ISSN 0021-9673

VOL. 685 NO. 2 18 NOVEMBER 1994

JOURNAL OF CHROMATOGRAPHY A

INCLUDING ELECTROPHORESIS AND OTHER SEPARATION METHODS

ELSEVIER

JOURNAL OF CHROMATOGRAPHY A

INCLUDING ELECTROPHORESIS AND OTHER SEPARATION METHODS

Scope. The *Journal of Chromatography A* publishes papers on all aspects of **chromatography, electrophoresis** and related methods. Contributions consist mainly of research papers dealing with chromatographic theory, instrumental developments and their applications. In the *Symposium volumes*, which are under separate editorship, proceedings of symposia on chromatography, electrophoresis and related methods are published. *Journal of Chromatography B: Biomedical Applications* —This journal, which is under separate editorship, deals with the following aspects: developments in and applications of chromatographic and electrophoretic techniques related to clinical diagnosis or alterations during medical treatment; screening and profiling of body fluids or tissues related to the analysis of active substances and to metabolic disorders; drug level monitoring and pharmacokinetic studies; clinical toxicology; forensic medicine; veterinary medicine; occupational medicine; results from basic medical research with direct consequences in clinical practice.

Submission of Papers. The preferred medium of submission is on disk with accompanying manuscript (see *Electronic manuscripts* in the Instructions to Authors, which can be obtained from the publisher, Elsevier Science B.V., P.O. Box 330, 1000 AH Amsterdam, Netherlands). Manuscripts (in English; *four* copies are required) should be submitted to: Editorial Office of *Journal of Chromatography A*, P.O. Box 681, 1000 AR Amsterdam, Netherlands, Telefax (+31-20) 5862 304, or to: The Editor of *Journal of Chromatography B: Biomedical Applications*, P.O. Box 681, 1000 AR Amsterdam, Netherlands. Review articles are invited or proposed in writing to the Editors who welcome suggestions for subjects. An outline of the proposed review should first be forwarded to the Editors for preliminary discussion prior to preparation. Submission of an article is understood to imply that the article is original and unpublished and is not being considered for publication elsewhere. For copyright regulations, see below.

Publication information. *Journal of Chromatography A* (ISSN 0021-9673): for 1995 Vols. 683–714 are scheduled for publication. *Journal of Chromatography B: Biomedical Applications* (ISSN 0378-4347): for 1995 Vols. 663–674 are scheduled for publication. Subscription prices for *Journal of Chromatography A*, *Journal of Chromatography B: Biomedical Applications* or a combined subscription are available upon request from the publisher. Subscriptions are accepted on a prepaid basis only and are entered on a calendar year basis. Issues are sent by surface mail except to the following countries where air delivery via SAL is ensured: Argentina, Australia, Brazil, Canada, China, Hong Kong, India, Israel, Japan, Malaysia, Mexico, New Zealand, Pakistan, Singapore, South Africa, South Korea, Taiwan, Thailand, USA. For all other countries airmail rates are available upon request. Claims for missing issues must be made within six months of our publication (mailing) date. Please address all your requests regarding orders and subscription queries to: Elsevier Science B.V., Journal Department, P.O. Box 211, 1000 AE Amsterdam, Netherlands. Tel.: (+31-20) 5803 642; Fax: (+31-20) 5803 598. Customers in the USA and Canada wishing information on this and other Elsevier journals, please contact Journal Information Center, Elsevier Science Inc., 655 Avenue of the Americas, New York, NY 10010, USA, Tel. (+1-212) 633 3750, Telefax (+1-212) 633 3764.

Abstracts/Contents Lists published in Analytical Abstracts, Biochemical Abstracts, Biological Abstracts, Chemical Abstracts, Chemical Titles, Chromatography Abstracts, Current Awareness in Biological Sciences (CABS), Current Contents/Life Sciences, Current Contents/Physical, Chemical & Earth Sciences, Deep-Sea Research/Part B: Oceanographic Literature Review, Excerpta Medica, Index Medicus, Mass Spectrometry Bulletin, PASCAL-CNRS, Referativnyi Zhurnal, Research Alert and Science Citation Index.

US Mailing Notice. *Journal of Chromatography A* (ISSN 0021-9673) is published weekly (total 52 issues) by Elsevier Science B.V., (Sara Burgerhartstraat 25, P.O. Box 211, 1000 AE Amsterdam, Netherlands). Annual subscription price in the USA US$ 5389.00 (US$ price valid in North, Central and South America only) including air speed delivery. Second class postage paid at Jamaica, NY 11431. **USA POSTMASTERS**: Send address changes to *Journal of Chromatography A*, Publications Expediting, Inc., 200 Meacham Avenue, Elmont, NY 11003. Airfreight and mailing in the USA by Publications Expediting.

See inside back cover for Publication Schedule, Information for Authors and information on Advertisements.

0021-9673/94/$07.00

Printed in the Netherlands

VOL. 685, NO. 2 JOURNAL OF CHROMATOGRAPHY A 18 NOVEMBER 1994

CONTENTS

(Abstracts/Contents Lists published in Analytical Abstracts, Biochemical Abstracts, Biological Abstracts, Chemical Abstracts, Chemical Titles, Chromatography Abstracts, Current Awareness in Biological Sciences (CABS), Current Contents/Life Sciences, Current Contents/Physical, Chemical & Earth Sciences, Deep-Sea Research/Part B: Oceanographic Literature Review, Excerpta Medica, Index Medicus, Mass Spectrometry Bulletin, PASCAL-CNRS, Referativnyi Zhurnal, Research Alert and Science Citation Index)

REGULAR PAPERS

Column Liquid Chromatography

Gas Chromatography

(Continued overleaf)

Contents (continued)

ELSEVIER

Journal of Chromatography A, 685 (1994) 203–211

JOURNAL OF CHROMATOGRAPHY A

Hydrogen bonding XXXV. Relationship between high-performance liquid chromatography capacity factors and water–octanol partition coefficients

Michael H. Abraham[a,*], Harpreet S. Chadha[a], Albert J. Leo[b]

[a]*Department of Chemistry, University College London, 20 Gordon Street, London WC1H 0AJ, UK*
[b]*Medicinal Chemistry Project, Pomona College, Claremont, CA 91711, USA*

First received 31 March 1994; revised manuscript received 19 July 1994

Abstract

The solvation equation $\log SP = c + rR_2 + s\pi_2^H + a\Sigma\alpha_2^H + b\Sigma\beta_2^H + vV_x$ has been applied to reversed-phase HPLC capacity factors, as $\log k'$, for solutes on a C_{18} bonded phase, with various water–methanol mobile phases, using data by Yamagami and Takao. Here, SP is a property for a series of solutes in a fixed solvent system, and the explanatory variables are solute descriptors as follows: R_2 is an excess molar refraction, π_2^H is the solute dipolarity/polarizability, $\Sigma\alpha_2^H$ and $\Sigma\beta_2^H$ are the solute overall or effective hydrogen-bond acidity and basicity, and V_x is the McGowan characteristic volume; c, r, s, a, b and v are constants. It is shown that the blend of factors that influence $\log k'$ in any given system is not the same as that which influences $\log P_{oct}$. In particular, solute hydrogen-bond acidity considerably influences $\log k'$, but has no effect on $\log P_{oct}$. It follows that when $\log k'$ values are used to estimate $\log P_{oct}$, great care has to be taken to match the training set of solutes in the correlation equation, with the solutes for which $\log P_{oct}$ is to be determined.

1. Introduction

The use of reversed-phase high-performance liquid chromatography (RP-HPLC) to determine water–octanol partition coefficients is a well-established and widely practiced method [1–5]. Values of the RP-HPLC capacity factor, k', are obtained for a training set of solutes with known water–octanol partition coefficients, P_{oct}, using a given stationary phase and a given mobile phase, and a correlation equation of the type

$$\log k' = o \log P_{oct} + q \quad (1)$$

is constructed. Then further measurements of $\log k'$ in the same system can be used to estimate P_{oct} for other solutes. How good the estimations are, depends not only on the choice of the RP-HPLC system, but also on the choice of the training set of solutes. Xie et al. [2] used a training set of phenols in order to estimate $\log P_{oct}$ for phenols, and obtained a good correlation between $\log P_{oct}$ from an RP-HPLC method, and $\log P_{oct}$ from the traditional shake-flask (sf) method. The RP-HPLC procedure of Xie et al. [2] differs slightly from that summarized as Eq.

* Corresponding author.

0021-9673/94/$07.00
SSDI 0021-9673(94)00686-5

1, in that the capacity factors determined at different water–methanol mobile phase compositions were extrapolated to zero methanol composition, and the resulting log k'_w values used to calculate log P_{oct}. For 21 phenolic solutes, the relationship between log P_{oct} by the sf method, and log P_{oct} by the RP-HPLC method is given by

$$\log P_{oct,sf} = 0.0616 + 0.9861 \log P_{oct,RP\text{-}HPLC}$$
$$n = 21,\ \rho = 0.9803,\ \text{S.D.} = 0.12,\ F = 468 \qquad (2)$$

Here and elsewhere, n is the number of solutes, ρ is the correlation coefficient, S.D. is the standard deviation in the dependent variable, and F is the F-statistic. If a wide range of solutes is considered, the regression equation, either in terms of Eq. 1 or Eq. 2, is not so good. For example, Vallat et al. [5] determined log k'_w both directly using buffered water as the mobile phase, and by extrapolation from buffered water–methanol mobile phases, with a deactivated C_8 stationary phase. For 70 varied solutes they found

$$\log P_{oct} = 0.30 + 1.09 \log k'_{w,C_8}$$
$$n = 70,\ \rho = 0.9476,\ \text{S.D.} = 0.29,\ F = 599 \qquad (3)$$

They attributed the rather poor correlation shown in Eq. 3 to the different hydrogen-bond properties of the RP-HPLC C_8 system and the water–octanol system, on the lines suggested by Kamlet and co-workers [6,7] several years ago. As might be expected, a plot of log P_{oct} vs. log k'_w revealed clear family-dependent lines [5]. Vallat et al. [5] also examined a novel octadecylpolyvinyl alcohol (ODP) stationary phase in a similar way, and obtained

$$\log P_{oct} = -0.06 + 0.83 \log k'_{w,ODP}$$
$$n = 40,\ \rho = 0.9823,\ \text{S.D.} = 0.23,\ F = 1048 \qquad (4)$$

The ODP system seems to mimic hydrogen-bond and other properties of the water–octanol system rather well [5], and gives a better correlation over a varied set of solutes. However, the RP-HPLC systems mostly used in the determination of log P_{oct} values are nearer the C_8 system, and in these cases, the training set of solutes will normally be chosen so as to resemble as closely as possible the solutes for which log P_{oct} is unknown. Unless the training set is carefully chosen, Eq. 1 may not hold. An elegant demonstration of this has recently been provided by Yamagami and Takao [4], who obtained log k' values on a typical C_{18} bonded stationary phase, Capcell Pak, with various water–methanol mixtures as the mobile phase. They used a variety of substituted furans and heterocyclic compounds (see Table 1), as a training set, and showed that Eq. 1 held only for restricted families of solute. Even when taking the two sets of solutes in Table 1 separately, a plot of log k' against log P_{oct} gave rise to families of lines, rather than to one single line, for any given water–methanol mobile phase. Yamagami and Takao [4] also obtained log k'_w values through extrapolation of log k' to zero methanol concentration using results from water–methanol mixtures containing 30–70% (v/v) methanol, but found again that a plot of log k'_w against log P_{oct} gave rise to families of lines. Although Yamagami and Takao [4] took the two sets of solutes in Table 1 separately, similar results are found if the two sets are treated together, as shown in Figs. 1–3. Note that solutes 32–35 in set B in Table 1 also occur in set A; we keep both because the log k' values given by Yamagami and Takao [4] are slightly different from one set to the other.

Yamagami and Takao [4] divided the solutes in set A in Table 1 into three groups of substituents, (i) H, alkyl, halogen, OMe and COMe, (ii) CO_2R and $CONMe_2$, and (iii) CONHMe and $CONH_2$. They suggested that solutes with hydrogen-bond acidic groups would undergo hydrogen-bonding more effectively with octanol (or rather wet octanol) than with the less basic stationary phase, so that log P_{oct} is larger than expected, or log k' is smaller than expected, by comparison with the other substituted furans. A similar argument was put forward to explain the deviant behaviour of indole and 3-car-

Table 1
Solutes and their descriptors used in the calculations

No.	Solute	R_2	π_2^H	$\Sigma\alpha_2^H$	$\Sigma\beta_2^H$	V_x
Set A						
1	Furan	0.369	0.53	0.00	0.13	0.5363
2	2-Methylfuran	0.372	0.50	0.00	0.14	0.6772
3	2-Ethylfuran	0.361	0.50	0.00	0.14	0.8181
4	2-Methoxyfuran	0.408	0.76	0.00	0.25	0.7359
5	2-O · COMe-furan	0.570	1.20	0.00	0.58	0.8925
6	2-CO_2Me-furan	0.560	1.00	0.00	0.50	0.8925
7	2-CO_2Et-furan	0.560	1.00	0.00	0.50	1.0334
8	2-Br-5-CO_2Et-furan	0.785	1.13	0.00	0.45	1.0675
9	2-CONMe$_2$-furan	0.810	1.10	0.00	0.89	1.0745
10	3-CO_2Me-furan	0.477	0.84	0.00	0.46	0.8925
11	3-CO_2Et-furan	0.429	0.86	0.00	0.46	1.0334
12	3-CONMe$_2$-furan	0.710	0.94	0.00	0.98	1.0745
13	2-CONH$_2$-furan	0.910	1.20	0.10	0.83	0.7927
14	2-CONHMe-furan	0.850	1.15	0.36	0.76	0.9336
15	2-CONHEt-furan	0.800	1.15	0.36	0.81	1.0745
16	3-CONH$_2$-furan	0.810	1.11	0.49	0.67	0.7927
17	3-CONHMe-furan	0.750	0.87	0.36	0.82	0.9336
18	3-CONHEt-furan	0.700	0.89	0.36	0.85	1.0745
Set B						
19	Pyrazine	0.629	0.95	0.00	0.62	0.6342
20	2-CO_2Me-pyrazine	0.750	1.28	0.00	0.92	0.9904
21	2-Me-5-CO_2Me-pyrazine	0.750	1.28	0.00	0.96	1.1313
22	2-Me-6-CO_2Me-pyrazine	0.750	1.28	0.00	0.98	1.1313
23	2-Cl-5-CO_2Me-pyrazine	0.850	1.27	0.00	0.85	1.1128
24	2-MeO-6-CO_2Me-pyrazine	0.780	1.30	0.00	0.87	1.1900
25	Pyrimidine	0.606	1.00	0.00	0.65	0.6342
26	2-CO_2Me-pyrimidine	0.730	1.33	0.00	1.04	0.9904
27	5-CO_2Me-pyrimidine	0.730	1.33	0.00	0.82	0.9904
28	Pyridazine	0.670	0.85	0.00	0.81	0.6342
29	4-CO_2Me-pyridazine	0.790	1.18	0.00	0.97	0.9904
30	Benzene	0.610	0.52	0.00	0.14	0.7164
31	Methyl benzoate	0.733	0.85	0.00	0.46	1.0726
32	Furan	0.369	0.53	0.00	0.13	0.5363
33	2-CO_2Me-furan	0.560	1.00	0.00	0.50	0.8925
34	3-CO_2Me-furan	0.477	0.84	0.00	0.46	0.8925
34	2-Br-5-CO_2Et-furan	0.785	1.13	0.00	0.45	1.0675
36	N-Methylpyrrole	0.559	0.79	0.00	0.31	0.7180
37	2-CO_2Me-pyrrole	0.740	1.06	0.00	0.40	0.9936
38	Thiophene	0.687	0.57	0.00	0.15	0.6411
39	Benzofuran	0.888	0.83	0.00	0.15	0.9053
40	2-CO_2Me-benzofuran	1.080	1.31	0.00	0.46	1.2615
41	Indole	1.200	1.12	0.44	0.22	0.9460
42	2-CO_2Me-indole	1.320	1.45	0.12	0.52	1.3026
43	3-CO_2Me-indole	1.320	1.45	0.44	0.49	1.3026

bomethoxyindole in set B in Table 1. Whether or not such an explanation is quantitatively correct can only be ascertained through an analysis that includes proper descriptors of solute hydrogen-bond acidity and basicity. This is the aim of the present work.

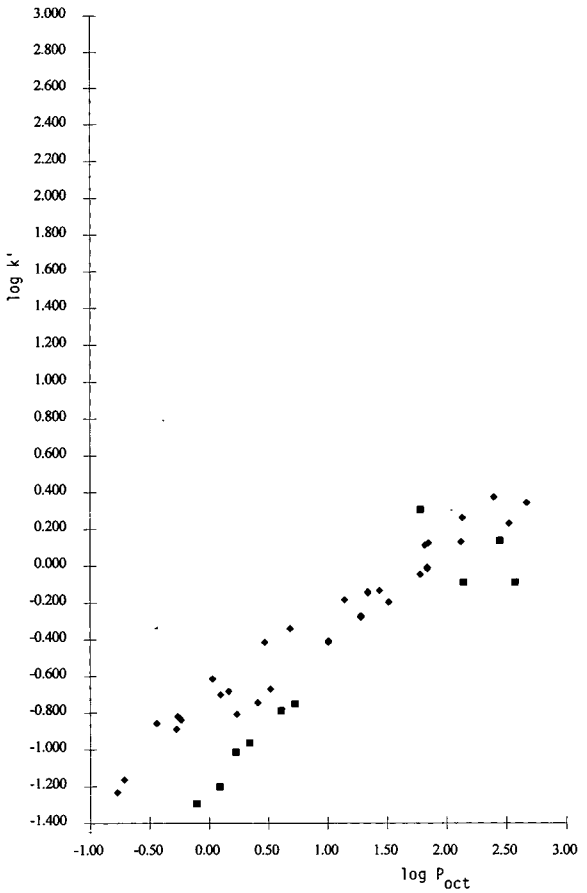

Fig. 1. Plot of log k' with mobile phase 70% methanol vs. log P_{oct} for all the entries in Table 1. Solutes with potential hydrogen bond acidic sites are denoted as ■.

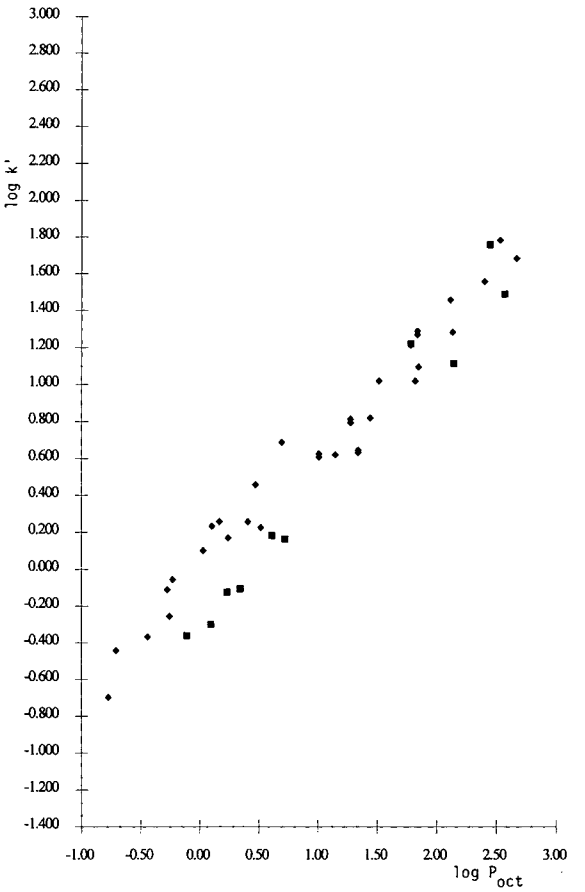

Fig. 2. Plot of log k' with mobile phase 30% methanol vs. log P_{oct} for all the entries in Table 1. Solutes with potential hydrogen bond acidic sites are denoted as ■.

2. Methodology

Our analysis is based [8] on the general solvation equation,

$$\log SP = c + rR_2 + s\pi_2^H + a\Sigma\alpha_2^H + b\Sigma\beta_2^H + vV_x \quad (5)$$

Here, SP is a property for a series of solutes in a fixed solvent system; in this work, SP will either be k' for solutes in a given RP-HPLC stationary phase–mobile phase system, or will be water–octanol partition coefficients for a series of solutes. The explanatory variables in Eq. 5 are solute descriptors as follows: R_2 is an excess molar refraction that can be obtained for complicated solutes by simple addition of fragments [8], π_2^H is the solute dipolarity/polarizability, $\Sigma\alpha_2^H$ and $\Sigma\beta_2^H$ are the solute overall or effective hydrogen-bond acidity and basicity, and V_x is the McGowan characteristic volume that can be calculated from molecular structure [8]; c, r, s, a, b and v are constants. Hence for any new solute to be examined, three descriptors need to be assigned, viz. π_2^H, $\Sigma\alpha_2^H$ and $\Sigma\beta_2^H$. We have shown in some detail [9] exactly how these can be obtained, provided that a number of water–solvent log P values are available. Yamagami et

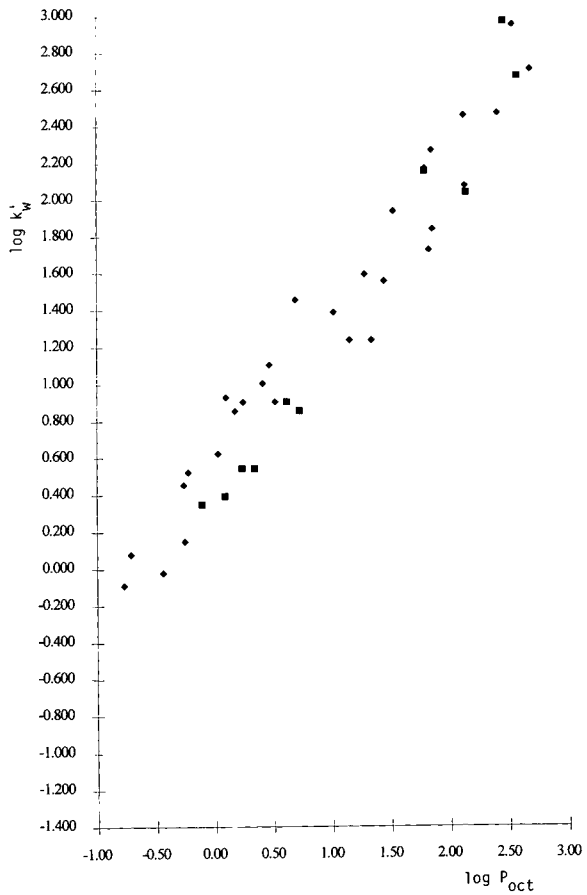

Fig. 3. Plot of log k'_w vs. log P_{oct} for all the entries in Table 1. Solutes with potential hydrogen bond acidic sites are denoted as ◘.

al. [10] have determined such log P values in water–octanol, water–chloroform, water–octane and water–dibutyl ether systems for the pyrazines, pyrimidines, and pyridazines in Table 1, enabling us to calculate the required descriptors. We have already determined those for many of the other compounds [8,9], leaving assignments to be made for solutes 4–18. This was done using structurally related compounds as examples, and the total set of descriptors was tested using the log P_{oct} values listed [4]. The assigned descriptors are given in Table 1.

The general Eq. 5 has been applied to a large number of water–solvent partitions [9]. The most relevant is the water–octanol system, for which the most recent [11] equation is

$$\log P_{oct} = 0.088 + 0.562R_2 - 1.054\pi_2^H + 0.034\Sigma\alpha_2^H - 3.460\Sigma\beta_2^H + 3.841V_x$$
$$n = 613, \quad \rho = 0.9974, \quad \text{S.D.} = 0.116, \quad F = 23162 \qquad (6)$$

The constants in Eq. 5 can be used to characterize the system in question; thus in Eq. 6 they provide information on the difference in properties of octanol (or wet octanol) and water. The r constant shows that solute polarizability favors octanol, and the s constant that solute dipolarity/polarizability favors water —hence octanol is itself more polarizable than water but water is more dipolar than octanol. The a constant is a measure of the difference in hydrogen-bond basicity between octanol and water (because acidic solutes interact with basic solvents), and shows that the two solvents have almost exactly the same basicity. On the other hand, the b constant indicates that water is much more acidic than octanol. Finally, the large positive v constant shows that octanol will interact with lipophilic solutes to a much greater extent than will water. There is no reason why Eq. 5 should not be applied in the same way to log k' values; indeed, Miller and Poole [12] have already shown this to be the case for a Baker-bond C_{18} stationary phase with various water–methanol mobile phases. We shall discuss these results later.

3. Results and discussion

The log k' values of Yamagami and Takao [4] refer to six water–methanol mixtures for the solutes in set A in Table 1, over the range 0–70% methanol, and to three water–methanol mixtures, from 30–70%, for solutes in set B in Table 1. There are not really enough solutes (18) in set A to carry out a complete analysis with Eq. 5, but since such a wide range of mixtures has been used, we thought it of interest to apply the equation, anyway. A summary of the resulting regression equations is in Table 2.

Table 2
Summary of regression Eq. 5 for solutes 1–18[a]

Methanol (%)	c	r	s	a	b	v	ρ	S.D.	F
0	−0.84	0.16	−0.10	−1.11	−1.93	3.96	0.9979	0.04	570
5	−0.63	0.36	−0.36	−1.06	−2.11	3.67	0.9969	0.05	384
15	−0.49	0.47	−0.52	−0.96	−2.33	3.34	0.9969	0.06	381
30	−0.39	0.56	−0.68	−0.84	−2.33	2.86	0.9976	0.05	508
50	−0.42	0.51	−0.76	−0.68	−2.09	2.28	0.9989	0.03	1051
70	−0.67	0.32	−0.73	−0.60	−1.74	1.88	0.9975	0.04	482
Log k'_w	−0.17	0.80	−0.66	−1.11	−2.83	3.59	0.9926	0.10	160
30[b]	−0.32	0.44	−0.58	−0.43	−2.52	3.34	0.9950	0.07	241
50[b]	−0.41	0.34	−0.74	−0.31	−2.00	2.75	0.9880	0.11	103
70[b]	−0.71	0.16	−0.44	−0.32	−1.59	2.12	0.9900	0.08	124
100[b]	−0.98	0.01	−0.19	−0.03	−0.62	1.22	0.9320	0.08	17

[a] With a Capcell Pak C_{18} phase, ref. [4].
[b] With a Bakerbond C_{18} phase, and a different solute set, ref. [12].

Although we do not regard the regression equations as definitive, the constants make general chemical sense, and the interpretation of them follows exactly that of the water–octanol equation, above. The main factors that influence log k' are solute dipolarity/polarizability, hydrogen-bond acidity and hydrogen-bond basicity that all favor the mobile phase and lead to a reduction in log k', and solute volume that favors the stationary phase and leads to an increase in log k'. The variation of the constants with mobile phase composition is interesting. As the methanol content increases, the difference between mobile phase and stationary phase basicity decreases and hence the magnitude of the a constant decreases; however the b constant reaches a maximum in magnitude at around 15–30% methanol. As the difference in hydrophobicity decreases with increasing methanol content, so does the v constant decrease. Surprisingly, the s constant increases in magnitude as the methanol content increases, so that the difference in dipolarity/polarizability between stationary phase and mobile phase becomes larger. However it must be noted that the stationary phase is not constant over the range of mobile phase composition. At 0% methanol, it will be saturated with water, at 100% methanol it will be saturated with methanol, and at intermediate compositions it will be saturated with some solvent composition, not necessarily the same as that in the mobile phase. Although the equations of Miller and Poole [12] refer to a different C_{18} phase, and a different (and also limited) solute set, they resemble quite closely those we find. A selection of the Miller–Poole equations is given in Table 2 for comparison. The trend of the constants in the Miller–Poole equations is practically the same as for the solute 1–18 set, and shows, additionally, that as the mobile phase approaches 100% methanol, the a constant becomes negligible.

The equation in log k'_w is not as good as the others, no doubt because the log k'_w values themselves are linearly extrapolated from the 30–70% methanol results. Because the linearity in the extrapolation does not hold at low methanol content, the log k'_w equation is not the same as that at 0% methanol, obtained from the actual experimental log k' values at 0%.

We can see from a direct comparison of Eq. 6 with the equations summarized in Table 2, why log k' values will not always be linear with log P_{oct}. Such linearity will hold if the constants in the log k' equation are similar to those in Eq. 6, or if there is a simple relationship between them. Otherwise, Eq. 1 will not be expected to hold, as a generality, unless the solute set contains only functionally related solutes. Most importantly, if

a solute set contains solutes that differ widely in their hydrogen-bond acidity, then the linear Eq. 1 will break down, simply because log P_{oct} is not influenced by solute acidity, whereas log k' in most water–methanol mixtures is so influenced. The suggestion of Yamagami and Takao [4] that hydrogen-bond acidity of the solute leads to deviations from Eq. 1 is thus confirmed, but in order to quantify the effect we first prefer to analyse results for the total data set in Table 1.

A summary of the regression equations obtained using all 43 data points is in Table 3. There is a satisfactory agreement between the constants in Table 2 (set A) and those in Table 3 (sets A and B), except that the s constant in Table 3 decreases with increase in methanol content, more as expected. All the equations in Table 3 include a substantial a constant, so that our comments on the influence of acidic solutes, above, hold for this larger data set. We can show the effect of our analysis using the various descriptors in Eq. 5, by comparing a plot of observed and calculated log k'_w values (Fig. 4), with the plot shown in Fig. 3. Another, more quantitative, way is to add log P_{oct} as a descriptor to those in Eq. 5, leading to a method of analysis that we refer to as the log P_{plus} method,

$$\log SP = c + rR_2 + s\pi_2^H + a\Sigma\alpha_2^H + b\Sigma\beta_2^H + vV_x + o \log P_{oct} \quad (7)$$

We shall discuss the application of the log P_{plus} equation elsewhere, and now just apply it to the results for the 43 data points, as a comparison with the constants in Table 3. The application of

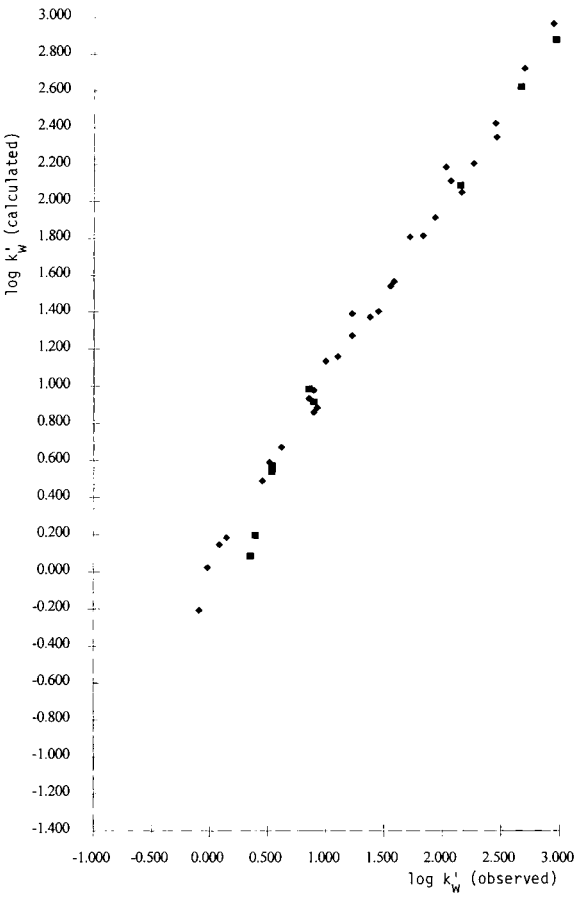

Fig. 4. Plot of observed vs. calculated log k'_w on Eq. 3 with the constants in Table 3. Solutes with potential hydrogen bond acidic sites are denoted as □.

Eq. 7 is not straightforward with the present data, because of cross-correlations of the original descriptors with log P_{oct}. The best equations are summarized in Table 4; in all cases, the differ-

Table 3
Summary of regression Eq. 5 for solutes 1–43

Methanol (%)	c	r	s	a	b	v	ρ	S.D.	F
30	−0.43	0.36	−0.61	−0.89	−2.24	2.92	0.9979	0.05	1761
50	−0.45	0.18	−0.47	−0.76	−2.02	2.23	0.9961	0.06	932
70	−0.64	0.05	−0.27	−0.78	−1.72	1.61	0.9838	0.09	223
Log k'_w	−0.21	0.70	−0.94	−1.04	−2.60	3.83	0.9948	0.09	711

Capcell Pak C_{18} phase, ref. [4].

Table 4
Summary of the log P_{plus} regression Eq. 7 for solutes 1–43

Methanol (%)	c	a	v	o	ρ	S.D.	F
30	−0.53	−0.83	0.57	0.65	0.9972	0.05	2283
Log k'_w	−0.31	−0.78	0.98	0.80	0.9968	0.07	1991
30	−0.03	−0.67		0.67	0.9838	0.12	604
50	−0.44	−0.76		0.58	0.9916	0.08	1179
70	−0.80	−0.91		0.46	0.9728	0.11	352
Log k'_w	0.55	−0.50		0.83	0.9714	0.20	335

Capcell Pak C_{18} phase, ref. [4].

ence between the log k' (or log k'_w) regression with log P_{oct} and the best regression with the log P_{plus} equation, depends on the $a\Sigma\alpha_2^H$ term, together with a vV_x term in two cases. For comparison, the constants are given in all four cases with just a two-term equation. Then it is clear that the $a\Sigma\alpha_2^H$ term is numerically largest for the 70% methanol system, and smallest for the 30% methanol system. This may seem contrary to the results in Table 3, where the $a\Sigma\alpha_2^H$ term is numerically the largest for the 30% system, but the effect of the hydrogen-bond term depends also on the magnitude of the other terms in Eq. 6.

We can now calculate from the two-term equation summarised in Table 4, exactly how the solute hydrogen-bond acidity contributes to the deviation in the log k' against log P_{oct} equation. In the first set of solutes (Table 1), the CONHR-substituted furans have $\Sigma\alpha_2^H$ equal to 0.36 units, which will lead to deviations of 0.24 log units in log k' for 30% methanol, 0.27 log units for 50% methanol, 0.33 units for 70% methanol, and 0.18 units in log k'_w. Because the o constants in Eq. 1 are all less than unity (0.667, 0.573, 0.454 and 0.829 respectively), these deviations in log k' or log k'_w correspond to deviations in any calculated log P_{oct} value of 0.36 (30%), 0.47 (50%), 0.73 (70%) and 0.22 (log k'_w). Yamagami and Takao [4] pointed out the deviant behaviour of indole and 3-carbomethoxyindole in set B, Table 1. Since $\Sigma\alpha_2^H$ is no less than 0.44 units for these two solutes, the calculated deviations will be even larger than those for the CONHR-furans.

We have highlighted the solute hydrogen-bond acidity as a possible factor in deviations from Eq. 1, but even for non-acidic solutes, such deviations can also arise, but to a less extent. This can be seen by scaling the equations in log k' in order to make the vV_x term exactly the same as that in the log P_{oct} Eq. 6, so that for the 30% methanol system

$$1.32 \log k' = 0.48R_2 - 0.80\pi_2^H - 1.17\Sigma\alpha_2^H - 2.95\Sigma\beta_2^H + 3.84V_x \quad (8)$$

There is no comparison between the a constant in Eq. 8 and that in Eq. 6, as we have discussed above. But also, the s constants differ by 0.20 units, and the b constants by 0.45 units, with the same (adjusted) v constants. Thus if Eq. 1 is applied to solutes with a very wide range of $\Sigma\beta_2^H$ values and similar V_x values, then deviations will also occur.

It might be thought that log k' values determined at 100% methanol could be used to advantage in Eq. 1, because the a constant becomes numerically smaller with increasing methanol content. Indeed the Miller–Poole equation (Table 2) for log k' values on Baker-bond C_{18} with 100% methanol mobile phase shows that the a constant is not significant. However, this does not help very much in the estimation of log P_{oct} values, because the blend of factors in the given Eq. 5 is still quite different to that in Eq. 6. We can show this in the same way as before, by multiplying Eq. 5 for 100% methanol, in Table 2, by the factor 3.15 throughout,

$$3.15 \log k' = -3.09 + 0.04R_2 - 0.60\pi_2^H - 0.09\Sigma\alpha_2^H - 1.95\Sigma\beta_2^H + 3.84V_x \quad (9)$$

A comparison of Eq. 9 with Eq. 6 shows that solutes of the same volume but of different R_2, π_2^H or $\Sigma\beta_2^H$ value cannot lie on the same log k' vs. log P_{oct} plot. This is the reason why 100% methanol is almost never used as the mobile phase in log P_{oct} determinations.

We have therefore shown, through the general Eq. 5, how large deviations can arise in any log k' vs. log P_{oct} equation when the solute hydrogen-bond acidity varies through the given solute set if aqueous methanol is used as the mobile phase. Deviations, although smaller in nature, can also occur if other solute properties such as hydrogen-bond basicity vary widely in the solute set. Large deviations can arise when methanol itself is the mobile phase, because the blend of factors that influence log k' is now quite different to the blend that influences log P_{oct}. Although our analysis has concentrated on RP-HPLC data for a particular C_{18} stationary phase, the results obtained here are likely to be general for C_{18} and similar phases, and indicate how extreme care must be taken to match the properties of the training set of solutes to those for which log P_{oct} values are to be estimated.

Acknowledgement

We are grateful to Dr. Colin F. Poole for a preprint of his paper prior to publication.

References

[1] A. Nahum and Cs. Horváth, *J. Chromatogr.*, 192 (1980) 315.
[2] T.M. Xie, B. Hulthe and S. Folestad, *Chemosphere*, 13 (1984) 445.
[3] C. Yamagami, T. Ogura and N. Takao, *J. Chromatogr.*, 514 (1990) 123.
[4] C. Yamagami and N. Takao, *Chem. Pharm. Bull.*, 40 (1992) 925.
[5] P. Vallat, W. Fan, N. El Tayar, P.-A. Carrupt and B. Testa, *J. Liq. Chromatogr.*, 15 (1992) 2133.
[6] P.C. Sadek, P.W. Carr, R.M. Doherty, M.J. Kamlet, R.W. Taft and M.H. Abraham, *Anal. Chem.*, 57 (1985) 2971.
[7] M.J. Kamlet, M.H. Abraham, P.W. Carr, R.M. Doherty and R.W. Taft, *J. Chem. Soc., Perkin Trans. 2*, (1988) 2087.
[8] M.H. Abraham, *Chem. Soc. Rev.*, 22 (1993) 73.
[9] M.H. Abraham, *J. Phys. Org. Chem.*, 6 (1993) 660.
[10] C. Yamagami, N. Takao and T. Fujita, *J. Pharm. Sci.*, 82 (1993) 155.
[11] M.H. Abraham, H.S. Chadha, G.S. Whiting and R.C. Mitchell, *J. Pharm. Sci.*, 83 (1994) 1085.
[12] K.G. Miller and C.F. Poole, *J. High. Resolut. Chromatogr.*, 17 (1994) 125.

ELSEVIER

Journal of Chromatography A, 685 (1994) 213–220

JOURNAL OF CHROMATOGRAPHY A

Synthesis of a polymeric-based stationary phase for carbohydrate separation by high-pH anion-exchange chromatography with pulsed amperometric detection ☆

Claudio Corradini[a,*], Danilo Corradini[a], Christian G. Huber[b], Gunther K. Bonn[c]

[a]*Istituto di Cromatografia del C.N.R., Area della Ricerca di Roma, P.O. Box 10, I-00016 Monterotondo Stazione (Rome), Italy*

[b]*Institute of Analytical Chemistry and Radiochemistry, Leopold-Franzens University, A-6020 Innsbruck, Austria*

[c]*Department of Analytical Chemistry, Johannes-Kepler University, A-4040 Linz, Austria*

First received 9 May 1994; revised manuscript received 15 July 1994

Abstract

Spherical highly cross-linked styrene–divinylbenzene copolymer particles were chemically modified by direct nitration, followed by reduction with tin metal and quaternization with iodomethane to produce a superficial layer of quaternized amino functions. Besides being simple and economical, the proposed method of synthesis leads to an anion exchanger that allows the use of shorter columns (75 × 4.6 mm I.D.) than those currently employed for carbohydrate separation by high-performance anion-exchange chromatography with pulsed amperometric detection under alkaline conditions. The new sorbent has proved to be highly selective for isomeric disaccharides and individual oligomers of an homologous series of maltooligosaccharides of up to 21 glucose residues. Extended exposure of columns packed with this sorbent to high pressure and strong alkaline solutions did not have any untoward effect on mechanical stability and chromatographic performance.

1. Introduction

The pK_a values of neutral carbohydrates usually fall in the range 12–14, and at high pH their hydroxyl groups are either partially or completely ionized, enabling this class of compounds to be separated as anions by high-performance anion-exchange chromatography (HPAEC) [1]. Furthermore, alkaline conditions allows the detection of carbohydrates by pulsed amperometric detection (PAD) at a gold electrode. PAD is characterized by high sensitivity, relative specificity for compounds with hydroxyl groups, it allows gradient elution techniques and no sample derivatization is requested [2]. This renders HPAEC–PAD a powerful tool for the highly selective separations of carbohydrates [3–8]. Silica-based columns cannot be used for these applications, due to their poor stability at high pH. Under these conditions separations are performed on polystyrene–divinylbenzene (PS–DVB)-based columns.

Most of the anion-exchange columns currently employed for carbohydrate separations by HPAEC–PAD are packed with electrostatically

* Corresponding author.

☆ Presented at the *16th International Symposium on Column Liquid Chromatography, Baltimore, MD, 14–19 June 1992*, paper L 127.

0021-9673/94/$07.00
SSDI 0021-9673(94)00665-2

latex-coated pellicular polymeric-based anion-exchange sorbents [9–11]. These sorbents are prepared by a proprietary process, which permits the independent manufacture of polymeric nonporous pellicular sulphonated resins and anion-exchange latex particles functionalized with quaternary ammonium compounds that are brought together only at the last steps of preparing a column. Another anion exchanger, specifically designed by Dionex for the separation of weakly ionizable carbohydrates such as mono- and disaccharides, sugar alcohols, and aldoses consists of a 8.5 μm diameter macroporous poly(vinylchloro–divinylbenzene) with quaternary ammonium functional groups [12]. Furthermore, the use of a macroporous poly(N,N,N,-trimethylammoniummethylstyrene–divinylbenzene) strong anion exchanger manufactured by a proprietary process [13] has also been reported [14,15].

Several other methods have been reported to produce surface-functionalized polystyrene-based anion exchangers, mainly for the separation of organic or inorganic ionic species [16,17], and proteins and nucleic acids [18,19].

The aim of this study was to develop a new, simple method for preparing a strong anion exchanger by chemical modification of highly cross-linked PS–DVB microspheres and to examine the potential of this new sorbent for the separation of carbohydrates by HPAEC–PAD under alkaline conditions. Chemical functionalization of the support was obtained by direct nitration, followed by reduction with granulated tin metal and quaternization with iodomethane. Details of this synthesis and applications of the resultant sorbent for the separation of isomeric disaccharides and individual oligomers of maltooligosaccharides by HPAEC–PAD in short columns of 75 × 4.6 mm I.D. are reported.

2. Experimental

2.1. Materials

All saccharides used as authentic standards, including maltooligosaccharides with degrees of polymerization 2–7 were obtained from Sigma (St. Louis, MO, USA). Dextrin 10 and dextrin 20 (maltodextrin) starch hydrolysates were purchased from Fluka (Buchs, Switzerland). Sodium hydroxide (50%, w/w) solution and anhydrous sodium acetate were purchased from J.T. Baker (Deventer, Netherlands). Anhydrous N,N-dimethylformamide, 1,2,2,6,6-pentamethylpiperidine and iodomethane were from Aldrich (Milwaukee, WI, USA). Reagent-grade fuming nitric acid, concentrated sulphuric acid, granulate tin metal, hydrochloric acid, HPLC-grade water, and other reagent-grade solvents and salts were purchased from Carlo Erba (Milan, Italy).

2.2. Equipment

The experiments were performed on a Dionex (Sunnyvale, CA, USA) Model 4000i gradient pump module equipped with a Model PAD II pulsed amperometric detector consisting of an amperometric flow-through cell with a gold working electrode and a silver–silver chloride reference electrode. The following working pulse potentials and durations were used for detection of analytes: $E_1 = 0.10$ V ($t_1 = 300$ ms); $E_2 = 0.60$ V ($t_2 = 120$ ms); $E_3 = -0.60$ V ($t_3 = 300$ ms). The response time of the PAD was set to 1 s. A Dionex DXP single-piston pump was used to add 0.3 *M* sodium hydroxide to the column effluent through a tee at 0.2 ml/min before the PAD cell during elution with sodium hydroxide concentrations lower than 40 m*M*. The sample loop volume was 10 μl. The Dionex eluent degas module was employed to sparge and pressurize the eluents with helium. This both degases and prevents adsorption of carbon dioxide and subsequent production of carbonate which would act as displacing ion and shorten retention times. Chromatographic data were collected and plotted using the Dionex Auto Ion 450 chromatography workstation.

2.3. Synthesis of the packing material

Spherical highly cross-linked PS–DVB particles having a mean diameter of 2.8 μm, and surface area of 7 m^2/g were prepared and characterized as previously reported [20]. The

PS–DVB beads were superficially nitrated and reduced by a modification of the method proposed by Maa et al. [18], and then reacted with iodomethane to produce a superficial layer of quaternized amino groups.

Nitration

Dry PS–DVB beads (5 g) were dispersed in a 6-fold excess (v/w) of N,N-dimethylformamide by sonication for about 10 min. The suspension was added dropwise under stirring at 2–5°C to 60 ml of a 75% (v/v) mixture of fuming nitric acid and sulphuric acid contained in a 250-ml three-neck flask equipped with a stirrer and a thermometer, and cooled by an ice bath. Stirring of this mixture was protracted for 3 h. The reaction mixture was then heated to 60°C and maintained at this temperature (± 2°C) under stirring for an additional 6 h. The resulting nitrated PS–DVB beads were filtered on a sintered-glass filter and washed successively with water, 0.15 *M* sodium hydroxide, water to neutrality, and N,N-dimethylformamide. Then the particles were air-dried overnight.

Reduction

The nitrated PS–DVB beads were placed in the three-neck flask and dispersed in 30 ml of N,N-dimethylformamide by sonication for about 5 min. A 2-g amount of granulated tin metal was added to the reaction mixture cooled in an ice bath. From a dropping funnel, 60 ml of concentrated hydrochloric acid were added dropwise under stirring maintaining the temperature at 5–10°C. Thereafter, the reaction mixture was slowly warmed up to room temperature, stirred for an additional 2 h, then heated at 90°C and left at this temperature overnight under continuous stirring. The reduced product was filtered on a sintered-glass filter and washed successively with water, 1.0 *M* sodium hydroxide, water and then methanol. At the end, particles were left overnight under vacuum in an oven at 60°C.

Quaternization

The resulting amino groups were methylated following the procedure reported by Rounds and Regnier [19]. A 700-μl volume of 1,2,2,6,6-pentamethylpiperidine was added to the particles, which were previously suspended in 35 ml of dry N,N-dimethylformamide. The reaction mixture was sonicated for a few minutes, then 3 ml of iodomethane were added. The suspension was heated at 60°C for 10 h under stirring. After cooling, the reaction mixture was filtered on a sintered-glass filter and washed successively with water, methanol, triethylamine, methanol and then dried at 60°C under vacuum.

2.4. HPLC columns and procedures

Columns were packed using the following high-pressure slurry packing technique. The polymeric sorbent (1.25 g) was suspended in 20 ml of HPLC-grade water, sonicated for 3 min and packed into a 75 × 4.6 mm I.D. polyether ether ketone (PEEK) column (Alltech, Deerfield, IL, USA). Water was used as the driving solvent at a constant pressure of 40 MPa, by using a Model DSTV 122 pneumatic pump (Haskel, Burbank, CA, USA).

Eluents were prepared by suitable dilution of 50% sodium hydroxide solution with HPLC-grade water. After each run the sodium hydroxide concentration was ramped to 300 m*M* in 5 min and then maintained at this level for a further 15 min to clean the column. The column was then reequilibrated to the starting conditions for 15 min.

3. Results and discussion

3.1. Characterization of the column

The complete synthetic route to the strong-anion-exchange packing material is depicted in Fig. 1. In order to evaluate the mechanical stability of the polymeric-based sorbent, the pressure drop of a 75 × 4.6 mm I.D. column packed with the above stationary phase was measured upon eluting it with water at various flow-rates. The results are presented in Fig. 2 as a plot of column pressure drop versus flow-rate, which shows good linearity up to column inlet pressure of 27.6 MPa (4000 p.s.i.), the practical upper limit of the pumping system used.

The resistance of the PS–DVB-based sorbent

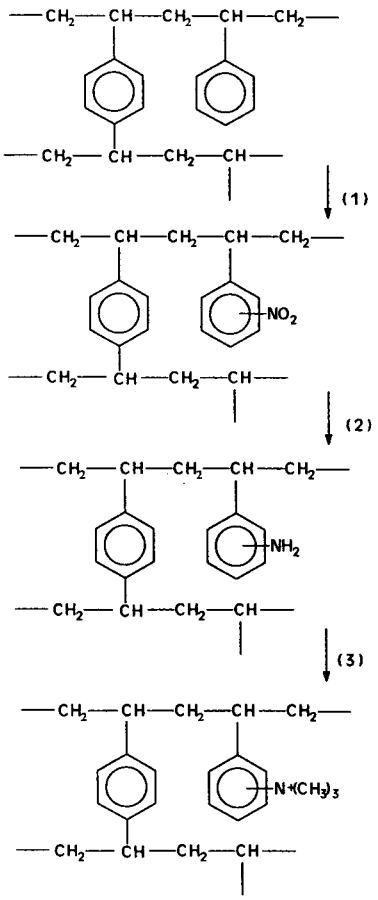

Fig. 1. Synthetic route to the quaternized amino phase on highly cross-linked poly(styrene–divinylbenzene) 2.8-μm particles. (1) Direct nitration, (2) reduction of nitro groups and (3) quaternization of amino groups.

to prolongate exposure to alkaline mobile phase and pressure was investigated by measuring the column performance during a test consisting of alternative elution of the column with aqueous solutions containing (A) sodium hydroxide (50 mM) and (B) a mixture of sodium acetate (400 mM) and sodium hydroxide (50 mM). At the end of the test (84 h) more than 2000 column volumes (over 2500 ml) of the two eluents were pumped through the column with no noticeable effect on retention and peak shape of a carbohydrate test mixture. Furthermore, the column used for this test withstood over 600 sample

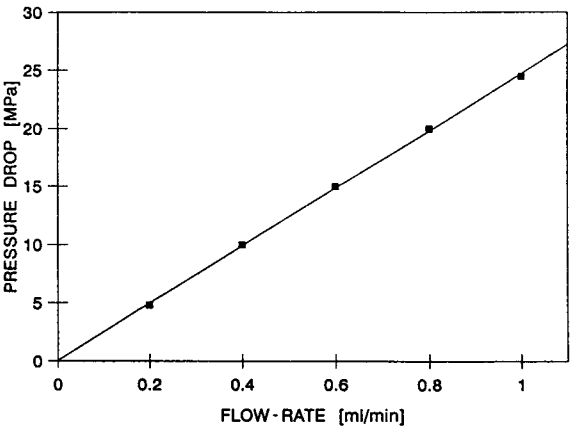

Fig. 2. Plot of pressure drop versus flow-rate of water at 25°C. Column, 75 × 4.6 mm I.D. packed with 2.8-μm highly cross-linked PS–DVB-based strong anion exchanger.

injections under various mobile phase conditions without loss of performance.

The loading capacity of the 75 × 4.6 mm I.D. column packed with the microparticulate sorbent was examined by injecting increasing levels of an equimolar mixture of maltose and turanose. Elution was performed under isocratic conditions with 50 mM sodium hydroxide as the mobile phase. Under these conditions, 10 μg (ca. 30 nmol) of each disaccharide was the upper loading limit for resolution. Plots of the peak area generated by the pulsed amperometric detector versus the concentration were constructed for these two saccharides and were found to be linear in the range from 4 to 32 μg/ml (see Fig. 3).

3.2. Retention behaviour and selectivity

The chromatogram of a mixture of authentic standards of glucose, turanose, maltose, panose and maltotriose is reported in Fig. 4. This mixture was used to evaluate the retention behaviour of the stationary phase in relation to the ionic strength of the mobile phase. The standard mixture was eluted isocratically with mobile phases containing sodium hydroxide at various concentrations ranging from 40 to 60 mM. The retention times of all carbohydrates

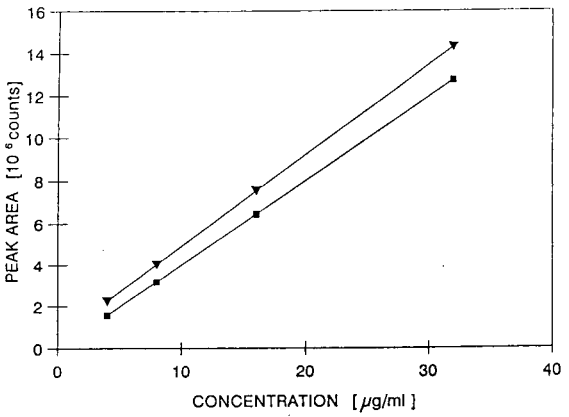

Fig. 3. Dependence of peak area generated by PAD on the concentration of injected sample. Column, 75 × 4.6 mm I.D. packed with 2.8-μm highly cross-linked PS–DVB-based strong anion exchanger; eluent, 50 m*M* sodium hydroxide; flow-rate, 0.5 ml/min; temperature, 25°C; sample: ▼ = turanose, □ = maltose. Detector, PAD 2; attenuation, 1000 nA.

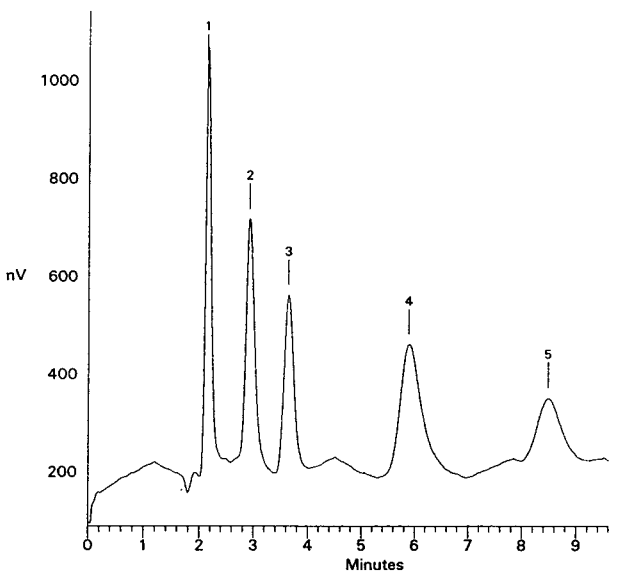

Fig. 4. Separation of (1) glucose, (2) turanose, (3) maltose, (4) panose and (5) maltotriose on column 75 × 4.6 mm I.D. Chromatographic conditions as in Fig. 3, except isocratic elution with 40 m*M* sodium hydroxide.

decreased with increasing sodium hydroxide concentration as shown in Fig. 5. Glucose was eluted first, while the disaccharides turanose and maltose and the trisaccharides panose and maltotriose showed higher retention times, which can be explained on the basis of an increasing number of negative charges on the oligosaccharides owing to the increasing number of hydroxyl groups. Fig. 6 demonstrates that the oligomers of the homologous maltooligosaccharides glucose, maltose and maltotriose, showed a linear relationship between the logarithmic retention time and the number of glucose residues in the homologous series. However, besides chain

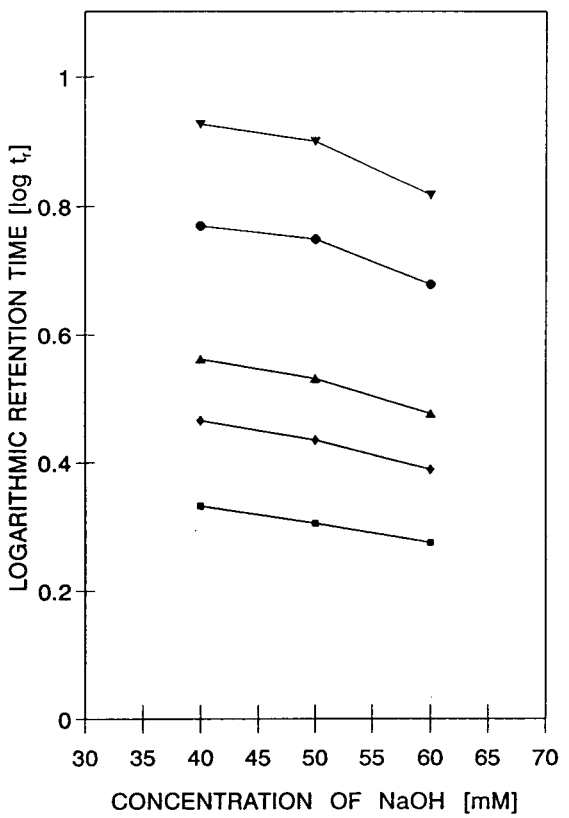

Fig. 5. Plots of the logarithmic retention time as a function of the concentration of sodium hydroxide in the eluent. Chromatographic conditions as in Fig. 3, except concentration of sodium hydroxide in the eluent as indicated in the graph. Samples: □ = glucose; ◆ = turanose; ▲ = maltose; ○ = panose; ▼ = maltotriose.

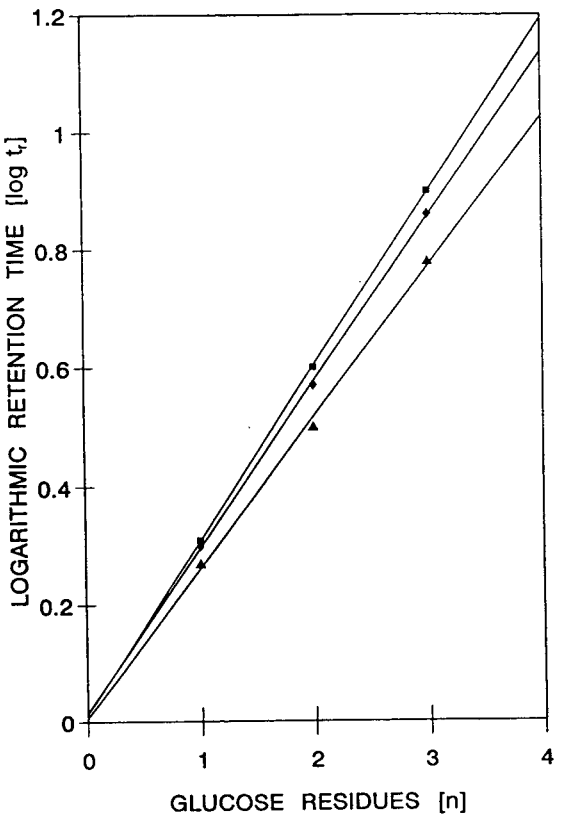

Fig. 6. Dependence of the logarithmic retention time on the chain length of homologous maltooligosaccharides. Eluent aqueous solution of sodium hydroxide at (□) 40, (◆) 50 and (▲) 60 m*M*. Other conditions as in Fig. 3.

length, saccharide composition and linkage position are expected to affect the chromatographic retention of oligosaccharides [21,22].

Disaccharides were selectively retained under isocratic conditions with mobile phases containing sodium hydroxide at concentrations ranging from 6 to 45 m*M*. When performing isocratic analysis at these low sodium hydroxide concentrations, postcolumn addition of 0.3 *M* sodium hydroxide at a flow-rate of 0.2 ml/min was necessary to maintain optimum detector sensitivity and minimize baseline drift. The retention times of twelve disaccharides are listed in Table 1.

Separation of oligosaccharides by AEC is strongly affected, besides their acidity, by the accessibility of oxyanions to functional groups attached to the stationary phase [23]. The disaccharides trehalose, isomaltose, gentiobiose, nigerose and maltose are similar in structure (they are all composed of two D-glucosyl residues), and differ only in the configuration of their glycosidic bonds. These disaccharides follow the elution order showed in HPAEC using a currently available strong anion-exchange sorbent [24], and the differences in the retention times are believed to be related either to the different acidity of the substituted hydroxyl groups or to the different configuration of the glycosidic bond, which causes their orientation to differ when adsorbed to the stationary phase. The greater retention time of the trisaccharide maltotriose compared to the trisaccharide isomaltotriose is an other example of the selectivity of the stationary phase for isomeric forms.

The effective separation of individual components of an homologous series of maltooligosaccharides of different provenance was achieved using linear gradient elution. The chromatogram of the mixture containing maltooligosaccharides of up to 21 glucose residues is reported in Fig. 7. The first peak in the chromatogram corresponds to glucose, the second peak to maltose, etc. The number of each peak, which corresponds to the number of glucose residues in the linear maltooligosaccharide, was confirmed by adding authentic standard of maltooligosaccharides of known degree of polymerization. Maltooligosaccharides of up to 13 glucose residues were eluted during the gradient development, whereas the homologues of greater than 13 glucose residues eluted at the end of the gradient during the following isocratic step. A plot of the adjusted elution volume versus the number of glucose residues in the maltooligosaccharide oligomers is reported in Fig. 8.

4. Conclusions

The results of this study have demonstrated that the synthesized polystyrene-based quaternary amine stationary phase is a highly selective, alkaline-resistant sorbent for high-pH AEC of oligo- and polysaccharides. Isocratic elution with

Table 1
Structures and retention times of neutral di- and trisaccharides by HPAEC–PAD

Trivial name	Structure[a]	Retention time (min)
α,α-Trehalose	α-D-Glc*p*-(1↔1)-α-D-Glc*p*	3.04
Sucrose	α-D-Glc*p*-(1↔2)-β-D-Fru*f*	3.41
Melibiose	α-D-Gal*p*-(1→6)-D-Glc	4.14
Lactose	β-D-Gal*p*-(1→4)-D-Glc	4.49
Lactulose	β-D-Gal*p*-(1→4)-Fru*f*	4.52
Xylobiose	β-D-Xyl*p*-(1→4)-D-Xyl	4.55
Isomaltose	α-D-Glc*p*-(1→6)-D-Glc	4.71
Gentiobiose	β-D-Glc*p*-(1→6)-D-Glc	5.19
Palatinose	α-D-Glc*p*-(1→6)-D-Fru*f*	5.95
Turanose	α-D-Glc*p*-(1→3)-D-Fru	6.55
Nigerose	α-D-Glc*p*-(1→3)-D-Glc	7.01
Maltose	α-D-Glc*p*-(1→4)-D-Glc	7.74
Melezitose	α-D-Glc*p*-(1→3)-β-D-Fru*f*-(2↔1)-α-D-Glc*p*	4.03
Raffinose	α-D-Gal*p*-(1→6)-α-D-Glc*p*-(1↔2)-β-D-Fru*f*	4.13
Isomaltotriose	α-D-Glc*p*-(1→6)-α-D-Glc*p*-(1→6)-D-Glc	5.67
Maltotriose	α-D-Glc*p*-(1→4)-α-D-Glc*p*-(1→4)-D-Glc	19.78

Isocratic elution with 6 m*M* sodium hydroxide solution at a flow-rate of 0.5 ml/min; temperature 25°C.
[a] Abbreviations as recommended by the International Union of Pure and Applied Chemistry (IUPAC) and the International Union of Biochemistry (IUP) as reported in ref. [25] .

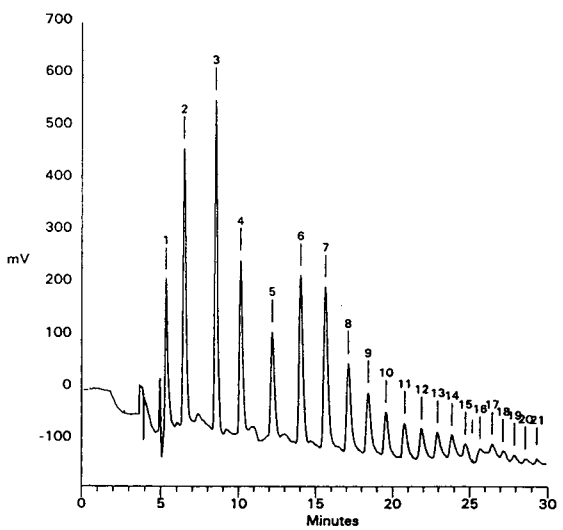

Fig. 7. Separation of linear maltooligosaccharide oligomers of up to 21 glucose residues. Chromatographic conditions as in Fig. 3, except 20 min linear gradient from 0 to 0.2 *M* sodium acetate in 50 m*M* sodium hydroxide, followed by 10 min isocratic elution with the mobile phase containing 0.2 *M* sodium acetate. Peak numbers indicate the number of glucose residues in the separated maltooligomers.

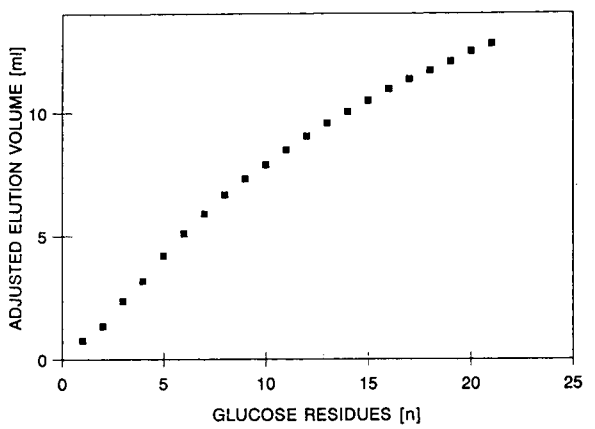

Fig. 8. Dependence of adjusted elution volume on the number of glucose residues in the homologous maltooligosaccharides. Chromatographic conditions as in Fig. 7.

mobile phases containing sodium hydroxide at low concentration has been found to be satisfactory for resolution of isomeric disaccharides, whereas oligo- and polysaccharides are selectively eluted by increasing the sodium acetate concentration during the analysis. Moreover, the use of a short column enables a considerable saving

in time, eluent consumption and instrument usage, which can be advantageous in routine analysis process monitoring and method development.

Acknowledgements

The contributions of Miss Anette Holbek and Miss Charlotte Anker to some of the experiments is gratefully acknowledged. Part of this work was supported by a grant from the Austrian National Bank (No. 4539).

References

[1] Y.C. Lee, *Anal. Biochem.*, 189 (1990) 151.
[2] W.R. LaCourse, *Analusis*, 21 (1993) 181.
[3] M.R. Hardy, R.R. Townsend and Y.C. Lee, *Anal. Biochem.*, 170 (1988) 54.
[4] K. Koizumi, Y. Kubota, T. Tanimoto and Y. Okada, *J. Chromatogr.*, 454 (1988) 303.
[5] D.A. Martens and W.T. Frankenberger, Jr., *Chromatographia*, 30 (1990) 651.
[6] J. van Riel and C. Olieman, *Carbohydr. Res.*, 215 (1991) 39.
[7] T. Hayase, M. Sheykhanazari, V.P. Bhavanandan, A.V. Savage and Y.C. Lee, *Anal. Biochem.*, 211 (1993) 72.
[8] A.T. Hotchkiss and K.B. Hicks, *Carbohydr. Res.*, 247 (1993) 1.
[9] R.D. Rocklin and C.A. Pohl, *J. Liq. Chromatogr.*, 6 (1983) 1577.
[10] J.D. Olechno, S.R. Carter, W.T. Edwards and D.G. Gillen, *Am. Biotechnol. Lab.*, 5 (1987) 38.
[11] *Technical Note 20*, Dionex, Sunnyvale, CA, March 1989.
[12] R.E. Majors, *LC·GC Int.*, 6 (1993) 196.
[13] D.P. Lee, *J. Chromatogr. Sci.*, 22 (1984) 327.
[14] D.P. Lee and M.T. Bunker, *J. Chromatogr. Sci.*, 27 (1989) 496.
[15] K. Mopper, C.A. Shultz, L. Chevolot, C. Germain, R. Revuelta and R. Dowson, *Environ. Sci. Technol.*, 26 (1992) 133.
[16] L.M. Warth, J.S. Fritz and J.O. Naples, *J. Chromatogr.*, 462 (1989) 165.
[17] R.C. Ludwig, *J. Chromatogr.*, 592 (1992) 101.
[18] Y.-F. Maa, S.-C. Lin, Cs. Horváth, U.-C. Yang and D.M. Crothers, *J. Chromatogr.*, 508 (1990) 61.
[19] M.A. Rounds and F.E. Regnier, *J. Chromatogr.*, 443 (1988) 73.
[20] S. Wongyai, J.M. Varga and G.K. Bonn, *J. Chromatogr.*, 536 (1991) 155.
[21] K. Koizumi, Y. Kubota, T. Tanimoto and Y. Okada, *J. Chromatogr.*, 464 (1989) 365.
[22] T.J. Paskach, H.-P. Lieker, P.J. Reilly and K. Thielecke, *Carbohydr. Res.*, 215 (1991) 1.
[23] M.R. Hardy and R.R. Townsend, *Proc. Natl. Acad. Sci. U.S.A.*, 85 (1988) 3289.
[24] K. Koizumi, Y. Kubota, H. Ozaki, K. Shigenobu and M. Fukuba, *J. Chromatogr.*, 595 (1992) 340.
[25] J.F. Kennedy and C.A. White, *Bioactive Carbohydrates In Chemistry, Biochemistry and Biology*, Ellis Horwood, Chichester, 1983, pp. 15–42.

ELSEVIER

Journal of Chromatography A, 685 (1994) 221–227

JOURNAL OF CHROMATOGRAPHY A

Calibration of gel-permeation columns in the high-molecular-mass range: Fixed human thrombocytes for the estimation of interstitial volume and the haemocyanin of the Vineyard snail *Helix pomatia* as a molecular mass calibration substance

W.K.R. Barnikol*, H. Pötzschke

Institut für Physiologie und Pathophysiologie, Johannes Gutenberg-Universität, 55099 Mainz, Germany

First received 4 May 1994; revised manuscript received 20 July 1994

Abstract

Human thrombocytes, fixed with formaldehyde, are shown to be a universal indicator of the interstitial volume in gel-permeation chromatography (size-exclusion chromatography) for gels of all molecular mass separation ranges. The fixed thrombocytes are simple to prepare and to handle.

Furthermore, native or intramolecularly cross-linked haemocyanin of the Roman snail *Helix pomatia* is shown to be well suited as a molecular mass calibration substance. We propose $8.8 \cdot 10^6$ as its molecular mass for calibration. This haemocyanin can therefore be added to the list of globular protein molecular mass calibration substances in the range of very high molecular masses.

1. Introduction

The aim of our research is the development of a new kind of an artificial oxygen transporter based on polymerized haemoglobins. Preliminary measurements with gel-permeation chromatography (GPC) have shown soluble hyperpolymeric haemoglobins with broad distributions of molecular masses which are partially greater than $6 \cdot 10^6$ [1–4]. Two problems arise in the measurement of values and distributions of those molecular masses with GPC: firstly, suitable high-molecular-mass calibration substances are needed, and secondly, for a gel-specific calibration, valid for all lengths of columns and qualities of packing, a simple assessment of the interstitial volume (V_0) is necessary. Suitable gels are available, e.g. Sephacryl S-500 HR, Sephacryl S-1000 SF and Sepharose CL-2B from Pharmacia (Freiburg, Germany).

One phenomenon of GPC, when different substances of the same class are used, is that there is a linear relationship between a distribution coefficient, e.g. the volume fraction (FV), and the logarithm of the molecular mass (log M) of the substance. FV is calculated as $(V_e - V_0)/(V_t - V_0)$, where V_e is the elution volume and V_t the total mobile phase volume. The latter is easily assessed by using small molecules, in this case vitamin B_{12}. The ratio V_t/V_T of vitamin B_{12}

* Corresponding author.

0021-9673/94/$07.00
SSDI 0021-9673(94)00690-3

is 0.97 (with Sepharyl S-500 HR), where V_T is the total (geometrical) volume of the column.

However, a reliable, practical and sufficiently accurate measurement of V_0 of a column, filled with the gels as mentioned above, is a problem. A substance is needed whose molecules are, at least partially, greater than the greatest pores of the separation gel, thus allowing the determination of the absolute exclusion limit of the gel. Synthetic polymers with broad molecular mass distribution, for example Blue Dextran 2000 with a mean molecular mass of $2 \cdot 10^6$, are often used. Applying this substance to gels with a separation range for medium molecular masses results in a definite exclusion maximum, but with gels having separation ranges of high molecular masses, Blue Dextran 2000 is not suitable for indication of the interstitial volume.

Manufacturers of these gels do not offer suitable substances for measurement of the interstitial volume, but instead recommend killed bacteria or viruses, which are not readily available to all investigators. Calculation of the interstitial volume as a fraction of the total column volume, as also recommended for GPC in the high-molecular-mass separation range, is insufficient for an accurate determination of molecular masses under the actual conditions of chromatography, e.g. quality of filling of the column, type of eluent, flow-rate, temperature, dimensions of the column, kind of specimen, etc.

Therefore, we here describe a method for determination of the interstitial volume using fixed human thrombocytes, which can readily be prepared in every biomedical laboratory at any time.

Ideal molecular mass calibration substances should be of uniform molecular mass and similar in shape and molecular density as compared to the substances to be analyzed. For our purpose we use native proteins, which should be of very high molecular mass. Uniform "giant" proteins do exist, for example the erythrocruorin of the earth-worm *Lumbricus terrestris*. This erythrocruorin is suitable as a molecular mass calibration substance [5], but its molecular mass is "only" $3.34 \cdot 10^6$. Therefore, the use of the haemocyanin of the snail *Helix pomatia* (Roman snail) as a molecular mass calibration substance in GPC is also described. Its molecular mass is much higher, with light-scattering and sedimentation measurements yielding $7.55 \pm 0.5 \cdot 10^6$ [6] and $9 \cdot 10^6$ [7], respectively.

2. Materials and methods

2.1. Production of fixed human thrombocytes

Venous blood is taken from a cubital vein using a plastic syringe, previously flushed with a heparin solution (5000 IU/ml). The heparinized blood is centrifuged in 10-ml polycarbonate tubes for 5 min with a relative centrifugal acceleration of 500 *g*. The supernatant is the so-called platelet-rich plasma (PRP). In a polyethylene reaction vessel, 150 μl of 37% formaldehyde solution are added to 1 ml of PRP at room temperature and mixed, the mixture is then allowed to react for 24 h. To prevent formation of gels, the suspension is diluted to one third after this time, preferentially with the elution medium used: the protein concentration is then approximately 2 g/dl.

2.2. Preparation of haemocyanin

The shell of the snail is opened by filing a hole on the right side of the shell at the beginning of the second winding — above the marginal lung vein. The aperture is widened by carefully breaking off the edges of the hole with a pair of tweezers. The visible vein is then opened with a pointed pair of scissors or a scalpel, the opalescent haemolymph flows out and can be collected into a small tube. Pressing back the body of the snail into its shell with a finger through the natural aperture enhances the yield considerably: up to 2 ml of the haemolymph, containing 3 g/dl haemocyanin [8], may be obtained. Alternatively, although with lower yield, the haemolymph may be aspirated from the marginal vein using a cannula. Normally, the snails survive this procedure. Before use for calibration, the haemolymph is diluted to one third, preferably

with the eluent, and filtered through a 0.45-μm filter.

2.3. Intramolecular cross-linking of haemocyanin

A 3-μmol amount of divinyl sulfone (Sigma, Deisenhofen, Germany; 30 μl of a freshly prepared 0.1 mol/l solution in electrolyte BIKU, see below) are added to 1 ml of the diluted haemocyanin solution (ca. 1% in concentration) or to 300 μl of the original haemolymph. After 24 h at room temperature, 60 μmol lysine (60 μl of a 1 mol/l solution in electrolyte BIKU) are added to the mixture and the whole solution is allowed to react for another 24 h.

2.4. Chromatography

The columns used were 1 cm in diameter and about 80 cm in length. The flow-rate of the aqueous eluent was 5.25 ml/h and detection was carried out in flow-through cuvettes with a dead volume of about 50 μl and an optical pathlength of 1 cm. Haemoglobin and erythrocruorin were detected at a wavelength of 425 nm, all other proteins and calibration substances at 275 nm. Chromatographic gels were Sepharose CL-2B, Sephacryl S-400 HR, Sephacryl S-500 HR and Sephacryl S-1000 SF, all purchased from Pharmacia (Freiburg, Germany). Eluents were isosmotic (with plasma) aqueous electrolytes compounded as follows: (1) BIKU: 125 m*M* NaCl–4.5 m*M* KCl–20 m*M* $NaHCO_3$, pH 8.5; (2) HENA: 144 m*M* NaCl–10 m*M* 4-(2-hydroxyethyl)-1-piperazineethanesulphonic acid (HEPES buffer), pH 7.4; and (3) Helix-Ringer: 63 m*M* NaCl–4.2 m*M* KCl–13.2 m*M* $MgCl_2$–10.3 m*M* $CaCl_2$–10 m*M* Tris buffer, pH 7.5. All three contained 0.2 g/dl NaN_3.

Volume fractions (FV) were calculated as mentioned above. The interstitial volume (V_0) was determined with Blue Dextran 2000 (Pharmacia) or with fixed human thrombocytes, and the total mobile phase volume (V_t) with vitamin B_{12} (Sigma, Deisenhofen, Germany). Calibration proteins and their molecular masses were: ribonuclease A 13 700, haemoglobin 64 500, bovine serum albumin 67 000, alcohol dehydrogenase 141 000, ferritine 440 000, thyroglobulin 669 000 (all from Pharmacia), and *Lumbricus terrestris*-erythrocruorine $3.34 \cdot 10^6$.

3. Results

3.1. Measurements of V_0

Fig. 1A and B show original chromatograms of determinations of the interstitial volume using the same column, filled with Sephacryl S-400 HR. Determinations were carried out with Blue Dextran 2000 (Fig. 1A) and with fixed PRP (fPRP) as the indicator (Fig. 1B) for comparison. The interstitial volumes, determined from these chromatographic runs, were 31.04 and 30.59 ml, respectively.

Fig. 1C and D show analogous original chromatograms using Sephacryl S-500 HR gel. It is evident that Blue Dextran 2000 is not sufficient to indicate the interstitial volume (Fig. 1C), whereas the suspension of fixed thrombocytes is (Fig. 1D). Finally, Fig. 1E and F show analogous results on a column filled with Sephacryl S-1000 SF; the interstitial volume is clearly indicated by the fixed thrombocytes (Fig. 1F), but not by Blue Dextran 2000 (Fig. 1E).

The values of the interstitial volume, determined with both indicators on Sephacryl S-400 HR, did not differ significantly. Corresponding values of the other gels are in the same range. The standard errors are small and, hence, relative standard deviations are also small, lying between 1 and 3%. Table 1 summarizes the results for all gels used.

3.2. Haemocyanin as calibration substance

The haemocyanin of the snail *Helix pomatia* was eluted on all gels used without any sign of dissociation into subunits, always with Helix-Ringer as eluent, and for comparison also with HENA on Sephacryl S-400 HR. Fig. 2 shows a typical original chromatogram with Sephacryl S-400 HR. With all gels the FV–log *M* functions were measurable, using the mentioned calibra-

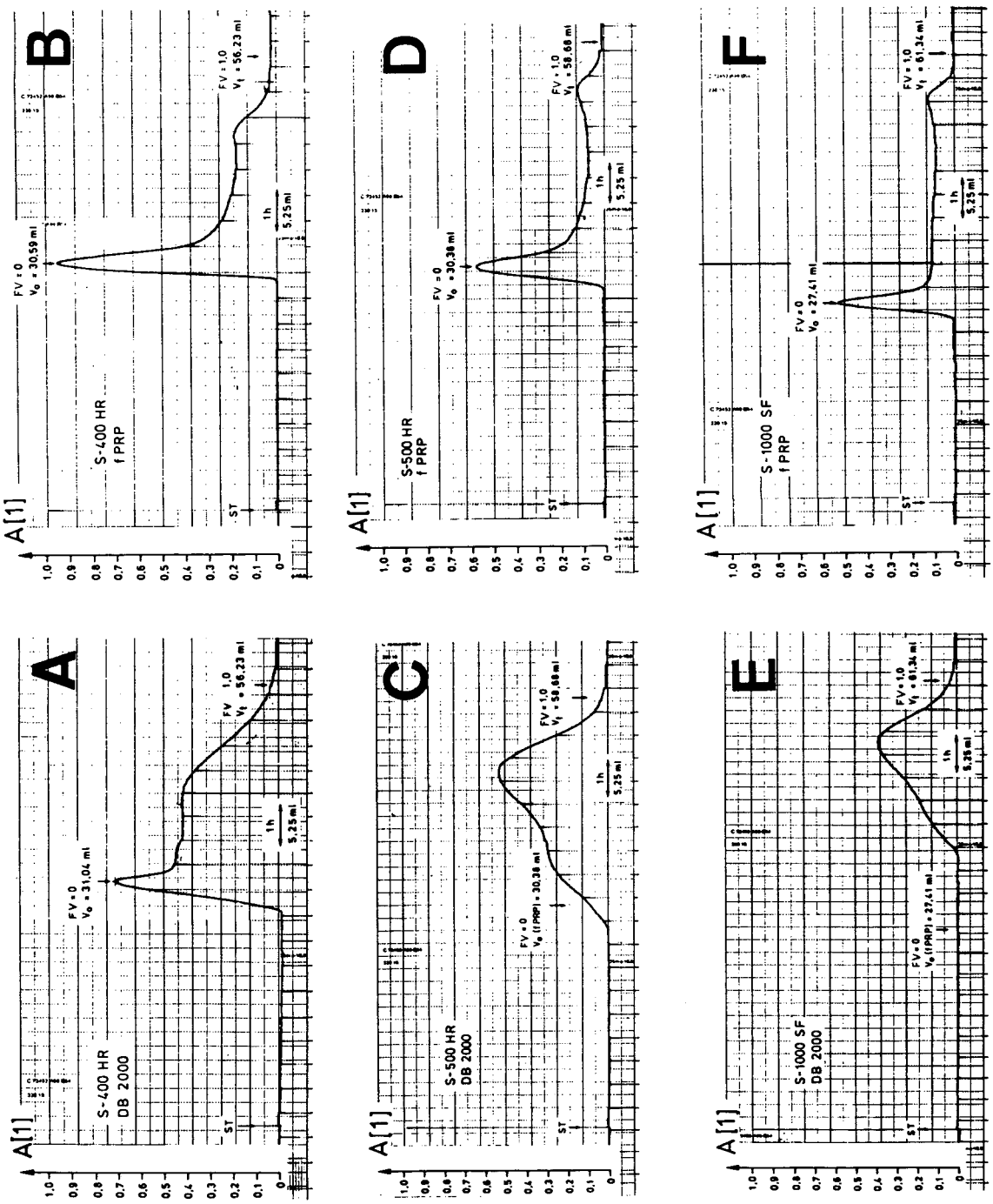

Fig. 1. Examples of original gel-permeation chromatograms of Blue Dextran 2000 (DB 2000: A, C and E) and fixed human thrombocytes (fPRP: B, D and F) for the indication of V_0 on Sephacryl gels S-400 HR (A and B), S-500 HR (C and D) and S-1000 SF (E and F). Eluent HENA; ST = start; A = absorbance.

Table 1
Values for interstitial volume (V_0) of columns packed with different gels, measured with Blue Dextran 2000 (DB 2000) and fixed human thrombocytes (fPRP)

GPC-gel	S-400 HR		S-500 HR	S-1000 SF
V_0 indicator	DB 2000	fPRP	fPRP	fPRP
V_0 (ml)	31.044	30.586	30.019	28.587
	30.815	30.356	29.894	27.476
	30.806	29.255	30.837	28.014
	30.753	29.308	30.380	27.956
	29.156	30.296		27.081
				28.330
$\bar{V}_0$ (ml)	30.52	29.96	30.28	27.91
$s_{\bar{V}_0}$ (ml)	0.77	0.63	0.42	0.56
$s_{\bar{V}_0}/\bar{V}_0$	0.03	0.02	0.01	0.02

$\bar{V}_0$ = Arithmetic average; $s_{\bar{V}_0}$ = standard deviation; $s_{\bar{V}_0}/\bar{V}_0$ = relative standard deviation.

tion proteins together with haemocyanin; Fig. 3 shows the results. Within the error of measurement, the functions are approximately linear, and all corresponding correlation coefficients are greater than 0.992. The molecular mass of haemocyanin ($8.3 \cdot 10^6$) used for these calculations, was taken as the mean from light-scattering measurements ($7.55 \cdot 10^6$ [6]) and from sedimentation measurements ($9 \cdot 10^6$ [7]).

When using BIKU (pH 8.5) as the eluent on Sephacryl S-400 HR, the chromatograms of the haemocyanin are analogous to those of mixtures of proteins of lower hydrodynamic volumes. The mean elution volumes correspond to a molecular mass of about $1.5 \cdot 10^6$. This may be explained by the well known dissociation of the haemocyanin into subunits in solutions with pH values different from the physiological one. Such subunits are still complexes of the smallest subunits [9]. In contrast, haemocyanin treated with divinyl sulfone has the same elution volume in all eluents used.

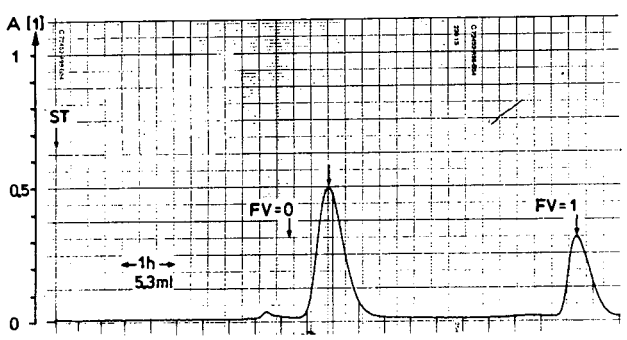

Fig. 2. Gel-permeation chromatogram of haemocyanin from the snail *Helix pomatia* on Sephacryl S-400 HR gel. Eluent Helix-Ringer; ST = start; A = absorbance.

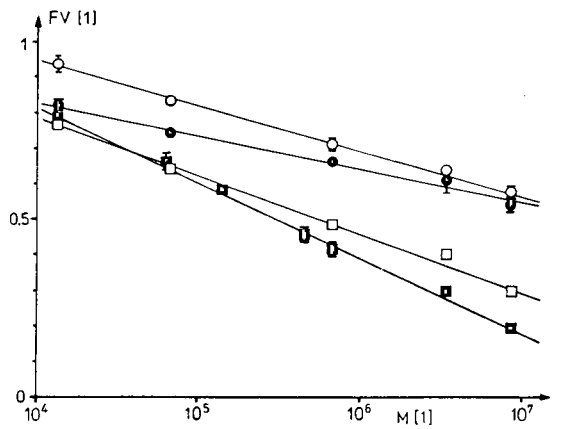

Fig. 3. FV–log M calibration curves of native proteins on different GPC gels, and their coefficients of correlation r. ○ = Sepharose CL-2B, $r = -0.998$; ● = Sephacryl S-1000 SF, $r = -0.993$; □ = Sephacryl S-500 HR, $r = -0.997$; ■ = Sephacryl S-400 HR, $r = -0.999$. Eluent was HENA for Sephacryl S-400 HR, for all other gel types it was BIKU for *Lumbricus*-erythrocruorin, Helix-Ringer for *Helix*-haemocyanin, and HENA for the other proteins. The lengths of the bars indicate the standard deviations ($n = 3$–7).

4. Discussion

The results presented here show that fixed human thrombocytes are suitable for determination of the interstitial volume. Dilution of the thrombocytes after fixation is recommended to avoid gelatinization, which could result in column obstruction. In the event of gelatinization, occurring even at this recommended dilution, repeated preparation with greater dilution is advised. Normally a suspension of fixed thrombocytes is stable for months. But following prolonged storage, the suspension should be prefiltered, for example through a 0.8-μm filter, in order to remove invisible minute gel particles, which may have formed.

The Sephacryl gels investigated here are similar in their chemical structure and gel particle size. They differ only in porosity, and thus in their range of separation of molecular volumes. Therefore it can be assumed that interstitial volumes, determined with fixed thrombocytes on Sephacryl S-500 HR and on Sephacryl S-1000 SF are accurate (accuracy of the mean) since with Sephacryl S-400 HR the same values are obtained (within the limits of measurement error), as determined with Blue Dextran 2000 and with fixed thrombocytes.

A determination of the interstitial volume with fixed thrombocytes is also possible on gels with different chemical structure, for example on Sepharose CL-2B. Five measurements of V_0 resulted in a mean of 26.03 ml and a standard deviation of 0.18 ml. On this gel, Blue Dextran 2000 is again not sufficient for the indication of V_0.

Fixed human thrombocytes are probably also suitable as V_0 indicators for other gel types, and fixed thrombocytes from animals may also be suitable for this purpose.

With one column filling many determinations of the interstitial volume and analytical runs are possible alternately, always with reproducible values. This shows that there are no specific interactions between fixed thrombocytes and the gels, and, especially, gel columns do not become obstructed.

Haemocyanin from the snail *Helix pomatia* is eluted in Helix-Ringer and in HENA with no sign of dissociation; chromatograms resemble those of molecular homogeneous substances. Under these conditions there seems to be no dissociation into subunits, which has been described for different degrees related to ionic strength, acidity and concentration of Ca^{2+} [9]. Molecular masses determined under the conditions described here are always maximal values, and therefore probably correspond to the undissociated molecule.

To our knowledge, Largier and Polson [10] are the only investigators who have used a complete haemocyanin as a calibration substance in GPC with an aqueous eluent. It was the haemocyanin of a maritime snail, *Burnupena cincta*, with a molecular mass of $6.6 \cdot 10^6$. This snail is only found in the sea around South Africa and thus its haemocyanin is not easy to obtain. In addition, the molecular mass of this haemocyanin is relatively low.

Calibration functions determined using the haemocyanin of *Helix pomatia* are almost linear, with corresponding correlation coefficients close to one. However, as Fig. 3 also shows, in all gels except Sepharose gel, the volume fractions for the earth-worms erythrocruorin lie above the calibration line; those for the haemocyanin lie below it. Because GPC separates molecules according to their hydrodynamic volumes, it follows, that the molecular volume of the erythrocruorin is "too small" and that of the haemocyanin is "too large". A possible explanation is that the molecular density of the erythrocruorin is higher than that of the haemocyanin. In accordance with this, the molecular mass of the haemocyanin, as assessed by measured volume fractions and the mean (linear) calibration line of the other calibration points, is higher than that measured by sedimentation and with light scattering. With the Sephacryl gels S-400 HR, S-500 HR and S-1000 SF, and with Sepharose CL-2B we calculated the molecular masses to be $9.8 \cdot 10^6$, $10 \cdot 10^6$, $12 \cdot 10^6$ and $8.3 \cdot 10^6$, respectively. The mean molecular mass of haemocyanin regarding all three methods (sedimentation, light scattering and GPC) is $8.8 \cdot 10^6$. Despite the discussed systematic deviations, which

are within the limit of the measurement error, the linearity of the calibration curves legitimizes the use of the haemocyanin of *Helix pomatia*, which is easily accessible and easy to handle, as a calibration protein in GPC. It can therefore be added to the list of calibration proteins in the high-molecular-mass range.

Nevertheless it would be useful to have more values of the molecular mass of this haemocyanin, assessed by light scattering and/or with sedimentation, especially in the ionic medium used in this investigation. We propose to take the above-mentioned value $8.8 \cdot 10^6$ as the molecular mass for calibration, which is the average of all available values.

*Intra*molecular cross-linking of the haemocyanin using divinyl sulfone as described above does not produce detectable *inter*molecular cross-links, in contrast to analogous treatment (addition in the same molar ratio to haemocyanin) with glutaraldehyde, another bifunctional cross-linker for proteins. Its reaction products contain polymers of the haemocyanin or its subunits, which makes the reaction products unsuitable for molecular mass calibrations. The relative amount of divinyl sulfone, as mentioned above, is the minimum necessary for a complete intramolecular stabilization, as evidenced by chromatography.

Some other proteins, catalase, ferritin and thyroglobulin, when treated in an analogous manner with divinyl sulfone (application in the same mass ratio related to the proteins), are also not polymerized (results not shown here).

As an extension of the application of the erythrocruorin from the earth-worm *Lumbricus terrestris* as a calibration substance in GPC [5], erythrocruorins from the near-related earthworms *Lumbricus rubellus* and *Dendrobena veneta* may be used alternatively. These erythrocruorins have the same molecular mass and all of these earth-worms are available from shops specializing in fishing equipment.

Acknowledgement

We thank Beate Krumm for skillful technical assistance and careful evaluation of chromatograms.

References

[1] W.K.R. Barnikol and O. Burkhard, *Adv. Exp. Med. Biol.*, 215 (1987) 129.
[2] W.K.R. Barnikol and O. Burkhard, *Biomater., Artif. Cells, Artif. Organs*, 16 (1988) 639.
[3] W.K.R. Barnikol and O. Burkhard, *Adv. Exp. Med. Biol.*, 248 (1989) 335.
[4] H. Pötzschke and W.K.R. Barnikol, *Biomater., Artif. Cells, Immob. Biotech.*, 20 (1992) 287.
[5] W.K.R. Barnikol, O. Burkhard and H. Pötzschke, *J. Chromatogr.*, 497 (1989) 231.
[6] Th.T. Hershovits and M.W. Russell, *Biochemistry*, 23 (1984) 2812.
[7] E.J. Wood, M.F. Chaplin, C. Gielens, J. De Sadeleer, G. Preaux and R. Lontie, *Comp. Biochem. Physiol.*, 82B (1985) 179.
[8] K. Schlieper, *Praktikum der Zoophysiologie*, Fischer, Stuttgart, 4th ed., 1977, p. 113*ff*.
[9] R.J. Siezen and R. van Driel, *J. Mol. Biol.*, 90 (1974) 91.
[10] J.F. Largier and A. Polson, *Biochim. Biophys. Acta*, 79 (1964) 626.

ELSEVIER

Journal of Chromatography A, 685 (1994) 229–235

JOURNAL OF CHROMATOGRAPHY A

Comparative high-performance liquid chromatographic analyses of cholesterol and its oxidation products using diode-array ultraviolet and laser light-scattering detection

S. Kermasha[a,*], S. Kubow[b], M. Goetghebeur[a]

[a]*Department of Food Science and Agricultural Chemistry, McGill University, 21 111 Lakeshore, Ste. Anne de Bellevue, Québec, H9X 3V9, Canada*

[b]*School of Dietetics and Human Nutrition, McGill University, 21 111 Lakeshore, Ste. Anne de Bellevue, Québec, H9X 3V9, Canada*

First received 13 June 1994; revised manuscript received 29 July 1994

Abstract

Comparative high-performance liquid chromatographic (HPLC) analyses of cholesterol and its oxidization products (COPS) showed that cholesterol, cholestane, 7-ketocholesterol and 7α, 7β-, 20- and 25-hydroxycholesterol were detected by both ultraviolet (UV) and laser light-scattering detection (LLSD). In addition, the use of LLSD allowed the detection of cholestanetriol and α- and β-epoxides. The limits of detection of COPS varied from 0.5 to 25 μg/ml, depending on both the compound and the detector. The HPLC analyses demonstrated a linear correlation between the UV response and concentrations of products in the range 0–500 μg/ml whereas a linear correlationship with LLSD was obtained by plotting logarithmic coordinates in the same range.

1. Introduction

Cholesterol oxidation products (COPS) are found in many common foods and have been shown to be atherogenic, cytotoxic, mutagenic and possibly carcinogenic [1–3]. Because of these properties, concern has been expressed that substantial amounts may form in cholesterol-containing foods during storage and processing [3,4]. Cholesterol α-oxide along with the β-isomer have received much attention owing to their possible association with carcinogens, atherogenesis and cholesterol metabolism [5]. Gray et al. [6] have found abnormally high concentrations of cholesterol α-oxide in the sera of hypercholesterolaemic and high blood pressure pateints but none in those of normal healthy persons. Addis et al. [7] suggested that the quantification of COPS in human plasma lipoproteins could be used as a tool for studying their potential role in heart disease.

The increasing interest in the biological role of COPS has led to the development of chromatographic methods for their identification and determination [8]. Park and Addis [9] reported the use of capillary gas chromatography (GC) for the determination of COPS in foods. Combined GC and mass spectrometry (MS) has also

* Corresponding author.

0021-9673/94/$07.00
SSDI 0021-9673(94)00718-7

been used for the identification of COPS [10–13]. MS, although being considered the best detection method available, requires expensive instrumentation and is not routinely available to most investigators [4].

The development of high-performance liquid chromatography (HPLC) for the determination of COPS in foods [12] and plasma from rats [4] has also been reported. Tsai and Hudson [14] demonstrated that HPLC could resolve a variety of oxygenated derivatives of cholesterol with polar groups on various carbon atoms of the isoprenoid side-chain. The method proposed by Csiky [15] did not give a good baseline resolution of 25-hydroxycholesterol, as it appeared as a shoulder peak on a large UV absorption peak.

An important issue in the determination of cholesterol oxides concerns the autoxidation of cholesterol [16]. Several studies have appeared in which the extent of cholesterol oxide artifact during analysis was determined by HPLC with radioactivity detection [16] and GC–MS and stable isotope techniques [17].

Stolyhwo et al. [18] reported that laser light-scattering detection (LLSD) is extremely unresponsive to changes in the physical environment that result in the absence of background and baseline drift, even with a gradient elution system. Although LLSD has been reported as a reliable tool in the HPLC of triacylglycerols [19], little is known about its application for the detection of cholesterol and its COPS. As far as the authors are aware, there is no information regarding the use of LLSD in the HPLC of cholesterol and COPS. The objective of this research was to develop a rapid and accurate comparative method for the characterization and determination of cholesterol oxidation products using ultraviolet (UV) and LLS detection.

2. Experimental

2.1. Materials

Standards of cholesterol and its derivatives were purchased from Sigma (St. Louis, MO, USA) and Research Plus (Bayonne, NJ, USA). These standards included cholesta-3,5-dien-7-one (cholestane), 3β-hydrocholest-5-en-7-one (7-ketocholesterol), cholesta-5-ene-3β,7α-diol (7α-hydroxycholesterol), cholesta-5-ene-3β,7β-diol (7β-hydroxycholesterol), cholest-5-ene-3β,20-diol (20-hydroxycholesterol), cholest-5-ene-3β,25-diol (25-hydroxycholesterol), 5,6α-eopxy-5α-cholestan-3β-ol (α-epoxide), 5,6β-epoxy-5α-cholestan-3β-ol (β-epoxide) and 5α-cholestane-3β,5α,6β-triol (cholestanetriol). Chloroform, 2-propanol and hexane (Omnisolv grade) were BDH products (CM Industries, Hawthorne, NY, USA). A mixture was prepared to contain 500 μg/ml of cholestane, cholesterol, 20-hydroxycholesterol, 25-hydroxycholestero, α-epoxide, β-epoxide, 7-ketocholesterol, 7α-hydroxycholesterol and cholestanetriol and also 250 μg/ml of 20-hydroxycholesterol, β-epoxide and 7β-hydroxycholesterol.

2.2. Apparatus

The mixture of cholesterol and oxidation products (COPS) was separated on a μ-Porasil (10 μm) HPLC column (300 × 3.9 mm I.D.) obtained from Waters–Millipore (Bedford, MA, USA). The HPLC system used for the analyses was Beckman Gold (Beckman Instruments, San Ramon, CA, USA) using computerized integration and data handling (Beckman Model 126). The system was equipped with two detectors. The UV absorbance was monitored with a Beckman diode-array UV detector (Model 168) whereas the light scattering was determined with a laser light-scattering detector (Varex, Burtonsville, MD, USA). A Beckman analog interface (Model 406) was used to transfer data from the mass detector to the Gold system. Injection was achieved through a Model 9095 automatic injector (Varian, Walnut Creek, CA, USA) fitted with a 20-μl loop.

2.3. HPLC of COPS using UV detection

HPLC of COPS with UV detection were performed according to a modification of the procedure described by Csallany et al. [20]. Elution was carried out with a gradient elution

system, using a mixture of hexane and 2-propanol containing from 99.6% to 79.3% of hexane at a flow-rate of 1 ml/min for 56 min. UV detection was performed simultaneously at two different wavelengths, 206 and 233 nm.

2.4. HPLC of COPS using laser light-scattering detection

The HPLC separation of COPS was performed with a mixture of hexane and 2-propanol, using a linear decreasing gradient from 99.6% to 79.3% of hexane, at a flow-rate of 1 ml/min for 56 min. Detection was performed at a temperature setting of 120°C and a stream of inert gas (N_2) at a flow-rate of 40 ml/min and a sensitivity range of 1.

3. Results and discussion

3.1. Optimization of HPLC analyses

UV maximum absorbance analyses of standard COPS compounds were performed. The results (data not shown) indicated that 7α-and 7β-hydroxycholesterol exhibited one specific maximum absorbance (λ_{max}) at 207 and 208 nm, respectively, whereas 7-ketohydroxycholesterol demonstrated two specific λ_{max} at 207 and 234 nm. Csallany et al. [20] reported that the λ_{max} for 7-ketohydroxycholesterol is 202 nm whereas that of cholesterol, 7α- and 7β-hydroxycholesterol and 25-hydroxycholesterol is 233 nm. Hence, to achieve the optimum detection of cholesterol and COPS, the HPLC–UV analyses were performed using two different wavelengths, 206 and 233 nm.

Preliminary work on the optimization and selection of the most appropriate temperature and N_2 flow-rate for setting the LLS detector indicated that both high sensitivity and a stable baseline were obtained for COPS at 120°C with a flow-rate of inert gas of 30 ml/min. The optimization of the conditions for HPLC–LLSD demonstrated that a gradient elution solvent system from 99.6% to 79.3% of hexane at a flow-rate of 1 ml/min for 56 min provided a chromatogram with well separated and highly resolved peaks. The available literature on LLSD [18,19,21] suggested that, in addition to instrumental factors, optimization of factors such as temperature and gas flow-rate are also important for the sensitivity.

3.2. UV and LLS detection of standard cholesterol and COPS

Fig. 1 shows the chromatograms for the HPLC of cholesterol and COPS using (A and B) UV detection and (C) LLSD. The results demon-

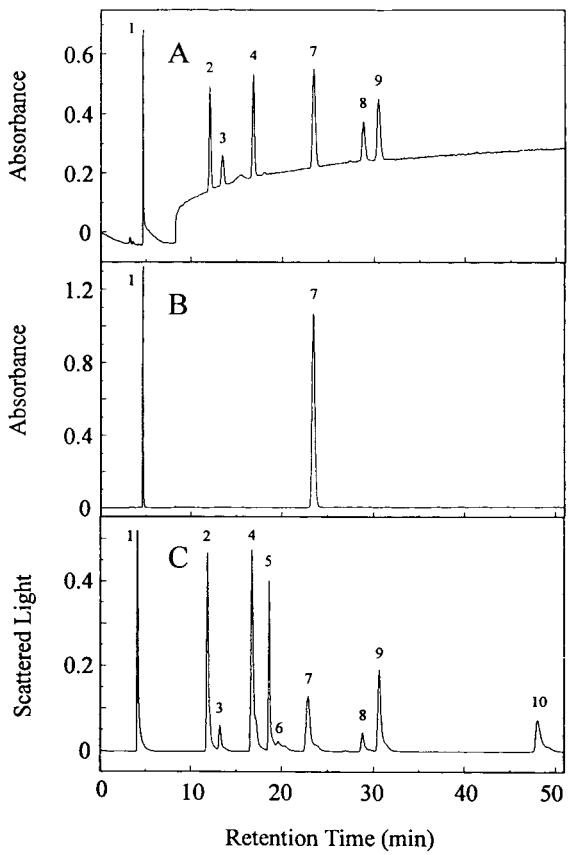

Fig. 1. HPLC of cholesterol and its oxidization products on a (μ-Porasil (10-μm) column (300 × 3.9 mm I.D.) with (A,B) diode-array UV detection at (A) 206 nm and (B) 233 nm and (C) laser light-scattering detection. Peaks: 1 = cholestane; 2 = cholesterol; 3 = 20-hydroxycholesterol; 4 = 25-hydroxycholesterol; 5 = α-epoxide; 6 = β-epoxide; 7 = 7-ketocholesterol; 8 = 7β-hydroxycholesterol; 9 = 7α-hydroxycholesterol; 10 = cholestanetriol.

strate a much more stable and better baseline with LLSD than that obtained with UV detection. In addition, LLSD provided a higher resolution of COPS than was achieved with UV detection. The results also show that cholesterol, cholestane, 7-ketocholesterol, 7α- and 7β-hydroxycholesterol and 20- and 25-hydroxycholesterol were detected by both UV and LLSD methods, whereas cholestanetriol and α- and β-epoxide were detected only with LLSD. In addition, the use of UV detection at 206 nm allowed an increase in the sensitivity of detection of 7-ketocholesterol.

It has been reported that the use of UV detection in HPLC analyses allowed the determination of cholesterol, 7α- and 7β-hydroxycholesterol, 7-ketocholesterol [9] and 25-hydroxycholesterol [20], whereas the use of refractometric detection also permits the detection of cholestanetriol, α- and β-epoxide and 20-hydroxycholesterol [14]. However, Stolyhwo et al. [18] reported that the LLSD response is more sensitive than that of the refractometer.

3.3. Limits of detection

The minimum detectable concentrations of COPS were calculated on the basis of a signal-to-noise ratio of 3 [20]. The results (Tables 1 and 2) indicate that the limits of detection of cholesterol, cholestane and 7-ketocholesterol (10, 1 and 0.5 μg/ml, respectively) with UV detection were 2.5, 2.5 and 20 times lower than those (25, 2.5 and 10.0 μg/ml, respectively) obtained with LLSD. As the molar absorptivity of 7-ketocholesterol is high [20], its detection by HPLC–UV was the most sensitive. The results (Tables 1 and 2) also show that the limit of detection of 7α-hydroxycholesterol (10.0 μg/ml) with LLSD was 2.5 times lower than that (25 μg/ml) obtained with UV detection. The results also indicate that the limits of detection of 20-hydroxycholesterol (12.5 μg/ml), 25-hydroxycholesterol (10.0 μg/ml) and 7β-hydroxycholesterol (12.5 μg/ml) were the same with both UV and LLS detection. Hence LLSD was the most sensitive for the detection of cholestane, 25-hydroxycholesterol, 7α-hydroxycholesterol, α-epoxide, 7-ketocholesterol and cholestanetriol.

It has been reported that the limit of detection of 25-hydroxycholesterol in serum by HPLC–UV was 10 ng/ml [4], whereas the lowest concentration of this compound in plasma, detected by gas chromatography with flame ionization detection (GC–FID), was 100 ng/ml [7]. The limits of detection of 7α- and 7β-hydroxycholesterol by HPLC–UV were 1.7 and 1.5 μg/ml, respectively, [20] and 50 μg/ml with refractometric detec-

Table 1
Quantitative chromatographic parameters for HPLC of cholesterol and its oxidation products using diode-array UV detection

Compound	Retention time (min)	Detection limit[a] (μg/ml)	Range of linearity[b] (μg/ml)	R^{2} [c]	Precision[d]
Cholesterol	11.7	10.0	10.0–500	0.995	1.8
Cholestane	4.2	1.0	1.0–500	0.994	1.5
20-Hydroxycholesterol	13.2	12.5	12.5–250	0.991	6.5
25-Hydroxycholesterol	16.7	10.0	10.0–500	0.991	3.1
7α-Hydroxycholesterol	30.6	25.0	50.0–500	0.999	1.8
7β-Hydroxycholesterol	28.8	12.5	12.5–500	0.992	5.1
7-Ketocholesterol	22.9	0.5	0.5–500	0.996	1.0

[a] Detection limit is the minimum detectable concentration of COPS calculated on the basis of a signal-to-noise ratio of 3.
[b] Range of linearity is determined by the lower and higher limits of quantification of the calibration graph.
[c] Correlation coefficient (R^2) of the calibration graph, calculated on the basis of triplicate injections of each product.
[d] Precision is the percentage deviation of the mean as obtained by three replicate analyses of the sample; the sample contained 50.0 μg/ml of each compound.

Table 2
Quantitative chromatographic parameters for HPLC of cholesterol and its oxidation products using laser light-scattering detection

Compound	Retention time (min)	Detection limit[a] (μg/ml)	Range of linearity[b] (μg/ml)	R^2 [c]	Precision[d]
Cholesterol	11.7	25.0	25.0–500	0.999	18.2
Cholestane	4.2	2.5	2.5–100	0.991	3.0
20-Hydroxycholesterol	13.2	12.5	12.5–500	0.999	12.1
25-Hydroxycholesterol	16.7	10.0	10.0–500	1.000	8.2
7α-Hydroxycholesterol	30.6	10.0	10.0–1000	0.998	6.6
7β-Hydroxycholesterol	28.8	12.5	12.5–500	0.997	2.9
α-Epoxide	18.4	10.0	10.0–500	0.999	5.0
β-Epoxide	19.4	50.0	50.0–500	0.999	11.7
7-Ketocholesterol	22.9	10.0	10.0–1000	0.997	8.3
Cholestanetriol	47.7	10.0	10.0–1000	0.993	8.6

[a–d] See Table 1.

tion [5]. The lowest concentrations of 7α- and 7β-hydroxycholesterol detected by GC–FID were 1 μg/ml [8] and 0.4 μg/ml [7]. The limit of detection of 7-ketocholesterol was reported to be 0.38 μg/ml using HPLC–UV [20], whereas the lowest concentration detected by GC–FID was 0.9 μg/ml [2]. It has also been reported that α- and β-epoxides and cholestanetriol could be determined only with GC–FID and their lowest concentration reported with 1 μg/ml [8,22]. Pie et al. [23] reported that the lowest concentration of 20-hydroxycholesterol detected by GC–FID was 0.57 μg/ml.

Although α- and β-epoxides and cholestanetriol have been separated by HPLC with refractometric detection [14], the determination of these compounds was not reported. Fig. 1 demonstrates that the HPLC–LLSD method developed here allowed the quantification of α- and β-epoxides and cholestanetriol that had previously only been determined using GC–FID [8,22,24]. However, GC–FID may be considered as a destructive method as it requires the derivatization of COPS and heating of the sample, whereas HPLC can be regarded as a non-destructive and rapid method [25]. Hence the development of HPLC–LLSD could provide a reliable method for the determination, under mild conditions, of COPS, particularly α-and β-epoxides and cholestanetriol. However, special attempts to suppress autoxidation of cholesterol should be included in the analyses of foodstuffs and biological samples [16,17].

3.4. Linearity and precision of UV and LLSD responses

In order to test the applicability of HPLC–UV and –LLSD for the determination of cholesterol and major COPS, each compound was investigated for its linear response. Calibration graphs were constructed for cholesterol and each of the COPS studied in the range 0–1000 μg/ml.

The plots of compound concentration versus peak area obtained in HPLC–UV analyses are shown in Fig. 2. The results (Table 1) show that good linearity was obtained for the calibration graphs for HPLC–UV of 7-ketocholesterol in the range 0.5–500 μg/ml whereas the ranges of linearity were 1–500 μg/ml for cholestane, 10–500 μg/ml for cholesterol and 25-hydroxycholesterol, 12.5–500 μg/ml for 7β-hydroxycholesterol, 12.5–250 μg/ml for 20-hydroxycholesterol and 50–500 μg/ml for 7α-hydroxycholesterol. The correlation coefficients (Table 2) for COPS were between 0.991 and 0.999.

The plots of compound concentration versus peak area obtained in HPLC–LLSD analyses demonstrate a non-linear response. However, a linear correlation with LLSD was obtained by

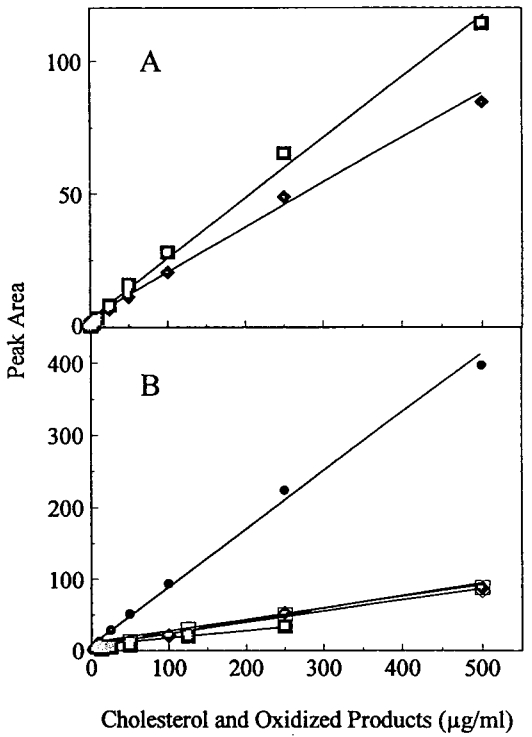

Fig. 2. Calibration graph for HPLC of cholesterol and its oxidization products using diode-array UV detection. (A) ◆ = cholesterol; ○ = cholestane. (B) ◘ = 20-hydroxycholesterol; ◆ = 25-hydroxycholesterol; □ = 7β-hydroxycholesterol; ◇ = 7α-hydroxycholesterol; ○ = ketocholesterol.

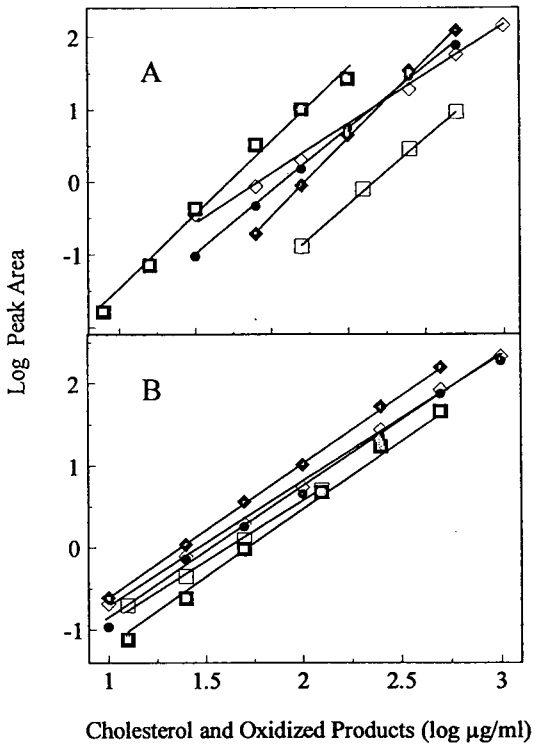

Fig. 3. Calibration graph for HPLC of cholesterol and its oxidization products using laser light-scattering detection. (A) ◆ = cholesterol; ◘ = cholestane; ○ = α-epoxide; □ = β-epoxide; ◇ = cholestanetriol. (B) ◘ = 20-hydroxycholesterol; ◆ = 25-hydroxycholesterol; □ = 7β-hydroxycholesterol; ◇ = 7α-hydroxycholesterol; ○ = 7-ketocholesterol.

plotting log peak area versus log (product concentration) (Fig. 3). The results (Table 2) show that good linearity in logarithmic coordinates was obtained for cholestane in the range of 2.50–100 μg/ml whereas the ranges of linearity were 10–1000 μg/ml for 7α-hydroxycholesterol, 7-ketocholesterol and cholestanetriol, 10–500 μg/ml for 25-hydroxycholesterol and α-epoxide, 12.5–500 μg/ml for 20- and 7β-hydroxycholesterol, 25–500 μg/ml for cholesterol and 50–500 μg/ml for β-epoxide. The correlation coefficients (Table 2) were between 0.991 and 1.000. Stolyhwo et al. [18] reported that a plot of peak area versus sample size for dioctyl phthalate was linear in logarithmic coordinates over a ratio of sample size of 500:1. Similar correlation coefficients have been obtained in analyses of cholesterol and COPS using a GC–FID system equipped with a capillary column [26].

The results (Tables 1 and 2) also indicate that the accuracy (1.0–6.5%) of UV detection of COPS was better than that obtained using LLSD (2.9–18.2%). A comparative study of cholesterol analyses [27] indicated that the relative standard deviations (R.S.D.s) for GC and HPLC–UV analyses were 9 and 8%, respectively. Pie et al. [23] reported that the R.S.D.s of GC analyses of COPS varied from 0.4 to 15%. The results obtained here (Tables 1 and 2) demonstrate that

the determination of cholesterol and COPS by HPLC with UV and LLS detection is very reliable.

4. Conclusions

The results suggest that the use of LLSD in the HPLC of cholesterol and COPS could provide a reliable tool for the determination of these compounds. In addition, the HPLC-LLSD analyses allowed the detection of α- and β-epoxides and cholestane–triol under mild conditions, which previously could only be achieved by GC–FID. The present study demonstrated an excellent analytical resolution among cholesterol and nine commonly encountered oxidization of these toxicologically important compounds. The method should be useful in research dealing with cholesterol and COPS in foodstuffs and biological samples.

Acknowledgement

The authors thank Mrs. A. Reid for technical assistance.

References

[1] P.B. Addis, *Food Chem. Toxicol.*, 24 (1986) 1021.
[2] P.B. Addis and S.W. Park, in R.A. Scanlon and S.L. Taylor (Editors), *Food Toxicology: a Perspective on the Relative Risks (Proceedings, 1988 IFT–IUFOST Basic Symposium)*, Marcel Dekker, New York, 1989, Ch. 11.
[3] S. Kubow, *Free Rad. Biol. Med.*, 12 (1992) 63.
[4] I.L. Kou and R.P. Holmes, *J. Chromatogr.*, 330 (1985) 339.
[5] L.S. Tsai and C.A. Hudson, *J. Food Sci.*, 50 (1985) 229.
[6] M.F. Gray, T.D.V. Lawrie and C.J.W. Brooks, *Lipids*, 6 (1971) 836.
[7] P.B. Addis, H.A. Emmanuel, S.D. Bergmann and J.H. Zavoral, *Free Rad. Biol. Med.*, 7 (1989) 179.
[8] W.B. Zhang and P.B. Addis, *J. Food Sci.*, 55 (1990) 1673–1675.
[9] S.W. Park and P.B. Addis, *J. Food Sci.*, 50 (1985) 1437.
[10] N.B. Javitt, E. Kok, S. Burstein, B. Cohen and J. Kutscher, *J. Biol. Chem.*, 256 (1981) 12644.
[11] L.L. Smith, J.L. Teng, Y.Y. Lin, P.K. Seitz and L. McGehee, *J. Steroid Biochem.*, 14 (1981) 889.
[12] S.W. Park and P.B. Addis, *J. Agric. Food Chem.*, 34 (1986) 653.
[13] S.W. Park and P.B. Addis, *J. Food Sci.*, 51 (1986) 1380.
[14] L.S. Tsai and C.A. Hudson, *J. Am. Oil Chem. Soc.*, 57 (1981) 931.
[15] I. Csiky, *J. Chromatogr.*, 241 (1982) 381.
[16] B.A. Wasilchuk, P.W. Le Quesne and P. Vouros, *Anal. Chem.*, 64 (1987) 1077.
[17] K. Kudo, G.T. Emmons, E.W. Casserly, D.P. Via, L.C. Smith, J.S. Pyrek and G.J. Schroepfer, Jr., *J. Lipid Res.*, 30 (1989) 1097.
[18] A. Stolyhwo, H. Colin, A. Martin and G. Guiochon, *J. Chromatogr.*, 288 (1984) 253.
[19] S. Kermasha, S. Kubow, M. Safari and A. Reid, *J. Am. Oil Chem. Soc.*, 70 (1993) 169.
[20] A.S. Csallany, S.E. Kindom, P.B. Addis and J.H. Lee, *Lipids*, 24 (1989) 645.
[21] A. Stolyhwo, H. Colin and G. Guiochon, *J. Chromatogr.*, 265 (1983) 1.
[22] B.D. Sanders, P.B. Addis, S.W. Park and D.E. Smith, *J. Food Protect.*, 52 (1989) 109.
[23] J.E. Pie, K. Spahis and C. Seillan, *J. Agric. Food Chem.*, 38 (1990) 973.
[24] S.W. Park and P.B. Addis, *J. Food Sci.*, 52 (1987) 1500.
[25] E. Heftmann and I.R. Hunter, *J. Chromatogr.*, 165 (1979) 238.
[26] S.W. Park and P.B. Addis, *Anal. Biochem.*, 149 (1985) 275.
[27] F. Cheillan, H. Lafont, E. Termine, Y. Hamann and G. Lesgards, *Lipids*, 24 (1989) 225.

ELSEVIER

Journal of Chromatography A, 685 (1994) 237–241

JOURNAL OF CHROMATOGRAPHY A

Studies of gramicidin S analogues having various ring sizes by reversed-phase high-performance liquid chromatography

Makoto Tamaki[a,*], Sadatoshi Akabori[a], Ichiro Muramatsu[b]

[a]*Department of Chemistry, Faculty of Science, Toho University, Miyama, Funabashi, Chiba 274, Japan*
[b]*Department of Chemistry, College of Science, Rikkyo University, Nishi-ikebukuro, Tokyo 171, Japan*

First received 29 March 1994; revised manuscript received 22 July 1994

Abstract

Many gramicidin S analogues containing six to fourteen amino acid residues were synthesized and their chromatographic behaviour was investigated using reversed-phase high-performance liquid chromatography. Cyclo(-Val-Leu-Orn-Leu-D-Phe-Pro-Val-Orn-Leu-D-Phe-Pro-) gave double peaks in the chromatogram, whereas the other peptides gave a single peak. The influences of the concentration of this peptide, column temperature and flow-rate on the chromatographic separation were examined. The isomeric conformers were separated from each of the double peaks and were in equilibrium with each other at low temperatures. These results suggested that the presence of the additional L-Leu residue preceding the Orn residue gives rise to moderate stabilization of their conformers.

1. Introduction

Gramicidin S (GS) (Fig. 1) [1] is an antibiotic cyclodecapeptide with a rigid β-pleated sheet conformation [2,3]. A characteristic feature of this conformation is the orientation of the side-chains in such a way that the two charged Orn side-chains are situated on one side of the molecule and the four hydrophobic Val and Leu side-chains on the other. (Note: amino acid residues with no prefix are of L-configuration unless stated otherwise. The abbreviations for amino acids and peptides are in accordance with the rules of the IUPAC–IUB Commission of Biochemical Nomenclature.) This arrangement is apparently maintained by a rigid ring structure containing two type II′ β-turns composed of D-Phe–Pro.

In order to investigate the contribution of the ring size to the secondary structure and the antibiotic activity of this antibiotic, we synthesized numerous GS analogues containing six to fourteen amino acid residues (Fig. 1) [4–6]. These GS analogues have the D-Phe–Pro sequence in each molecule. A Leu residue having a hydrophobic side-chain was used to enlarge the ring size. In the high-performance liquid chromatographic (HPLC) studies of these synthetic peptides using a reversed-phase column, we found that one of the GS analogues containing eleven amino acid residues gives double peaks in the chromatogram.

Recently, in studies of the HPLC behaviour of a cyclic dodecapeptide, gratisin (GR), we reported that the analogues having D-X–D-Y–L-Pro

* Corresponding author.

0021-9673/94/$07.00
SSDI 0021-9673(94)00721-7

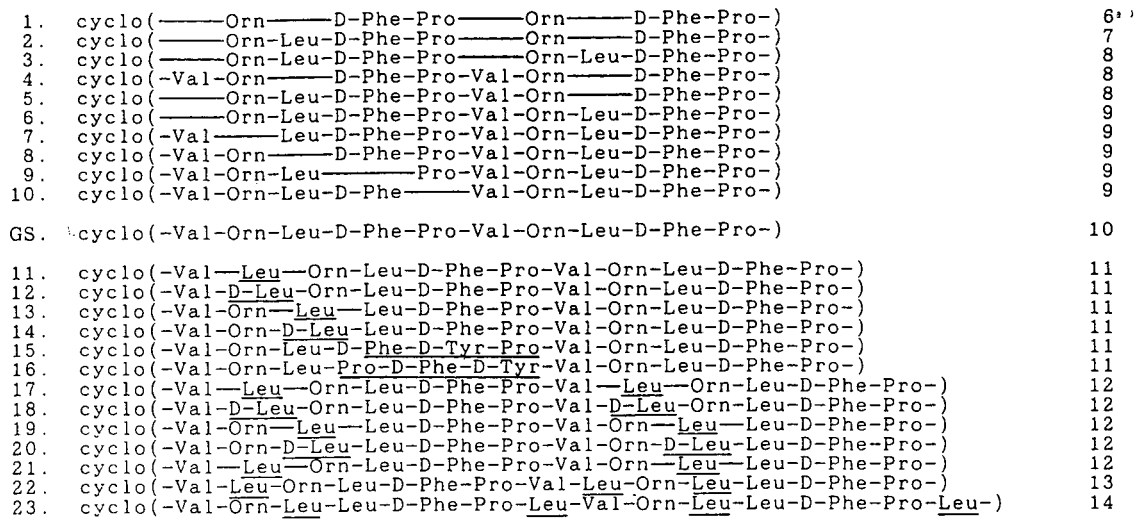

Fig. 1. Primary structures of synthetic peptides and gramicidin S. [a] Number of amino acid residues in each cyclic peptide.

or L-Pro–D-X–D-Y sequences (X and Y = amino acid residue) and strong antibiotic activity gave double peaks on the chromatogram, but that GR analogues containing D-X–L-Pro–L-Y sequences did not show the presence of conformers [7].

In this paper, we report the HPLC behaviour of GS analogues that have various ring sizes and contain the D-Phe–L-Pro sequence at the β-turn part, and discuss the effect of the ring structures on the formation of stable conformers.

2. Experimental

2.1. Synthesis of peptides

Cyclic peptides related to GS were synthesized by a conventional liquid-phase method [4,5]. Their primary structures are shown in Fig. 1 [4–6]. Syntheses of cyclo(–Val–Orn–Leu–D-Phe–Val–Orn–Leu–D-Phe–Pro–) and cyclo(–Val–Orn–Leu–Pro–D - Phe–D - Tyr–Val–Orn–Leu–D-Phe–Pro–) have not previously been reported. Cyclo(–Val–Orn–Leu–D-Phe–Val–Orn –Leu–D-Phe–Pro–) · 2HCl, m.p. 248–250°C (decomp.); $[\alpha]_D^{25}$ – 128.1° (*c* 0.3, EtOH). MS [fast atom bombardment (FAB)], *m/z* 1044 ($C_{55}H_{85}O_9N_{11}$; M + H^+). Amino acid analysis: Val, 2.00; Orn, 2.05; Leu, 2.10; Phe, 2.20: Pro, 0.95. Found: C, 56.45; H, 8.34; N, 13.21%. Calculated for $C_{55}H_{85}O_9N_{11} \cdot 2HCl \cdot 3H_2O$: C, 56.40; H, 8.00; N, 13.15%. Cyclo(–Val–Orn–Leu–Pro–D - Phe–D - Tyr–Val–Orn–Leu–D - Phe –Pro–) · 2HCl, m.p. 225°C (decomp.); $[\alpha]_D^{25}$ – 131.0° (*c* 0.5, EtOH). MS (FAB), *m/z* 1304 ($C_{69}H_{102}O_{12}N_{13}$; M + H^+). Amino acid analysis: Val, 2.10; Orn, 2.00; Leu, 2.20; Phe, 2.10: Pro, 1.90; Tyr, 1.00. Found: C, 57.72; H, 7.87; N, 12.63%. Calculated for $C_{69}H_{102}O_{12}N_{13} \cdot 2HCl \cdot 3.5H_2O$: C, 57.45; H, 7.82; N, 12.6%.

The homogeneities of the synthetic peptides were confirmed by means of TLC, HPLC, elemental analysis, fast-atom bombardment mass spectrometry and amino acid analysis of their acid hydrolysates.

2.2. HPLC analysis

HPLC was carried out using an 800 Series system (Jasco, Tokyo, Japan) consisting of a model 880 intelligent HPLC pump, a Model 875-UV intelligent UV–Vis detector, a Model 860-CO column oven and a Model 7125 syringe-loading sample injector (Rheodyne, Cotati, CA, USA). A Finepak SIL C_{18} column (250 × 4.6 mm I.D.) (Jasco) was used. The mobile phase was methanol–5% aqueous sodium perchlorate (4:1, v/v), the flow-rate was 1 ml/min and the

wavelength of detection was 220 nm. About 1 mg of each synthetic peptide was dissolved in 1 ml of the mobile phase and the resulting solution (10 μl) was injected into the chromatograph. The peak area was recorded using a Chromatopac C-R3A integrator (Shimadzu, Kyoto, Japan).

3. Results and discussion

The HPLC of peptides **1–23** and GS was usually performed at 20°C. Peptide **11**, containing eleven amino acid residues and possessing strong antibiotic activity, gave double peaks (Fig. 2), although other analytical results showed the homogeneity of the peptide. The other peptides with various ring sizes gave a single peak and did not show such phenomena, although these peptides also have the D-Phe–Pro sequence at the β-turn part.

The area ratio of the two peaks remained unchanged on diluting the sample injected, suggesting that the phenomena are not caused by intermolecular aggregation.

Next, the effect of column temperature (10, 20, 25, 30, 40 and 50°C) on the elution of peptide **11** was investigated (Fig. 2). With an increase in the column temperature, the two peaks gradually coalesced and resulted in a single peak.

The effect of flow-rate on the shape of the peak of peptide **11** is shown in Fig. 3. With a decrease in the flow-rate, the peptide was eluted as a broader peak.

The two isomers of peptide **11** isolated on a preparative scale by HPLC at 10°C were rechromatographed under the same conditions after storage for 1.5 h at 10°C (Fig. 4). The chromatograms of each isomer reverted to the original profile, suggesting that the two conformers slowly interconvert at low temperature.

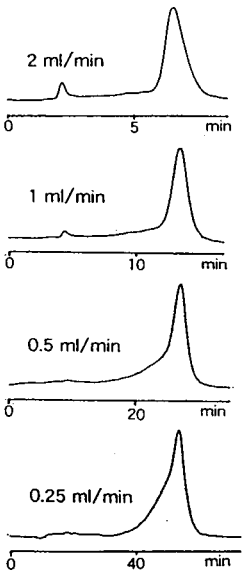

Fig. 3. Effect of flow-rate (0.25–2 ml/min) on the peak shape of peptide **11**. Column temperature, 20°C.

Similar examples of multiple peaks on HPLC separation have been reported for several biologically active peptides [7–11] and model dipeptides [12] which contain the Pro residue. These phenomena were ascribed to the slow interconversion by *cis–trans* isomerization of the X–Pro imide bond. The present HPLC results for peptide **11** may also be caused by *cis–trans* isomerization of the D-Phe–Pro imide bond.

Recently, in HPLC studies of a cyclic dodecapeptide, gratisin (GR), we reported that

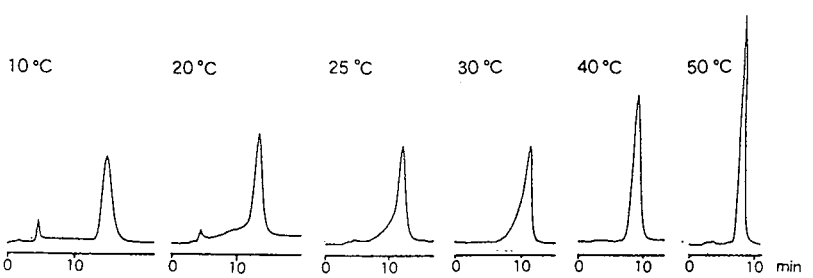

Fig. 2. Effect of column temperature (10–50°C) on the elution of peptide **11**. Flow-rate, 1 ml/min.

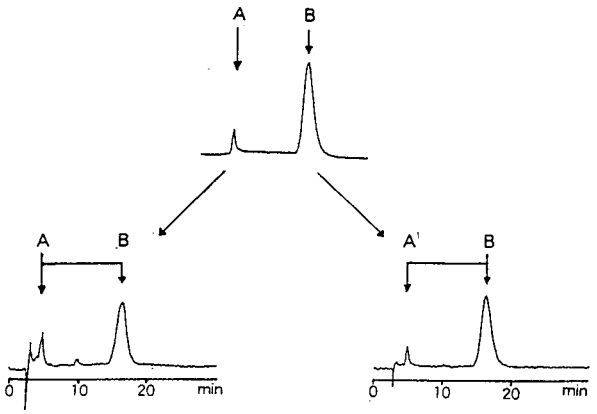

Fig. 4. Rechromatography of the isolated conformers (A, B) of peptide **11** after storage at 10°C for 1.5 h. Column temperature, 10°C; flow-rate, 1 ml/min.

GR analogues having D-X–D-Y–L-Pro or L-Pro–D-X–D-Y sequences (X and Y = amino acid residue) and strong activities gave double peaks in the chromatogram [7]. Peptides **15** and **16**, which contain eleven amino acid residues and one D-Phe–D-Tyr–L-Pro or L-Pro–D-Phe–D-Tyr sequence in the molecule, respectively, gave a single peak in the chromatograms. Further, peptide **17**, which contains twelve amino acid residues and the same hexapeptide sequence, Val–Leu–Orn–Leu–D-Phe–Pro, as peptide **11**, also gave a single peak. These results indicated that a special sequence resulting in the stabilization of conformers in cyclic undecapeptides on the chromatogram was different from that in cyclic dodecapeptides (GR-peptides). In addition, the presence of the additional L-Leu residue preceding the Orn residue in peptide **11** may be necessary to give rise to stabilization of their conformers.

The circular dichroism (CD) spectra of peptides **11–14** containing eleven amino acid residues at room temperature (ca. 20°C) in aqueous solution resembled each other, although the positions and the configurations of the additional Leu residue are different in each molecule, suggesting that the conformations of these peptides are similar to each other [6]. In the present studies, peptides **12–14** gave a single peak and peptide **11** gave double peaks in the chromatogram. On the basis of the chromatogram of the latter peptide, the conformer eluted slowly from the column was the main component. Therefore, the structure of the main conformer may be similar to those of peptides **12–14**.

The antibiotic activity of peptide **11** is slightly lower than those of peptides **13** and **14** [6]. In studies of the HPLC behaviour of peptides related to GS and GR, it was reported that the antibiotics with stronger activity exhibited a higher effective hydrophobicity, and were eluted more slowly from an octadecylsilica gel column [13]. Hence the lower activity of peptide **11** may be brought about by the presence of the conformational equilibrium.

Further detailed conformational analyses of these cyclic peptides are needed in order to understand clearly the phenomena mentioned above.

Acknowledgment

We are grateful to the staff of the Research Laboratory of Asahi Chemical Industry (Ohito, Shizuoka, Japan) for the assay of the synthetic peptides.

References

[1] A.R. Battersby and L.C. Craig, *J. Am. Chem. Soc.*, 73 (1951) 1887.
[2] D.C. Hodgkin and B.M. Oughton, *Biochem. J.*, 65 (1957) 752.
[3] N. Izumiya, T. Kato, H. Aoyagi, M. Waki and M. Kondo, *Synthetic Aspects of Biologically Active Cyclic Peptides–Gramicidin S and Tyrocidines*, Kodansha, Tokyo, and Halsted Press, New York, 1979.
[4] M. Tamaki and S. Akabori, *Bull. Chem. Soc. Jpn.*, 64 (1991) 2569.
[5] M. Tamaki, M. Takimoto and I. Muramatsu, *Bull. Chem. Soc. Jpn.*, 61 (1988) 3925.
[6] M. Tamaki, S. Akabori and I. Muramatsu, in Y. Shimonishi (Editor), *Peptide Chemistry 1990*, Protein Research Foundation, Osaka, 1991, p. 281.
[7] M. Tamaki, S. Akabori and I. Muramatsu, *J. Chromatogr.*, 574 (1992) 65.
[8] D. Bonding and C. States, *J. Biol. Chem.*, 258 (1983) 12247.

[9] L. Rusconi, G. Perseo, L. Franzoi and P.C. Montecucchi, *J. Chromatogr.*, 349 (1985) 117.
[10] Y. Nishiuchi and S. Sakakibara, in U. Ragnarsson (Editor), *Peptides 1984*, Almqvist and Wiksell International, Stockholm, 1984, p. 537.
[11] J.C. Gesquiere, E. Diesis and A. Tartar, in G. Jung and E. Bayer (Editors), *Peptides 1988*, Walter de Gruyter, Berlin, 1988, p. 112.
[12] W.R. Melander, J. Jacobson and Cs. Horvath, *J. Chromatogr.*, 234 (1982) 269.
[13] M. Tamaki, M. Takimoto, S. Nozaki and I. Muramatsu, *J. Chromatogr.*, 413 (1987) 287.

ELSEVIER

Journal of Chromatography A, 685 (1994) 243–251

JOURNAL OF CHROMATOGRAPHY A

Determination of ginsenosides in ginseng crude extracts by high-performance liquid chromatography

Wu-Chang Chuang, Shuenn-Jyi Sheu*

Department of Chemistry, National Taiwan Normal University, Taipei, Taiwan

First received 24 May 1994; revised manuscript received 2 August 1994

Abstract

A high-performance liquid chromatographic method for the simultaneous determination of ginsenosides Rb_1, Rb_2, Rc, Rd, Re, Rf, Rg_1, Rg_2, R_0 and malonylginsenosides Rb_1, Rb_2, and Rc was developed. Detection at 198 nm with linear gradient elution with dihydrogenphosphate buffer–far-UV-grade acetonitrile was found to be the most suitable and the contents of the ginsenosides in a non-pretreatment ginseng extract could easily be determined within 45 min. Validation of this method and differences in column selectivity are described.

1. Introduction

Ginseng, the roots of *Panax ginseng* C.A. Meyer, is one of the most commonly used Chinese herbal drugs, possessing CNS-stimulating, cardiotonic and hypotensive effects, etc. [1]. Active constituents of this plant are found to be a complex mixture of saponins often referred to as ginsenosides, and more than 30 ginsenosides are known. This study considered eight major neutral saponins, ginsenosides Rb_1 (**1**), Rb_2 (**2**), Rc (**3**), Rd (**4**), Re (**5**), Rf (**6**), Rg_1 (**7**) and Rg_2 (**8**), an acidic saponin, ginsenoside R_0 (**9**) [2,3], and three acidic malonates of the dammarane saponins, malonylginsenosides Rb_1 (**10**), Rb_2 (**11**) and Rc (**12**) [4], as shown in Fig. 1.

In the last 15 years, many attempts have been made to assay ginseng by high-performance liquid chromatography (HPLC) either in the normal-phase mode or more recently in the reversed-phase mode [5–13]. However, none of these methods is entirely adequate, as their resolution is limited to at the most six or even less than six of the ginsenosides. Yamaguchi et al. [14] have developed a method for the simultaneous determination of all twelve compounds on an amino column in 70 min, but failed to separate well **6** from **7**, **3** from **11** and **2** from **10**. Further, all of the previously reported methods require tedious pretreatment of ginseng extracts before analysis.

We describe here the development of a direct and rapid method for determining these twelve ginsenosides in ginseng crude extracts within 45 min. The column selectivity was also investigated by studying eleven kinds of commercial columns under the selected conditions.

* Corresponding author.

0021-9673/94/$07.00
SSDI 0021-9673(94)00724-1

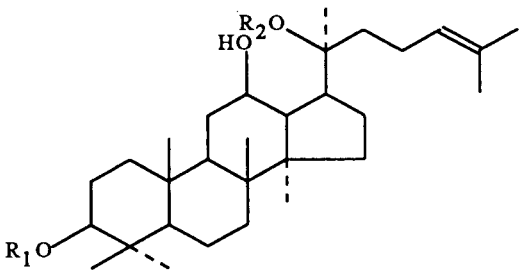

20-S-Protopanaxadiol(R1=R2=H)

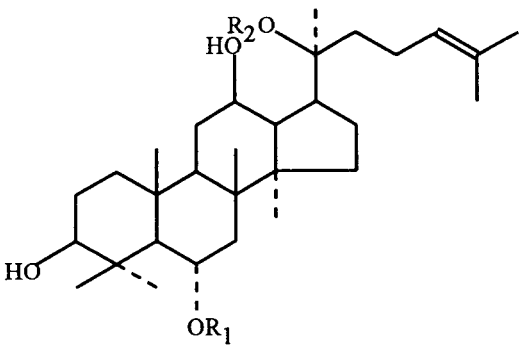

20-S-Protopanaxatriol(R1=R2=H)

1 Rb1: R1= D-Glc(β1-2)D-Glc-
R2= D-Glc(β1-6)D-Glc-

2 Rb2: R1= D-Glc(β1-2)D-Glc-
R2= L-Ara(pyr)(α1-6)D-Glc-

3 Rc: R1= D-Glc(β1-2)D-Glc-
R2= L-Ara(fur)(α1-6)D-Glc-

4 Rd: R1= D-Glc(β1-2)D-Glc-
R2= D-Glc-

5 Re: R1= L-Rha(α1-2)D-Glc-
R2= D-Glc-

6 Rf: R1= D-Glc(β1-2)D-Glc-
R2= H-

7 Rg1: R1= D-Glc-
R2= D-Glc-

8 Rg2: R1= L-Rha(α1-2)D-Glc-
R2= H-

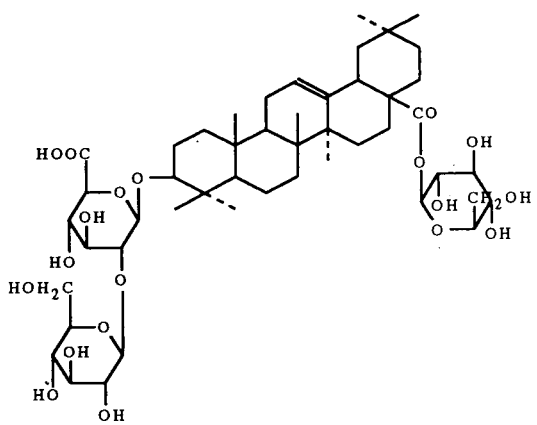

Oleanolic acid

9 R0

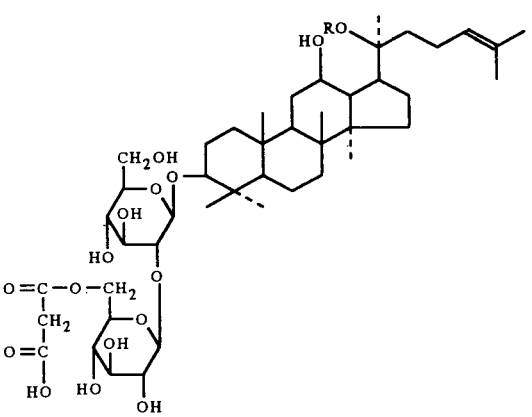

Malonyl-ginsenoside

10 mRb1: R= D-Glc(β1-6)D-Glc-
11 mRb2: R= L-Ara(pyr)(α1-6)D-Glc-
12 mRc: R= L-Ara(fur)(α1-6)D-Glc-

Fig. 1. Structures of the twelve ginsenosides.

2. Experimental

2.1. Reagents and materials

Ginsenosides **1–7** were purchased from Extrasynthese (Genay, France) and potassium dihydrogenphosphate and acetophenone from Nacalai Tesque (Kyoto, Japan). Deionized water from a Milli-Q system (Millipore, Bedford, MA, USA) was used to prepare all buffers and sample solutions. Acetonitrile and methanol were of far-UV grade (Mallinckrodt, Paris, KY, USA). Ginseng was purchased from the Chinese herbal market in Taipei (Taiwan).

2.2. Preparation of ginseng extracts

A 2.0-g sample of pulverized ginseng was extracted by refluxing with 50% ethanol (7 ml) for 15 min, then centrifuged at 1500 *g* (Universal, Hettich Zentrifugen) for 5 min. Extraction was repeated three times. The extracts were combined and filtered through a No. 1 filter-paper. After adding 1 ml of internal standard solution (80 μl of acetophenone in 500 ml of 50% ethanol), the ginseng extract was diluted to 25 ml with 50% ethanol. A 20-μl volume of this solution was injected directly into the HPLC system.

2.3. Apparatus and conditions

The HPLC system consisted of two LC-6AD pumps, an SCL-6B system controller, a Rheodyne Model 7125 injector (20-μl loop) and an SPD-M6A photodiode-array detector, all purchased from Shimadzu (Kyoto, Japan).

The separations were obtained by linear gradient elution, using eluents A and B [A = 10 m*M* KH_2PO_4–CH_3CN (80:20); B = H_2O–CH_3CN (15:85)] according to the following profile: 0–15 min, 98–96% A, 2–4% B; 15–25 min, 96–85% A, 4–15% B; 25–40 min, 85–75% A, 15–25% B; 40–50 min, 75–0% A, 25–100% B; 50–62 min, 100% B. The flow-rate was kept constant at 1.0 ml/min.

The columns used are listed in Table 1. A precolumn of μBondapak C_{18} and Novapak silica (both from Millipore, Milford, MA, USA) was used to protect the column.

3. Results and discussion

3.1. Analytical conditions

HPLC of the neutral saponins of ginseng has been studied extensively. Two methods for the separation of all the major acidic and neutral saponins have been developed by Yamaguchi et

Table 1
Columns used

No.	Column	Producer and location	Column I.D. (mm)
I	Cosmosil $5C_{18}$	Nacalai Tesque (Kyoto, Japan)	4.6
II	Cosmosil $5C_{18}$-MS	Nacalai Tesque	4.6
III	Cosmosil $5C_{18}$-AR	Nacalai Tesque	4.6
IV	Vercopak 5ODS	GL Science (Tokyo, Japan)	4.6
V	Vercopak ODS-2	GL Science	4.6
VI	Inertsil ODS-2	GL Science	4.6
VII	Inertsil ODS-80A	GL Science	4.6
VIII	Lichrosorb RP-18	Merck (Darmstadt, Germany)	4.0
IX	LiChrospher 60RP-SelectB	Merck	4.0
X	Purosphere RP-18	Merck	4.0
XI	Nucleosil 100 $5C_{18}$	Macherey–Nagel (Düren, Germany)	4.0

Length = 25 cm and particle size = 5 μm for all columns.

al. [14] and Kanazawa et al. [13]. The former used aqueous acetonitrile containing 1.0% H_3PO_4 as mobile phase whereas the latter used a mixture of acetonitrile and 50 m*M* KH_2PO_4 solution. In our preliminary study, we found that the addition of dihydrogenphosphate to the mobile phase and the selection of a suitable reversed-phase column are two main determining factors in achieving good resolution.

Buffer concentration

Among the five kinds of columns available in our laboratory (I, III, IV, VIII and X), we found that the Cosmosil $5C_{18}$ (Nacalai Tesque) gave the best separation in our preliminary study. This column was therefore chosen as the basis of our study in searching for the optimum eluent composition and flow-rate. First, we prepared eight KH_2PO_4 buffer solutions of different concentrations: 0 m*M* (pH 6.39), 2m*M* (pH 5.94), 5 m*M* (pH 5.92), 10 m*M* (pH 5.88), 20 m*M* (pH 5.76), 30 m*M* (pH 5.62), 40 m*M* (pH 5.55) and 50 m*M* (pH 5.55). Using these eluents, the capacity factors (k') of the column towards each ginsenoside were obtained. The results are given in Table 2.

From the results in Table 2, it can be seen that by using the mobile phase without KH_2PO_4, a good result was obtained only for neutral saponins and not for the acidic compounds. With the addition of a low concentration of KH_2PO_4 (2 m*M*) to the mobile phase, a much better separation of both kinds of saponins was obtained, which is in agreement with the result of Yamaguchi et al. [14]. Increasing the buffer concentration from 2 to 50 m*M* not only varies the retention time but also narrows the peak width of most of the components in ginseng. As shown in Table 2, satisfactory resolution was obtained with concentrations of 5, 10, 40 and 50 m*M*. However, when the individual chromatograms in Fig. 2 were closely examined, it was found that the separation of **5** from **7** and **6** from **11** using 5 m*M* buffer was incomplete, and the peak of **8** was partially overlapped with some minor impurities when using 40 and 50 m*M* buffers. Further, an appreciable amount of salt precipitated out in the course of analysis when a high concentration of buffer (e.g., 50 m*M* KH_2PO_4 or higher) was used, and thus contaminated the column. Hence a buffer solution containing 10 m*M* KH_2PO_4 was adopted in subsequent studies.

Column selectivity

The mobile phase and stationary phase, which are the factors governing HPLC separation, have mutual influences on each other. We therefore fixed the concentration of buffer at 10 m*M* KH_2PO_4 as discussed above and compared the

Table 2
Correlation of buffer concentration of KH_2PO_4 with capacity factor (k') of the saponins

Ginsenoside	KH_2PO_4 concentration (m*M*)							
	0	2	5	10	20	30	40	50
7	5.95	5.62	4.21	5.30	5.54	4.39	5.92	7.05
5	6.21	5.84	4.40	5.52	5.89	4.65	6.12	7.18
9	8.00	9.24	9.01	9.44	9.58	9.85	9.55	9.98
10	8.00	9.58	9.31	9.70	9.74	9.93	9.80	10.20
12	8.00	9.93	9.69	9.91	10.09	10.22	10.21	10.61
6	10.46	10.37	9.92	10.38	10.54	10.55	10.64	11.09
11	8.00	10.36	10.11	10.56	10.50	10.55	10.43	10.85
8	11.13	11.05	10.67	11.08	11.01	10.85	11.07	11.40
1	11.27	11.19	10.80	11.25	11.14	10.99	11.20	11.55
3	11.78	11.71	11.31	11.75	11.62	11.42	11.71	12.05
2	12.34	12.28	11.85	12.32	12.16	11.90	12.26	12.59
4	13.58	13.53	13.11	13.57	13.57	13.05	13.52	13.79

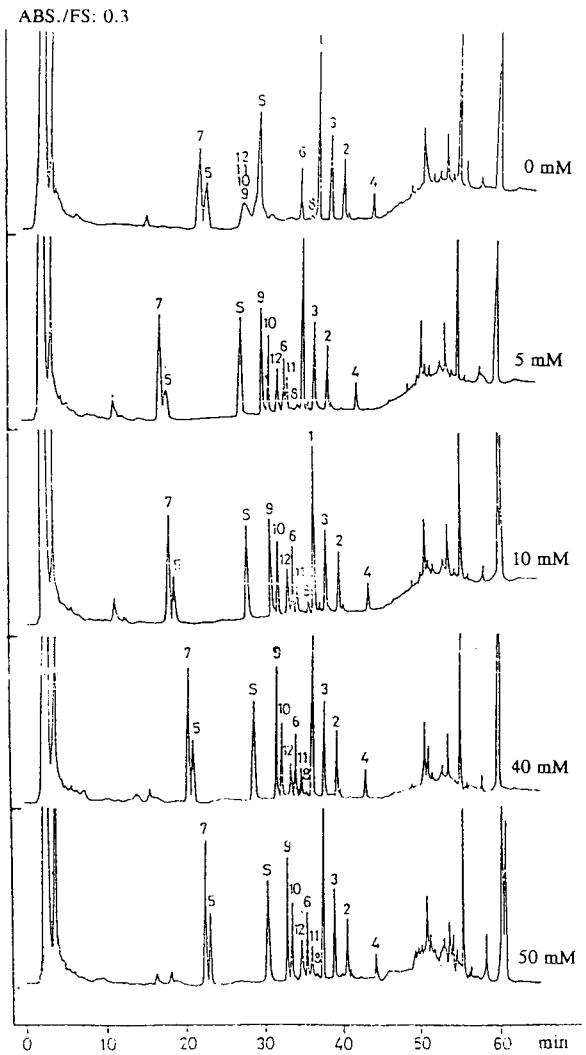

Fig. 2. HPLC of white-ginseng extract eluted with KH_2PO_4 buffers of different concentrations (column I).

selectivities of the eleven commercial C_{18} columns (all 25 cm in length). After a series of experiments, the capacity factors (k') of the ginsenosides were as shown in Table 3.

The data in Table 3 showed that **1–4** could be well separated no matter which column was used. However, great variations occurred in the separations of **5** from **7** and of **6** and **8–12**. Examining the individual chromatograms in detail, it was found that all the columns except I, III and XI failed to separate completely the compounds in the middle region (**8–12**). In addition, columns IV, V, VII and VIII did not give satisfactory separations of **5** and **7**.

Among columns I, III and XI, which are the columns that can give a fairly good separation for all the ginsenosides, column I was found to be the best one owing to a higher resolution in the separation of **8** from **11**. Therefore, column I was adopted (Fig. 3).

A precolumn is mainly used to protect the column, and the packing material used is normally in accordance with that in the analytical column. Our experiments revealed that precolumns of μBondapak C_{18} gave poorly reproducible retention times in the separation of **7** and **5** (19.20 ± 1.04 min, 20.18 ± 0.85 min, $n = 6$); an improvement was obtained using silica (19.37 ± 0.06 min, 20.26 ± 0.05 min, $n = 6$). Therefore, precolumns of the Novapak silica type were the best choice in this study. Moreover, the HPLC system should be completely washed for 17 min after each run to maintain the column reproducibility.

3.2. Method validation

Identification

Ginsenosides **1–7** in the samples were identified by comparing the retention times of authentic ginsenoside standards with those obtained from the sample chromatograms. As malonylginsenosides are known to be thermally unstable and will be decomposed on heating, the identification of **10–12** was carried out by comparing the chromatograms of heat-treated samples with those of the original samples, and also with those reported by Kanazawa et al. [13] and Yamaguchi et al. [14]. Ginsenoside R_0 (**9**), an acidic saponin of oleanolic acid, which has similar characteristics to malonyl ginsenosides except for its thermal stability, was identified by comparing the chromatograms with the published data [13,14]. On the other hand, on varying the detection wavelength from 195 to 220 nm, this acidic saponin was found to give the only large signal in the chromatogram at 220 nm (Fig. 4). Ginsenoside Rg_2 (**8**) was identified by repeating

Table 3
Correlation of column selectivity with capacity factor (k') of the saponins

Ginsenoside	Column										
	I	II	III	IV	V	VI	VII	VIII	IX	X	XI
7	5.30	3.94	3.54	7.08	4.29	4.41	3.32	3.78	3.58	6.09	5.47
5	5.52	4.20	3.82	7.23	4.50	4.71	3.34	4.07	3.86	6.38	5.77
9	9.44	8.98	8.70	10.41	9.44	9.49	8.43	8.97	8.67	0.98	9.43
10	9.70	8.98	8.90	10.41	9.56	9.61	8.17	9.33	8.67	0.98	9.68
12	9.91	9.11	9.23	10.41	9.96	10.02	8.76	9.67	8.90	0.98	10.04
6	10.56	9.58	9.38	10.92	10.10	10.07	9.07	9.39	9.45	10.25	9.86
11	10.38	9.98	9.59	11.23	10.40	10.43	9.07	10.00	9.38	0.98	10.36
8	11.08	9.98	9.79	11.67	10.40	10.43	9.33	10.14	9.80	12.08	10.85
1	11.25	10.29	10.00	11.87	10.70	10.78	9.47	10.84	9.93	12.25	11.18
3	11.75	10.76	10.44	12.40	11.19	11.28	9.88	11.29	10.37	12.84	11.68
2	12.32	11.63	10.93	12.89	11.73	11.81	10.28	11.77	10.77	13.41	12.09
4	13.57	12.45	12.03	14.10	12.97	13.01	11.34	12.78	11.73	14.23	13.18

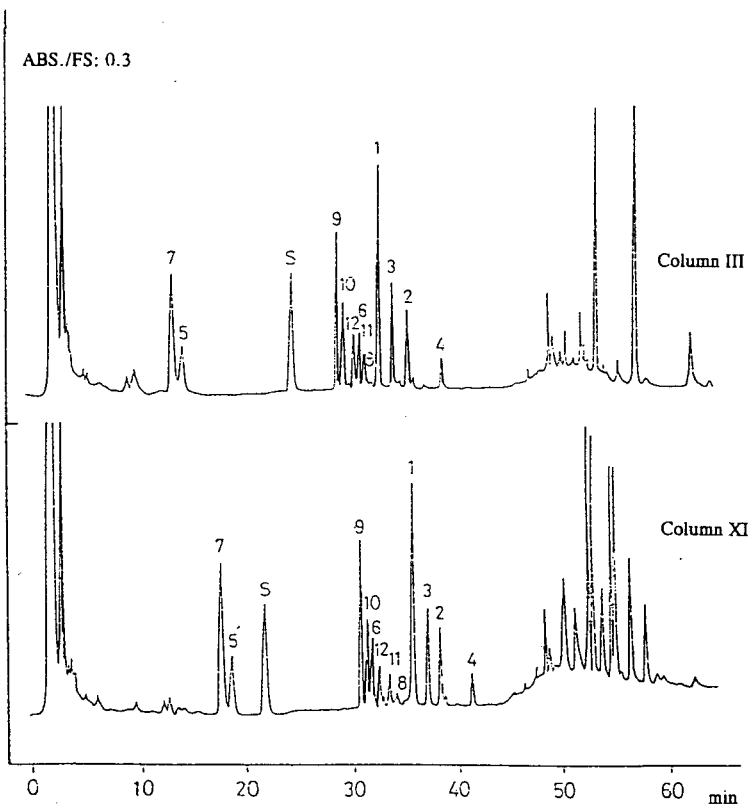

Fig. 3. HPLC of white-ginseng extract separated on different columns.

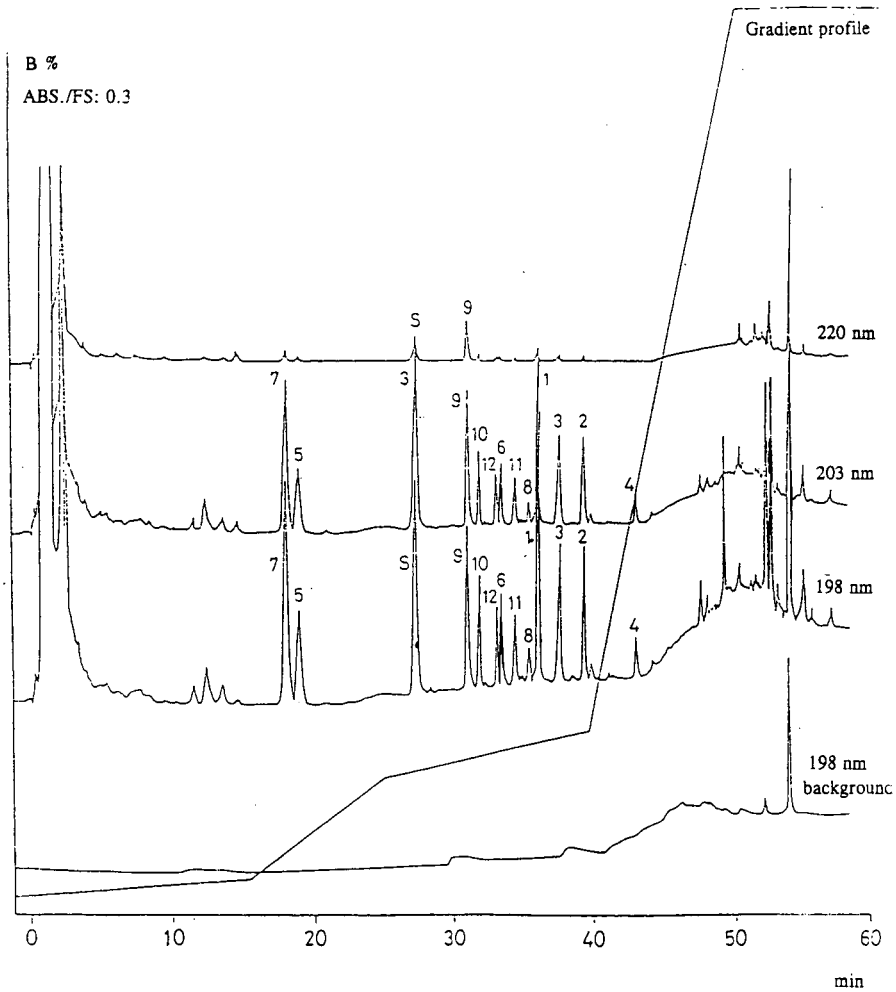

Fig. 4. HPLC of white-ginseng extract with detection at various wavelengths.

the methods reported by Pietta et al. [9] Kanazawa et al. [10].

Detection limit

For the HPLC detection of ginsenosides, the detection wavelength was 203 nm (the detection limit of each ginsenoside was about 5 μg [10,11]). With the use of far-UV-grade acetonitrile (Mallinckrodt), which has a weaker absorbance in the low wavelength region, detection at lower wavelengths was feasible in this study. After scanning with an SPD-M6A photodiode-array detector with wavelengths ranging from 195 to 380 nm, it was found that strong absorbance occurred only at wavelengths below 200 nm. In comparison, the peak sensitivity of ginsenosides monitored at 198 nm was about 1.5 times those at 203 nm, as shown in Fig. 4. Therefore, 198 nm was chosen as the detection wavelength. The detection limit of each ginsenoside at this wavelength was about 0.2 μg (0.01 mg/ml, signal-to-noise ratio = 2, sample size 8 μl). However, under such conditions, baseline drift occurred as shown in Fig. 4. Hence it was difficult to determine the peaks with retention times longer than 46 min.

Precision

The reproducibility (relative standard deviation) of the proposed method, on the basis of peak-area ratios for six replicate injections, was 0.04–3.09%, as shown in Table 4. The variation of the retention time of each peak was less than 0.5% for six replicate injections.

Linearity

The linearity of the peak-area ratio (y) vs. concentration (x, mg/ml) curve for each of the seven ginsenosides was investigated in the range 0.01–1.00 mg/ml. Results of the regression analysis and the correlation coefficients (r) were as follows: **1**, $y = 2.34x + 0.03$ ($r = 0.9988$); **2**, $y = 2.09x + 0.04$ ($r = 0.9990$); **3**, $y = 3.03x + 0.05$ ($r = 0.9992$); **4**, $y = 2.13x + 0.04$ ($r = 0.9987$); **5**, $y = 2.60x + 0.01$ ($r = 0.9998$); **6**, $y = 2.31x + 0.03$ ($r = 0.9992$); **7**, $y = 3.45x + 0.02$ ($r = 0.9988$).

Accuracy

The results of a standard addition recovery study for the seven ginsenosides from ginseng are summarized in Table 5. The recoveries were 98.5–103.2%, with the exception of **6** (95.5% and 96.8%). All the tailing factors of the peaks are very close to unity.

Table 5
Data for recoveries of ginsenosides ($n = 3$)

Ginsenoside	Added (mg)	Recovery (%)
7	0.1000	100.3
	0.2000	99.5
5	0.1000	101.2
	0.2000	102.3
6	0.1000	95.5
	0.2000	96.8
1	0.1000	98.5
	0.2000	100.5
3	0.1000	101.5
	0.2000	100.9
2	0.1000	101.2
	0.2000	103.2
4	0.1000	99.4
	0.2000	98.8

3.3. Determination of ginsenosides in various ginseng samples

When the test solutions of various ginsengs were analysed by HPLC under the selected conditions, the calculated contents of ginsenosides given in Table 6 were obtained. These

Table 4
Reproducibility of separation of ginsenosides

Ginsenoside	Intra-day		Inter-day	
	Ratio[a]	R.S.D. (%)[b]	Ratio[a]	R.S.D. (%)[b]
7	1.14	2.53	1.13	1.18
5	0.50	3.09	0.51	2.43
9	0.67	0.96	0.67	0.95
10	0.38	0.41	0.37	0.40
12	0.30	0.73	0.31	1.01
6	0.30	2.18	0.29	2.81
11	0.19	1.54	0.15	0.78
8	0.02	2.08	0.02	1.98
1	1.01	1.90	1.03	1.50
3	0.49	0.56	0.49	0.82
2	0.33	0.70	0.32	0.33
4	0.15	0.33	0.14	0.45

[a] Ratio = peak area of ginsenoside/peak area of internal standard (acetophenone).
[b] $n = 6$.

Table 6
Contents (mg/g) of ginsenosides in ginseng samples (±S.D., $n = 3$)

Ginsenoside	Sample[a]		
	1	2	3
7	3.96 ± 0.05	3.56 ± 0.08	4.23 ± 0.04
5	2.22 ± 0.02	2.91 ± 0.03	6.77 ± 0.01
6	0.84 ± 0.04	1.45 ± 0.04	2.51 ± 0.03
1	3.31 ± 0.06	5.67 ± 0.01	11.34 ± 0.06
3	1.71 ± 0.03	3.86 ± 0.04	9.47 ± 0.08
2	1.93 ± 0.02	3.51 ± 0.01	8.13 ± 0.02
4	0.43 ± 0.01	1.77 ± 0.04	7.53 ± 0.02
Total	14.40 ± 0.17	22.71 ± 0.10	49.96 ± 0.13

[a] 1 = White-ginseng; 2 = red-ginseng; 3 = Ginseng hair-root.

results indicate that the proposed HPLC method is suitable for the determination of ginsenosides in various ginseng samples. Moreover, no pretreatment is needed in this method.

Acknowledgement

Financial support from the National Science Council, Republic of China, is gratefully acknowledged (NSC 83-0208-M003-001).

References

[1] H.Y. Hsu, Y.P. Chen, S.J. Sheu, C.H. Hsu, C.C. Chen and H.C. Chang, *Chinese Material Medica—A Concise Guide*, Modern Drug Press, Taipei, 1985, pp. 31–32.
[2] O. Tanaka and R. Kasai, in W. Herz, H. Grisebach, G.W. Kirby and CH. Tamm (Editors), *Progress in the Chemistry of Organic Natural Products*, Vol. 46, Springer, New York, 1984, p. 1.
[3] O. Tanaka, R. Kasai and T. Morita, *Abstr. Chin. Med.* 1, (1986) 130.
[4] I. Kitagawa, T. Taniyama, T. Hayashi and M. Yoshikawa, *Chem. Pharm. Bull.*, 31 (1983) 3353.
[5] O. Sticher and F. Soldati, *Planta Med.*, 36 (1979) 30.
[6] H. Besso, Y. Saruwatar, K. Futamura, K. Kunihiro, T. Fuwa and O. Tanaka, *Planta Med.*, 37 (1979) 226.
[7] O. Sticher and F. Soldati, *Planta Med.*, 39 (1980) 348.
[8] H. Kaizuka and K. Takahashi, *J. Chromatogr.*, 258 (1983) 145.
[9] P. Pietta, P. Mauri and A. Rava, *J. Chromatogr.*, 256 (1986) 212.
[10] H. Kanazawa, Y. Nagata, Y. Matsushima, M. Tomoda and N. Takai, *Chromatographia*, 24 (1987) 517.
[11] H. Kanazawa, Y. Nagata, Y. Matsushima, M. Tomoda and N. Takai, *J., Chromatogr.*, 507 (1990) 327.
[12] T.G. Peterson and B. Palmqvist, *J. Chromatogr.*, 504 (1990) 139.
[13] H. Kanazawa, Y. Nagata, Y. Matsushima, M. Tomoda and N. Takai, *J. Chromatogr.*, 537 (1991) 469.
[14] H. Yamaguchi, R. Kasai, H. Matsura, O. Tanaka and T. Fuwa, *Chem. Pharm. Bull.*, 36 (1988) 3468.

ELSEVIER

Journal of Chromatography A, 685 (1994) 253–257

JOURNAL OF CHROMATOGRAPHY A

Preparative separation of stereoisomeric 1-methyl-4-methoxymethylcyclohexanecarboxylic acids by pH-zone-refining counter-current chromatography

Chagit Denekamp[a], Asher Mandelbaum[a], Adrian Weisz[b,*], Yoichiro Ito[c]

[a]*Department of Chemistry, Technion–Israel Institute of Technology, 32000 Haifa, Israel*

[b]*Office of Cosmetics and Colors, US Food and Drug Administration, Washington, DC 20204, USA*

[c]*Laboratory of Biophysical Chemistry, National Heart, Lung, and Blood Institute, National Institutes of Health, Bethesda, MD 20892, USA*

First received 26 April 1994; revised manuscript received 18 July 1994

Abstract

The application of pH-zone-refining counter-current chromatography (CCC) to the preparative separation of stereoisomeric acids is described. The separation was accomplished on the basis of the difference in acidity of the two stereoisomers. pH-Zone-refining CCC of 400 mg of a crude synthetic mixture of stereoisomeric 1-methyl-4-methoxymethylcyclohexanecarboxylic acids yielded 49.5 and 40 mg of the pure *Z*- and *E*-stereoisomers, respectively. The two-phase solvent system consisted of hexane–ethyl acetate–methanol–water (1:1:1:1). Trifluoroacetic and octanoic acids were used as retainer acids. The eluent base was aqueous ammonia. The eluted fractions were monitored by gas chromatography–mass spectrometry.

1. Introduction

As part of an ongoing investigation of stereochemical effects in the fragmentation of organic gas-phase ions on chemical ionization and electron ionization [1,2], pure methyl esters of *Z*- and *E*-1-methyl-4-methoxymethylcyclohexanecarboxylic acids (**Z-1** and **E-1**, respectively, Fig. 1) were needed. The synthetic preparation of these compounds resulted in a crude mixture of methyl esters of **Z-1** and **E-1**. This mixture was considered appropriate to subject to a preparative separation technique recently developed in our laboratories, pH-zone-refining counter-current chromatography (CCC) [3,4], which enables effective separations of organic acid components of multigram mixtures [3–8]. This technique requires the addition of a retainer acid [e.g.,

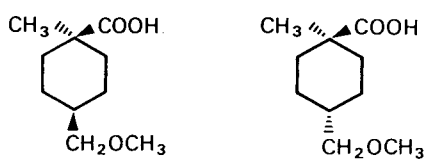

Z-1 **E-1**

Fig. 1. Structures of 1-methyl-4-methoxymethylcyclohexanecarboxylic acids: **Z-1** (*cis* isomer) and **E-1** (*trans* isomer).

* Corresponding author.

0021-9673/94/$07.00
SSDI 0021-9673(94)00669-5

trifluoroacetic acid (TFA)] to the sample solution or stationary phase to enhance partitioning of the analytes into the stationary organic phase. Isocratic elution with an eluent base (e.g., aqueous ammonia) elutes the acid components as well-resolved rectangular peaks in the order of their pK_a values and hydrophobicities [3]. In addition, a spacer acid (e.g., octanoic acid) is sometimes used to aid the separation. Although UV detection (which produces a series of broad rectangular peaks) may not indicate that separations have occurred, monitoring the pH of the eluted fractions results in a series of plateaus that correspond to the separated components. Because equatorial and axial carboxyl groups in cyclohexanecarboxylic acids differ in acidity by approximately 0.5 pK units [9,10], **Z-1** and **E-1** were considered appropriate compounds to be separated by pH-zone-refining CCC.

2. Experimental

2.1. Materials

Hexane, ethyl acetate, methanol and water were chromatography grade. TFA (Sigma, St. Louis, MO, USA), octanoic acid (Eastman-Kodak, Rochester, NY, USA) and aqueous ammonia (>25% NH_3 in water, Fisher Scientific, Pittsburgh, PA, USA) were used as received. The crude mixture of **Z-1** and **E-1** was prepared by the following route: 1,4-cyclohexanedimethanol (*cis–trans* mixture, Aldrich, Milwaukee, WI, USA) was partially methylated to 1-hydroxymethyl-4-methoxymethylcyclohexane [11]. Oxidation of the latter compound to 4-methoxymethylcyclohexanecarboxylic acid ($KMnO_4$, NaOH in water) followed by methylation with iodomethane and lithium diisopropylamide (LDA) in tetrahydrofuran [12] yielded the crude mixture of the methyl esters of **Z-1** and **E-1**. These esters were hydrolyzed to **Z-1** and **E-1** for the purpose of the present separation. The detailed procedure will be reported elsewhere [2].

2.2. Apparatus

The separation was performed using a commercial high-speed CCC centrifuge (P.C. Inc., Potomac, MD, USA) that holds an Ito multilayer-coil separation column and a counterweight whose centers revolve 10 cm around the centrifugal axis. A multilayer column was constructed by one of us (Y.I.) from polytetrafluoroethylene tubing (ca. 165 m × 1.6 mm I.D., with a total capacity of approximately 325 ml). The β value (a centrifugal parameter) [13] ranged from 0.5 at the internal terminal to 0.85 at the external terminal. The column consisted of 16 coiled layers. Similar columns are commercially available from P.C. Inc., Pharma-Tech Research Corp. (Baltimore, MD, USA) and Shimadzu (Kyoto, Japan).

2.3. Solvent system, sample solution and separation procedure

The two-phase solvent system consisted of hexane–ethyl acetate–methanol–water (1:1:1:1). The solvent system was thoroughly equilibrated in a separatory funnel and the two phases were separated shortly before use. To the lower phase was added aqueous ammonia (3.4 mmol NH_3/1000 ml, pH 9.89). To the upper phase (500 ml) were added 100 μl of TFA (1.3 mmol) and 100 μl of octanoic acid (0.63 mmol).

For the preparative separation, 400 mg of the crude mixture containing **Z-1** and **E-1** was dissolved in 3 ml of the above solvent system (2.5 ml of unacidified upper phase and 0.5 ml of unbasified lower phase).

The separation was initiated by filling the column with the stationary (upper) phase by using a metering pump (Accu-Flo pump; Beckman, Palo Alto, CA, USA). The sample solution was injected through the sample port into the column by syringe. The mobile (lower) phase was then pumped into the column at a flow-rate of 3 ml/min while the column was rotated at 800 rpm in the head-to-tail mode. The column effluent was monitored with a UV detector (Uvicord S; LKB Instruments, Stockholm,

Sweden) at 206 nm, to which was attached an LKB 6-channel strip-chart recorder at a chart speed of 1 cm/20 min with a full-scale response of 2 absorbance units. Fractions (6 ml) were collected using a fraction collector (Ultrorac, LKB Instruments). The pH of each eluted fraction was measured with a pH meter (Accumet 1001; Fisher Scientific, Pittsburgh, PA, USA). All fractions of interest were brought to dryness by freeze-drying and were analyzed by gas chromatography–mass spectrometry (GC–MS).

2.4. Gas chromatography–mass spectrometry

The system used consisted of a Hewlett-Packard 5890 Series II gas chromatograph interfaced with an HP-5971 mass-selective detector. Full scan data were acquired. The gas chromatograph was equipped with a Supelcowax 10 fused-silica capillary column, 30 m × 0.25 mm I.D. and 0.25 μm film thickness (Supelco, Bellefonte, PA, USA). The initial column temperature was 40°C, and the solvent delay was 7 min. The column temperature was increased from 40 to 200°C at 15°C/min and from 200 to 270°C at 5°C/min. The injector temperature was 225°C.

A small portion of the dry residue from each fraction of interest was redissolved in ethyl acetate and injected (1 μl) into the GC–MS system.

3. Results and discussion

GC–MS analysis of the crude mixture used in the present work showed that the *Z* and *E* isomers were well separated along with several other components (Fig. 2); 400 mg of this mixture were preparatively separated by pH-zone-refining CCC. UV detection and pH monitoring of the eluted fractions from the CCC separation produced the counter-current chromatogram shown in Fig. 3a. The solvent front (first fraction containing mobile phase) emerged at fraction 13. Retention of the stationary phase, calculated from the volume of stationary phase collected from the column after the separation,

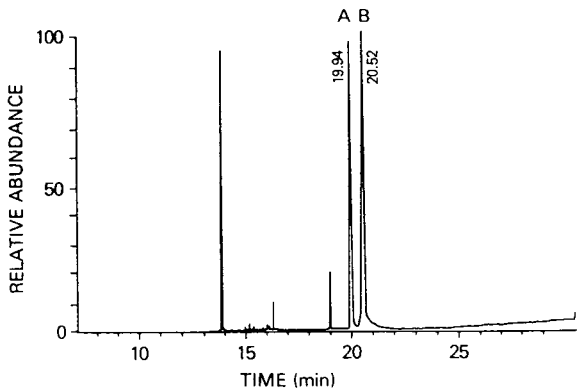

Fig. 2. GC–MS analysis of the crude synthetic mixture of **Z-1** (peak A) and **E-1** (peak B).

was 70.7%. The chromatogram obtained by UV detection has a broad rectangular shape. The low, flat absorbance line (following a sharp peak which represents impurities eluting between the TFA and octanoic acid, respectively, in Fig. 3a) represents saturation of the detector. This saturation is due to the strong absorbance at 206 nm of ethyl acetate, a component of the solvent system used. The two hatched areas correspond to the two descending pH plateaus. Each hatched area represents elution of a pure compound. The eluates corresponding to these areas were collected in fractions 42–63 and 69–76.

Fractions 42–63 contained a single component (40 mg) whose GC retention time (Fig. 3b) was identical to that of peak B in Fig. 2. Fractions 69–76 contained a single component (49.5 mg) whose GC retention time (Fig. 3c) was identical to that of peak A in Fig. 2. The structural assignments (fractions 42–63: **E-1**; fractions 69–76: **Z-1**) were made by comparing the nuclear magnetic resonance (NMR) spectra of the two separated stereoisomers with the NMR spectrum of the *cis* isomer, **Z-1**, whose configuration was determined by X-ray crystallography [2]. The separation of these stereoisomers by pH-zone-refining CCC was possible because of the difference in acidity (pK_a) of axial- and equatorial-oriented carboxyl groups in cyclohexanecarboxylic acids [9,10]. The axial carboxyl group in **Z-1** interacts with the hydrogens in positions 1 and 3,

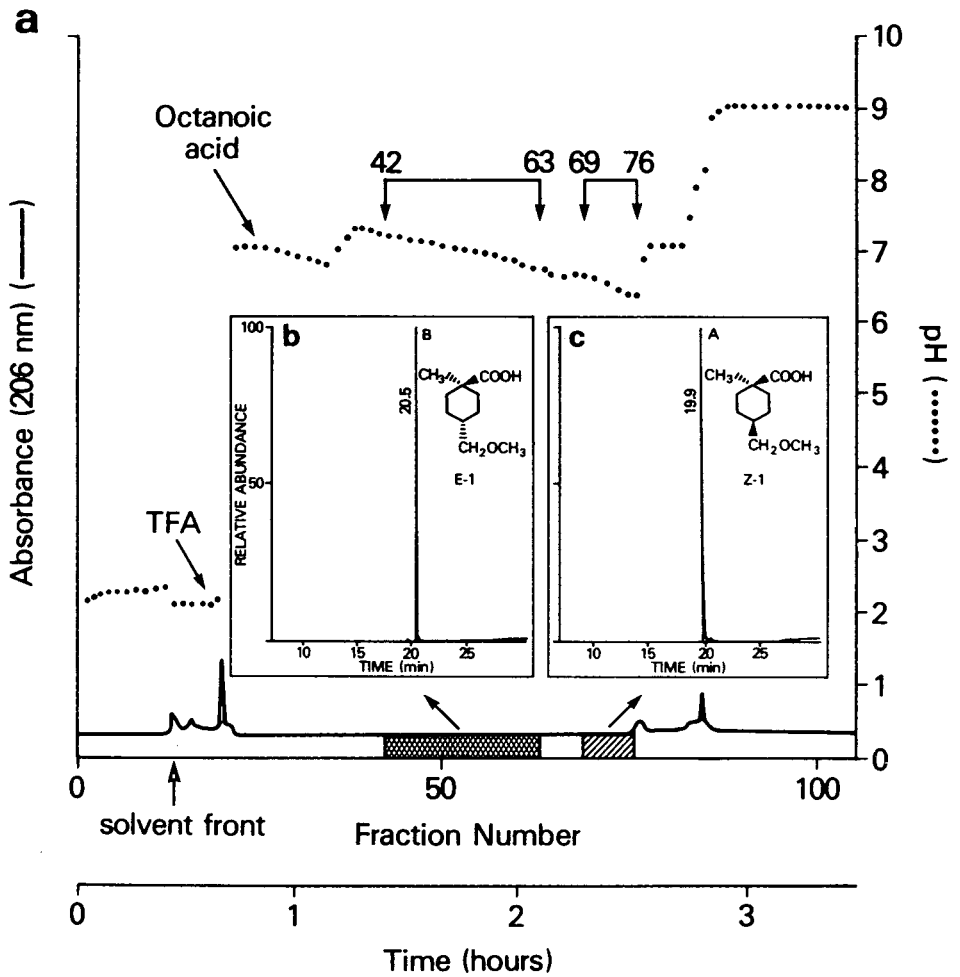

Fig. 3. pH-Zone-refining CCC of 400 mg of a synthetic mixture of **Z-1** and **E-1** (see Fig. 2). (a) Counter-current chromatogram and pH profile of the separation. (b) GC–MS analysis of combined fractions 42–63. (c) GC–MS analysis of combined fractions 69–76.

resulting in hindrance of solvation and hence acid weakening [10] (Fig. 4). In pH-zone-refining CCC, acids elute in descending order of acidity [3]. Thus in the present separation, *trans* isomer **E-1** with its equatorial carboxyl group elutes before the weaker acid, isomer **Z-1**.

Not surprisingly, the strongest acid present (TFA) elutes immediately after the solvent front, followed by octanoic acid (Fig. 3a). The *trans* acid **E-1** elutes at the end of the pH plateau formed by octanoic acid. A sharp impurity peak appears at the point of transition between the respective pH plateaus of TFA and octanoic acid. Without addition of the octanoic acid, impurities that eluted immediately after TFA would have contaminated the early fractions of the first eluted isomer (**E-1**). Octanoic acid was chosen as a second retainer acid on the basis of preliminary experiments with retinoic acids that indicated similar hydrophobicities of retainer acid and analytes result in purified product even in the first eluted fractions [14]. Octanoic acid

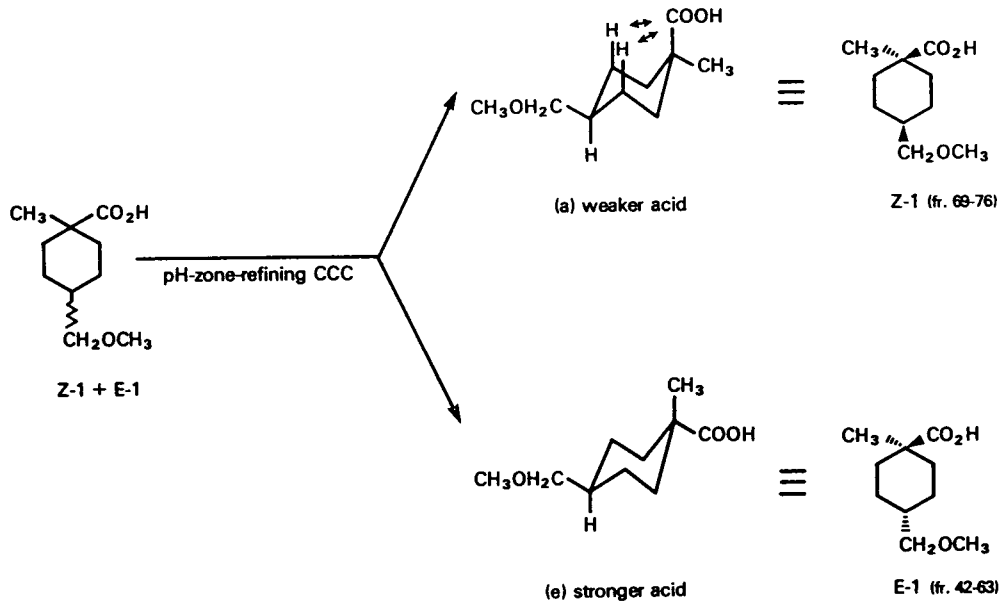

Fig. 4. Schematic diagram of the conformational isomers **Z-1** and **E-1**. In pH-zone-refining CCC the stronger acid (e) elutes before the weaker acid (a).

facilitates the purification of the analytes by acting as a spacer between the analytes and those impurities having comparable hydrophobicities.

Overall, the present study reveals the value of pH-zone-refining CCC for preparative-scale separation of stereoisomeric cyclohexanecarboxylic acids. The results presented here, in conjunction with previous work [7], suggest the great potential of this technique for separating other closely related organic acids.

Acknowledgement

The authors gratefully acknowledge Dr. M. Kapon, Department of Chemistry, Technion–Israel Institute of Technology, for the X-ray crystallographic analysis.

References

[1] A. Etinger, A. Idina and A. Mandelbaum, *J. Am. Chem. Soc.*, 115 (1993) 7397–7401.
[2] C. Denekamp and A. Mandelbaum, in preparation.
[3] A. Weisz, A.L. Scher, K. Shinomiya, H.M. Fales and Y. Ito, *J. Am. Chem. Soc.*, 116 (1994) 704–708.
[4] Y. Ito and A. Weisz, *pH-Zone-Refining Countercurrent Chromatography; US Pat. 5,332,504*, July 26, 1994.
[5] Y. Ito, K. Shinomiya, H.M. Fales, A. Weisz and A.L. Scher, presented at the *ACS National Meeting, Chicago, IL, 22-27 August 1993*, abstract AGFD154.
[6] A. Weisz, K. Shinomiya and Y. Ito, presented at the *44th Pittsburgh Conference and Exposition on Analytical Chemistry and Applied Spectroscopy, Atlanta, GA, 8–12 March 1993*, abstract 865.
[7] A. Weisz, D. Andrzejewski, R.J. Highet and Y. Ito, *J. Chromatogr. A*, 658 (1994) 505–510.
[8] A. Weisz, D. Andrzejewski and Y. Ito, *J. Chromatogr. A*, 678 (1994) 77–84.
[9] R.D. Stolow, *J. Am. Chem. Soc.*, 81 (1959) 5806–5811.
[10] G.B. Barlin and D.D. Perrin, in K.W. Bentley and G.W. Kirby (Editors), *Techniques of Chemistry, Vol. 4, Elucidation of Organic Structures by Physical and Chemical Methods*, Wiley-Interscience, New York, 2nd ed., 1972, pp. 661–664.
[11] R.A.W. Johnstone and M.E. Rose, *Tetrahedron*, 35 (1979) 2169–2173.
[12] P.E. Pfeffer and L.S. Silbert, *J. Org. Chem.*, 35 (1970) 262–264.
[13] Y. Ito, *J. Chromatogr.*, 301 (1984) 387–403.
[14] Y. Ito, unpublished results.

ELSEVIER

Journal of Chromatography A, 685 (1994) 259–262

JOURNAL OF CHROMATOGRAPHY A

Separation of alkaloids by pH-zone-refining counter-current chromatography

Ying Ma, Yoichiro Ito*, Edward Sokolosky, Henry M. Fales

Laboratory of Biophysical Chemistry, National Heart, Lung, and Blood Institute, National Institutes of Health, Bethesda, MD 20892, USA

First received 16 May 1994

Abstract

pH-Zone-refining counter-current chromatography was applied to the separation of alkaloids from a crude extract of *Crinum moorei* using a multilayer coil planet centrifuge. After methyl *tert.*-butyl ether and water were equilibrated, triethylamine (5–10 m*M*) was added to the organic phase and hydrochloric acid (5–10 m*M*) to the aqueous phase. The separation was performed by eluting the column with either the organic phase (displacement mode) or the aqueous phase (reverse-displacement mode) while the other phase was used as the stationary phase. From 3 g of the extract, crinine, powelline and crinamidine were separated in 2.5–7 h with minimum overlapping

1. Introduction

Counter-current chromatography (CCC) [1–3] is a liquid–liquid partition chromatography not requiring solid support in the separation column and offering various advantages including high sample recovery, high purity of fractions and large sample loading capacity. During the past decade, high-speed CCC has been widely used for preparative separations of natural products [3,4].

pH-Zone-refining CCC [5–8] is a recently developed preparative method which yields characteristic rectangular peaks of analytes comparable to those observed in displacement chromatography [9]. The method has been successfully applied to separations of ionizable compounds including various amino acid derivatives [5–7,10,11], hydroxyxanthene dyes [5,12,13], indole auxins [7], etc.

The technique operates in two different modes: reverse-displacement mode [5] and displacement mode [10]. In the reverse-displacement mode, the aqueous mobile phase elutes the analyte retained in the organic stationary phase by the action of a retainer. In the displacement mode, the displacer in the organic mobile phase transfers the analyte from the aqueous stationary phase to the organic mobile phase in a manner analogous to that observed in displacement chromatography. Both modes result in similar elution patterns of analytes except that the order of elution is reversed.

In this paper, pH-zone-refining CCC was applied to the separation of three basic alkaloids from a crude extract of *Crinum moorei* using both reverse-displacement and displacement modes. Each analyte was identified by both MS

* Corresponding author.

0021-9673/94/$07.00
SSDI 0021-9673(94)00667-9

and NMR. The advantages of each operation mode are discussed.

2. Experimental

2.1. CCC apparatus

A commercial model (Ito Multilayer Coil Separator/Extractor, Potomac, MD, USA) of the high-speed CCC centrifuge was used throughout the present studies. The basic design of the apparatus was given elsewhere [4].

The separation column was prepared in our laboratory by winding a single piece of 160 m × 1.6 mm I.D. polytetrafluoroethylene (PTFE) tubing around the column holder hub with 16 layers and 325 ml capacity.

The revolution speed of the apparatus was regulated with a speed controller (Bodine Electric Co., North Chicago, IL, USA). An optimum speed of 600–800 rpm was used in the present studies.

2.2. Reagents

Methyl *tert.*-butyl ether (HPLC grade), triethylamine (reagent grade) and hydrochloric acid (reagent grade) were purchased from Fisher Scientific, Fair Lawn, NJ, USA.

The crude alkaloid extract from *Crinum moorei Hook f.* was extracted as described by Boit [14] and stored at room temperature for ca. 35 years.

2.3. Preparation of solvent phases and sample solutions

The solvent pairs were prepared as follows: about equal volumes of methyl *tert.*-butyl ether and distilled water were thoroughly equilibrated in a separatory funnel at room temperature and the two phases separated. To the upper organic phase triethylamine was added to make the solution in that base 5–10 m*M* (pH 9.2–9.6) while the lower aqueous phase was acidified with hydrochloric acid to 5–10 m*M* (pH 2.3–1.7).

The sample solution was prepared by dissolving 3 g of crude alkaloids extract in 60 ml of a phase mixture consisting of equal volumes of each phase. The pH of the sample solution was adjusted to about 6.0 with HCl.

2.4. Separation procedures

Two different operation modes were employed. In the reverse-displacement mode the organic phase was used as the stationary phase and the lower aqueous phase as the mobile phase. In the displacement mode, the above relationship was reversed, i.e. the lower aqueous phase became the stationary phase and the upper organic phase the mobile phase.

In the reverse-displacement operation, the column was first entirely filled with the organic phase containing 5 m*M* triethylamine (retainer base) followed by sample injection through the sample port. Then, the acidified aqueous phase containing 5 m*M* HCl (eluent acid) was pumped into the inlet of the column in the head to tail elution mode while the column was rotated at the initial speed of 600 rpm. The revolution speed was raised to 800 rpm after 20 fractions had been collected. The above change of the column rotation minimized the carryover of the stationary phase. The effluent from the outlet of the column was continuously monitored with a UV monitor (Uvicord S; LKB Instruments, Bromma/Stockholm, Sweden) at 206 nm and collected into test tubes at 1-min intervals (3.3 ml/tube) with a fraction collector (Ultrorac, LKB Instruments).

In the displacement operation, the column was filled with the aqueous phase containing 10 m*M* HCl (retainer acid) followed by sample injection through the sample port. Then the organic phase containing 10 m*M* triethylamine (displacer) was eluted through the column at a flow-rate of 3.3 ml/min in the tail-to-head elution mode while the apparatus was rotated at 600 rpm. In this elution mode, the two phases establish a reversed pressure gradient through the column where the pressure at the column inlet often plunges into a negative range causing suction of extra solvent from the reservoir through one-way check valves of the metering pump. In order to

prevent this complication, a piece of long narrow PTFE tubing (3 m × 0.4 mm I.D.) was placed at the outlet of the monitor to raise the column pressure. This device also prevented formation of gas bubbles inside the flow cell of the UV monitor which would disturb recording of the elution curve.

In both operation modes, after the desired peaks were eluted, the apparatus was stopped and the column contents were collected into a graduated cylinder by connecting the inlet of the column to a nitrogen line at 80 p.s.i. (1 p.s.i. = 6894.76 Pa).The retention of the stationary phase relative to the total column capacity was computed from the volume of the stationary phase collected from the column.

2.5. *Analysis of fractions*

The pH value of each fraction was determined manually with a portable pH meter (Accumet Portable Laboratory, Fisher Scientific, Pittsburgh, PA, USA).

Alkaloids were identified by TLC (Kieselgel 60 F_{254}) using a solvent mixture composed of chloroform–methanol–32% acetic acid (16:4:1, v/v/v) (R_F values: 0.64 for crinine; 0.74 for powelline; and 0.85 for crinamidine) as well as by comparison of MS and NMR spectrum analyses with standard compounds[1].

3. Results and discussion

Fig. 1A shows a typical chromatogram obtained from 3 g of the crude alkaloid extract of *C. moorei Hook f.* by the reverse-displacement mode. Alkaloids were eluted as an irregular rectangular peak where three absorbance plateaus are observed at retention times of 42–90, 91–136 and 140–148 min. The pH measurement of the collected fractions also revealed three flat pH zones, I, II and III which respectively correspond to the above absorbance plateaus, suggesting the successful separation of three components. Lack of an ideal detector for these specific compounds (all bore similar UV absorption) means that fractions showing subtle changes in UV or pH must be examined carefully (TLC) to determine the onset of elution of the various species. Considerable amounts of impurities were eluted in the front and the back of the main peak, forming multiple peaks. TLC analysis of fractions corresponding to each zone boundary revealed that the mixing zones were no more than several milliliters. MS and NMR analyses of fractions corresponding to the main plateaus identified fractions of pure crinine (zone I), powelline (zone II) and crinamidine (zone III) as indicated in the diagram.

Fig. 1B shows a similar chromatogram obtained from 3 g of the same sample by the displacement mode of pH-zone-refining CCC. Three alkaloids (crinamidine, powelline and crinine) were also eluted together as rectangular peaks but, as expected, in the reverse order due to the reverse-displacement mode (Fig. 1A).

Each mode of pH-zone-refining CCC has its own specific advantages depending on the nature of the analytes. In the displacement mode, each analyte is collected as a free base (or acid) in the organic phase which can be easily evaporated. In the reverse-displacement mode, all analytes are eluted as their salts with the aqueous mobile phase. Although evaporation of fractions requires a longer time, some alkaloids are more stable in the salt form than in the free base and therefore have less risk of decomposition. The reverse-displacement mode also facilitates accurate pH monitoring through the aqueous mobile phase and further provides more stable retention of the stationary phase for low-interfacial-tension solvent systems suitable for the separation of polar compounds.

The overall results of our studies demonstrated that both reverse-displacement and displacement modes of pH-zone-refining CCC produced efficient separations of three alkaloids from gram quantities of *C. moorei* crude extract. The present method may be applied to various other alkaloids from natural products.

[1] One of us (H.M.F.) maintains a reference collection of several hundred amaryllidaceae alkaloids and their chemical degradation products. Inquiries are welcome.

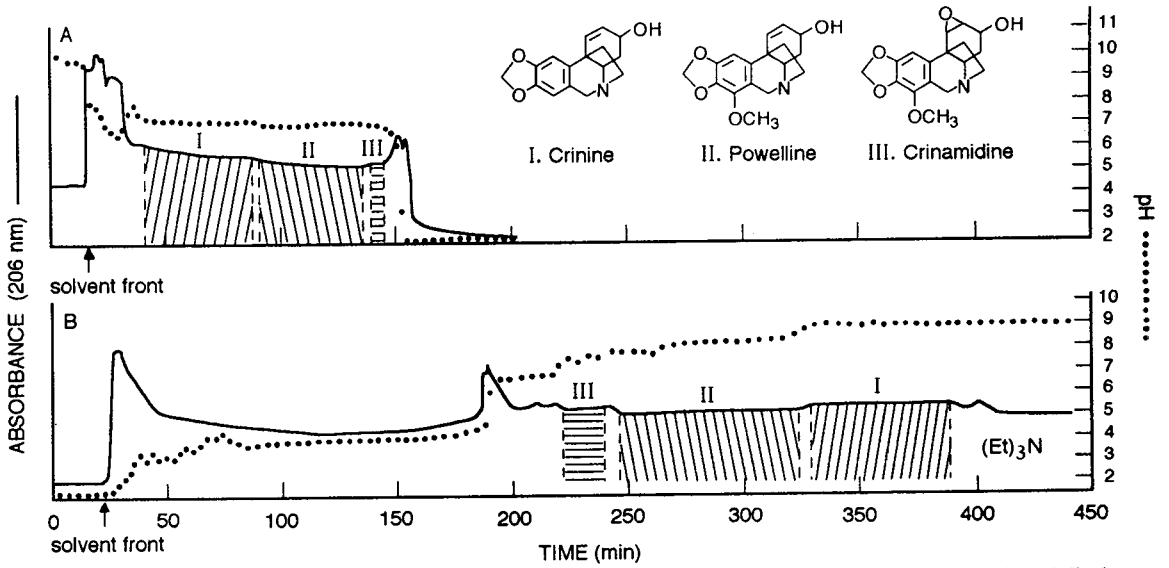

Fig. 1. Chromatograms of crude alkaloid extract of *Crinum moorei* obtained by reverse-displacement mode (A) and displacement mode (B) of pH-zone-refining CCC. Experimental conditions were as follows: apparatus: high-speed CCC centrifuge equipped with a multilayer coil of 1.6 mm I.D. and about 300 ml capacity; solvent system: methyl *tert.*-butyl ether–water; stationary phase: (A) upper phase (5 m*M* triethylamine) and (B) lower phase (10 m*M* HCl); mobile phase: (A) lower phase (5 m*M* HCl) and (B) upper phase (10 m*M* triethylamine); flow-rate: 3.3 ml/min; sample: crude alkaloid extract of *Crinum moorei*, 3 g dissolved in 30 ml of each phase; revolution: (A) 800 rpm (600 rpm until 66 ml of mobile phase was eluted) and (B) 600 rpm throughout.

References

[1] Y. Ito, in N.B. Mandava and Y. Ito (Editors), *Countercurrent Chromatography —Theory and Practice*, Marcel Dekker, New York, 1988, pp. 79–442.

[2] W.D. Conway, *Countercurrent Chromatography —Principle, Apparatus and Applications*, VCH, New York, 1990.

[3] Y. Ito, in E. Heftmann (Editor), *Chromatography —Fundamentals and Applications of Chromatography and Related Differential Migration Methods, Part A: Fundamentals and Techniques (Journal of Chromatography Library*, Vol. 51A), Elsevier, Amsterdam, 1992, Ch. 2.

[4] Y. Ito, *CRC Crit. Rev. Anal. Chem.*, 17 (1986) 65–143.

[5] A. Weisz, A.L. Scher, K. Shinomiya, H.M. Fales and Y. Ito, *J. Am. Chem. Soc.*, 116 (1994) 704–708.

[6] Y. Ito, in Y. Ito and W.D. Conway (Editors), *High-Speed Countercurrent Chromatography*, Wiley-Interscience, New York, in press.

[7] Y. Ito, K. Shinomiya, H.M. Fales, A. Weisz and A.L. Scher, in W.D. Conway and R. Petroski (Editors), *Countercurrent Chromatography*, American Chemical Society, Washington, DC, in press.

[8] A.L. Scher, in W.D. Conway and R. Petroski (Editors), *Countercurrent Chromatography*, American Chemical Society, Washington, DC, in press.

[9] Cs. Horváth, A. Nahum and J.H. Frenz, *J. Chromatogr.*, 218 (1981) 365–393.

[10] Y. Ito and Y. Ma, *J. Chromatogr. A*, 672 (1994) 101.

[11] Y. Ma and Y. Ito, *J. Chromatogr. A*, 678 (1994) 233.

[12] A. Weisz, D. Andrzejewski, R.J. Highet and Y. Ito, *J. Chromatogr. A*, 658 (1994) 505–510.

[13] A. Weisz, in Y. Ito and W.D. Conway (Editors), *High-Speed Countercurrent Chromatography*, Wiley-Interscience, New York, in press.

[14] H.-G. Boit, *Chem. Ber.*, 87 (1954) 1704.

ELSEVIER

Journal of Chromatography A, 685 (1994) 263–269

JOURNAL OF CHROMATOGRAPHY A

High-performance liquid chromatographic method for determination of dehydroabietic and abietic acids, the skin sensitizers in bindi adhesive

B.L. Lee, H.Y. Ong, D. Koh, C.N. Ong*

Department of Community, Occupational and Family Medicine, National University of Singapore, National University Hospital, Lower Kent Ridge Road, Singapore 0511, Singapore

First received 25 May 1994; revised manuscript received 22 June 1994

Abstract

A sensitive and selective high-performance liquid chromatographic (HPLC) method was developed for simultaneous determination of two common allergens, dehydroabietic (DHAA) and abietic acid in bindi adhesive with fluorimetric and ultraviolet (UV) absorbance detection. Bindi is a cosmetic item used by Indian women on their foreheads. The sample was ultrasonicated with 1 ml of acetonitrile for 30 min. A 0.6-ml aliquot of the extract was mixed with an equal volume of deionized water. After centrifugation, 1 ml of the supernatant was percolated through a preconditioned C_{18} solid-phase extraction column. After rinsing the column with 1 ml of acetonitrile–water (60:40, v/v), the analytes were eluted with 1 ml of mobile phase A and 50 μl of the eluent was used for HPLC analysis. The two mobile phases used for gradient elution were: (A) methanol–water (90:10, v/v) containing 0.06% (v/v) formic acid and (B) methanol–water (75:25, v/v) with 0.1% (v/v) formic acid. The flow-rate was set at 1.0 ml/min. DHAA was detected with fluorescence (excitation 225 nm and emission 285 nm) at 3.6 min. Abietic acid was detected at 6.1 min with UV at 238 nm. The lowest detection limits (signal-to-noise ratio 3) were 0.5 and 1.25 ng for DHAA and abietic acid, respectively. Analytical recovery and reproducibility generally exceeded 95 and 90%, respectively. DHAA and abietic acid were present in most of the bindi samples tested, with mean values 0.36 μg of DHAA ($n = 26$) and 0.31 μg of abietic acid ($n = 24$) per sample.

1. Introduction

Rosin (colophony) is a complex mixture of many compounds. It contains about 90% resin acids and 10% neutral matter. Owing to its very strong adhesive effect, it is commonly found in glues and adhesives. Resin acids found in rosin are generally of the abietic and pimaric types. Of these, the abietic type acids are easily oxidized and allergenic. Dehydroabietic acid (DHAA) and abietic acid are the major acids of the abietic type found in different types of rosin [1,2].

Bindi is a cosmetic item used by Indian women on their foreheads to enhance their appearance and as a mark of marital status. It usually originates from the Indian subcontinent. A patient with contact dermatitis to bindi adhesive was found to be sensitive to colophony on patch testing. The identification and confirmation of the presence of these allergens in bindi would provide useful information for patient management. Therefore, a method was developed to

* Corresponding author.

0021-9673/94/$07.00
SSDI 0021-9673(94)00691-1

measure the amount of DHAA and abietic acid in samples of bindi.

DHAA and abietic acid have previously been analyzed, both by gas chromatography [3–5] and by high-performance liquid chromatography (HPLC) [1,6–8]. The most recent HPLC method with ultraviolet (UV) absorbance detection enabled the determination of 0.015% of DHAA and 0.001% of abietic acid in 200 mg of contact adhesive [7]. However, this method was found to be insensitive and non-specific. In the present study, a gradient elution method was developed for baseline separation of DHAA and abietic acid in bindi adhesives. We used solid-phase extraction (SPE) for sample cleaning prior to HPLC analysis. This procedure eliminates matrix interferences and enhances the specificity of detection. The optimum detection conditions for DHAA and abietic acid using fluorimetry and UV spectrometry were also investigated. Measurement of DHAA by the fluorimetric method was at least 100 times more sensitive than by UV absorbance detection.

2. Materials and methods

2.1. Reagents and chemicals

Standards of the analytes of interest were purchased from two different chemical companies: DHAA from Helix Biotech (Richmond, Canada) and abietic acid from Wako (Tokyo, Japan). Formic acid, HPLC-grade methanol and acetonitrile were obtained from Merck (Darmstadt, Germany). Distilled and deionized water was used for the preparation of all solutions. The two mobile phases used for gradient elution were: (A) methanol–water (90:10, v/v) containing 0.06% (v/v) formic acid and (B) methanol–water (60:40, v/v) containing 0.1% (v/v) formic acid.

2.2. Standard preparation

The stock standards of DHAA and abietic acid were prepared from 10 mg of the respective acids dissolved in 10 ml of acetonitrile. A second stock solution containing each 10 μg/ml of DHAA and abietic acid were prepared by diluting the first solution with mobile phase A. Calibration curves were prepared by diluting the second stock solution to final concentrations of 0.01–1 μg/ml of DHAA and 0.025–1 μg/ml of abietic acid and with an injection volume of 50 μl.

2.3. Sample preparation

Twenty-nine bindi samples of different manufacturers were purchased in Singapore. Each piece of bindi sticker (10–20 mg) contains approximately 1–2 mg of adhesive. The SPE column used for sample cleaning was a 1-ml tube column containing 100 mg of C_{18} packing material (Supelco, USA). The column was preconditioned by rinsing with 1 ml of methanol and followed by 1 ml of water. One piece of bindi sticker was soaked in 1 ml of acetonitrile. After ultrasonication for 30 min, the sample was centrifuged at 1500 *g* for 2 min. An aliquot of 0.6 ml of sample was mixed with 0.6 ml of water. The mixture was centrifuged at 1500 *g* for 2 min and 1 ml of the supernatant was allowed to percolate through the preconditioned SPE column. The column was then washed with 1 ml of acetonitrile–water (60:40, v/v) and effluent was discarded. The analytes were then eluted with 1 ml of mobile phase A. An aliquot of 50 μl of the collected eluate was used for HPLC analysis. The results presented as observed are in μg/ml. After correction with a dilution factor of 2, the amount of DHAA and abietic acid contained in each bindi adhesive was calculated as μg per sample.

2.4. Chromatography

The HPLC system used consisted of a Waters Model 600E quaternary pumping system, a Model 996 photodiode array detector, a guard column connected to a Nova-Pak C_{18} analytical column (4 μm, 150 × 3.9 mm I.D.) and a Millennium 2010 software for peak identification and integration (Millipore, Milford, MA, USA). UV scans at peak apex were performed by the

present computerized system. The UV spectrum showed absorption maxima at 267 and 238 nm for DHAA and abietic acid, respectively. A Shimadzu Model RF-535 spectrofluorimetric detector (Kyoto, Japan) with slit width 15 nm was connected in series before the photodiode array detector. For DHAA determination, the excitation and emission wavelengths were set at 225 and 285 nm, respectively. Sample introduction was carried out using a Gilson autoinjector fitted with a 100-μl loop (Model 231-401; Villiers-le-Bel, France). The flow-rate was set at 1.0 ml/min with a gradient elution profile as follows: 0–0.8 min, 100% of mobile phase A; 1.2 min, A–B (50:50); 1.8–8 min, A–B (80:20) and 9–14 min, 100% A.

3. Results and discussion

3.1. Detection mode

HPLC determination of resin acids is generally carried out with UV absorbance detection [1,6–8]. In our initial experiment, DHAA and abietic acid were detected at 267 and 240 nm, respectively, by using a variable-wavelength detector (Model HP1050; Hewlett-Packard, Palo Alto, CA, USA). However, the detection of DHAA (0.5 μg/ml) at UV 267 nm was found to be rather insensitive (Fig. 1a). Using this detection method, most of the bindi samples containing less than 1 μg DHAA could not be detected. Therefore, a more sensitive and specific detection method by fluorimetry was developed. The maximum fluorescence of DHAA was obtained with excitation at 225 nm and emission at 285 nm. As shown in Fig. 1b, the peak height of DHAA was about 140 times higher than that measured with UV detection (Fig. 1a). The fluorimetric detection limit (signal-to-noise ratio 3) for DHAA was 0.01 μg/ml. On the other hand, a photodiode array detector was used for verification of abietic acid detection. It was found that the maximum UV absorbance was at 238 nm and the sensitivity is two times better than with the variable-wavelength detector. The lowest detection limit for abietic acid by using photodiode array detection was 0.025 μg/ml with a sample size of 50 μl.

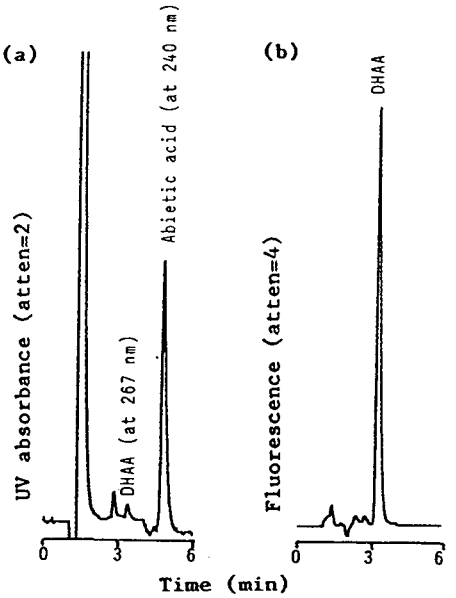

Fig. 1. Chromatograms for an injection of 50 μl of DHAA and abietic acid standards (0.5 μg/ml each) eluted with 100% of mobile phase A at 1.0 ml/min, and analyzed by (a) UV absorbance detection and (b) fluorimetric detection.

3.2. Efficiency of chromatographic analysis

DHAA and abietic acid are insoluble in water but readily dissolved in methanol or acetonitrile. For HPLC analysis, the chromatographic performances of the analytes were evaluated with different mobile phases in order to determine the optimum analytical condition. It was observed that the analytes were retained longer in a reversed-phase C_{18} column with 90% (v/v) methanol than with same concentration of acetonitrile. The retention time of these resin acids and other unknown components were also found to be susceptible to slight changes in the solvent concentration. However, the sensitivities of this effect among the analytes and components were not uniform. Furthermore, chromatographic performances of DHAA and abietic acid were poor if eluted with mobile phase containing less than 80% (v/v) methanol or 75% (v/v) acetonitrile.

Thus, separation of these resin acids in contact adhesive is usually difficult to achieve.

Nevertheless, it was found that addition of acetic or formic acid in 80% solvents in the mobile phase improved the chromatographic efficiency dramatically. Therefore, a gradient elution method using methanol-based solvent as the mobile phase with water and formic acid as modifier was developed. Using the present method, only two samples of the same manufacturer had DHAA closely eluted with interferences. The reliability of this method was verified by comparing the results obtained from the other 27 samples, with the same samples analyzed by using two other, different gradient profiles. The results showed close agreement among these three elution methods (data not shown) and the present method was considered the most efficient and time saving. In Fig. 2, chromatograms of a, b and c are a pure standard (0.5 μg/ml of DHAA and abietic acid), a blank and spiked sample (+0.5 μg/ml of DHAA and abietic acid), respectively. DHAA was determined by fluorimetric detection at 3.6 (±0.05) min. In Fig. 3, chromatograms of a, b and c are of the same injections of samples as in Fig. 2, abietic acid was detected at 6.1 (±0.05) min at UV 238 nm (photodiode array detection). The peaks were well separated with no spectroscopic evidence for coelution. Similar purity tests had been carried out for the rest of samples collected from different manufacturers, and results appeared promising. Only three samples had their abietic acid peaks interfered by adjacent peaks. The

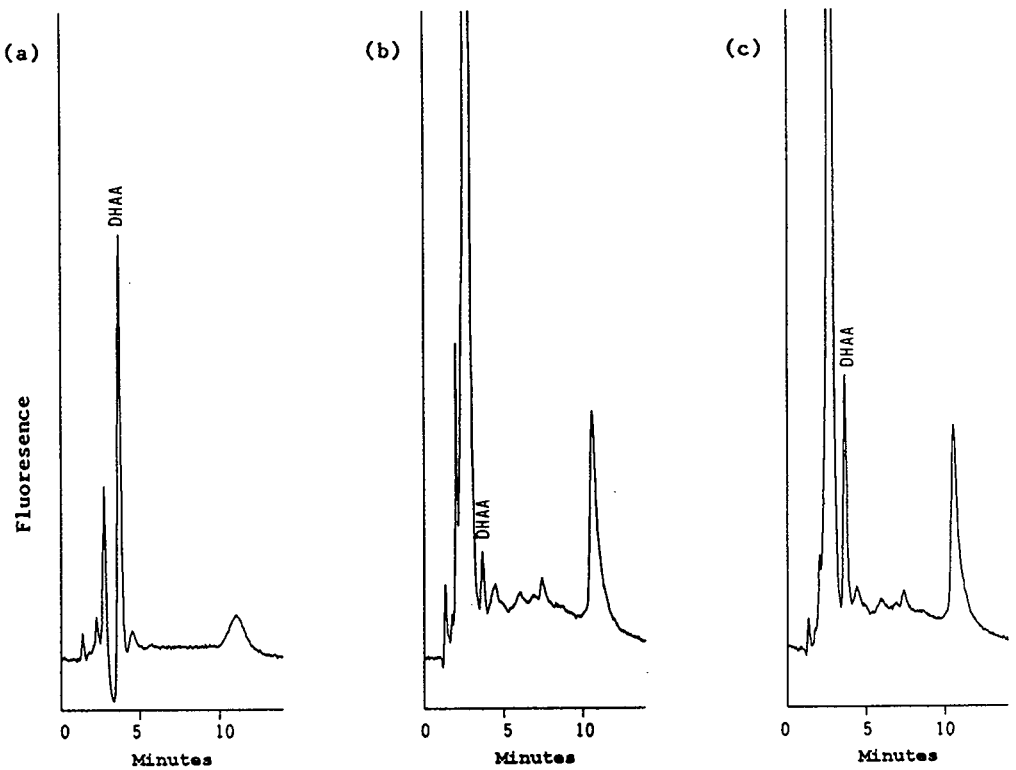

Fig. 2. Chromatograms of (a) a pure standard (0.5 μg/ml of DHAA and abietic acid), (b) a blank and (c) same sample supplemented with 0.5 μg/ml of DHAA and abietic acid, analyzed by the present gradient elution method with fluorimetric detection.

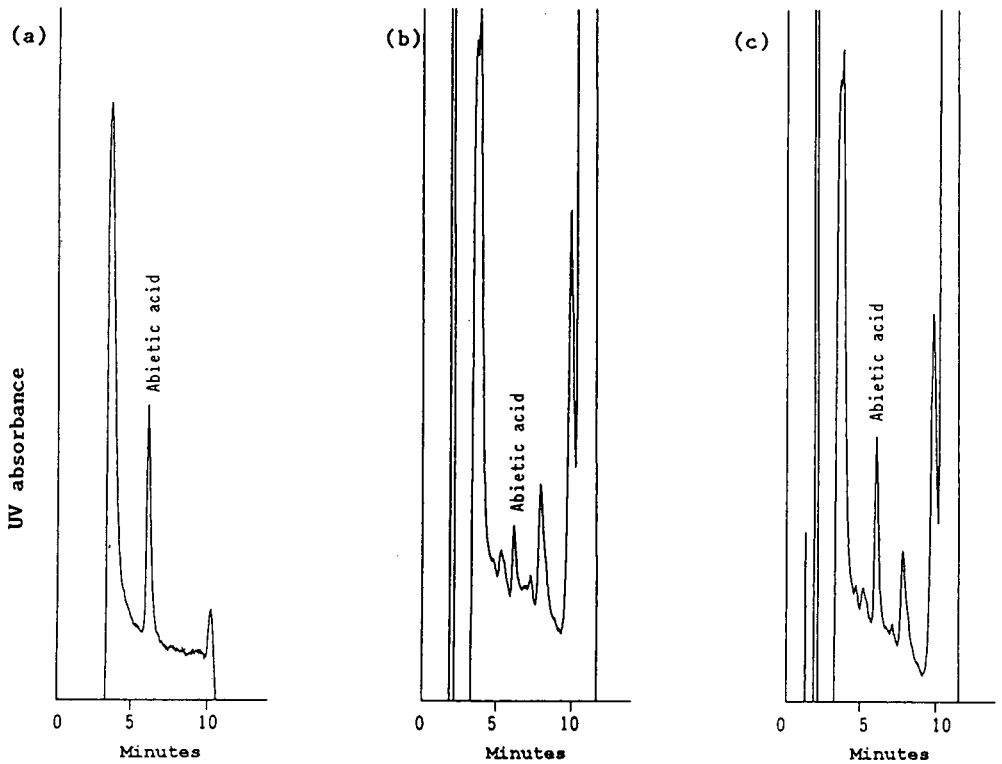

Fig. 3. Chromatograms of (a), (b) and (c) as in Fig. 2, but determined by photodiode array detection and reviewed at UV at 238 nm.

total analysis time was only 14 min per injection. Thus, the present HPLC method could be considered the most rapid, specific and reliable for identification and quantification of DHAA and abietic acid in bindi adhesive.

3.3. Sample preparation, recovery and reproducibility

Matrix interferences of the bindi samples varied from sample to sample due to different manufacturers. The HPLC determination of these resin acids was found to be rather complex either with UV or fluorimetric detection. Samples prepared by ultrasonication in dichloromethane, evaporation and reconstitution in methanol as suggested by Ehrin and Karlberg [7], showed serious interferences on HPLC analysis (data not shown). In our study, samples treated with acetonitrile alone were also difficult and non-specific due to void volume matrix interferences. Thus, the use of SPE for sample cleaning prior to HPLC analysis appears to be the most appropriate approach. The conditions and procedures had been worked out for maximum recovery. Pure standards with concentrations of 0.1, 0.2 and 0.5 μg/ml of DHAA and abietic acid, were processed with the same procedures as sample preparation and were used for determining the recovery, within-assay and day-to-day precision of the method. The mean recovery of various concentrations was 96% for DHAA and 102% for abietic acid (Table 1). The within-assay and day-to-day relative standard deviations

Table 1
Recovery and reproducibility ($n = 3$)

Sample (μg/ml)	Mean (μg/ml)	Recovery (%)	Relative standard deviation (%)	
			Within-day	Between-day
DHAA				
0.1	0.094	94	6.0	6.3
0.2	0.193	97	3.9	7.2
0.5	0.491	98	3.0	3.4
Mean		96	4.3	5.6
Abietic acid				
0.1	0.104	104	4.1	2.3
0.2	0.203	102	2.9	4.0
0.5	0.505	101	5.8	7.4
Mean		102	4.3	4.6

were generally less than 7% for both DHAA and abietic acid analysis ($n = 3$).

3.4. Linearity

Calibration was done by the external standard method. The calibration curves were linear for concentrations of DHAA in the range 0.01–1 μg/ml and 0.025–1 μg/ml for abietic acid. Typical regression equations and correlation coefficients (r) were $y = 102 + 1.6284 \cdot 10^4\ x$ ($r = 0.99$) for DHAA and $y = 41 + 3.815 \cdot 10^3\ x$ ($r = 0.99$) for abietic acid, where y is the peak height (μV) and x is the concentration of analytes (μg/ml). The relative standard deviations of slope and linearity of calibrations for between-day analysis ($n = 3$) were 0.6 and 0.08% for DHAA, and 3.4 and 0.08% for abietic acid; respectively.

3.5. Quantification of DHAA and abietic acid in bindi adhesive

DHAA and abietic acid are well known skin sensitizers. They can be found in various types of contact adhesives and facial cosmetics and can cause contact allergy [7–9]. In clinical practice, patients with contact dermatitis to these cosmetic items may be found to be sensitive to colophony on patch testing. The quantification of these allergens in actual contact items would be helpful for clinical diagnosis and management. Besides those samples that we were unable to measure due to interference or below detection limit, the mean value of DHAA for 26 samples was 0.36 (range 0.06–1.53) μg and that of abietic acid for 24 samples was 0.31 (range 0.05–0.81) μg per sample. The results demonstrate that DHAA and abietic acid are present in adhesives of most of the bindi samples tested in Singapore.

The proposed method was validated with 29 bindi samples available in Singapore. Approximately 1 mg of bindi adhesive containing as low as 0.002% of DHAA and 0.005% of abietic acid could be detected. The sensitivity of this proposed method for abietic acid analysis was 40 times higher than the earlier method [7]. An analytical run took only 14 min. The present method can be considered the most sensitive and reliable HPLC method for DHAA and abietic acid measurement in contact adhesives.

References

[1] A.T. Karlberg, K. Bohlinder, A. Boman, U. Hacksell, J. Hermansson, S. Jacobsson and J.L.G. Nilsson, *J. Pharm. Pharmacol.*, 40 (1988) 42.
[2] A.T. Karlberg, A. Boman, U. Hacksell, S. Jacobsson and J.L.G. Nilsson, *Contact Dermatitis*, 19 (1988) 166.
[3] R. Gref, *J. Chromatogr.*, 448 (1988) 428.
[4] H.B. Lee, T.E. Peart and J.M. Carron, *J. Chromatogr.*, 498 (1990) 367.

[5] A.T. Karlberg, A. Boman and C. Liden, *Contact Dermatitis*, 27 (1992) 224.
[6] A.F. Cunningham, G.C. Furneaux and D.E. Hillman, *Anal. Chem.*, 48 (1976) 2192.
[7] E. Ehrin and A.T. Karlberg, *Contact Dermatitis*, 23 (1990) 359.
[8] A.T. Karlberg, C. Liden and E. Ehrin, *Acta Derm. Venereol. (Stockholm)*, 71 (1991) 445.
[9] H.I. Maibach and P.G. Engasser, in A.A. Fisher (Editor), *Contact Dermatitis*, Lea & Febiger, Philadelphia, PA, 3rd ed., 1986, p. 379.

ELSEVIER

Journal of Chromatography A, 685 (1994) 271–278

JOURNAL OF CHROMATOGRAPHY A

Determination of Ni(II), Co(II) and Cu(II) as diethyldithiocarbamate complexes by high-performance liquid chromatography using hexadecyltrimethylammonium bromide in the mobile phase

María Paz San Andrés*, Soledad Vera, María Luisa Marina

Departamento de Química Analítica, Facultad de Ciencias, Universidad de Alcalá, 28871 Alcalá de Henares (Madrid), Spain

First received 19 May 1994; revised manuscript received 26 July 1994

Abstract

The enhancement of the selectivity and sensitivity in high-performance liquid chromatography due to the presence of the cationic surfactant hexadecyltrimethylammonium bromide (CTAB) in the mobile phase in the determination of three metal ions as complexes with sodium diethyldithiocarbamate was studied. The presence of an organic modifier such as 1-propanol in the mobile phase contributes to the decrease in the retention times of the complexes. The results show that under these conditions, the separation of the three metal ions is possible whereas in the absence of surfactant it is not possible. Also, the detection limits and selectivity are better in the presence of CTAB than in its absence. The method was applied to the determination of nickel and copper in real samples.

1. Introduction

High-performance liquid chromatography (HPLC) has been widely used for the separation and determination of metal ions as complexes [1]. Generally, ion-pair reversed-phase liquid chromatography in which a counter ion with opposite charge to the complex is introduced into the mobile phase has been employed. In this technique, two approaches are possible. In one, the metal ion complex is originated in the chromatographic system and in the other, the complex is formed prior to the chromatographic separation. The first possibility is called "on-column" complexation and implies that the mobile phase employed contains the complexing ligand. The second mode is "precolumn" complexation in which in most instances a solvent extraction step is necessary prior to the chromatographic separation. Optimum conditions for the solvent extraction of many metal ion complexes and their spectrophotometric characteristics have been reported [2]. Diethyldithiocarbamate (DDTC) has been used as a complexing agent to achieve the separation of metal ions by HPLC [3–12]. An organic solvent extraction step is usually used before introducing the complexes into the chromatographic system [3,4,8,10,11]. In some instances, the complexes are introduced into the chromatographic system directly formed in the mobile phase when it contains a high percentage of an organic modifier, e.g., metha-

* Corresponding author.

0021-9673/94/$07.00
SSDI 0021-9673(94)00707-1

nol or acetonitrile [5–7,12], also adding carbon tetrachloride to the mobile phase in order to facilitate the solubilization of the hydrophobic complexes.

In most instances, the detection mode was UV–Vis spectrophotometry and in a few instances electrochemical [5–8].

The influence of surfactants in analytical methods [13–17] and, in particular, in separation methods has been described [18]. Surfactants have been used in chromatography to improve the separation and determination of organic and inorganic compounds owing to the increase in the solubility of hydrophobic solutes that the surfactant micelles produce. In fact, when a surfactant is introduced into the mobile phase, the retention of the solutes is modified owing to the interactions between the stationary phase, the mobile phase and the solute contained in the mobile phase. Some equations have been proposed to describe this process and the interactions mentioned above [18–25].

In some studies different stationary phases and a mobile phase containing a surfactant have been used for determining metal ions by HPLC [26–28]. Also, an aqueous–organic mobile phase in a gradient with another that contains the surfactant has been employed [29].

In this work, the separation and determination of Co(II), Ni(II) and Cu(II) as diethyldithiocarbamate complexes was achieved by HPLC using hexadecyltrimethylammonium bromide as a surfactant in the mobile phase. The need for solvent extraction for the formation of the complexes was avoided owing to the presence of the surfactant in the mobile phase. The proposed method was applied to the determination of Ni(II) and Cu(II) in real samples and the results were compared with those obtained for the same samples by flame atomic absorption spectrometry (FAAS).

2. Experimental

2.1. Reagents

All reagents were of analytical-reagent grade. Cu(II), Ni(II) and Co(II) solutions were prepared from their nitrate salts. The ligand, sodium diethyldithiocarbamate (DDTC), the cationic surfactant, hexadecyltrimethylammonium bromide (CTAB), and 1-propanol (PrOH) were used as received. All these reagents and the HNO_3 employed for the preparation of metallic samples, were obtained from Merck. Methanol (MeOH) for HPLC was supplied by Scharlau. Deionized water was obtained using a Milli-Q system (Millipore).

2.2. Apparatus

A Waters liquid chromatograph was used with a Model 510 pump, a Model 481 UV–Vis detector, a Model 740 integrator and a Rheodyne injection valve with an injection volume of 20 μl.

A LiChrosorb RP-18 column (150 × 3.9 mm I.D.; particle size 10 μm), obtained from Sugelabor, was used in all HPLC runs.

The FAAS measurements were carried out in a Perkin-Elmer Model 2380 atomic absorption spectrometer.

2.3. Procedure

The mobile phases consisted of the cationic CTAB surfactant at an appropriate concentration, the ligand (DDTC) and an organic modifier (methanol or 1-propanol), which was needed to reduce the retention times. These mobile phases were prepared by weighing the necessary amounts of CTAB (at concentrations between 0.03 and 0.25 M) and 10^{-4} M DDTC and dissolving them in a mixture of 1-propanol or methanol and deionized water with the percentage of the alcohol varying from 20 to 50% (v/v). All mobile phases were filtered and placed in an ultrasonic bath for 20 min for degasification before introduction into the chromatographic system.

The complexes were prepared by dissolving the necessary amount of each salt directly in the mobile phase. These complexes were then injected into the chromatographic system. The variation of the retention times of the three complexes as a function of the concentration of CTAB in the mobile phase [with 45% (v/v) of 1-propanol as organic modifier and DDTC at a

concentration 10^{-4} *M*] was determined. Next, the variations of retention times as a function of the concentration of DDTC in the mobile phase [with 0.03 *M* CTAB and 45% (v/v) 1-propanol] and finally as a function of percentage of organic modifier in the mobile phase using 1-propanol and methanol (with 0.03 *M* CTAB and 10^{-4} *M* DDTC) were determined.

Detection was carried out by UV–Vis spectrophotometry using a wavelength of 326 nm for the Ni(II) and Co(II) complexes and 440 nm for the Cu(II) complex.

2.4. Sensitivity and detection limits

The sensitivity and detection limits for the LC determination of the three complexes were determined using a mobile phase containing the surfactant with the composition 0.03 *M* CTAB–10^{-4} *M* DDTC–45% (v/v) 1-propanol and, in order to compare the results obtained in the presence of CTAB with those in the absence of surfactant, a mobile phase with the same composition but without CTAB was employed. The amounts of the metal ions injected ranged from 0.23 to 26 ng for Ni(II) and Co(II) and from 0.25 to 210 ng for Cu(II).

2.5. Determination of nickel and copper in real samples

The amounts of nickel and copper contained in metallic samples of a copper alloy which were anodized with nickel were determined. Six pieces of three different sizes (two of each) were used. For these determinations, the metal alloy pieces were dissolved completely in a minimum volume of concentrated nitric acid, transferred to a volumetric flask and diluted to 250 ml with deionized water. The samples were prepared by diluting appropriate volumes of these solutions with the mobile phase [0.03 *M* CTAB–10^{-4} *M* DDTC–45% (v/v) 1-propanol] to 25 ml. Next, 20 μl of sample were injected into the chromatograph. The amount of each metal contained in the samples was determined form appropriate calibration graphs.

In order to compare the HPLC results with those of another method of analysis, the concentrations of copper and nickel were also determined by FAAS. Each sample was measured six times and both the means and standard deviations were calculated.

3. Results and discussion

3.1. Retention of the complexes in the chromatographic system

Diethyldithiocarbamate complexes of Co(II), Ni(II) and Cu(II) are insoluble in aqueous solution in the absence of CTAB and organic modifier, and only partially soluble when the 1-propanol content of the mobile phase is ≤35% (v/v) in the absence of CTAB. The presence of CTAB leads to solubilization of the metal ion complexes in aqueous medium and a decrease in their retention in the stationary phase, decreasing the analysis time and improving the selectivity.

The influence of the concentration of CTAB in the mobile phase on the retention of the three metal complexes was examined. The CTAB concentration ranged from 0.02 to 0.08 *M*. 1-Propanol was added to the mobile phase at a concentration of 45% (v/v) in order to decrease the retention of the metal complexes. Fig. 1 shows that the variation of the inverse of the capacity factor (k') as a function of surfactant concentration is linear over the range of CTAB

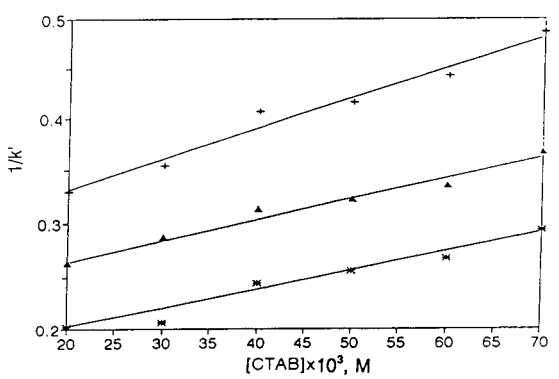

Fig. 1. Variation of the inverse of the capacity factor (k') with the concentration of CTAB in the mobile phase. ▲ = Ni(II); + = Co(II); * = Cu(II). Mobile phase: 10^{-4} *M* DDTC–45% (v/v) 1-PrOH–CTAB.

concentrations studied. This result is in agreement with the equations that have been proposed [17,18] to relate these parameters in the case of organic compounds with mobile phases in the absence (or with low percentages) of alcohols.

The retention of the DDTC complexes agrees with Armstrong's model [19,21] in which three equilibria are involved: the solute distribution between the mobile micellar pseuso-phase and the bulk mobile phase, the solute partitioning between the stationary phase and the mobile micellar pseudo-phase and the distribution of the solute between the bulk mobile phase and the stationary phase. According to this model, when the concentration of surfactant in the mobile phase increases, the solute affinity for this phase increases and the solute retention decreases. The experimental results are in agreement with this behaviour.

The concentration of DDTC was keep constant at 10^{-4} *M*. Fig. 2 shows the variation of the sensitivity (in peak area) as a function of ligand concentration in the mobile phase. Maximum sensitivity is obtained at DDTC concentrations of 10^{-4} *M* and above. The decrease in sensitivity at concentrations lower than 10^{-4} *M* is due to the fact that at these low concentrations are insufficient to complex the metals completely.

A mobile phase 10^{-4} *M* in DDTC and 0.03 *M* in CTAB were chosen with the aim of determining the variation of the capacity factor as a function of organic modifier concentration in the mobile phase. Two short-chain alcohols, methanol and 1-propanol, were used as organic modifiers. Figs. 3 and 4 show the variation of the logarithm of the capacity factor of the three DDTC complexes as a function of the percentage of methanol and 1-propanol, respectively, in the mobile phase. Fig. 3 shows that the logarithm of the capacity factor varies linearly with methanol percentage as in reversed-phase

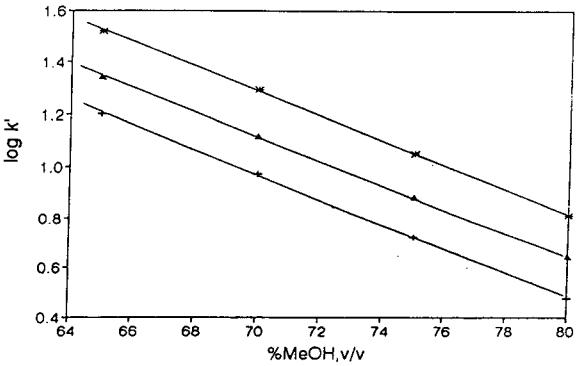

Fig. 3. Variation of the logarithm of the capacity factor (k') with the MeOH concentration in the mobile phase. ▲ = Ni(II); + = Co(II); * = Cu(II). Mobile phase: 0.03 *M* CTAB–10^{-4} *M* DDTC–MeOH.

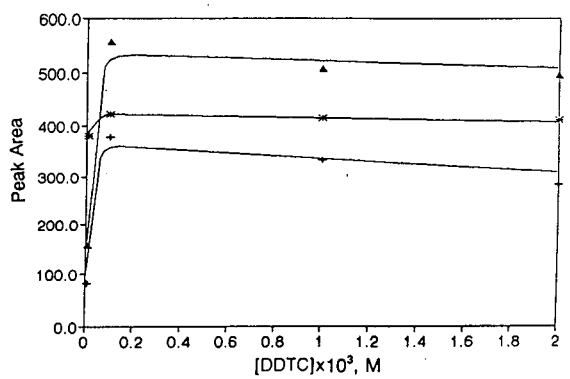

Fig. 2. Variation of the peak area with the concentration of DDTC in the mobile phase. ▲ = Ni(II); + = Co(II); * = Cu(II). Mobile phase: 0.03 *M* CTAB–45% (v/v) 1-PrOH–DDTC.

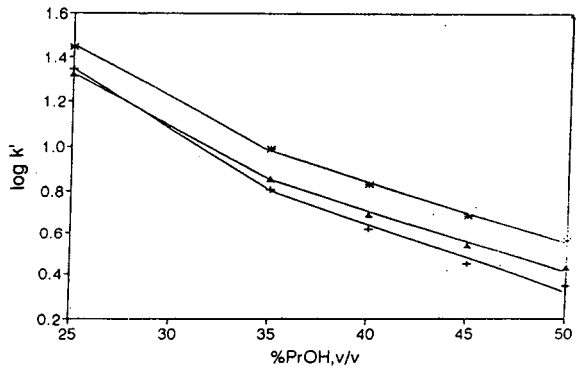

Fig. 4. Variation of the logarithm of the capacity factor (k') with 1-PrOH concentration in the mobile phase. ▲ = Ni(II); + = Co(II); * = Cu(II). Mobile phase: 0.03 *M* CTAB–10^{-4} *M* DDTC–1-PrOH.

HPLC with conventional aqueous–organic mobile phases [30]. However, with 1-propanol, a linear variation is obtained only for concentrations >35% (v/v). For both alcohols, the solute retention decreases when the percentage of organic modifier in the mobile phase increases. However, according to eluent strength, the percentage of alcohol necessary to obtain short retention times is much lower when using 1-propanol than methanol.

With respect to the selectivity, Fig. 3 shows that separation selectivity does not vary as a function of the methanol percentage in the mobile phase. However, with 1-propanol, the selectivity increases as its concentration increases. In fact, although Cu(II) can be separated from Ni(II) or Co(II) with any 1-propanol percentage, the separation of Ni(II) from Co(II) is possible only with >40% (v/v) 1-propanol. For these reasons, a mobile phase containing 45% (v/v) 1-propanol was utilized to achieve the separation of DDTC complexes.

The observed increase in selectivity with increases in the 1-propanol percentage in the mobile phase (Fig. 4) is the opposite of that seen in reversed-phase HPLC with conventional aqueous–organic mobile phases. However, our results are in good agreement with those obtained by others who added surfactants to the mobile phase [31] and reported an increase in selectivity with eluent strength.

As can be observed in Fig. 4, a change in the elution order of the Ni(II) and Co(II) complexes occurs. This change is obtained when the concentration of 1-propanol ranges from 25% to 35%. The behaviour of these complexes at these 1-propanol percentages cannot be studied in the absence of CTAB because in these media the DDTC complexes are not soluble and the retention times are very long.

Fig. 5 shows a chromatogram for the separation of the three DDTC complexes using the mobile phase 0.03 *M* CTAB–10^{-4} *M* DDTC–45% (v/v) 1-propanol. The separation selectivity is fairly good although it is better for the Co(II)–Cu(II) and Ni(II)–Cu(II) separations than for the Co(II)–Ni(II) separation. The Ni(II)–Co(II)–Cu(II) separation can be achieved with an analysis time of less than 5 min. Fig. 6 shows a chromatogram for the separation of the same complexes using a mobile phase with the same DDTC and 1-propanol concentrations but in the absence of CTAB. In this instance it is not possible to separate Ni(II) and Co(II), even

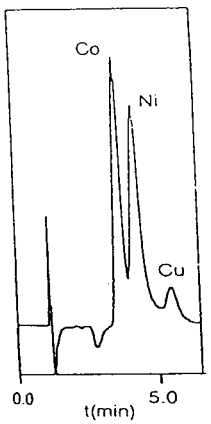

Fig. 5. Chromatogram of a mixture of Ni(II), Co(II) and Cu(II) in the presence of CTAB in the mobile phase. Mobile phase: 0.03 *M* CTAB–10^{-4} *M* DDTC–45% (v/v) 1-PrOH.

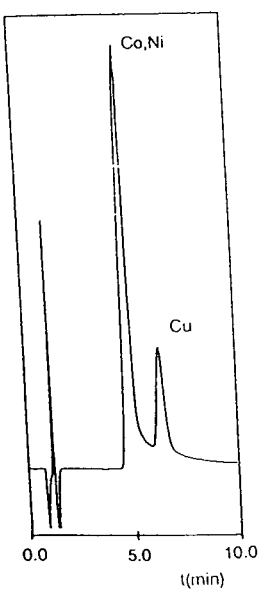

Fig. 6. Chromatogram of a mixture of Ni(II), Co(II) and Cu(II) in the absence of CTAB in the mobile phase. Mobile phase: 10^{-4} *M* DDTC–45% (v/v) 1-PrOH.

Table 1
Detection limits and sensitivity for the three metal ion complexes by HPLC with the mobile phases (1) 10^{-4} *M* DDTC–45% (v/v) 1-PrOH and (2) 10^{-4} *M* DDTC–0.03 *M* CTAB–45% (v/v) 1-PrOH

Mobile phase	Metal ion	Detection limit (pg)	Sensitivity	Linear range (ng)	Wavelength (nm)
1	Ni(II)	134.4	2.5671	0.23–16	326
	Co(II)	77.9	1.9236	0.23–16	326
	Cu(II)	314.8	0.8820	0.25–140	440
2	Ni(II)	68.1	3.1547	0.23–14	326
	Co(II)	67.2	2.3676	0.23–17	326
	Cu(II)	35.4	0.8123	0.25–180	440

Table 2
Results obtained for the determination of Ni(II) and Cu(II) in metal samples by HPLC with the mobile phase 0.03 *M* CTAB–10^{-4} *M* DDTC–45% (v/v) 1-PrOH and by FAAS

Analysis No.	Cu(II) (mg)		Ni(II) (mg)		Sample mass (g)[a]	Cu(II) (%)		Ni(II) (%)	
	FAAS (λ = 325 nm)	HPLC (λ = 440 nm)	FAAS (λ = 232 nm)	HPLC (λ = 326 nm)		FAAS	HPLC	FAAS	HPLC
1	224.3 ± 2.0	223.9 ± 2.8	15.6 ± 0.3	14.9 ± 0.9	–	–	–	–	–
2	927.9 ± 8.6	923.1 ± 11.5	18.5 ± 0.2	17.9 ± 0.7	–	–	–	–	–
3	804.2 ± 9.4	803.5 ± 13.6	10.3 ± 0.2	10.1 ± 0.2	1.5253 ± 0.0040	52.7	52.7	0.7	0.7
4	831.4 ± 7.8	841.0 ± 10.8	11.9 ± 0.2	11.9 ± 0.3	1.5253 ± 0.0040	54.5	55.1	0.8	0.8
5	419.4 ± 2.9	417.4 ± 9.0	6.6 ± 0.1	6.4 ± 0.2	0.7054 ± 0.0019	59.4	59.2	0.9	0.9
6	400.4 ± 5.8	410.0 ± 9.1	6.1 ± 0.1	6.2 ± 0.2	0.7054 ± 0.0019	56.8	58.1	0.9	0.9

[a] Mass of samples corresponding to the mean of eight pieces of size 3 and 4, or to the mean of eleven pieces of size 5 and 6. Samples in analyses Nos. 1 and 2, 3 and 4, and 5 and 6 were of the same size.

partially, showing that the presence of the surfactant is necessary for this separation.

3.2. Sensitivity and detection limits

The sensitivity and detection limit for the determination of the three complexes using a mobile phase of $10^{-4}M$ DDTC–45% (v/v) 1-propanol, first containing and then without CTAB, were determined. The sensitivity is defined as the gradient of the calibration graph of peak area versus the amount in nanograms of metal cation injected. The detection limit is defined as the amount of metal cation necessary to obtain a peak height double that of the background noise. Peak heights were measured rather than peak areas because they are more reproducible and also because it is not possible to measure the peak area of the background noise.

The results are summarized in Table 1. The sensitivity obtained in the presence of CTAB is greater than that in its absence for Ni(II) and Co(II). For the determination of Cu(II) no difference in the sensitivity was observed in the presence and absence of CTAB. The increase produced in the sensitivity means that in the presence of CTAB peaks are obtained with a greater height for the same concentration of metal cation, so either a larger amount of complex was formed, or the peaks obtained had a greater efficiency than in the absence of CTAB, in addition to as modifying the retention of the complexes.

The detection limits are greater, in all instances, when CTAB is presence in the mobile phase, as shown in Table 1. The detection limits obtained in the presence of CTAB decrease in all instances, the difference being greatest for Cu(II), with a decrease of 279 pg.

3.3. Determination of the nickel and copper in metallic samples

Using the proposed method, nickel and copper were determined in metallic samples. These samples were components used in electronics, composed of a copper alloy anodized with a nickel alloy to give a covering of depth between 3 and 15 μm. A chromatogram of one of these samples is shown in Fig. 7. To investigate the validity of the proposed method, nickel and copper were also determined by FAAS and the results obtained with the two methods were compared.

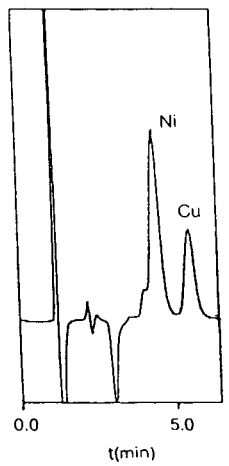

Fig. 7. Chromatogram of a real sample containing Ni(II) and Cu(II) in the presence of CTAB in the mobile phase. Mobile phase: 0.03 M CTAB–10^{-4} M DDTC–45% (v/v) 1-PrOH.

Three different sizes of metallic sample were available, and two of each size were chosen. Table 2 gives the results, as the average of six analyses each sample with the corresponding standard deviation for the proposed HPLC method in presence of CTAB and FAAS.

The results obtained by HPLC show good agreement with those obtained by FAAS. Hence the HPLC method in the presence of CTAB is valid for the proposed purpose.

4. Conclusions

The complexes of Co(II), Ni(II) and Cu(II) with DDTC, which are insoluble in aqueous solution, dissolved in the cationic micellar medium CTAB, making it possible to introduced them into a chromatographic system without first having conduct a solvent extraction. A sensitive and valid HPLC method for determination of these metals has been developed.

This work shows the possibility of separating metal ions as complexes formed on-column in RP-HPLC using a surfactant in the mobile phase, which increases the solubility of the complexes, the sensitivity and the selectivity of the detection. When the complexes are formed precolumn, the ligand and complex decomposition prevent a good separation and detection of the peaks of the complexes.

One of the main advantages of RP-HPLC with UV–Visible detection over ion chromatography is that in RP-HPLC only the metal ions that form complexes with the ligand in the mobile phase are detected, avoiding interferences from other species, and in addition RP-HPLC allows the separation and determination of non-ionic complexes.

This method allows the separation and determination of metal complexes using a mobile phase that contains a surfactant, 1-propanol and a complexing ligand at the pH value of the mobile phase in the absence of other additives in a short analysis time and with better sensitivity and detection limits than in the absence of the surfactant.

Acknowledgements

We gratefully acknowledge the support of this work through a research grant from the University of Alcalá de Henares (ref. 91B/14 and 92/27) and DGICYT (Spain) (ref. PS90-0026). We also thank Pedro Gámez for supplying the metal samples analysed.

References

[1] M.L. Marina, J.C. Díez-Masa and M.V. Dabrio, *J. Liq. Chromatogr.*, 12 (1989) 1973.
[2] K.L. Cheng, K. Ueno and T. Imamura (Editors), *CRC Handbook of Organic Analytical Reagents*, CRC Press, Boca Raton, FL, 1982, p. 389.
[3] G. Schwedt, *Chromatographia*, 11 (1978) 145.
[4] O. Liska, J. Lehotay, E. Brandsteterova, G. Guiochon and H. Colin, *J. Chromatogr.*, 172 (1979) 384.
[5] A.M. Bond and G.G. Wallace, *Anal. Chem.*, 53 (1981) 1209.
[6] A.M. Bond and G.G. Wallace, *Anal. Chem.*, 54 (1982) 1706.
[7] A.M. Bond and G.G. Wallace, *Anal. Chem.*, 55 (1983) 718.
[8] A.M. Bond and G.G. Wallace, *Anal. Chim. Acta*, 164 (1984) 223.
[9] R.M. Smith, A.M. Butti and A. Thakur, *Analyst*, 110 (1985) 35.
[10] I. Martí, N. Manero and M. Almarcha, *Técnicas de Laboratorio*, 11 (1988) 373.
[11] S.R. Hutchins, P.R. Haddad and S. Dilli, *J. Chromatogr.*, 252 (1982) 185.
[12] L. Svoboda and P. Prokes, *Collect. Czech. Chem. Commun.*, 57 (1992) 1843.
[13] E. Pelizzetti and E. Pramauro, *Anal. Chim. Acta*, 169 (1985) 1.
[14] G.L. McIntire, *CRC Crit. Rev. Anal. Chem.*, 21 (1990) 257.
[15] F. Fernández, M. L. Marina and A.R. Rodríguez, in J.J. Durig (Editor), *Vibrational Spectra and Structure*, Elsevier, Amsterdam, 1991, p. 113.
[16] M.P. San Andrés, M.L. Marina and S. Vera, *Talanta*, 41 (1994) 179.
[17] M.P. San Andrés, M.L. Marina and S. Vera, *Analyst*, 119 (1994), in press.
[18] W.L. Hinze and D.W. Armstrong (Editors), *Ordered Media in Chemical Separations*, (*ACS Symposium Series* No. 342), American Chemical Society, Washington, DC, 1987.
[19] D.W. Armstrong, *Sep. Purif. Methods*, 14 (1985) 213.
[20] J.G. Dorsey, *Adv. Chromatogr.*, 27 (1987) 167.
[21] D.W. Armstrong and F. Nome, *Anal. Chem.*, 53 (1981) 1662.
[22] M. Arunyanart and L.J. Cline Love, *Anal. Chem.*, 56 (1984) 1557.
[23] A. Berthod and J.G. Dorsey, *Analusis*, 16 (1988) 75.
[24] L.J. Cline Love, J.G. Habarta and J.G. Dorsey, *Anal. Chem.*, 56 (1984) 1132A.
[25] T. Okada, *Anal. Chem.*, 60 (1988) 2116.
[26] Y. Zhao and Ch. Fu, *Analyst*, 116 (1991) 621.
[27] H. Sirén, *Chromatographia*, 29 (1990) 144.
[28] T. Okada, *Anal. Chem.*, 64 (1992) 589.
[29] H. Irth, G.J. de Jong, U.A. Th. Brinkman and R.W. Frei, *Anal. Chem.*, 59 (1987) 98.
[30] Cs. Horváth, *High-Performance Liquid Chromatography —Advances and Perspectives*, Vol. 2, Academic Press, New York, 1980, 176.
[31] A.S. Kord and M.G. Khaledi, *Anal. Chem.*, 64 (1992) 1894.

ELSEVIER

Journal of Chromatography A, 685 (1994) 279–285

JOURNAL OF CHROMATOGRAPHY A

Use of microwave irradiation for rapid synthesis of perfluorooctanoyl derivatives of fatty alcohols, a new derivative for gas chromatography–mass spectrometric and fast atom bombardment mass spectrometric study

Amitava Dasgupta[a,*], William C. Thompson[a], Sohail Malik[b]

[a]*Department of Pathology, University of New Mexico School of Medicine, 2211 Lomas Boulevard N.E., Albuquerque, NM 87106, USA*

[b]*Department of Laboratory Medicine, University of Washington, Seattle, WA, USA*

First received 23 March 1994; revised manuscript received 18 July 1994

Abstract

Structural analyses of fatty alcohols as acetate, trifluoroacetate and trimethylsilyl derivatives are frequently used in lipid biochemistry. Those derivatives produce molecular ions (m/z) <400. Perfluorooctanoyl derivatives of fatty alcohols which can produce ions in the range of 600–700 (m/z) have never been studied before. We prepared perfluorooctanoyl derivatives of fatty alcohols by heating them with perfluorooctanoyl chloride for 15 min at 60°C. Using low-power microwave irradiation (240 W), we can reduce the reaction time to only 2 min. The yields of the derivatives were quantitative by both microwave technique and conventional heating as evidenced by absence of starting material (fatty alcohols) in the HPTLC analysis. The mass spectral fragmentation patterns of the derivatives obtained by microwave irradiation are identical to the derivatives prepared by conventional heating. We also prepared trimethylsilyl derivatives of fatty alcohols, a widely used derivative, in 1.5 min using microwave irradiation (power 3, 240 W) where the conventional technique requires 20 min. We conclude that microwave irradiation can be employed for rapid preparation of perfluorooctanoyl and trimethylsilyl derivatives of fatty alcohols for gas chromatography–mass spectrometric analysis.

1. Introduction

Fatty alcohols and aldehydes have been isolated from lipids of bacteria, animals and plants [1–4]. Surface lipids usually contain a complex mixture of fatty acids esterified to fatty alcohols (wax esters), hydrocarbons, non-esterified fatty acids and sterols. Free and esterified fatty alcohols are also found in large quantities in germinating seeds for the purpose of energy storage. Wax esters are also abundant in marine organisms, for example the oil of the sperm whale contains 70% wax ester while the oil of deep sea fish orange roughy contains 95% wax esters. For analysis, wax esters are hydrolyzed to liberate fatty acids and fatty alcohols. After separation, fatty alcohols are derivatized and analyzed by gas chromatography (GC) or GC–mass spectrometry (MS) [5,6].

The presence of mycobacteria in drinking

* Corresponding author.

0021-9673/94/$07.00
SSDI 0021-9673(94)00673-3

water represents a significant public health problem. Hydrolysis of wax esters from those mycobacteria produces characteristic fatty alcohols which are derivatized and analyzed by GC–MS for identification of those bacteria in drinking water [7,8]. The Sjogren–Larsson syndrome, an autosomal recessive disorder is due to the defect in fatty alcohol cycle. Affected patients usually survive childhood, but life expectancy is decreased. Cultured skin fibroblast of these patients accumulate fatty alcohols and analysis of fatty alcohol after derivatization is used as a diagnostic aid for this disease [9,10].

Long-chain fatty acyl coenzyme A thioesters have been implicated as substrates for several metabolic reactions [11] and their concentrations can be increased in many pathological conditions like ischemia. The assay of those compounds can be performed by taking advantage of borohydride reduction of those thioesters to fatty alcohols [12].

Usually, fatty alcohols are analyzed after converting them to acetate, trifluoroacetyl or trimethylsilyl derivatives. Those derivatives usually produce characteristic ions in the mass range < 400. Recently, derivatization of amphetamine and methamphetamine with perfluorooctanoyl chloride have been described [13]. We studied the possibility of derivatizing fatty alcohols with that reagent in order to produce ions in the much higher mass region 600–700 for unambiguous structural analysis. To our knowledge, this particular derivative of fatty alcohols has not been reported before.

Recently, microwave irradiation was demonstrated to produce dramatic acceleration of reaction rates. Dayal et al. [14] described a method for rapid hydrolysis of bile acid methyl esters using a commercially available microwave oven. Microwave-induced rapid acceleration of reaction rates for Diels–Alder, Ene, Claisen reaction, hydrolysis of proteins and peptides had been described [15–17]. The use of microwave irradiation for rapid epoxidation of fatty acid esters, cyclization of dioxostearates and oxounsaturated fatty acids esters into furanoid derivatives, conversion of epoxystearate to oxostearate and substitution of a tosyl group by an azide group have also been described in the literature [18]. We previously reported microwave-induced rapid transesterification of lipids and accelerated synthesis of fatty acyl pyrrolidides for GC–MS study [19]. We also reported the use of microwave oven for rapid preparation of conventional acetate and trifluoroacetyl derivatives of fatty alcohols [20]. Now we would like to report synthesis of perfluorooctanoyl derivative of fatty alcohols, a new derivative, and conventional trimethylsilyl derivatives using microwave irradiation.

2. Experimental

Cetyl, stearyl, oleyl, linoleyl, arachidonyl, arachidyl alcohol and eicosenol were purchased from Sigma (St. Louis, MO, USA). The derivatizing agent bis(trimethylsilyl)trifluoroacetamide was also purchased from Sigma while perfluorooctanoyl chloride was procured from PCR (Gainsville, FL, USA). The derivatizing reactions were carried out in reaction vials with a total capacity of 1 ml (Pierce, Rockford, IL, USA). The vials were capped with mini inert valves also available from Pierce.

The HPTLC plates coated with silica were obtained from EM Separations (Gibbstown, NJ, USA). The developing solvent was hexane–ethyl acetate (65:35). After developing, bands were visualized by spraying with 4% copper sulfate in 30% phosphoric acid followed by heating. The microwave oven used in this study has a total capacity of 800 W (Samsung, Model MW 5510 T). The GC–MS analysis was carried out using a Model 5890 gas chromatograph coupled with 5970 series mass-selective detector (Hewlett-Packard, Palo Alto, CA, USA). The capillary column used was an Ultra-2, also available from Hewlett-Packard. The initial oven temperature of the gas chromatograph was 180°C. After maintaining the temperature for 2 min, the temperature was increased at a rate of 4°C/min to reach an oven temperature of 240°C. Then the

oven temperature was increased at a rate of 10°C/min to reach a final oven temperature of 280°C. The mass spectrometer was operated in a scan mode with a scan range of 40–800 m/z, or a scan range of 200–800 m/z.

The fast atom bombardment (FAB) MS study was performed using a Model VG 70-SEQ mass spectrometer manufactured by Varian Instruments. The matrix used for this study was 3-nitrobenzoyl alcohol. The samples were bombarded with xenon atom beams with 8 keV energy.

2.1. Preparation of perfluorooctanoyl derivatives

We added 50 μl of derivatizing reagent to 0.01–0.05 mg of the fatty alcohol. The reaction was also complete in 2 min under microwave irradiation (power 3, 240 W). Gjerde et al. [13] recommended 30 min of heating at 60°C for conversion of amphetamine and methamphetamine to their corresponding perfluorooctanoyl derivative. Our study indicated that quantitative conversion of fatty alcohol to perfluorooctanoyl derivative can be achieved by heating the reaction mixture at 60°C for 15 min. After the reaction, excess derivatizing reagents were evaporated to dryness and the residue was reconstituted in ethyl acetate and injected into the GC–MS system.

2.2. Preparation of trimethylsilyl derivatives

We added 300 μl of bis(trimethylsilyl)trifluoroacetamide to 0.1–0.2 mg of fatty alcohol. Under microwave irradiation, the reaction was completed in 1.5 min under low power (power 3, 240 W) as evidenced by complete disappearance of starting material in the HPTLC analysis. For conventional conditions, the reaction mixture was allowed to stand at the room temperature for 20 min. Since fatty alcohols are stable only in excess derivatizing agent no work-up was performed. The reaction mixture was directly injected into the GC–MS system.

3. Results and discussion

3.1. Microwave technique for rapid derivatization

The microwave provides a rapid and convenient method for preparation of perfluorooctanoyl derivatives of fatty alcohols for structural analysis by GC–MS. The R_F values by HPTLC of derivatives prepared by microwave irradiation and conventional technique are always the same. Analysis of reaction products after microwave irradiation by HPTLC showed quantitative conversion of fatty alcohols to the perfluorooctanoyl derivatives. We also did not observe any undesirable decomposition products. The quantitative conversion of fatty alcohols to the corresponding derivatives either by microwave irradiation or conventional heating was also evidenced by the absence of underivatized alcohol peaks in the gas chromatogram. Moreover, the GC retention times and MS fragmentation patterns of fatty alcohol derivatives prepared by microwave irradiation were identical to those fatty alcohol derivatives prepared by conventional heating. Therefore, microwave irradiation produced derivatives which have the same chemical identity as derivatives produced by conventional heating (Table 1, Fig. 1).

We also use microwave irradiation for rapid derivatization of fatty alcohols with bis(trimethylsilyl)trifluoroacetamide because trimethylsilyl derivatives of fatty alcohols are widely used by investigators in lipid biochemistry. Weppelman et al. [21] recommended 20 min incubation of reaction mixture at room temperature for complete conversion to trimethylsilyl derivatives while Myher and Kuksis [22] recommended an incubation period of 30–60 min for complete conversion. Our results indicate that reaction was complete in 20 min. On the other hand the conversion of fatty alcohols to the corresponding trimethylsilyl derivatives was complete in 90 s under low-power microwave irradiation (power level 3, 240 W). The R_F value of trimethylsilyl derivatives of fatty alcohols prepared by microwave irradiation was the same as

Table 1
Mass spectral characterization of perfluorooctanoyl derivatives of fatty alcohols prepared by microwave irradiation and conventional heating

Compound	Mass spectral fragmentation pattern					
	Microwave			Conventional heating		
	M^{+} [a]	Base[a]	Other peaks[a]	M^{+} [a]	Base[a]	Other peaks[a]
Cetyl	–	43 (100)	620 (1), 224 (10)	–	43 (100)	620 (1), 224 (8)
Stearyl	–	43 (100)	648 (1), 252 (13)	–	43 (100)	648 (1), 252 (9)
Oleyl	664 (9)	55 (100)	578 (1), 369 (2)	664 (7)	55 (100)	578 (1), 369 (2)
Linoleyl	662 (15)	67 (100)	578 (3), 564 (4)	662 (13)	67 (100)	578 (3), 564 (3)
Arachidyl	–	57 (100)	676 (1), 479 (1)	–	57 (100)	676 (1), 479 (1)
11-Eicosenol	692 (3)	55 (100)	578 (1), 369 (1)	692 (3)	55 (100)	578 (1), 369 (1)
Arachidonyl	686 (2)	79 (100)	588 (9), 548 (9)	686 (2)	79 (100)	588 (8), 548 (8)

[a] m/z Values; relative intensities in parentheses.

the derivatives prepared by conventional technique. Similarly, the GC retention times were also similar. The MS fragmentation patterns were also identical again indicating that trimethylsilyl derivatives prepared by microwave irradiation had the same chemical identities as the derivatives prepared by the conventional technique (Table 2).

3.2. Electron impact and FAB mass spectra of fatty alcohol derivatives

The major advantage of derivatizing fatty alcohol with perfluorooctanoyl chloride is the significant increase in the molecular ion peak. For example, the perfluorooctanoyl derivative of arachidonyl alcohol (20:4) showed a molecular

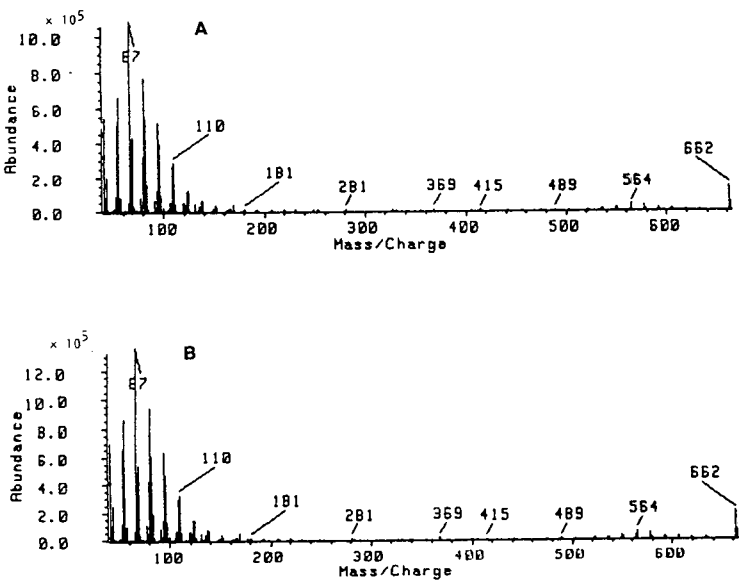

Fig. 1. Mass spectral fragmentation patterns of the perfluorooctanoyl derivative of linoleyl alcohol prepared by (A) conventional heating and (B) microwave irradiation.

Table 2
Mass spectral characterization of trimethylsilyl derivatives of fatty alcohols prepared by microwave irradiation and conventional heating

Compound	Mass spectral fragmentation pattern					
	Microwave			Conventional heating		
	M^+ [a]	Base[a]	Other peaks[a]	M^+ [a]	Base[a]	Other peaks[a]
Cetyl	299 (100)	299 (100)	314 (1), 75 (24)	299 (100)	299 (100)	314 (1), 75 (29)
Stearyl	327 (100)	327 (100)	342 (1), 75 (26)	327 (100)	327 (100)	342 (1), 75 (30)
Oleyl	325 (29)	75 (100)	340 (8), 297 (8)	325 (25)	75 (100)	340 (7), 297 (6)
Linoleyl	323 (12)	75 (100)	338 (3), 295 (2)	323 (14)	75 (100)	338 (4), 295 (2)
Arachidyl	355 (100)	355 (100)	339 (1), 75 (23)	355 (100)	355 (100)	339 (1), 75 (30)
11-Eicosenol	353 (31)	75 (100)	368 (11), 325 (10)	353 (29)	75 (100)	368 (9), 325 (8)
Arachidonyl	347 (1)	79 (100)	362 (2), 271 (2)	347 (1)	79 (100)	362 (2), 271 (1)

[a] m/z Values; relative intensities in parentheses.

ion peak at m/z 686 while the conventional trimethylsilyl derivative showed a weak M − 15 peak at m/z 347. In our previous study with microwave-induced rapid preparation of acetyl and trifluoroacetyl derivatives of fatty alcohols, the molecular ion peaks of arachidonyl alcohol were observed only at m/z 332 and m/z 386 respectively [20].

The strongest peaks in the perfluorooctanoyl derivatives of fatty alcohols were observed in the lower mass region (m/z 40–100) while the peaks in the higher mass region (m/z 200–600) showed much lower relative abundances. This feature is also common to other conventional fluoro derivatives of fatty alcohols, for example, the molecular ion peak (m/z 686) and peaks at m/z 588 and m/z 548 in the mass spectrum of the perfluorooctanoyl derivative of arachidonyl alcohol showed relative abundances of 2, 9 and 8%, respectively, relative to the base peak at m/z 79. The relative abundances of molecular ion peak (m/z 386) and peaks at m/z 288 and 248 in the mass spectrum of the trifluoroacetyl derivative of the same alcohol were 3, 10 and 12%, respectively, relative to the base peak at m/z 79 [20]. The trimethylsilyl derivative of arachidonyl alcohol also showed a base peak at m/z 79. However, the M − 15 peak at m/z 347 has a relative abundance of only 1% and the two other peaks at higher mass range at m/z 362 and m/z 271 had relative abundances of only 2% each.

In order to circumvent this problem, we studied FAB mass spectra of perfluorooctanoyl derivatives of fatty alcohols. Interestingly, saturated alcohols showed a weak M − 1 ion peak while any molecular ion or M − 1 peaks were absent in the electron impact mass spectra for those alcohols. The molecular ion peaks are also absent in conventional trifluoroacetyl or acetate derivatives of fatty alcohols [20]. Therefore, FAB-MS analysis has a distinct advantage over conventional electron impact for unambiguous determination of molecular mass of saturated alcohol. We also observed molecular ion peaks and M − 1 peaks in the FAB mass spectra of unsaturated alcohols. With some derivatized alcohol, specially arachidonyl alcohol, the M − 1 peak at m/z 685 was even stronger than molecular ion peak at m/z 686 (Fig. 2). We observed peaks with slightly higher relative abundances in the higher range of mass spectrum in FAB mode compared to the electron impact mode, but again the strongest peaks were observed in the lower mass range ($m/z < 200$) as observed with the electron impact mass spectra (Fig. 2). We did not observe any additional strong diagnostic peak in the higher mass range in the FAB spectra compared to electron impact spectra. Therefore, for unsaturated alcohols, FAB mass

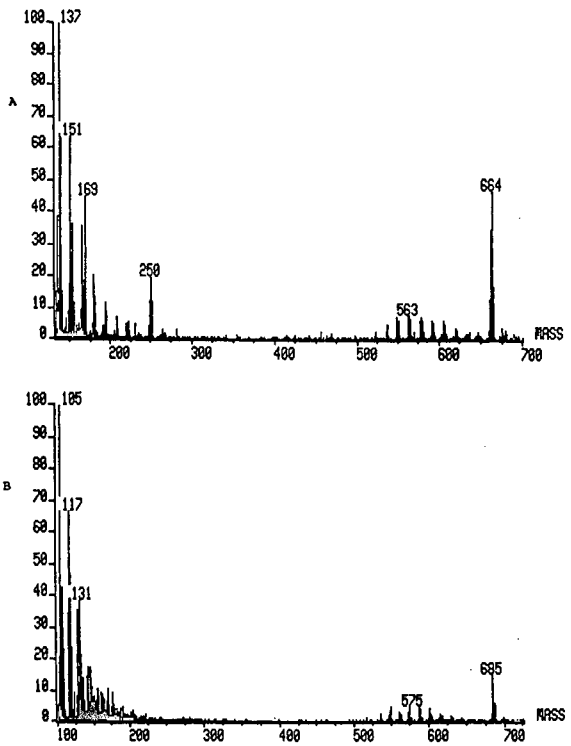

Fig. 2. Fast atom bombardment mass spectrum of perfluorooctanoyl derivatives of (A) oleyl alcohol and (B) arachidonyl alcohol.

spectra did not have any distinct advantage over the conventional electron impact mass spectra for structural analysis.

Since a FAB facility is not available to all laboratories, we studied the possibility of scanning the mass spectrometer of our GC–MS system from m/z 200 to 800 in order to increase the intensities of peaks in the higher mass range. We observed the same fragmentation patterns for all compounds as expected compared to spectra obtained by scanning the mass spectrometer from m/z 40 to 800. However, we observed significant increases in the relative abundances of all peaks in the higher mass ranges for all alcohols. For all unsaturated alcohols, except for arachidonyl alcohol the molecular ion peaks became the base peak. Other characteristic peaks in the 500–650 regions were more prominent when the mass spectrometer was scanned from m/z 200 to 800. For example, the molecular ion peak for arachidonyl derivative has a relative abundance of 40.1% when the mass spectrometer was scanned from m/z 200 to 800 compared to the relative abundance of 2% when scanning from m/z 40 to 800. Similarly, the diagnostic peaks at m/z 588 and m/z 548 had relative abundances of 97.7 and 100% compared to the relative abundances of 8.0 and 7.9%, respectively, when the mass spectrometer was scanned from m/z 40 to 800. Our results showed an excellent signal-to-noise ratio for those diagnostic peaks in the higher mass range when the mass spectrometer was scanned from m/z 200 to 800 (Fig. 3). However the sensitivity of detection was lower when we operated our mass spectrometer in that mode.

3.3. Perfluorooctanoyl versus trimethylsilyl derivatives

The major advantage of derivatizing fatty alcohols with perfluorooctanoyl chloride is the significant increase in the molecular ion peak in the mass spectrum as well as lower volatility of the derivative which can aid in eliminating interfering peaks in the gas chromatogram. Extracts from serum or another biological matrix often contains relatively volatile compounds that show up in the lower temperature zone of a gas chromatogram.

The molecular ion peaks of perfluorooctanoyl derivatives of unsaturated fatty alcohols showed higher abundance than saturated fatty alcohols (M − 1 peaks were present only in the FAB mode). On the other hand M − 15 peaks were very strong in the trimethylsilyl derivatives of saturated fatty alcohols, while the peaks were relatively weak with unsaturated alcohols (Tables 1 and 2). Because of these opposite characteristics in the molecular ion peaks for saturated versus unsaturated alcohol, perfluorooctanoyl and trimethylsilyl derivatives can provide complementary structural information for identification of fatty alcohols.

Our results clearly indicate that microwave irradiation is a rapid and convenient way of preparing perfluorooctanoyl and trimethylsilyl

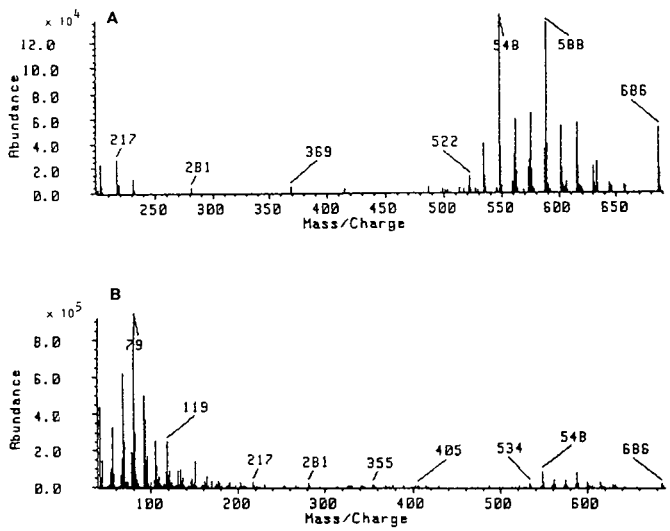

Fig. 3. Mass spectral characteristics of the perfluorooctanoyl derivative of arachidonyl alcohol. (A) Scan from m/z 200 to 800; (B) scan from m/z 40 to 800.

derivatives of fatty alcohols for structural identifications. Moreover, perfluorooctanoyl derivatives of fatty alcohols, a derivative not studied before, offer unique advantages of longer retention times and more characteristic peaks in higher mass region for identification purpose.

References

[1] W.F. Naccarato, R.A. Gelman, J.C. Kawalek and J.R. Gibertson, *Lipids*, 7 (1972) 275.
[2] A.P. Tulloch, *Lipids*, 5 (1970) 247.
[3] P.E. Kolattukudy, *Lipids*, 5 (1970) 259.
[4] T. Takahashi and H.H.O. Schmid, *Lipids*, 5 (1970) 243.
[5] J.C. Nevenzel, *Lipids*, 5 (1970) 308.
[6] R.A. Moreau and A.H.C. Huang, *Arch. Biochem. Biophys.*, 194 (1979) 422.
[7] S. Alugupalli, L. Larsson, M. Slosarek and M. Jaresova, *Appl. Environ. Microbiol.*, 58 (1992) 3538.
[8] L. Larsson, J. Jimenez, P. Valero-Guillen, F.M. Luengo and M. Kubin, *J. Clin. Microbiol.*, 27 (1989) 2388.
[9] W.B. Rizzo, A.L. Dammann, D.A. Craft, S. Black, A. Tilton, D. Africk, E.C. Carballo, G. Holmgren and S. Jagell, *J. Pediatr.*, 115 (1989) 228.
[10] W.B. Rizzo, A.L. Dammann, D.A. Craft, *J. Clin. Invest.*, 81 (1988) 738.
[11] D. Riendeau and E. Meighen, *Experientia*, 41 (1985) 707.
[12] M.R. Prasad and J. Saulter, *Anal. Biochem.*, 162 (1987) 202.
[13] H. Gjerde, I. Hasvold, G. Pettersen and A. Christophersen, *J. Anal. Toxicol.*, 17 (1993) 65.
[14] B. Dayal, G. Salen and V. Dayal, *Chem. Phys. Lipids*, 59 (1991) 97.
[15] R.J. Giguere, A.M. Namen, B.O. Lopez, A. Arepally, D.E. Ramos and G. Majetich, *Tetrahedron Lett.*, 28 (1987) 6553.
[16] R.N. Gedye, F.E. Smith and K.C. Westway, *Can. J. Chem.*, 66 (1988) 17.
[17] S.H. Chou and K.T. Wang, *J. Chromatogr.*, 491 (1989) 424.
[18] M. Lie Ken Jie and C. Yan-Kit, *Lipids*, 23 (1988) 367.
[19] A. Dasgupta, P. Banerjee and S. Malik, *Chem. Phys. Lipids*, 62 (1992) 281.
[20] A. Dasgupta and P. Banerjee, *Chem. Phys. Lipids*, 65 (1993) 217.
[21] R.M. Weppelman, W.J.A. Vandenheuvel and C.C. Wang, *Lipids*, 11 (1976) 209.
[22] J.J. Myher and K. Kuksis, *Lipids*, 9 (1974) 382.

ELSEVIER

Journal of Chromatography A, 685 (1994) 287–293

JOURNAL OF CHROMATOGRAPHY A

Selective thermolysis of the enol forms of acetoacetates during gas chromatography, revealed by combined matrix-isolation Fourier transform infrared and mass spectrometry

P. Jackson[a], D. Carter[a], G. Dent[a], B.W. Cook[b], J.M. Chalmers[c], I.R. Dunkin[d,*]

[a]*Zeneca Specialties Research Centre, P.O. Box 42, Hexagon House, Blackley, Manchester M9 8ZS, UK*

[b]*ICI Chemicals and Polymers, P.O. Box 8, The Heath, Runcorn, Cheshire WA7 4QD, UK*

[c]*ICI Materials, Wilton Research Centre, P.O. Box 90, Wilton, Middlesborough, Cleveland TS6 8JE, UK*

[d]*Department of Pure and Applied Chemistry, University of Strathclyde, 295 Cathedral Street, Glasgow G1 1XL, UK*

First received 31 May 1994

Abstract

The thermal decompositions of methyl and ethyl acetoacetates have been observed by combined gas chromatography (GC)–mass spectrometry–matrix-isolation Fourier transform infrared spectrometry. Under the conditions employed, keto and enol forms could be separated by GC and, by careful control of interface temperatures, the thermolysis of the individual components could be studied. Each enol acetoacetate form was almost completely converted to a keto-ketene and an alcohol. The keto-acetoacetate forms were only partially decomposed, with reaction products identical to those of the enol forms, indicating that the preferred mechanism of thermal degradation is via the enol-acetoacetate form.

1. Introduction

1.1. Gas chromatography with combined matrix-isolation Fourier transform infrared and mass spectrometry

Recently, work has been performed to evaluate the complementary information obtained from combined matrix-isolation (MI) Fourier transform (FT) infrared (IR) spectrometric and mass spectrometric (MS) examination of peaks eluting from a gas chromatography (GC) column using a Mattson Cryolect GC–MS–MI-FT-IR instrument. The FT-IR spectra are recorded from a portion of the GC eluent trapped in an argon matrix at approximately 11 K on a rotating, gold-coated drum. The mass spectra are recorded in parallel using a VG Trio-1 operating in positive ion electron ionization (EI^+) mode.

During a part of this work, it was noticed that a GC-isolated component, identified as an acetoacetate, had a strong band in the IR spectrum at 2150 cm^{-1}, which was inconsistent with its presumed structure. Similar IR bands appear in several Cryolect matrix-isolation IR reference spectra of acetoacetates, but do not appear in any of the liquid or vapour-phase spectra of acetoacetates.

In this paper we report a study of the GC of methyl and ethyl acetoacetates using the Mattson

* Corresponding author.

0021-9673/94/$07.00
SSDI 0021-9673(94)00672-5

Cryolect instrument. It was found that, with the conditions employed, the keto and enol forms of the acetoacetates are not rapidly equilibrated and are eluted separately. It was also found that high temperatures in the transfer line connecting the GC column with the matrix spray-on device can induce a selective thermolysis of the enol forms.

1.2. Chromatography of acetoacetates

It has been known for a long time (see, e.g., [1]–[3]) that acetoacetates exist as equilibrium mixtures of the keto (**1**) and enol (**2a** ⇌ **2b** ⇌ **2c**) forms (Fig. 1). The rate of equilibration in the pure state is not very rapid, but traces of H^+ or OH^- catalyse this process. As long ago as 1911, Knorr et al. [4], by careful work at low temperatures, were able to prepare reasonably pure samples of the keto and enol forms of ethyl acetoacetate (**1**, R = Et), and estimated the proportions of keto and enol forms in the equilibrium mixture from refractive index measurements. Recently it has been demonstrated that low-temperature HPLC on silica or modified silica columns can separate the keto and enol forms of both methyl and ethyl acetoacetates, and evidence for a third equilibrium component, possibly the unconjugated enol (**3**, R = Et), was obtained in the latter case [5,6]. The enol form was found to revert to the equilibrium mixture if the eluate was heated to 90°C for 1 min. These HPLC studies showed that the equilibrium constant for ethyl acetoacetate (K = [enol]/[keto]) varies considerably with the medium, e.g. at 25°C from ca. 0.05 in water, through 0.092 in the pure liquid (8% enol), to ca. 1 in hexane and cyclohexane [5]. In the pure liquid at 25°C, methyl acetoacetate (**1**, R = Me) contains about 6% of the enol and is thus slightly less enolized than the ethyl analogue. In the measurement of keto–enol equilibrium constants, HPLC has an advantage over NMR methods, since it can be conveniently applied to more dilute solutions. With unsymmetrical β-dicarbonyl compounds, e.g. **1**, two isomeric *cis*-enols, **2a** and **2c**, are distinguishable in principle, but linewidth measurements in the ^{17}O NMR spectra of some β-diketones suggest that interconversion of these is usually very rapid [7].

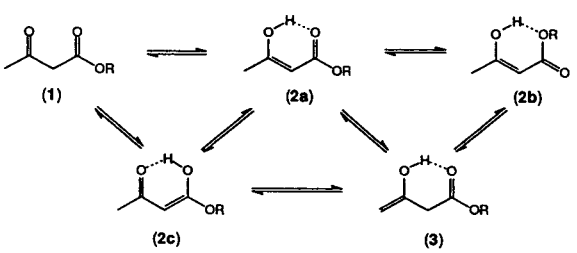

Fig. 1. Keto–enol equilibria in acetoacetates.

Studies of acetoacetates by GC have shown that, in a sufficiently hot injector system, decomposition can occur either intramolecularly [8] or by reaction with traces of water [9]. The term *reaction gas chromatography* has been applied to the use of GC in these conditions [8,10]. When the decomposition yields unstable primary products, they cannot be observed directly by conventional means. The development of MI-FT-IR as a method of examining the components eluted from a GC column provides the opportunity to trap these reactive decomposition products in a low-temperature matrix and identify them by IR spectrometry.

2. Experimental

Methyl and ethyl acetoacetates were 99% pure standards obtained as commercial samples (Aldrich), which were checked for purity by routine techniques. The sample studied here was prepared as a 1:1 mixture of the two acetoacetates as an approximately 0.1% solution in dichloromethane.

The Mattson Cryolect GC–MS–MI-FT-IR instrument [11] was equipped with a CP-SIL-8-CB capillary column (25 m × 0.32 mm I.D., film thickness 0.25 μm). Samples were introduced to the column using split injection (approximately 30:1 split ratio) at 150°C and the following GC temperature program was used for the separation: 50°C (2 min), 10°C/min to 150°C (2 min). Components were eluted using helium as the carrier gas, and the eluate was split three ways

after separation using a simple three-hole ferrule and balanced capillary transfer lines. One stream (20%) passed to a conventional flame ionization detection (FID) system, the second (40%) to the MS transfer line, and the third (40%) to the matrix-deposition system. Here the eluate was diluted with a large excess of argon (approximately 1000:1) and deposited through a fine capillary tip as an argon matrix on a rotating, gold-coated drum at ca. 11 K. The resulting matrix had a helical path on the outer surface of the drum, with the individual components of the sample spatially separated in the matrix. The cryogenic drum could be relocated by a computer-controlled stepper motor to position any part of the matrix in the IR beam. Each component could thus be examined by FT-IR spectrometry. The instrument provides precise control of the temperatures of the injector system, the GC column, the transfer capillaries and the matrix-deposition tip.

3. Results and discussion

Fig. 2 shows a GC–FT-IR chromatogram of a 1:1 mixture of methyl and ethyl acetoacetates obtained with transfer line and deposition tip temperature of 180°C. The chromatogram shows four separated components, denoted *A–D*. The major two components (*C* and *D*) can be identified as the keto forms of methyl and ethyl acetoacetates, respectively, and the minor components (*A* and *B*) as the corresponding enols. The reasons for these assignments are as follows. The mass spectra of components *A* and *C* were identical, with a molecular ion at *m/z* 116, in accordance with the formula $C_5H_8O_3$, while components *B* and *D* had a molecular ion at *m/z* 130, indicating the formula $C_6H_{10}O_3$. The MI-FT-IR spectra of components *A–D* are shown in Figs. 3–6, respectively. The major components, *C* and *D*, had IR absorptions in the carbonyl (C = O) stretching region at 1724–1755 cm^{-1} (Figs. 5 and 6); whereas the minor components, *A* and *B*, each had weaker carbonyl absorptions (relative to other bands in the spectra) at lower wavenumber (1655–1683 cm^{-1}) and an additional band at 1636–1638 cm^{-1}, which is consistent with a carbonyl group adjacent to an unsaturated carbon–carbon bond (Figs. 3 and 4). The keto forms both exhibit two bands in the carbonyl stretching region, as expected for molecules containing both ketone and ester functionalities, but the possibility of site-effect splitting cannot be excluded (see, e.g., [12]). Each of the enols also showed more than one carbonyl band.

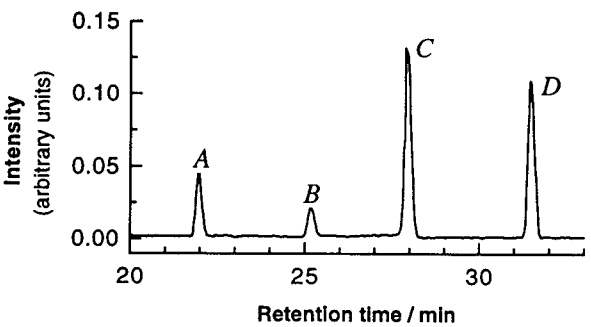

Fig. 2. GC–FT-IR chromatogram of a 1:1 mixture of methyl and ethyl acetoacetates (**1**, R = Me and R = Et), obtained with a GC injector temperature of 150°C and transfer-line temperature of 180°C. The GC conditions were as follows: column CP-SIL-8-CB, 25 m × 0.32 mm I.D., 0.25 μm film thickness; program 50°C (2 min), 10°C/min to 150°C (2 min). Peaks: *A* = methyl acetoacetate enol; *B* = ethyl acetoacetate enol; *C* = methyl acetoacetate keto; *D* = ethyl acetoacetate keto.

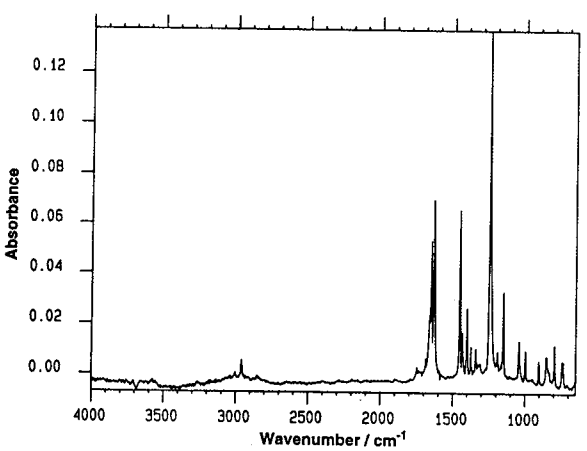

Fig. 3. Argon MI-FT-IR spectrum in the range 4000–650 cm^{-1} obtained from component *A* of Fig. 2 (methyl acetoacetate enol). The GC–matrix-isolation interface transfer-line temperature was 180°C.

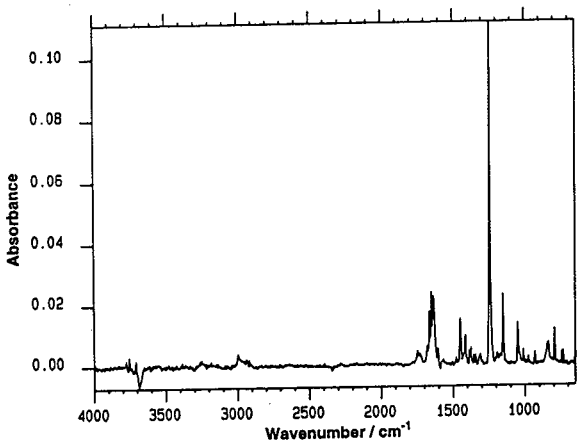

Fig. 4. Argon MI-FT-IR spectrum in the range 4000–650 cm^{-1} obtained from component *B* of Fig. 2 (ethyl acetoacetate enol). The GC–matrix-isolation interface transfer-line temperature was 180°C.

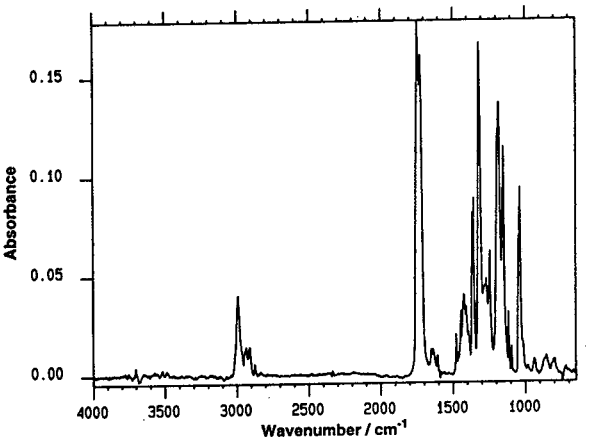

Fig. 6. Argon MI-FT-IR spectrum in the range 4000–650 cm^{-1} obtained from component *D* of Fig. 2 (ethyl acetoacetate keto). The GC–matrix-isolation interface transfer-line temperature was 180°C.

These could be due to the presence of more than one enol isomer in each case (cf. **2a**, **2b**, **2c** and **3**), but could equally reflect matrix site effects. Neither enol had an obvious O–H stretching absorption, but a study of matrix-isolated salicylaldehyde and derivatives by Gebicki and Krantz [13] has shown that sometimes only weak, very broad O–H bands are found for intramolecular hydrogen bonds. It seems that the matrix-isolated enols in our experiments fall into this category.

The observed solvent effect on keto–enol equilibria (see above) [5] establishes that enols are less polar than the corresponding keto forms. This accords with our observation that the enols are eluted first from the GC column. The measured peak-area ratios (keto:enol) in Fig. 2 are approximately 4:1 for each of the acetoacetates. This is in fair agreement with data reported previously for ethyl acetoacetate at room temperature in dichloromethane [5], but the peak areas in the GC–FT-IR chromatogram —computed from IR intensities— can vary considerably depending on the functional groups present. GC–FID traces, which are probably more reliable as indicators of the relative mol quantities, gave ratios varying between 8.7:1 and 16.4:1. It is likely that these measurements reflect the equilibrium in solution, but the possibility of rapid tautomerization in the GC injector (possibly catalysed by trace acidic impurities) must also be considered. Nevertheless, it is clear from the clean chromatographic peak shapes that such rapid tautomerization did not occur in the GC column during elution, and the dissimilarity of the keto and enol FT-IR spectra indicates that

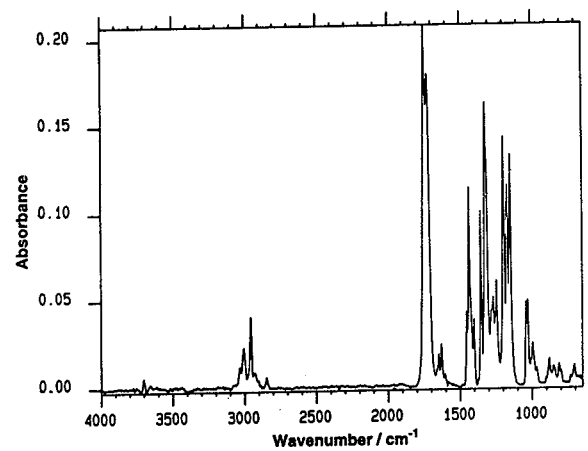

Fig. 5. Argon MI-FT-IR spectrum in the range 4000–650 cm^{-1} obtained from component *C* of Fig. 2 (methyl acetoacetate keto). The GC–matrix-isolation interface transfer-line temperature was 180°C.

neither did such tautomerization occur in the transfer line or matrix-deposition tip at 180°C.

When the transfer-line temperature was raised from 180 to 250°C, the resulting FT-IR spectra of the four components showed clear signs of thermally induced decomposition. Each spectrum contained characteristic ketene C=C=O stretching bands at 2133–2143 cm^{-1} (Figs. 7 and 8) (cf., e.g., [14]). The ketenes clearly arise by thermolysis in the transfer line, and the two enols show a much greater degree of decomposition than the keto forms.

The formation of ketenes from the thermolysis of acetoacetates has already been suggested [8], although their direct observation has not previously been achieved. The proposed mechanism of thermolysis involves an enol as the key intermediate, and predicts that a keto-ketene (**4**) and an alcohol are the products (Fig. 9). The advantage of MI-FT-IR is that it allows direct observation of unstable species such as ketenes (**4**). Under this scheme, any ketene found arising from the keto form of acetoacetates probably arises via the corresponding enol. It should be noted, however, that a mechanism can be postulated for the direct transformation to ketenes

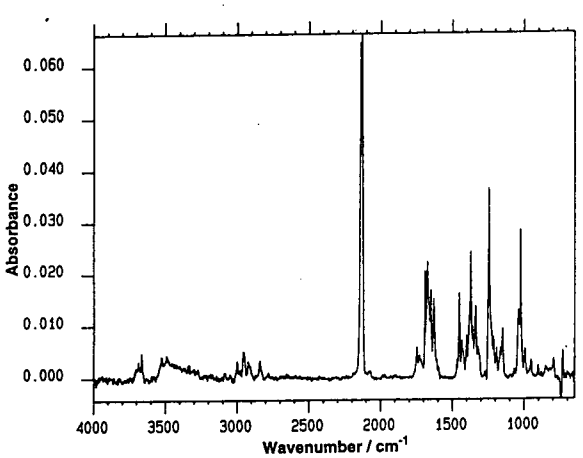

Fig. 7. Argon MI-FT-IR spectrum in the range 4000–650 cm^{-1} obtained from the enol form of methyl acetoacetate (component *A* of Fig. 2) with the GC–matrix-isolation interface transfer-line temperature increased to 250°C. Very similar results were obtained for the enol form of ethyl acetoacetate under these conditions.

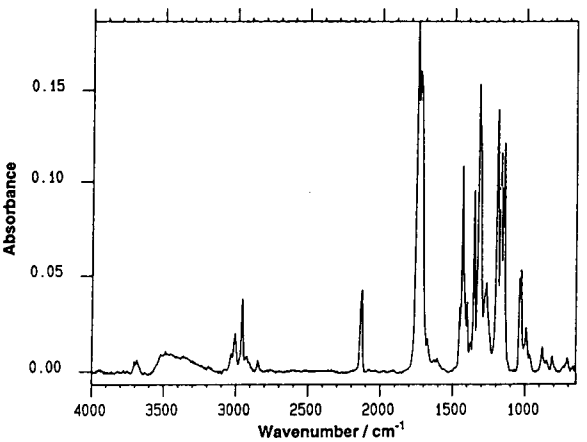

Fig. 8. Argon MI-FT-IR spectrum in the range 4000–650 cm^{-1} obtained from the keto form of methyl acetoacetate (component *C* of Fig. 2) with the GC–matrix-isolation interface transfer-line temperature increased to 250°C. Very similar results were obtained for the keto form of ethyl acetoacetate under these conditions.

from the keto form (Fig. 10). The key step is the retro-ene reaction of *trans*-keto form (**5**), which would yield ketene (**6**) and the enol of an ester (**7**). It is likely that this ester enol would tautomerize very rapidly to the normal ester form (**8**).

The validity of the mechanism of Fig. 9 is supported in our experiments by the selective thermolysis of the enols to ketenes. Because the MI-FT-IR spectra of the thermolysed enols un-

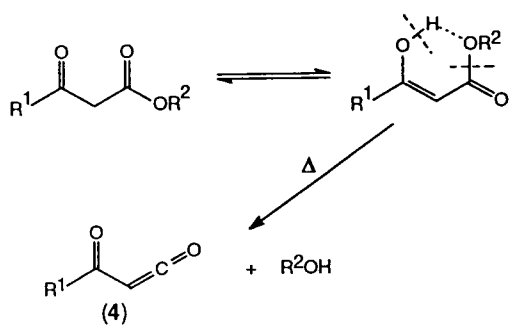

Fig. 9. Thermolytic cleavage pathway for the enol form of acetoacetates.

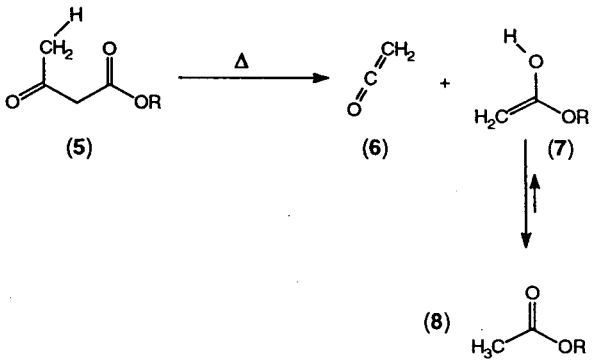

Fig. 10. Possible thermolytic cleavage pathway for the keto form of acetoacetates.

doubtedly arise from mixtures containing unchanged enols and the products, the carbonyl regions of the spectra have numerous absorptions, and it is not immediately possible to confirm that the ketenes formed are indeed keto-ketenes (**4**). It is likewise impossible to determine if only one enol conformer —specifically **2b**— is thermolysed, as predicted by the mechanism, or if the various enols are in rapid equilibrium. The presence of weak, broad O–H stretching bands around 3400 cm^{-1} in the product spectra of the thermolysed keto acetoacetates in our experiments suggests that the observed ketenes do indeed arise via the enols with concomitant alcohol formation, as shown in Fig. 9. It is just possible, however, that acetate enols (**7**) could survive long enough to be trapped in the argon matrices and thus give rise to the observed O–H stretches.

Conclusive evidence for Fig. 9 is finally provided by consideration of the spectrum derived by subtraction of the spectrum in Fig. 3 from that of Fig. 7 (with a suitable scaling factor). This has the effect of revealing the spectra of the thermolysis products only, no longer containing bands due to unreacted acetoacetate. The subtracted spectra from both the enol and keto forms of methyl acetoacetate give rise to identical data (though weaker in the keto case), with the presence of methanol clearly indicated by reference to a library spectrum of pure matrix isolated methanol, as illustrated in Fig. 11.

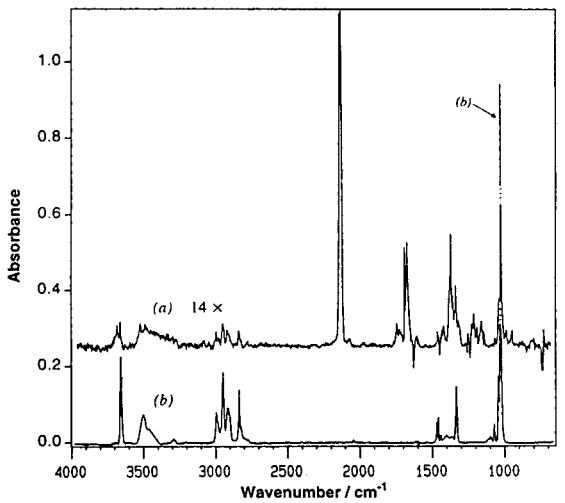

Fig. 11. (a) Argon MI-FT-IR spectrum derived by subtracting the scaled spectrum obtained from the enol of methyl acetoacetate with a transfer-line temperature of 180°C from that obtained with a transfer tube temperature of 250°C. The resulting spectrum contains bands due to the thermolysis products only. (b) Reference MI-FT-IR spectrum of methanol. Note that spectrum (a) has an absorbance-scale expansion of 14 × compared with spectrum (b); and note the overlap of the two spectra at the strong band of methanol at ca. 1020 cm^{-1}.

Likewise, the subtracted spectra obtained from both forms of ethyl acetoacetate are identical, indicating the presence of ethanol. In every case, the remaining bands in the FT-IR spectra are identical, including ketene stretching at 2133–2143 cm^{-1} and carbonyl stretching at 1682–1698 cm^{-1} indicating the formation of keto-ketene (**4**). Band splitting can again be explained in terms of matrix effects.

It should be noted that the analysis of the eluted components by MS did not indicate any differences in spectra between keto and enol forms obtained with both high and low transfer line temperatures. Mixtures of enol decomposition products, the enol itself and, indeed, the keto form would appear to have very similar mass spectra, since the ion fragmentation reactions occurring in the mass spectrometer would include analogues of the thermal fragmentation, or be preceded by thermal decomposition in the ionization source (temperature 250°C).

The foregoing results clearly indicate that the

thermal decomposition of acetoacetates proceeds preferentially via the enol form, as indicated in Fig. 9, with the resulting keto-ketene and alcohol formed. The formation of identical products from the keto acetoacetate indicates that this transformation also progresses via tautomerization to the enol form with subsequent enol degradation.

4. Conclusions

The addition of MI-FT-IR to the available techniques for analysing components eluted from GC columns greatly enhances the ease of identifying the components. In the present study, it was possible to demonstrate the separation of enol and keto forms of both methyl and ethyl acetoacetates.

The MI-FT-IR technique can also give insights into reactions which may occur at various stages of the chromatographic process. At a transferline temperature of 250°C, the enols of methyl and ethyl acetoacetates undergo an efficient thermolysis to yield, in each case, a keto-ketene and an alcohol. This observation gives experimental support to a previously proposed decomposition pathway of acetoacetates. The decompositions were avoided when the temperature in the transfer tube was lowered to 180°C. It is clear that some care must be exercised in choosing temperatures and other parameters in this type of chromatographic study. The inadvertent thermolysis of eluates could lead to anomalous IR spectra being recorded, and indeed this is already found in some of the available reference spectra.

References

[1] L.P. Hammond, *Physical Organic Chemistry*, McGraw-Hill, New York, 1st ed., 1940, pp. 245–246.
[2] J.M. Brown, in D. Barton, W.D. Ollis and I.O. Sutherland (Editors), *Comprehensive Organic Chemistry*, Vol. 2, Pergamon, Oxford, 1979, 1979, pp. 803–804.
[3] J. March, *Advanced Organic Chemistry*, Wiley, New York, 4th ed., 1992, pp. 70–72.
[4] L. Knorr, O. Rothe and H. Averbeck, *Ber.*, 44 (1911) 1138.
[5] M. Moriyasu, A. Kato and Y. Hashimoto, *J. Chem. Soc., Perkin Trans 2*, (1986) 515.
[6] M. Moriyasu, A. Kato and Y. Hashimoto, *J. Chromatogr.*, 400 (1987) 143.
[7] M. Gorodetsky, Z. Luz and Y. Masur, *J. Am. Chem. Soc.*, 89 (1967) 1183.
[8] H. Binder, L. Weis and P. Janz, *J. Chromatogr.*, 303 (1984) 375.
[9] H. Thoma and G Spiteller, *Liebigs Ann. Chem.*, (1983) 1237.
[10] B.A. Bierl, M. Beroza and W.T. Ashton, *Microchim. Acta*, I (1969) 637.
[11] P. Jackson, G. Dent, D. Carter, D.J. Schofield, J.M. Chalmers, T. Visser and M. Vredenbregt, *J. High Resolut. Chromatogr.*, 16 (1993) 515.
[12] H.E. Hallam, in H.E. Hallam (Editor), *Vibrational Spectroscopy of Trapped Species*, Wiley, New York, 1973, Ch. 3, pp. 67–132.
[13] J. Gebicki and A. Krantz, *J. Chem. Soc., Perkin Trans 2*, (1984) 1617.
[14] C.B. Moore and G.C. Pimentel, *J. Chem. Phys.*, 38 (1963) 2816.

ELSEVIER

Journal of Chromatography A, 685 (1994) 295–302

JOURNAL OF CHROMATOGRAPHY A

Retention of 4-cyanophenyl herbicides on water-insoluble β-cyclodextrin support

Tibor Cserháti*, Esther Forgács

Central Research Institute for Chemistry, Hungarian Academy of Sciences, P.O. Box 17, 1525 Budapest, Hungary

First received 23 November 1993; revised manuscript received 25 April 1994

Abstract

The retention of eight cyanophenyl herbicides on water-insoluble β-cyclodextrin polymer beads (BCDP) was determined by thin-layer chromatography using BCDP as stationary phase. The effects of pH, salt concentration in the aqueous eluent systems and the various physico-chemical parameters of herbicides on the herbicide–BCDP interaction were calculated by using principal component analysis. The pH of the eluent exerted a higher influence than the salt concentration on the retention of herbicides. The hydrophobicity and steric characteristics of solutes had the highest impact on their retention behaviour. Calculations revealed that BCDP showed a mixed retention mechanism and hydrophobic and hydrophilic forces in addition to steric parameters are involved in the interaction.

1. Introduction

Owing to their capacity to form inclusion complexes, cyclodextrins (CDs) are used in the stabilization and formulation of drugs, flavours and fragrances and also in agrochemistry [1]. A CD derivative, the water-insoluble CD, has been proved to be a useful agent for removing organic impurities from solutions [2].

CDs have been extensively applied in thin-layer chromatography (TLC) to modify the retention of various solutes. CDs can be covalently bonded to the silica surface [3,4]. The use of silica-bonded CDs in chromatography has been reviewed previously [5–8]. Silica-bonded β-CD plates have been successfully applied to the separation of racemic and diastereomeric mixtures and structural isomers [9]. In other studies β-CD was used as an eluent additive for the separation of enantiomeric drugs and dansyl-amino acids [10,11]. Amino acid and alkaloid enantiomers have been well separated by reversed-phase TLC using maltosyl-β-CD as an eluent additive [12]. Polymerized β-CD derivatives bonded to silica [13] or to organic supports [14] have also been used in liquid chromatography for the successful separation of various bioorganic compounds. Enantiomer separation of various amino acid derivatives was achieved by adding β-CD to the eluent [15,16]. Hydroxypropyl-β-CD was also suitable for the RP-TLC separation of enantiomers of derivatized amino acids [17,18]. Nitro-substituted aromatic hydrocarbon isomers were separated using α- and β-CD additives [19]. The presence of α-CD in the eluent considerably improved the separation of substituted phenolic and naphtholic compounds [20]. Both α- and β-CDs improved

* Corresponding author.

0021-9673/94/$07.00
SSDI 0021-9673(94)00642-3

the separation of cresols, nitrophenols, nitroanilines and nitronaphthalenes [21]. As the solubility of β-CD is low in common reversed-phase eluents, urea-solubilized β-CD solutions were used for the separation of polycyclic aromatic hydrocarbons and pesticides [22,23]. Hydroxypropyl-β-CDs appeared to be the most effective for increasing the TLC migration of laser dyes of the coumarin, rhodamine and bimane types [24].

The herbicidal character of 3,5-dihalo-4-hydroxy-benzonitriles has been known since 1963 [25]. They are primarily inhibitors of the photosynthetic electron transport chain [26] and uncouplers of oxidative photophosphorylation [27]. 3,5-Disubstituted 4-hydroxybenzonitriles containing a nitro group have a similar mode of action [28].

The objectives of this investigation were to study the possible application of water-insoluble β-CD polymer beads as TLC sorbents and to find the physico-chemical parameters of solutes that influence the retention. As it has been demonstrated that TLC can be successfully used to predict the retention of solutes in HPLC [29,30], the data can help in the prediction of the retention behaviour of solutes on a water-insoluble β-CD polymer-coated HPLC column [31,32].

2. Experimental

Water insoluble β-CD polymer (BCDP) was a pilot product of the Cyclolab Research and Development Laboratory (Budapest, Hungary). It was prepared by cross-linking β-CD monomers with epichlorohydrin and ethylene glycol bis(epoxypropyl) ether. It was ground and the 10–50-μm fraction was used in the experiments. As the common TLC sorbents contain the same fraction, we assumed that it can be successfully used for these preliminary investigations.

TLC plates were prepared on 20 × 20 cm glass plates: 5 g of BCDP and 25 mg of poly(vinyl alcohol) were suspended in the intended eluent, spread on the glass surface and dried at room temperature. Owing to the considerable swelling of the β-CD polymer, the preparation of the TLC plates has to be carried out in the eluent. The use of poly(vinyl alcohol) was motivated by the low mechanical stability of the BCDP layer; it considerably increased the adhesion of polymer particles to the glass surface.

The structures of solutes are shown in Table 1. They were dissolved in methanol at a concentration of 5 mg/ml and 5-μl volumes of solution were spotted on the plates. The eluents were water–methanol (3:7, v/v) (eluent I), 0.1 *M* HCl–methanol (3:7, v/v) (II), 0.1 *M* NaOH–methanol (3:7, v/v) (III), 1 *M* $MgCl_2$–methanol (3:7, v/v) (IV) and 1 *M* glycine–methanol (3:7, v/v) (V). The choice of the various eluent additives was motivated by the supposition that the extent of dissociation of polar groups in the solutes may influence the capacity to interact with cyclodextrins [33–35], and the salts [36,37] and bulky additives may inhibit inclusion complex formation.

Development was carried out in sandwich chambers (22 × 22 × 3 cm) at room temperature, the distance of development being about 16 cm. After development, the spots were detected by their UV and visible spectra. Each determination was run in quadruplicate.

The R_M value characterizing the molecular lipophilicity in RP-TLC was separately calculated for each solute in each eluent system:

$$R_M = \log (1/R_F - 1) \quad (1)$$

Table 1
Structures of 4-cyanophenol derivatives

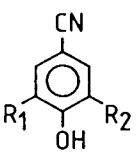

No.	R_1	R_2
1	H	H
2	H	Br
3	H	NO_2
4	NO_2	NO_2
5	Br	Br
6	I	NO_2
7	Cl	NO_2
8	Br	NO_2

To find the similarities and dissimilarities between the effects of the various eluent additives on the retention capacity of BCDP beads and to find the physico-chemical parameters of solutes governing their retention, principal component analysis (PCA) was applied [38]. PCA differs markedly from linear free energy calculations (LFE), which have also been applied to evaluate retention data [39,40]. LFE methods can calculate only the relationship between one chromatographic parameter (dependent variable) and one or more physico-chemical characteristics of the solute molecule. PCA with two-dimensional non-linear mapping [41] can evaluate the relationship between a large number of chromatographic and physico-chemical parameters without defining one as a dependent variable [42]. PCA was used twice:

(A) eluent systems I–V, the measured lipophilicity and adsorption capacity values of 4-cyanophenyl derivatives determined on impregnated and unimpregnated silica [43] being the variables; and

(B) Eluent systems I–V and the various calculated physico-chemical parameters of herbicides being the variables.

The physico-chemical parameters included in the calculation were the following:

π = Hansch–Fujita substituent constant characterizing hydrophobicity [44,45];

H-Ac and *H-Do* = indicator variables for proton acceptor and proton donor properties, respectively [46];

M-RE = molar refractivity [47];

F and *R* = electronic parameters characterizing the inductive and resonance effects, respectively [48];

σ = Hammett's constant, characterizing the electron-withdrawing power of the substituent [49];

Es = Taft's constant, characterizing steric effects of the substituent [50];

B_1 and B_4 = Sterimol width parameters determined by distance of substituents at their maximum point perpendicular to attachment [51,52].

The limit of variance explained was set to 95% in both instances. The two-dimensional non-linear map of principal component loadings and variables and the varimax rotation of PC loadings in two axes was also calculated. The iteration was carried out to the point where the difference between the last two iterations was less than 10^{-8}. Eluent systems and solutes form clusters on the map when their retention characteristic are similar and they are well separated when their retention behaviour is highly different. To compare the information contents of varimax rotation and the non-linear mapping technique, linear correlations were calculated between the corresponding coordinates.

3. Results and discussion

The R_F values of 4-cyanophenol derivatives are compiled in Table 2. Solutes show higher retention in acidic and lower retention in alkaline eluents; the effect of $MgCl_2$ and glycine is negligible. This finding indicates that the degree of dissociation of the polar head group has a considerable impact on the retention even on this support, and a change in pH may result in a change in retention order. These results entirely support previous conclusions [33–35] that the strength of inclusion complex formation may depend on the degree of dissociation of the guest molecule. We assume that the bulky substituted benzene ring enters the cavity of the β-CD polymer, forming inclusion complexes the stability of which depends on the steric correspondence of the interacting molecules. The polar groups probably point out of the cavity and can bind to the hydrophilic surface substructures on the outer part of the cavities (electrostatic interactions). We are well aware that the cross-linking of the CD may modify its inclusion complex-forming capacity [53]. However, the CD cavities remaining on the polymer surface and the irregular cavities formed during the polymerization process [54] may influence the retention of various solutes on β-CD polymer beads resulting in uncommon retention characteristics of the above support.

The results of principal component analyses A

Table 2
Retentions (R_F) of 4-cyanophenol derivatives on β-CD polymer beads

Compound	Eluent system									
	I		II		III		IV		V	
	Mean	S.D.	Mean	S.D.	Mean	S.D.	Mean	S.D.	Mean	S.D.
1	0.38	0.04	0.45	0.03	0.28	0.03	0.36	0.07	0.39	0.01
2	0.39	0.03	0.46	0.05	0.20	0.01	0.37	0.03	0.42	0.05
3	0.42	0.05	0.57	0.04	0.19	0.02	0.42	0.05	0.49	0.06
4	0.43	0.06	0.52	0.03	0.21	0.04	0.41	0.02	0.52	0.04
5	0.41	0.02	0.52	0.04	0.20	0.05	0.37	0.01	0.39	0.02
6	0.42	0.03	0.63	0.07	0.22	0.01	0.39	0.04	0.49	0.03
7	0.40	0.02	0.51	0.08	0.19	0.02	0.35	0.06	0.47	0.02
8	0.40	0.03	0.58	0.06	0.21	0.05	0.38	0.04	0.52	0.07

and B are compiled in Tables 3 and 4, respectively. In both instances the first principal component explains most of the variance, that is, the effect of various eluent additives can be explained by one background variable. Unfortunately, principal component analysis does not specify this background variable as a concrete physico-chemical entity but only indicates its mathematical possibility.

The measured physico-chemical parameters of the herbicides and also eluent systems I and V have a high loading in the first principal component, indicating that both the hydrophobicity and adsorption capacity of herbicides influence their binding to the BCDP surface. The relatively high loadings of acidic, basic and salt-containing eluents in the second, third and fourth principal components emphasizes the importance of the degree of dissociation of polar substructures in the retention and the consider-

Table 3
Similarities and dissimilarities between the effects of eluent additives on the retention characteristics of water-insoluble β-polymer beads and their measured physico-chemical parameters: results of principal component analysis A

No. of principal component	Eigenvalue	Variance explained (%)	Total variance explained (%)
1	4.60	65.72	65.72
2	0.98	13.97	79.69
3	0.74	10.62	90.31
4	0.41	5.82	96.13

Principal component loadings

Parameter	No. of principal component			
	1	2	3	4
Water	0.93	0.24	−0.04	0.06
0.1 *M* HCl	0.78	0.24	0.18	−0.54
0.1 *M* NaOH	−0.62	0.33	0.69	0.08
1 *M* $MgCl_2$	0.63	0.71	−0.11	0.26
1 *M* Glycine	0.96	−0.10	0.11	0.05
Lipophilicity	0.92	−0.27	−0.04	0.08
Adsorption capacity	0.75	−0.40	0.45	0.17

Table 4
Similarities and dissimilarities between the effects of eluent additives on the retention characteristics of water-insoluble β-CD polymer beads and their calculated physico-chemical parameters: results of principal component analysis B

No. of principal component	Eigenvalue	Variance explained (%)	Total variance explained (%)
1	8.79	62.81	62.81
2	3.17	22.67	85.48
3	0.97	6.91	92.39
4	0.70	5.01	97.40

Principal component loadings

Parameter	No. of principal component			
	1	2	3	4
Water	−0.88	0.23	0.32	−0.01
0.1 *M* HCl	−0.75	−0.05	0.42	0.40
0.1 *M* NaOH	0.58	0.27	−0.26	0.71
1 *M* $MgCl_2$	−0.46	0.62	0.59	0.00
1 *M* Glycine	−0.95	0.09	0.04	−0.03
π	−0.05	0.98	−0.17	−0.06
H-Ac	0.80	−0.55	0.22	0.00
M-RE	0.83	0.50	−0.02	−0.19
F	0.97	0.09	0.20	0.04
R	0.35	−0.91	0.19	0.00
σ	0.97	−0.08	0.23	0.03
Es	−0.97	−0.17	−0.14	0.04
B_1	0.88	0.46	0.12	0.00
B_4	0.96	0.20	0.16	−0.02

able influence of salt on the BCPD–herbicide interaction (Table 3). The distribution of variables on the two-dimensional non-linear map of PC loadings entirely supports our previous conclusions (Fig. 1: both the pH of eluent and the salt concentration exert marked effects on the retention of the solutes. Herbicides form distinct clusters according to the number of substituents on the two-dimensional non-linear map of PC variables (Fig. 2). This finding suggests that not only the lipophilicity and adsorption capacity but also the dimensions of the solute may influence the retention.

The various calculated physico-chemical parameters for 4-cyanophenyl herbicides and their retention behaviour on the BCDP layer are strongly related (Table 4). The steric characteristics (*Es*, B_1 and B_4 values) have a high loading in the first PC, proving again the importance of molecular dimensions in the herbicide–BCDP interaction.

The retention characteristics of eluent systems form a loose cluster with the lipophilicity and the steric effect of substituents on the two-dimensional non-linear map of PC loadings (Fig. 3). This finding suggests that more than one type of binding forces are involved in the herbicide–BCDP interaction. We assume that the ring structure of the herbicide enters the CD cavity on the surface of the BCDP (governed by the dimensions of the solute), and the binding forces between the cavity walls and the surface of guest molecules are of hydrophobic character (role of solute hydrophobicity). The dissociable hydroxyl group points towards the outer sphere of the BCDP and binds to it by hydrophilic forces. The strength of interaction depends in part on the degree of dissociation of the hydroxy group.

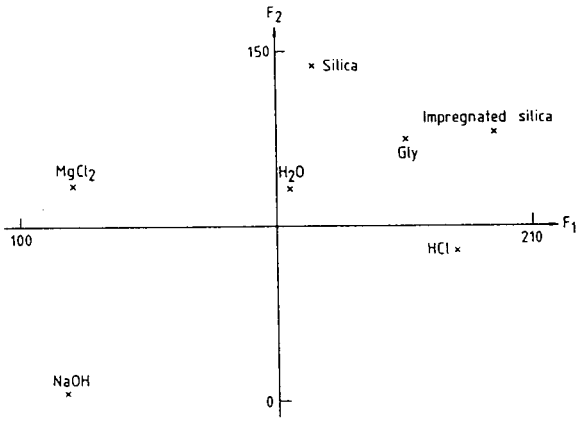

Fig. 1. Similarities and dissimilarities between the retention characteristics of various supports and eluent systems. Two-dimensional non-linear map of PC loadings; No. of iterations, 162; maximum error, $2.81 \cdot 10^{-2}$. H_2O = BCDP support, water–methanol (3:7, v/v); HCl = BCDP support, 0.1 *M* HCl–methanol (3:7, v/v); NaOH = BCDP support, 0.1 *M* NaOH–methanol (3:7, v/v); $MgCl_2$ = BCDP support, 1 *M* $MgCl_2$–methanol (3:7, v/v); Gly = 1 *M* glycine–methanol (3:7, v/v); Silica = adsorption capacity of solutes determined on unimpregnated silica; Impregnated silica = lipophilicity of solutes determined on impregnated silica.

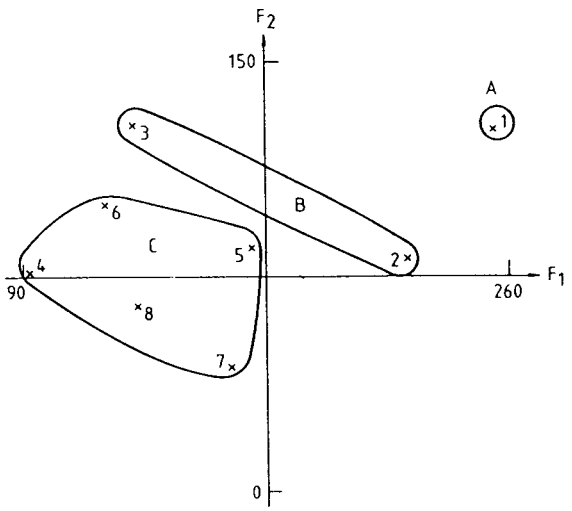

Fig. 2. Distribution of 4-cyanophenyl herbicides according to their retention behaviour. Two-dimensional non-linear map of PC variables. No. of iterations, 111; maximum error, $1.80 \cdot 10^{-2}$. Numbers refer to 4-cyanophenyl derivatives in Table 1. A = Unsubstituted 4-cyanophenol; B = monosubstituted 4-cyanophenols; C = disubstituted 4-cyanophenols.

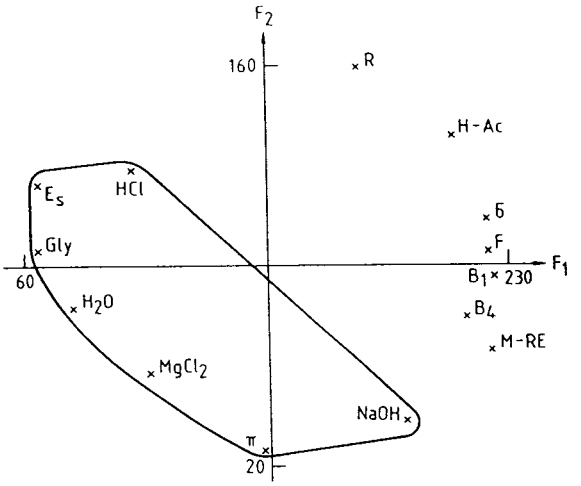

Fig. 3. Relationship between the retention behaviour and physico-chemical parameters of 4-cyanophenol derivatives. Two-dimensional non-linear map of PC loadings; No. of iterations, 79; maximum error, $1.62 \cdot 10^{-2}$. For symbols, see Fig. 1 and Experimental.

Good linear correlations were found between the coordinates of varimax rotation and the two-dimensional non-linear map:

$$\mathrm{Nlmap}_1 = -1.68 + (1.17 \cdot 10^{-2} \pm 6.69 \cdot 10^{-4}) \cdot \mathrm{varimax}_1$$

$$n = 14; \quad r_{\mathrm{calc.}} = 0.9810; \quad r_{99.9\%} = 0.7800$$

$$\mathrm{Nlmap}_2 = 1.04 - (1.10 \cdot 10^{-2} \pm 2.33 \cdot 10^{-3} \cdot \mathrm{varimax}_2$$

$$n = 14; \quad r_{\mathrm{calc.}} = 0.8064; \quad r_{99.9\%} = 0.7800$$

These data indicate that the information contents of the results of varimax rotation and two-dimensional non-linear mapping are similar but not identical. We must emphasize that this conclusion is possibly valid only for this data matrix and it is not the result of theoretical considerations, and therefore its use for other data matrices is probably subject to considerable error.

As the use of BCDP as a TLC support is relatively new [55], we do not have sufficient retention data to compare its advantages or

disadvantages with those of polymer-coated silica.

It can be concluded from our data that BCDP can be successfully used as a TLC support for the study of the interaction of various organic xenobiotics with BCDP, which facilitates the application of BCDP in environmental protection.

Acknowledgement

This work was supported by grant OTKA 2670.

References

[1] J. Szejtli, in J.L. Atwood, J.E. Davis and D.D. McNicoll (Editors), *Inclusion Compounds*, Vol. III, Academic Press, London, 1984, p. 331.
[2] P. Khanna and R. Dworschak, *Eur. Pat. Appl.*, 0 301 847 (1987).
[3] D.W. Armstrong, *US Pat. Appl.*, 84-635133 (1984).
[4] T. Vaisar, T. Tomas and E. Keulemansova-Smolkova, *Czech Pat.*, CS 88-4134 (1988).
[5] W.J. Timothy and D.W. Armstrong, *J. Liq. Chromatogr.*, 9 (1986) 407.
[6] E. Smolkova-Keulemansova, in O. Huber and J. Szejtli (Editors), *Proceedings of the 4th International Symposium on Cyclodextrins*, Kluwer, Dordrecht, 1988, p. 451.
[7] W.L. Hinze, *Sep. Purif. Methods*, 10 (1981) 159.
[8] S. Krysl and E. Smolkova-Keulemansova, *Chem. Listy*, 79 (1985) 919.
[9] A. Alak and D.W. Armstrong, *Anal. Chem.*, 58 (1986) 582.
[10] D.W. Armstrong, F.-Y. He and S.M. Han, *J. Chromatogr.*, 448 (1988) 345.
[11] J.W. LeFevre, *J. Chromatogr.*, 653 (1993) 293.
[12] J.D. Duncan and D.W. Armstrong, *J. Planar Chromatogr. Mod. TLC*, 3 (1990) 65.
[13] N. Thuaud, B. Sébille, A. Deratani, B. Pöppling and C. Pellet, *Chromatographia*, 36 (1993) 373.
[14] B. Zsadon, L. Dècsei, M. Szilasi, F. Tùdös and J. Szejtli, *J. Chromatogr.*, 270 (1983) 127.
[15] L. Lepri, V. Coas, P.G. Desideri and L. Checchini, *J. Planar Chromatogr. Mod. TLC*, 3 (1990) 311.
[16] L. Lepri, V. Coas and P.G. Desideri, *J. Planar Chromatogr. Mod. TLC*, 3 (1990) 533.
[17] J.D. Duncan and D.W. Armstrong, *J. Planar Chromatogr. Mod. TLC*, 4 (1991) 204.
[18] D.W. Armstrong, J. Faulkner, Jr., and S.M. Han, *J. Chromatogr.*, 452 (1988) 323.
[19] L. Lepri, V. Coas and P.G. Desideri, *J. Planar Chromatogr. Mod. TLC*, 4 (1991) 338.
[20] W.G. Burkert, C.N. Owensby and W.L. Hinze, *J. Liq. Chromatogr.*, 4 (1981) 1065.
[21] J. Debowski, G. Grassini-Strazza and D. Sybilska, *J. Chromatogr.*, 349 (1985) 131.
[22] W.L. Hinze, D.Y. Pharr, Z.S. Fu and W.G. Burkert, *Anal. Chem.*, 61 (1989) 422.
[23] D.Y. Pharr, Z.S. Fu, T.K. Smith and W.L. Hinze, *Anal. Chem.*, 61 (1989) 275.
[24] I.R. Politzer, K.T. Crago, K. Amos, K. Mitchel and T. Hollin, *Talanta*, 39 (1992) 953.
[25] K. Carpenter and B.J. Heywood, *Nature*, 200 (1963) 28.
[26] D. Paton and J.E. Smith, *Weed Res.*, 5 (1965) 75.
[27] T.E. Ferrari and D.E. Moreland, *Plant Physiol.*, 44 (1969) 429.
[28] Z. Szigeti, E. Tóth and G. Paless, *Photosynth. Res.*, 3 (1982) 347.
[29] J.K. Rozylo and M. Janicka, *J. Planar Chromatogr. Mod. TLC*, 3 (1990) 413.
[30] J.K. Rozylo and M. Janicka, *J. Liq. Chromatogr.*, 14 (1991) 3197.
[31] T. Cserháti and E. Forgács, *Anal. Chim. Acta*, 279 (1993) 107.
[32] E. Forgács and T. Cserháti, *J. Chromatogr. A*, 668 (1994) 395.
[33] T. Cserháti, J. Szejtli, and E. Fenyvesi, *J. Chromatogr.*, 439 (1988) 393.
[34] D. Sybilska, J. Lipkowski and J. Woycikowski, *J. Chromatogr.*, 237 (1982) 303.
[35] I. Sanemasa, T. Mizoguchi and T. Degichi, *Bull. Chem. Soc. Jpn.*, 57 (1984) 1358.
[36] T. Cserháti, B. Bordás, E. Fenyvesi and J. Szejtli, *J. Inclus. Phenom.*, 1 (1983) 53.
[37] T. Cserháti, B. Bordás, E. Fenyvesi and J. Szejtli, *J. Chromatogr.*, 259 (1983) 107.
[38] K.V. Mardia, J.T. Kent and J.M. Bibby, *Multivariate Analysis*, Academic Press, London, 1979, p. 213.
[39] E. Forgács, *Biochem. Mol. Biol. Int.*, 30 (1993) 1.
[40] E. Forgács, *J. Liq. Chromatogr.*, 16 (1993) 3757.
[41] J.W. Sammon, Jr., *IEEE Trans. Comput.*, C18 (1969) 401.
[42] T. Cserháti and Z. Illès, *J. Pharm. Biomed. Anal.*, 9 (1991) 685.
[43] Z. Szigeti and T. Cserháti, *Acta Phytopathol. Acad. Sci. Hung.*, 19 (1984) 347.
[44] T. Fujita, J. Iwasa and C. Hansch, *J. Am. Chem. Soc.*, 86 (1964) 5175.
[45] A. Leo, C. Hansch and M. Ames, *J. Pharm. Sci.*, 64 (1975) 559.
[46] C. Hansch and A. Leo, *Substituent Constants for Correlation Analysis in Chemistry and Biology*, Wiley, New York, 1979, p. 1.
[47] L. Pauling and D. Pressman, *J. Am. Chem. Soc.*, 67 (1945) 1003.

[48] R.W. Taft and I.C. Lewis, *J. Am. Chem. Soc.*, 80 (1958) 2436.
[49] L.P. Hammett, *Chem. Rev.*, 17 (1935) 125.
[50] R.W. Taft, *J. Am. Chem. Soc.*, 74 (1952) 3120.
[51] A. Verloop and J. Tipker, *Pestic. Sci.*, 7 (1976) 379.
[52] A. Verloop, W. Hoogenstraaten and J. Tipker, in J. Ariens (Editor), *Drug Design*, Vol. VII, Academic Press, New York, 1976, p. 165.
[53] E. Fenyvesi, T. Cserháti and J. Szejtli, in A.R. Hodges (Editor), *Proceedings of the 6th International Symposium on Cyclodextrins, Chicago, 21–24 April 1992*, Edition Santé, Paris, 1992, p. 267.
[54] T. Cserháti, Gy. Oros, É. Fenyvesi and J. Szejtli, *J. Inclus. Phenom.*, 1 (1983–84) 395.
[55] T. Cserháti, *Anal. Chim. Acta*, 292 (1994) 17.

ELSEVIER

Journal of Chromatography A, 685 (1994) 303–312

JOURNAL OF CHROMATOGRAPHY A

Synthesis and evaluation of anionic polymer-coated capillaries with pH-independent electroosmotic flows for capillary electrophoresis

Peng Sun, Adam Landman, Geoffrey E. Barker, Richard A. Hartwick*

Department of Chemistry, State University of New York at Binghamton, Binghamton, NY 13902, USA

First received 31 May 1994; revised manuscript received 5 July 1994

Abstract

A capillary coating method was developed using a sodium-2-acrylamido-2-methylpropanesulfonate (NaAMPS) polymer. Capillaries coated with this anionic polymer exhibited pH-independent electroosmotic flows (EOFs). Capillaries with a particular EOF rate could be synthesized simply by changing the molar ratio of NaAMPS to neutral acrylamide in the polymer mixture. The pH-independent EOF of the coated capillary changed less than 1.5% over 20 days of routine, intermittent use. Capillary lifetime with a continuously applied electric field of 286 V cm^{-1} was about 60 h. Reproducibility of the coating procedure was 1.7% R.S.D. in observed EOF for independently synthesized capillaries. The pH-independent EOF of these capillaries as well as their selectable flow-rates (via synthesis) should prove useful in micellar electrokinetic capillary chromatography (MECC) at low pH values and for expansion of the separation window in MECC, as well as for more versatile separations of various species in the capillary zone electrophoresis mode.

1. Introduction

One of the most important features in capillary electrophoresis (CE) is the presence of electroosmotic flow (EOF), which because of its relatively flat flow profile [1–3], detracts little from the efficiency of a separation. A second feature of EOF is that it is often 5–10 times faster than the intrinsic electrophoretic mobilities of ions typically separated using capillary zone electrophoresis (CZE). This permits the migration of cations, anions and neutrals in one direction, allowing them to be detected at one end of the capillary within a reasonable time. Since the EOF affects the dwell time of a solute in the capillary, both the separation efficiency and resolution are related to the magnitude of EOF [4]. Method development is complicated by the pH dependency of EOF, which when coupled with pK_a values of ionic moieties on the solute, can create complicated pH–resolution maps which exhibit critical behavior and can become extremely sensitive to localized electrolyte pH changes, contributing to poor overall precision. Since electroosmotic flow diminishes at pH values lower than 4 or 5, ion suppression of acidic molecules for separation by micellar electrokinetic capillary chromatography (MECC) is often not feasible. Further complications arise during electrokinetic injections, where the mass of solute injected is directly related to the EOF. Another problem with EOF is that, since concentration detectors are widely used in CE, reproducibility of quantitation using peak area is directly proportional to the reproducibil-

* Corresponding author.

0021-9673/94/$07.00
SSDI 0021-9673(94)00635-O

ity of the EOF. While mathematical corrections can be applied on a post-run basis, in general, a constant EOF rate contributes greatly to the ruggedness and versatility of electrically based separations. This has made the control of EOF one of the fundamental problems in CE.

EOF is the bulk flow of solution due to the effect of the electric field on counterions in the diffuse layer adjacent to the shear layer residing next to the negatively charged capillary wall (assuming the use of fused silica at alkaline pH conditions). The potential at the shear layer is termed the ζ potential. When an electric field is applied, the cationic counterions migrate toward the cathode and drag solvent with them, resulting in a bulk flow of solution toward the cathode [5]. The velocity profile for EOF has been studied by numerous investigators [6,7]. The electroosmotic mobility can be expressed as [7]:

$$\mu_{eo} = \frac{-\epsilon\psi_0}{\eta} \quad (1)$$

where ϵ is the electrical permittivity of the solvent, ψ_0 is the electrical potential at the capillary–solution interface, and η is the viscosity at the wall. The surface charge density σ^* can be expressed as:

$$\sigma^* = \epsilon\kappa\psi_0 \quad (2)$$

where κ is equivalent to the inversion of double layer thickness (κ^{-1}) which is related to ϵ and ionic concentration (C). Thus Eq. 1 can be written in terms of the surface charge density:

$$\mu_{eo} = \frac{\sigma^*}{\kappa\eta} \quad (3)$$

or

$$\mu_{eo} = \frac{\sigma^*\kappa^{-1}}{\eta} \quad (4)$$

It can be seen that in order to control EOF, one can control either the charge density on the capillary wall (σ^*), the double layer thickness (κ^{-1}) or the viscosity of the solution adjacent to the capillary wall (η). Fujiwara and Honda [8,9] reported two methods to control EOF by reducing the double layer thickness: (1) increasing the electrolyte concentration in the run buffer, or (2) decreasing the permittivity of the run buffer by the addition of organic solvent. The limitations of these approaches are increased Joule heating within the capillary due to the increased ion concentration and altered electrolyte solubility due to the presence of organic solvents in the run buffer. EOF can also be altered by changing the buffer viscosity with addition of soluble polymers to the run buffer [10,11], such as methylcellulose.

Most research for the control of EOF has been focused on altering the surface charge density (σ^*) and viscosity (η) on the capillary wall. In situations where little or no EOF is desired, along with reduced solute adsorption, polymeric wall coatings such as methylcellulose [12], trimethylsilane [1,13], polyacrylamide [14], polyvinylpyrrolidinone (PVP) [15], polyethylene glycol (PEG) [16], maltose [17], vinyl-bond polyacrylamide [18], polyethyleneimine (PEI) [19], polymethylglutamate [20], hydroxylated polyether [21], octyl, octadecyl [22] and epoxydiol [23] have been used. Another approach used to control EOF is that of applying a radial electric field across the capillary wall [24–26]. The applied radial voltage can be positive or negative, and hence the surface charge density may be enhanced or reduced. The EOF actually can be reversed by radial voltage or by using positively charged polymer coatings [19,27]. The dependence of EOF on buffer pH can also be reduced to some level by using non-ionic surfactant coatings [22,28].

For CE, an ideal surface modification would be one in which the surface charge density could be reproducibly synthesized to a desired level, have a charge density largely independent of pH, and be non-adsorptive to macromolecules. This would only be possible in capillaries with neutral charge or a constant charge at the surface [19]. Two approaches have been reported for the polymerization of 2-acryloylamido-2-methylpropanesulfonic acid monomer in capillaries at 120°C using azobisisobutyronitrile (AIBN) as a radical initiator [29,30]. In these two methods, capillaries were pretreated with trichloro-

vinylsilane [29] or 7-oct-1-enyltrimethoxysilane [30].

In this research a simple method is reported in which the sodium 2-acrylamido-2-methyl-1-propanesulfonate (NaAMPS) monomer has been polymerized or copolymerized with acrylamide at room temperature, thus producing a level of sulfonic acid groups bonded to the fused-silica wall surface. Capillaries coated by this anionic polymer have electroosmotic flows which can be varied from near zero (pure polyacrylamide) to a maximum value ca. 60% of the maximum flow of a bare silica capillary at alkaline pH. The EOF was found to be largely independent of pH, and highly reproducible. The stability, lifetime, coating and operating reproducibilities, as well as application potentials of these new capillaries are discussed.

2. Experimental

2.1 Chemicals

2-Acrylamido-2-methyl-1-propanesulfonic acid (AMPSA), β-cyclodextrin (β-CD), benzoic acid, 2-bromophenyl acetic acid, 4-bromophenyl acetic acid, 2-naphthalenesulfonic acid and methylphenol were obtained from Aldrich (Milwaukee, WI, USA). Acrylamide, N,N,N′,N′,-tetramethylenediamine (TEMED) and ammonium persulfate (APS) were purchased from Bio-Rad Labs. (Richmond, CA, USA). Dansyl-DL-amino acid samples and sodium dodecyl sulfate (SDS) were obtained from Sigma (St. Louis, MO, USA). 3-Methacryloxypropyltrimethoxysilane was purchased from Huls America (Bristol, PA, USA) and benzenesulfonic acid sodium salt from Eastman (Rochester, NY, USA). All other chemicals were obtained from Fisher Scientific (Fair Lawn, NJ, USA).

2.2. Apparatus

CE and MECC separations were performed on a laboratory-constructed instrument which included a Plexiglas box, a CZE 1000 PN 30 high-power supply (Spellman, Plainview, NY, USA), and a fully digital controller for the CZE 1000 unit, designed by Chamonix (Johnson City, NY, USA). The controller is commercially available for a variety of high-voltage supplies. Detection was achieved via a Spectra 100 UV detector (Thermo Separation Products, Freemont, CA, formerly Spectra-Physics), using a commercial "flow cell" with a single ball lens, also purchased from Thermo Separation Products. The electropherograms were processed on a SP-4400 integrator (Thermo Separation Products). Detection wavelength was 210 nm.

2.3. Capillary coating

Approximately 0.8 g of 2-acrylamido-2-methyl-1-propanesulfonic acid (AMPSA) was dissolved in 8 ml deionized water. A concentrated NaOH solution was added to neutralize this acidic solution to pH 7.0, and brought to a total volume of 10 ml with water. This 0.386 *M* NaAMPS solution (solution A) was degassed for 20 min using vacuum and sonication before polymerization. The 0.386 *M* acrylamide solution (solution B) was made by dissolving 0.275 g acrylamide in 10 ml deionized water. Pretreatment of the capillary using a bifunctional reagent was performed using the method developed by Hjertén [14]. Fused-silica capillaries (75 μm I.D. × 375 O.D., Polymicro Technology, Phoenix, AZ, USA) with detection windows were washed with 1 *M* NaOH solution for 30 min, then with deionized water for 15 min. Then these capillaries were filled with 1% (v/v) 3-methacryloxypropyltrimethoxylsilane solution (pH has been adjusted to 3.5 by acetic acid). After 1 h, the silane solution was removed. These capillaries were ready to be coated after rinsing with water.

About 5 mg of ammonium persulfate and 5 μl of TEMED were added to 5 ml of 0.386 *M* NaAMPS (solution A), then the mixed solution was pushed through the pretreated capillary and left in the capillary for 1 h. The capillary was rinsed with water and dried with air before use. Fig. 1 represents the scheme of this anionic polymer coating. To make capillaries with different EOF rates, solutions with different volume

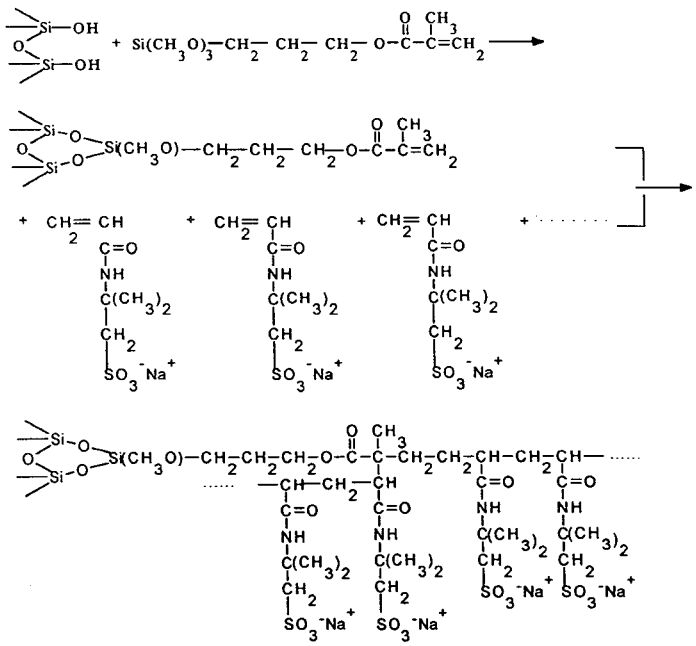

Fig. 1. NaAMPS polymer-coating procedure.

ratios of solution A to solution B were used to coat the capillaries. Methylphenol was used as a neutral marker to measure the EOF in this work.

2.4. Safety considerations

Caustic solutions are used in several steps of the synthesis. Suitable eye and skin protection should be employed for handling such solutions, realizing that splattering is possible as the solutions are forced through the capillaries under mild pressure.

3. Results and discussion

3.1. Effect of pH on EOF

Fig. 2 shows the effect of pH on EOFs for both coated and bare capillaries. NaAMPS polymer-coated capillary possesses a very stable flow over the pH range 2–9, while the bare capillary shows a strong dependence on pH. As described in Eq. 4, EOF is dependent on the surface charge density (σ^*), the double layer thickness (κ^{-1}) and the solution viscosity (η). In this experimental case, the same buffer solution is used in testing the EOF for both bare and coated

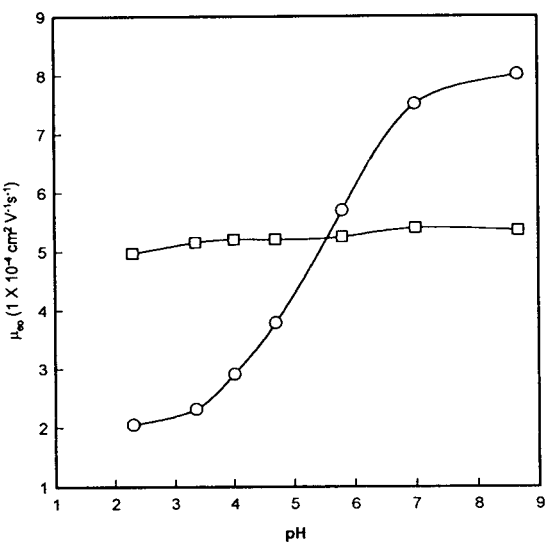

Fig. 2. pH effect on electroosmotic flow (μ_{eo}). □ = NaAMPS polymer-coated capillary; ○ = bare capillary.

capillaries. The major factor affecting the EOF is the surface charge density (σ^*). It results in dramatic difference in pH dependence between the two capillaries. For the bare capillary the surface charge density is controlled by the dissociation constant of the free hydroxyl groups on the silica surface. It can be calculated according to the following reaction [25]:

$$[SiOH_S] \rightleftharpoons [SiO_S^-] + [H^+]$$

where the $SiOH_S$ and SiO_S^- are surface functional groups given as function groups per units area. The charge density can be expressed as [25]:

$$\sigma^* = \frac{\gamma}{1 + \frac{[H^+]}{K}} \quad (5)$$

where γ is the number density of surface SiOH group, K is the dissociation constant (ca. $4.2 \cdot 10^{-10}$) for surface hydroxyl groups on fused silica and $[H^+]$ is the bulk buffer hydrogen ion concentration. Since the pK_a of the surface hydroxyl group is low, the ionization of this group will be vary at different pH. This results in the strong pH dependence of EOF.

For the NaAMPS polymer-coated capillary, the silica surface of the capillary is masked by a layer of NaAMPS polymer (Fig. 1). The sulfonic acid groups on the polymer are strongly acidic, and completely dissociate when pH is above 2. Consequently, the charge density on this polymer coating surface is very stable in pH range 2–9. This leads to a pH-independent EOF. Since the NaAMPS polymer coating has negatively charged sulfonate groups, this capillary exhibits a relatively fast EOF compared to the capillary coated with neutral polymers such as linear polyacrylamide [14]. In capillary modification using neutral or weakly charged polymer coatings, it is inevitable that an attempt to reduce sample–wall interaction will cause the loss of electroosmotic pumping. But EOF is needed in many practical cases to sweep the samples through the capillary to the detection end. The NaAMPS polymer coating is one method capable of solving this problem. The maximum EOF, $5.50 \cdot 10^{-4}$ cm^2 V^{-1} s^{-1}, produced by this new method is higher than that reported by Huang et al. [30], which is about $3.5 \cdot 10^{-4}$ cm^2 V^{-1} s^{-1}. Another advantage of this new method is that it is simpler than other methods [29,30]. Instead of at high temperature (120°C), polymerization is accomplished at room temperature.

3.2. Stability and lifetime of the NaAMPS polymer-coated capillary

The stability of the NaAMPS polymer-coated capillary is tested by measuring the EOF periodically during the course of research work. Fig. 3 shows the EOFs measured in pH range 3–9 on different days. It can be seen that the pH-independent EOF remains stable after 18 days. The lifetime of the coating is measured by maintaining an applied electric field strength of 288 V/cm (see Fig. 4). EOF begins to deviate after 60 h. The authors strongly believe that with the improvement of this coating procedure the lifetime can be improved.

3.3. Desirable EOFs

The reduction of pH dependence of EOF has been reported by Dougherty et al. [22] and Towns and Regnier [28]. In their methods, the pH dependence of EOF has been reduced to

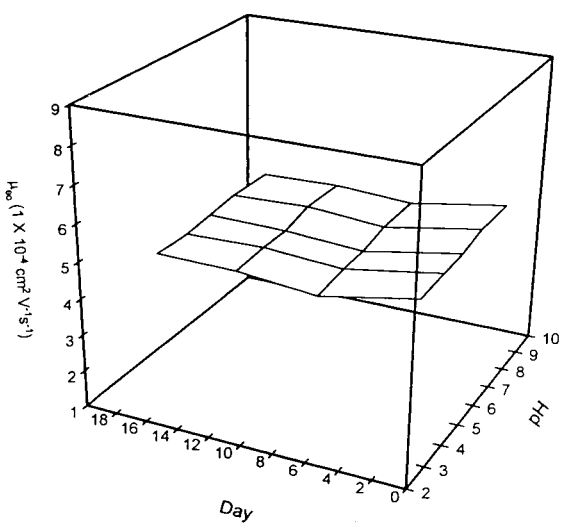

Fig. 3. Stability of NaAMPS polymer-coated capillary.

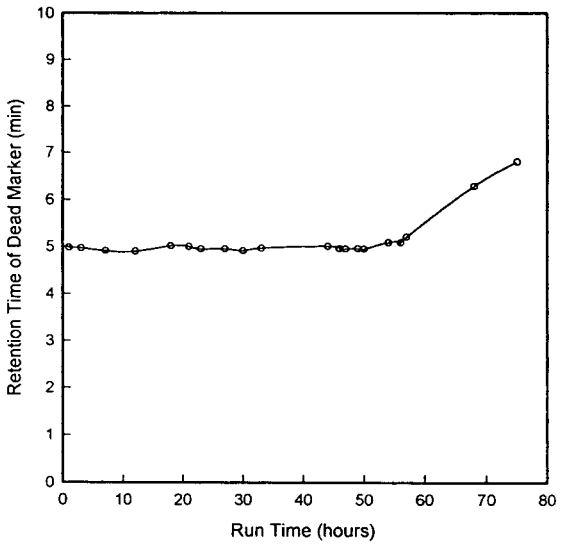

Fig. 4. Lifetime testing of NaAMPS polymer-coated capillary. Electric field: 18 kV; capillary: 63 cm total length and 42.2 cm effective length; buffer: 10 m*M* phosphate at pH 7.0; neutral marker sample: methylphenol in buffer.

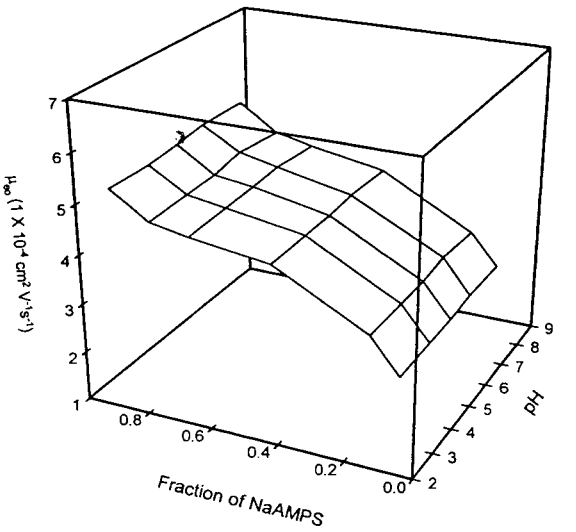

Fig. 5. Desirable electroosmotic flows of capillaries coated with polymers containing different NaAMPS molar fractions.

some level by using different coatings. However, the EOF rates are still not very stable in the pH range of 3–10. Also, in both methods the modified capillaries have low EOFs. When negatively charged NaAMPS polymer is used to coat the capillary, a relatively high EOF can be obtained, and this flow is very stable in pH range of 2–9 (Figs. 2 and 3). Another advantage of this method is that capillaries with different EOFs can be made by simply adding acrylamide solution to the NaAMPS solution before polymerization. The surface charge density (σ^*) on the polymer coating can be adjusted by changing the molar ratio of negatively charged NaAMPS to neutral molecule acrylamide in the monomer solution. Fig. 5 shows the pH-independent EOFs obtained from coatings containing different NaAMPS molar fractions. pH-independent flow can be adjusted to a desired level by this method. The coating reproducibility of this method is illustrated in Table 1. which shows the results of capillaries made on three different days. It can be seen that the reproducibility of EOF is good. The relative standard deviation is 1.7%. Similar reproducibility is obtained for capillaries with EOFs in the range reported in Fig. 5. This new method offers the possibility to make capillaries with desirable pH-independent EOFs. This allows one to vary pH to optimize selectivity without significantly affecting the EOF in CE separations.

3.4. Application potentials of NaAMPS polymer-coated capillary

In CE, acidic samples with low pK_a values are generally difficult to resolve at low-pH conditions on bare capillaries. Separations of 2-naphthalenesulfonic acid and benzenesulfonic acid on a bare capillary are represented in Fig. 6. At pH

Table 1
Coating reproducibility

No. of capillaries made at different days	μ_{eo} [a] ($1 \cdot 10^{-4}$ cm^2 V^{-1} s^{-1})	R.S.D. (%)
1	5.50	
2	5.34	1.7
3	5.33	

[a] All values of electroosmotic flows were the averages of three measurements.

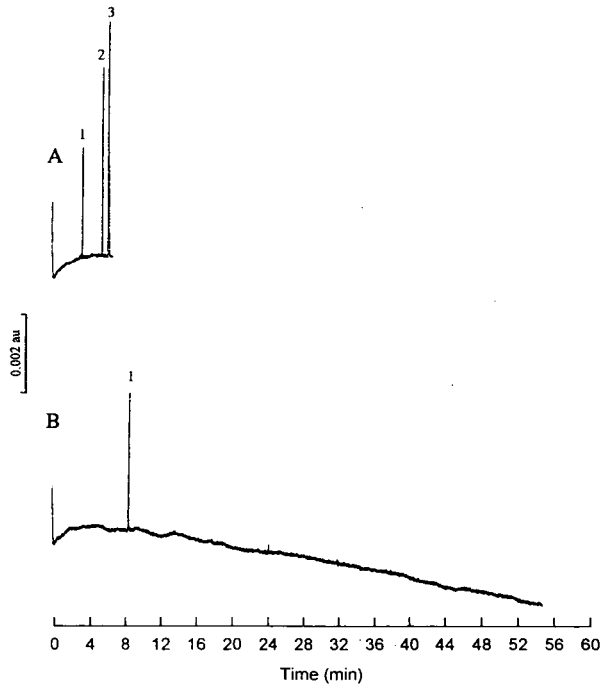

Fig. 6. Separations of acidic samples on bare capillary. Conditions: fused-silica capillary (75 μm I.D. × 375 μm O.D.) with 64.4 cm total length and 43.2 cm effective length; electric field, 288 V/cm. (A) pH 8.69; (B) pH 4.01. Peaks: 1 = methylphenol; 2 = 2-naphthalenesulfonic acid; 3 = benzenesulfonic acid.

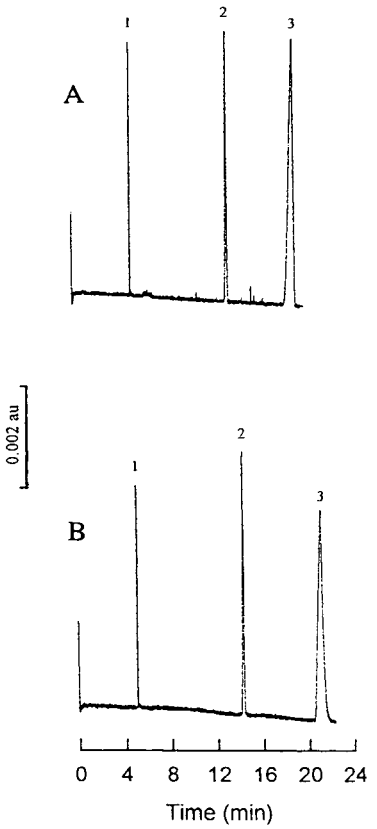

Fig. 7. Separations of acidic samples on NaAMPS polymer-coated capillary. Conditions as in Fig. 6. except that the capillary has a total length of 63 cm and effective length of 42.2 cm. (A) pH 8.69; (B) pH 4.01. Peaks: 1 = methylphenol; 2 = 2-naphthalenesulfonic acid; 3 = benzenesulfonic acid.

8.69, the bare capillary generates a high EOF, and all sample peaks exhibit short retention times. At pH 4.01 the two acidic samples maintain strong negative charges while the EOF becomes very slow. Only the neutral marker peak is detected. The two acidic samples are not observed in 55 min (Fig. 6B). On the NaAMPS polymer-coated capillary, all the neutral marker and two acidic samples elute at pH 8.69 and 4.01 (see Fig. 7). Sample retention times are similar for the two different pH conditions due to the pH-independent flow of the coated capillary. This example illustrates the ability to optimize selectivity for the separation of samples with very different pK_a values by changing the pH without affecting EOF rate.

CE has proven to be a powerful new technique for enantiomer separations [2]. Currently, the most commonly used chiral selector is cyclodextrin (CD) [31]. Chiral molecules of many pharmaceutical samples have been successfully separated using cyclodextrin as a run buffer additive. To obtain a good chiral separation, the mobility of the free sample species and the sample–CD complex must differ significantly from one another. Cross-linked polyacrylamide gel matrix [32] and dextran polymer network [33] have been used to achieve this requirement for the chiral separation of dansyl-DL-amino acids on coated capillaries. On a bare capillary, the EOF is relatively fast at pH 7 and the neutral β-CD molecules migrate with the EOF. The differences between the velocities of β-CD and the dansyl-DL-amino acid samples are too small

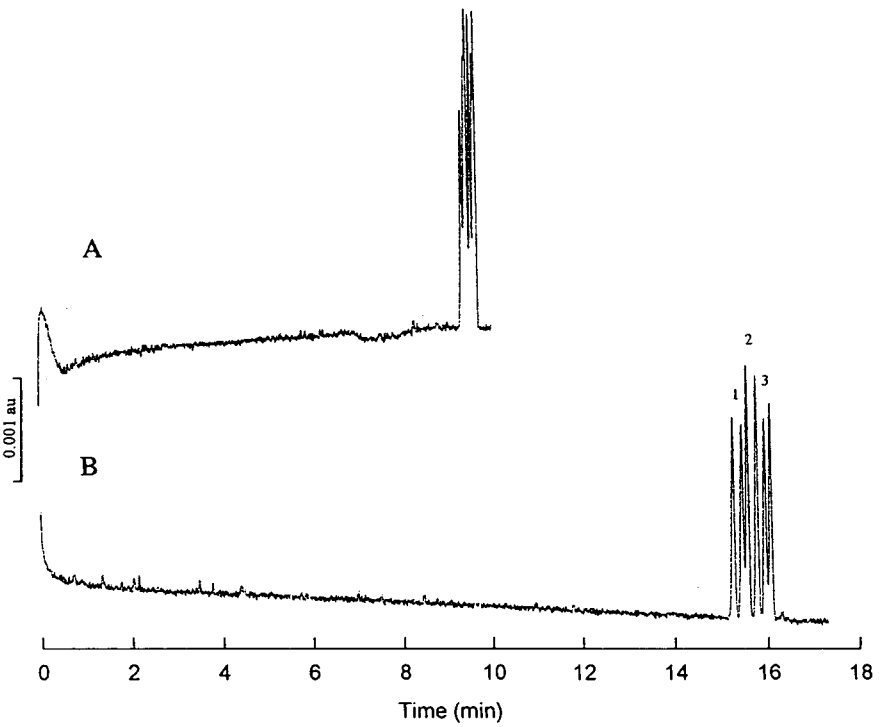

Fig. 8. Chiral separation of three dansyl-DL-amino acids. Conditions: electric field, 288 V/cm; buffer; 5 m*M* β-CD in 10 m*M* phosphate buffer at pH 7.0. (A) Bare capillary; (B) NaAMPS polymer-coated capillary. Peaks: 1 = dansyl-DL-norleucine; 2 = dansyl-DL-methionine; 3 = dansyl-DL-serine.

achieve chiral separation (Fig. 8A). A lower EOF is needed in this case to increase the difference between the free sample and CD–sample complex mobilities. This can be accomplished by using the NaAMPS polymer-coated capillary which possesses a lower EOF. Fig. 8B shows the chiral separation of three dansyl-CD-amino acids. All six enantiomers are resolved on this capillary at neutral pH.

Another application of the NaAMPS polymer-coated capillary with a pH-independent EOF is the use of MECC. MECC was first reported by Terabe et al. [34,35]. This method has provided an efficient means of separating a fairly wide variety of compounds of both biological and pharmaceutical significance [36]. One major limitation of MECC is the inability to perform separations at acidic pH (< pH 5) on a fused-silica capillary. In MECC, the net flow velocity of the micelles is equal to the summation of their electrophoretic velocity and the EOF velocity. At a low pH, the EOF velocity is too low and the micelles migrate toward the anode. Separations of neutral samples cannot be achieved under these conditions. The new NaAMPS polymer-coated capillary has a pH-independent EOF and provides the ability to run MECC separations at very low pH. Fig. 9 shows the separations of three samples, benzoic acid (pK_a = 4.20), 2-bromophenylacetic acid (pK_a = 4.05) and 4-bromophenylacetic acid (pK_a = 4.19). At pH 3.15, these samples cannot be baseline resolved without the addition of SDS to the run buffer (Fig. 9A). The MECC separation of these samples is represented in Fig. 9B. Good separation is obtained by MECC under these conditions. However, sample peaks cannot be detected on the bare capillary under the same

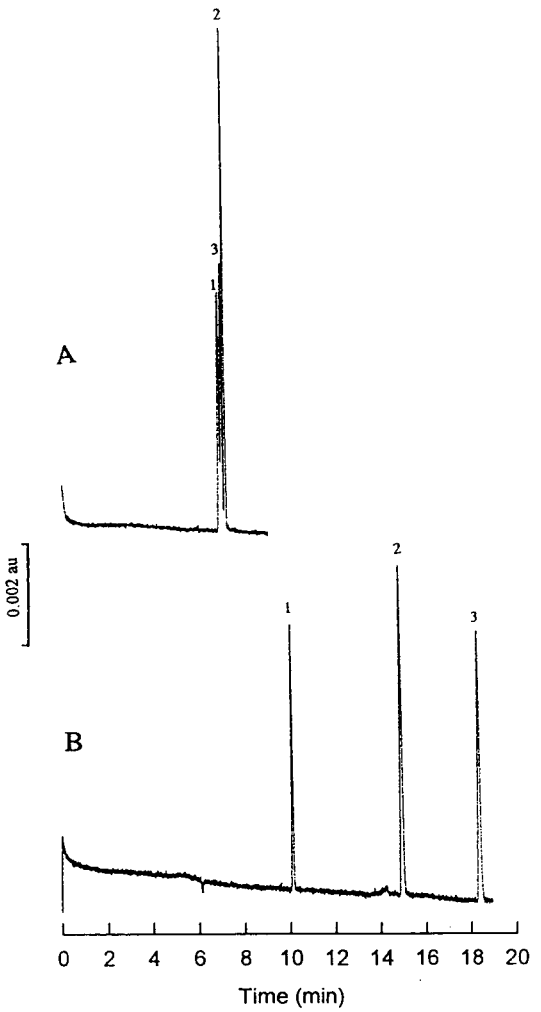

Fig. 9. Separations of three acidic samples on NaAMPS polymer-coated capillary. Conditions as in Fig. 7 except that run buffers are (A) 10 m*M* phosphate at pH 3.15 and (B) 50 m*M* SDS in 10 m*M* phosphate at pH 3.15. Peaks: 1 = benzoic acid; 2 = 2-bromophenylacetic acid; 3 = 4-bromophenylacetic acid.

conditions since the EOF is too low. Research is continuing in our laboratory to increase the applications of MECC using the new capillary coating. The preliminary results obtained so far [36] demonstrate that NaAMPS polymer-coated capillaries with desirable, pH-independent EOFs show very promising application potentials in MECC.

References

[1] J.W. Jorgenson and K.D. Lukacs, *Anal. Chem.*, 53 (1981) 1298.
[2] W.G. Kuhr, *Anal. Chem.*, 64 (1990) 403R.
[3] K.D. Altria and C.F. Simpson, *Chromatographia*, 24 (1987) 527.
[4] J.W. Jorgenson and K.D. Lukacs, *Science*, 222 (1983) 266.
[5] T.S. Stevens and H.J. Cortes, *Anal. Chem.*, 55 (1983) 1365.
[6] C.C. Rice and R. Witeheat, *J. Phys. Chem.*, 69 (1965) 4017.
[7] P.D. Grossman, in P.D. Grossman and J.C. Colburn (Editors), *Capillary Electrophoresis*, Academic Press, San Diego, CA, 1992, Ch. 1.
[8] S. Fujiwara and S. Honda, *Anal. Chem.*, 58 (1986) 1811.
[9] S. Fujiwara and S. Honda, *Anal. Chem.*, 59 (1987) 487.
[10] B.J. Herren, S.G. Shafer, J. Van Alstine, J.M. Harris and S.S. Snyder, *J. Colloid Interface Sci.*, 115 (1987) 46.
[11] J.R. Mazzeo and I.S. Krull, *Anal. Chem.*, 63 (1991) 2852.
[12] S. Hjertén, *Chromatogr. Rev.*, 9 (1967) 122.
[13] A.T. Balchunas and M.J. Sepaniak, *Anal. Chem.*, 59 (1987) 1466.
[14] S. Hjertén, *J. Chromatogr.*, 347 (1985) 191.
[15] R.M. McCormick, *Anal. Chem.*, 60 (1988) 2322.
[16] G.J.M. Bruin, J.P. Chang, R.H. Kuhlman, M.K. Zegers, J.C. Kraak and H. Poppe, *J. Chromatogr.*, 471 (1989) 429.
[17] G.J.M. Bruin, R. Huisden, J.C. Kraak and H. Poppe, *J. Chromatogr.*, 480 (1989) 339.
[18] K.A. Cobb, V. Dolnik and M. Novotny, *Anal. Chem.*, 62 (1990) 2478.
[19] J.K. Towns and F.E. Regnier, *J. Chromatogr.*, 516 (1990) 69.
[20] D. Bentrop, J. Kohr and H. Engelhardt, *Chromatographia*, 32 (1991) 171.
[21] W. Nashabeh and Z. El Rassi, *J. Chromatogr.*, 559 (1991) 367.
[22] A.M. Dougherty, C.L. Woolley, D.C. Williams, D.F. Swaile, R.O. Cole and M.J. Sepaniak, *J. Liq. Chromatogr.*, 14 (1991) 907.
[23] J.K. Towns, J. Bao and F.E. Regnier, *J. Chromatogr.*, 599 (1992) 227.
[24] C.S. Lee, W.C. Blanchard and C.T. Wu, *Anal. Chem.*, 62 (1990) 1550.
[25] M.A. Hayes and A.G. Ewing, *Anal. Chem.*, 64 (1992) 512.
[26] C.T. Wu, T. Lopes, B. Patel and C.S. Lee, *Anal. Chem.*, 64 (1992) 886.
[27] J.T. Smith and Z. El Rassi, *J. High Resolut. Chromatogr.*, 15 (1992) 573.
[28] J.K. Towns and F.E. Regnier, *Anal. Chem.*, 63 (1991) 1126.

[29] J. Kohr and H. Engelhardt, *J. Microcol. Sep.*, 3 (1991) 491.
[30] M. Huang, G. Yi, J.S. Bradshaw and M.L. Lee, *J. Microcol. Sep.*, 5 (1993) 199.
[31] S. Fanali, *J. Chromatogr.*, 474 (1989) 441.
[32] A. Guttman, A. Paulus, A.S. Cohen, N. Grinberg and B.L. Karger, *J. Chromatogr.*, 448 (1988) 41.
[33] P. Sun, G.E. Barker, G.J. Mariano and R.A. Hartwick, *Electrophoresis*, (1994) in press.
[34] S. Terabe, K. Otsuka, K. Ichikawa, A. Tsuchiya and T. Ando, *Anal. Chem.*, 56 (1984) 111.
[35] S. Terabe, K. Otsuka, K. Ichikawa and T. Ando, *Anal. Chem.*, 57 (1985) 834.
[36] A. Landman, P. Sun and R.A. Hartwick, *J. Chromatogr. A*, 669 (1994) 259.

ELSEVIER

Journal of Chromatography A, 685 (1994) 313–320

JOURNAL OF CHROMATOGRAPHY A

Evaluation of a neutral hydrophilic coated capillary for capillary zone electrophoretic separation of proteins

Tung-Liang Huang*, Paul C.H. Shieh, Edward V. Koh, Nelson Cooke

Beckman Instruments, Inc., 2500 Harbor Boulevard, Fullerton, CA 92634, USA

First received 5 April 1994; revised manuscript received 26 July 1994

Abstract

A neutral, hydrophilic coated capillary with negligible electroosmotic flow was characterized as to migration time reproducibility and separation efficiency for protein separation by capillary zone electrophoresis. Consecutive runs (over 200 runs) of the basic proteins at pH 6.0 yielded excellent migration time reproducibility ($<2\%$ R.S.D.) and high separation efficiency (ca. $3–5 \cdot 10^5$ plates/m). The acidic proteins were separated at pH 8.0 under the reversed polarity (cathode at the injection end), and excellent migration time reproducibility of less than 3% was achieved. Separation of egg white proteins at pH 3.0 showed migration time reproducibility of less than 0.5% R.S.D. ($n = 36$) for lysozyme, conalbumin and ovalbumin.

1. Introduction

Capillary zone electrophoresis (CZE) can serve as a fast, automated, and easily operated separation tool for analyzing proteins if the adsorption of proteins onto capillary wall can be eliminated for solving the problem of peak tailing and broadening, poor quantitation and irreproducibility of migration time. The adsorption of proteins are known to be incurred by electrostatic, hydrophobic, and, to a lesser extent, hydrogen bonding interactions between proteins and liquid–solid interface [1]. Much research has been devoted to minimize the interactions, and, basically, two major approaches have been employed in the research: the surface modification method [1–12] and the solution/colloids method [13–19]. With the former strategy, the capillary wall is bonded with a coating to deactivate the silanol groups on silica surface, and, for most cases, to increase the surface hydrophilicity; with the latter, buffer additives [13–17], high ionic strength [18,19], or pH extremes [20–23] are employed to prevent the adsorption. Generally, the latter approach is limited by the stability of protein at pH extremes and Joule heating accompanied by high ionic strength. When polymeric additives are used for reducing protein adsorption, the separation time is increased, and, in some cases, the resolution of two species of interest is limited due to the reduction of the difference of electrophoretic mobility with increased viscosity of running buffer. In contrast, with the bonded coating method, the buffer can still remain an adjustable parameter for optimizing the separation.

In this study, we have developed a neutral, hydrophilic coated capillary that allows basic and

* Corresponding author.

0021-9673/94/$07.00
SSDI 0021-9673(94)00702-0

acidic proteins separation at near neutral pH region (pH 6–8). This pH region is especially interesting since proteins often exist in native structures. An extensive evaluation of the coating will be reported, in terms of separation efficiency, migration time reproducibility and long-term stability, as applied to CZE separation of proteins.

2. Experimental

2.1. Materials

All proteins used were purchased as lyophilized powders from Sigma (St. Louis, MO, USA): α-lactalbumin (bovine milk, pI 4.8), β-lactoglobulin A (bovine milk, pI 5.1), carbonic anhydrase II (human erythrocytes, pI 5.4), carbonic anhydrase II (human erythrocytes, pI 5.9), myoglobin (horse heart, pI 7.2), ribonuclease A (bovine pancrease, pI 9.5), cytochrome c (bovine heart, pI 10.8) and lysozyme (chicken egg white, pI 11.0). Benzyl alcohol, hydrochloric acid, sodium hydroxide and the buffers for protein separations and electroosmotic flow (EOF) measurements were also supplied by Sigma. Egg white was taken from fresh chicken egg.

2.2. CZE

A P/ACE 2210 capillary electrophoresis instrument controlled by System Gold software (Beckman, Fullerton, CA, USA) was used in this study. Neutral, hydrophilic coated capillaries of 50 μm I.D. from eCAP neutral capillary methods development kit/proteins (Beckman) were used for protein separation. Protein mixtures were dissolved in deionized water at a concentration of 1 mg/ml for each protein; chicken egg white was diluted 1:10 in water. Unless specified, the separations were carried out at room temperature (25°C), with a field strength of 500 V/cm and detection at 214 nm. The proteins were introduced into the separation capillary by pressured injection for 1 s. Between runs, the column was rinsed with 0.1 M HCl for 0.5 min and then with the running buffer for 1.5 min. Running buffer in the vials was changed for every 30 runs.

When the buffer was changed to a different pH, the column was reconditioned by performing a 10-min rinse with the new buffer. The capillary was then equilibrated with the new buffer for another 10 min prior to performing a run.

3. Results and discussion

3.1. Electroosmotic flow

For the coated capillaries used in this study, the coating inside the capillary wall consists of two polymeric layers covalently bonded to each other [24]. The function of the first layer is to deactivate the silanol groups, and, thus, to reduce the electrostatic interaction between silica surface and proteins; the second layer serves as a hydrophilic shield to suppress the hydrophobic interactions between capillary wall and protein molecules. The coverage of the coating on capillary wall was evaluated by monitoring EOF of the coated capillaries. The plot of EOF vs. pH is given in Fig. 1. As shown in Fig. 1, the EOF of the coated capillary showed values ranging $1 \cdot 10^{-6}$–$5 \cdot 10^{-6}$ cm^2/V s at pH values 5–10, which are two orders of magnitude less than the EOF of fused-silica capillaries. The extremely low EOF in the coated capillaries can be attributed to at least two causes. First, the deactivation reaction of silanol groups on silica surface during coating processes reduces the surface charges arising from deprotonated silanol groups. Second, the viscosity of running buffer at the solid–liquid interface also plays an important role in affecting the magnitude of EOF. When hydrophilic polymers are bonded onto the silica surface, the viscosity at the interface is known to increase [25], leading to a slower EOF.

3.2. Basic protein separations

The separations of four basic proteins at pH 6.0 are shown in Fig. 2. Due to the strong

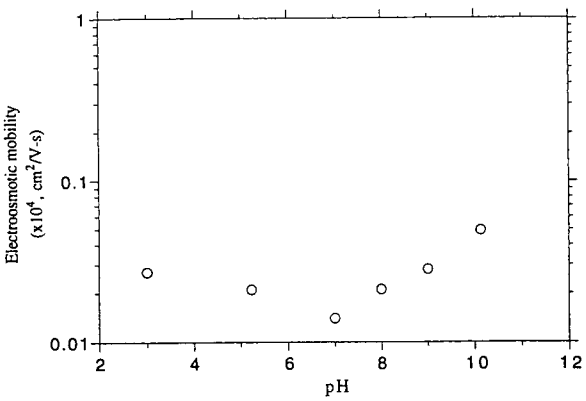

Fig. 1. EOF of the neutral coated capillaries. Conditions: 500 V/cm; 20 cm capillary separation length; benzyl alcohol used as EOF marker. The running buffers were: 20 m*M* citrate at pH 3.0, 50 m*M* 2-(N-morpholino)ethanesulfonic acid (MES) at pH 5.2, 20 m*M* 4-(2-hydroxyethyl)-1-piperazineethanesulfonic acid (HEPES) at pH 7.0, 20 m*M* N-[tris(hydroxymethyl)methyl]glycine (Tricine) at pH 8.0, 20 m*M* 2-(N-cyclohexylamino)ethanesulfonic acid (CHES) at pH 9.0 and 20 m*M* 3-cyclohexylamino-1-propanesulfonic acid (CAPS) at pH 10.1.

electrostatic interactions between positively charged proteins and deprotonated silanol groups, the basic proteins tend to adsorb onto bare silica surface, leading to poor peak shape and irreproducibility of migration time. In this sense, the basic proteins can serve as a sensitive probe of the charging state of the capillary surface. As shown in Fig. 2, all the four basic proteins showed good peak shape under the separation condition. After 216 consecutive runs under a high field strength of 500 V/cm, the migration time of the four proteins showed minimal change of less than 4 s, and the peak shapes of lysozyme, cytochrome *c* and ribonuclease A still remained good. The slightly tailing peak shape of myoglobin was due to the degradation of myoglobin kept in the sample vial for 61 h at 27°C during the 216 consecutive runs. The degradation of myoglobin with time at room temperature can be alleviated by using commercially available sample cooling systems, which use circulating coolant to keep the proteins at 4°C. The separation efficiency and migration time reproducibility of the basic proteins are shown in Table 1. The separation efficiencies of

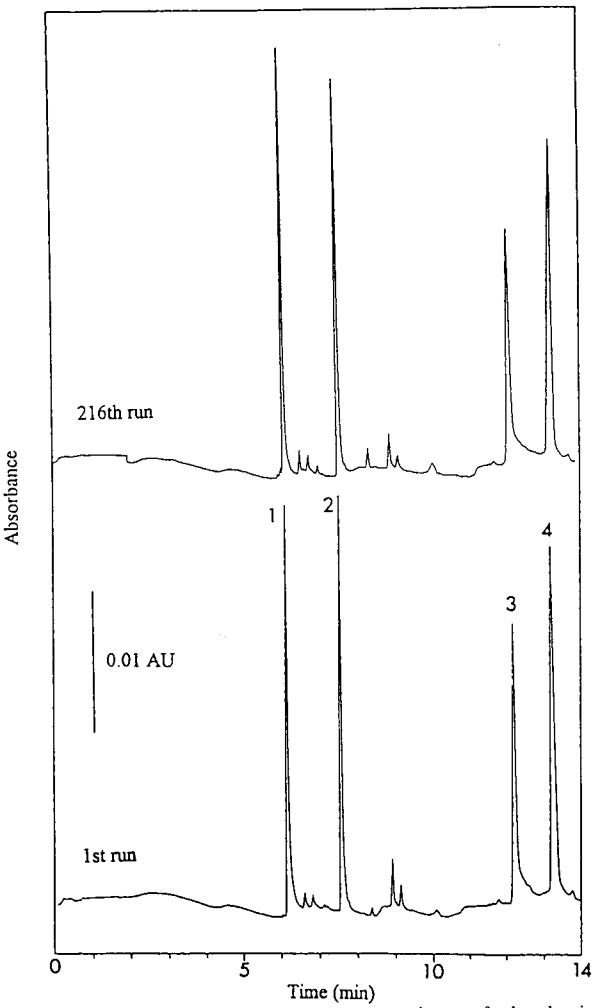

Fig. 2. Capillary electrophoretic separations of the basic proteins as in Table 1. Separation conditions: 20 m*M* citrate and 20 m*M* MES, pH 6.0; 500 V/cm; 20 cm capillary separation length.

the four proteins were all higher than $3 \cdot 10^5$/m for the first run, and, after 215 consecutive runs, the high efficiencies still remained, indicating the excellent stability of the coating. The relative standard deviations (R.S.D.s) of the basic proteins for overall 216 runs were all less than 2%. In this study, the running buffer in the vials was changed for every 30 runs. As will be discussed below, the migration time reproducibility could be further improved if the running buffer was changed more often.

Table 1
Column efficiencies and migration time reproducibility for consecutive runs at pH 6.0

Peak No.	Protein	Efficiency/m ($\times 10^3$)		Migration time[a]	
		1st run	216th run	Average (min)	R.S.D. (%)
1	Lysozyme	389	587	6.1	0.5
2	Cytochrome *c*	525	483	7.5	0.5
3	Myoglobin	587	465	12.1	1.0
4	Ribonuclease A	318	297	13.1	1.0

[a] $n = 216$ (1st–216th runs).

A detailed study of the migration time pattern of three basic proteins (lysozyme, cytochrome *c* and ribonuclease A) was carried out with another coated capillary, and the results were shown in Fig. 3. It is of interest to note that, for every 30 runs with a same vial of running buffer, the migration time of each protein tended to increase slightly with the number of run until the running buffer was replaced. When the running buffer was just changed, the migration time of each protein discontinuously shifted to a lower value. This phenomenon was more significant for the proteins with longer migration time, especially ribonuclease A. There are at least two possible causes for this effect. First, the evaporation of the buffer solution during the consecutive runs resulted in a more concentrated buffer with increased ionic strength, and thus reduced the electrophoretic mobility of proteins and the residual EOF. Second, the polarization of electrodes by an excess of counter-ions (or depletion of co-ions) leaded to a lower effective separation voltage. Thus, the migration times of proteins were increased due to a lower separation field strength. Nevertheless, this study suggests that if a running buffer vial can be replaced more frequently than 30 runs, the elution time of the last run will deviate to a lesser extent from the first run, and better migration time reproducibility can be achieved.

A detailed study of the separation efficiency vs. run number for 210 consecutive runs was also carried out, and no significant trend was observed for the four basic proteins (lysozyme, cytochrome *c*, myoglobin and ribonuclease A).

The capillary-to-capillary study of the migration time reproducibility (R.S.D.) was evaluated using separations of the basic proteins

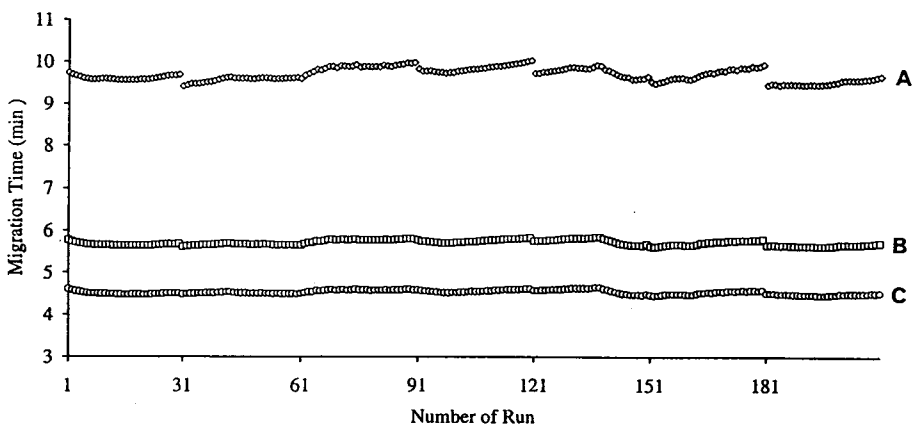

Fig. 3. Migration times of 210 consecutive runs for capillary electrophoretic separations of basic proteins. Separation conditions as in Fig. 2. A = Ribonuclease A; B = cytochrome *c*; C = lysozyme.

(lysozyme, cytochrome *c* and ribonuclease A) at pH 6.0. Six capillaries, with designations of Cap 1–6, were evaluated with 240 consecutive runs. The migration time reproducibility (R.S.D.) based on the first and last 20 runs ($n = 40$) was calculated and shown in Table 2. The Cap 1–3 were randomly chosen from the same lot, and Cap 1, 4, 5 and 6 were from four different lots. By our coating procedure, 140 coated capillaries of 45 cm long were prepared in one lot. As shown in Table 2, the R.S.D.s of migration times were all less than 2%, and the variation of the migration time reproducibility for the capillaries from different lots was not larger than that from the same lot, indicating the consistency of the coating techniques for obtaining coating capillaries with excellent migration time reproducibility.

3.3. Acidic protein separations

As mentioned above, the EOF of the coated capillaries is extremely low, and can be regarded as zero for normal CZE separation. For separation of the acidic proteins at the pH values near neutral, the separation has to be carried out under reversed-polarity mode (cathode is at the injection end), to drive the negatively charged proteins toward detection window by their own electrophoretic mobility. The separations of four acidic proteins at pH 8.0 under the reversed polarity are shown in Fig. 4. As shown in Fig. 4, all the four acidic proteins showed good peak shapes under the separation conditions. After 120 consecutive runs of separation under a high field strength of 500 V/cm, the migration times of the four proteins showed minimal change, and the peak shapes of α-lactalbumin, carbonic anhydrase II (p*I* 5.4) and carbonic anhydrase II (p*I* 5.9) still remained good. The broadening of the β-lactoglobulin A peak was found to be caused by degradation of β-lactoglobulin A molecules,

Table 2
Capillary-to-capillary variation of migration time reproducibility at pH 6.0

	Migration time reproducibility (R.S.D., %)[a]		
	Lysozyme	Cytochrome *c*	Ribonuclease A
Cap 1[b]	0.7	0.6	0.7
Cap 2	1.7	1.6	1.9
Cap 3	0.7	0.6	0.6
Cap 4	0.7	0.7	1.0
Cap 5	1.9	1.9	1.5
Cap 6	0.5	0.4	0.8

[a] Based on 1st–20th runs and 221st–240th runs ($n = 40$) for each capillary.
[b] Cap 1–3 were randomly chosen from a lot of 140 capillaries. Cap 1, 4, 5 and 6 were each randomly chosen from different lots; 140 capillaries were prepared in one lot.

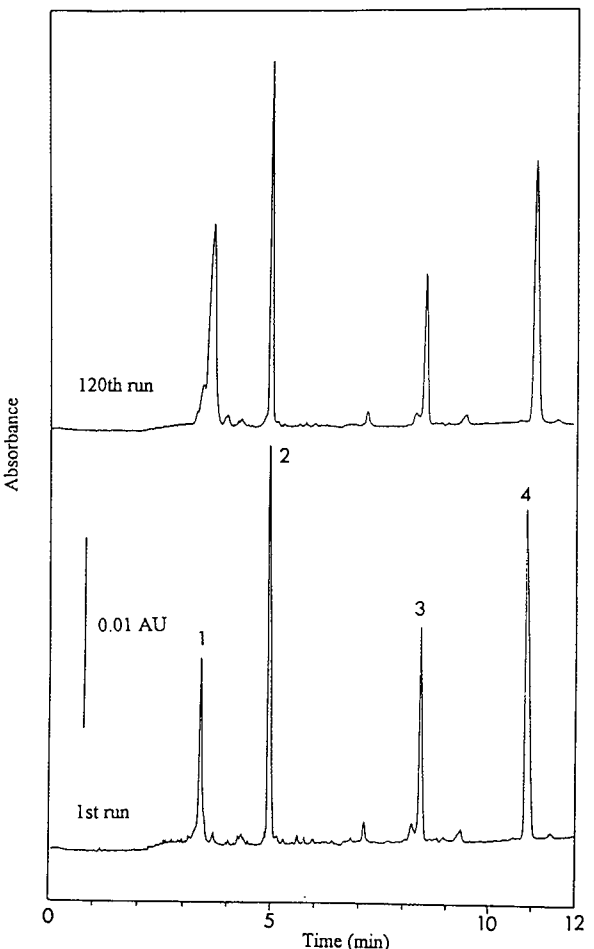

Fig. 4. Capillary electrophoretic separations of the acidic proteins as in Table 3. Separation conditions: 20 m*M* Tricine, pH 8.0; 500 V/cm; 20 cm capillary separation length.

as confirmed by the fact that a symmetrical and sharp peak shape was restored after replacing with a fresh sample vial. The separation efficiency and migration time reproducibility of the acidic proteins are shown in Table 3. As indicated in Table 3, after 120 consecutive runs, the efficiencies were still high (the low efficiency of β-lactoglobulin A is owing to degradation). Regarding the migration time reproducibility, except for β-lactoglobulin A, the R.S.D.s of the acidic proteins for 216 consecutive runs were less than 2%. Due to the degradation of protein molecules, β-lactoglobulin A showed a higher value of R.S.D. of 3%.

3.4. Egg white protein separations

The three major components of egg white proteins are lysozyme (p*I* 11.0, M_r 14 000), conalbumin (p*I* 6.6, M_r 77 000) and ovalbumin (p*I* 4.7, M_r 43 500) [26]. To elute these three components with a wide p*I* range in one run, 20 m*M* citrate buffer at pH 3.0 was used to separate the three proteins. As shown in Fig. 5, these three components eluted according to their charging states; lysozyme, the most positively charged protein, eluted first followed by conalbumin, the protein with the middle p*I*. The identification of each peak was confirmed by individual standard protein. Both lysozyme and conalbumin appeared with good peak shapes, while the ovalbumin peak appeared with a shoulder that has been observed and attributed to impurity [26,27].

Reproducibility of migration time of the egg white proteins was studied for over 36 consecutive runs, and the results were shown in Table 4. As seen in Table 4, the relative standard deviation (R.S.D.) for each component was all less than 0.5%. Data of reproducibility of the peak area and peak height for over 9 runs are listed in Table 5. The R.S.D.s of peak area and peak height for these three proteins were around 3%, suggesting little, if any, loss of protein molecules due to adsorption and the possibility of using CZE to quantify the egg white proteins.

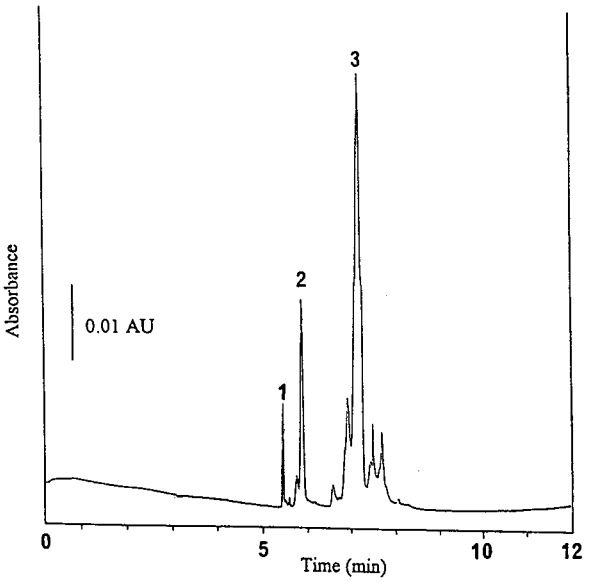

Fig. 5. Capillary electrophoretic separations of egg white proteins as in Table 4. Separation conditions: 20 m*M* citrate, pH 3.0; 324 V/cm; 30 cm capillary separation length.

Table 3
Column efficiencies and migration time reproducibility for consecutive runs at pH 8.0

Peak No.	Protein	Efficiency/m (× 10^3)		Migration time[a]	
		1st run	120th run	Average (min)	R.S.D. (%)
1	β-Lactoglobulin A	73	35	3.5	3.0
2	α-Lactalbumin	117	142	5.0	0.4
3	Carbonic anhydrase II (p*I* 5.4)	548	263	8.4	1.0
4	Carbonic anhydrase II (p*I* 5.9)	334	249	10.9	1.3

[a] $n = 120$ (1st–120th runs).

Table 4
Reproducibility of migration time for egg white proteins at pH 3.0

Peak No.	Protein	p*I*	Migration time[a]	
			Average (min)	R.S.D. (%)
1	Lysozyme	11.0	5.3	0.4
2	Conalbumin	6.6	5.8	0.3
3	Ovalbumin	4.7	7.1	0.4

[a] $n = 36$.

4. Conclusions

A neutral, hydrophilic coated capillary with negligible EOF was evaluated to show high separation efficiency, excellent migration time reproducibility, and long term stability as applied to CZE for protein separations. From the results shown above, the coated capillary combined with three buffers at pH 3.0, 6.0 and 8.0 can serve as a convenient analyzing tool for separations of proteins with a wide p*I* range. The pH 6.0 buffer is used for separations of neutral and basic proteins (p$I > 6.7$) under normal separation polarity (anode at the injection end), and the pH 8.0 buffer can be used for acidic proteins (p$I <$ 6.6) under reversed separation polarity (cathode at the injection end). With a field strength of 500 V/cm and a capillary separation length of 20 cm, model proteins with p*I* values ranging 3.5–6.6 (or 6.7–11.0) were observed to elute in 20 min with high separation efficiency by using the pH 6.0 (or the pH 8.0 buffer); with the pH 3.0 buffer, proteins with p*I* values ≥ 4 would elute in 10 min under a field strength of 500 V/cm and capillary separation length of 20 cm. In this sense, an unknown sample can be quickly scanned by carrying out the separation with pH 3.0 buffer, followed by the separations with pH 6.0 and/or pH 8.0 buffers to achieve better separation efficiency and resolution.

For CZE separation, development of a method for protein separation is by no mean an easy task, which involves the optimization of buffer type, ionic strength, pH, field strength and capillary separation length. The conjunction of the neutral coated capillary with three buffers of appropriate pH values (pH 3.0, 6.0 and 8.0) is then expected to make easier the development of methodology for protein separations by CZE.

Table 5
Reproducibility of peak area and peak height for egg white proteins at pH 3.0

Peak No.	Protein	R.S.D. (%)[a]	
		Peak area	Peak height
1	Lysozyme	3.0	2.5
2	Conalbumin	3.5	3.7
3	Ovalbumin	3.6	2.9

[a] $n = 9$.

Acknowledgement

The authors gratefully acknowledge Professor Barry L. Karger, Northeastern University, Barnett Institute, Boston, MA, USA, for his helpful discussion.

References

[1] Z. Zhao, A. Malik and M.L. Lee, *Anal. Chem.*, 65 (1993) 2747–2752.
[2] G.J.M. Bruin, J.P. Chang, R.H. Kuhlman, K. Zegers, J.C. Kraak and H. Poppe, *J. Chromatogr.*, 471 (1989) 429–436.
[3] K.A. Cobb, V. Dolnik and M. Novotny, *Anal. Chem.*, 62 (1991) 2478–2483.
[4] W. Nashabeh and Z. El Rassi, *J. Chromatogr.*, 559 (1991) 367–383.

[5] J.E. Sandoval and J.J. Pesek, *Anal. Chem.*, 63 (1991) 2634–2641.
[6] J. Kohr and H. Engelhardt, *J. Microcol. Sep.*, 3 (1991) 491–495.
[7] J.K. Towns and F.E. Regnier, *Anal. Chem.*, 63 (1991) 1126–1132.
[8] M. Huang, W.P. Vorkink and M.L. Lee, *J. Microcol. Sep.*, 4 (1992) 233–238.
[9] M. Gilges, H. Husmann, M.-H. Kleemiss, S.R. Motsch and G. Schomburg, *J. High Resolut. Chromatogr.*, 15 (1992) 452–457.
[10] S.A. Swedberg, *Anal. Biochem.*, 185 (1990) 51–70.
[11] D. Schmalzing, C.A. Piggee, F. Foret, E. Carrilho and B.L. Karger, *J. Chromatogr. A*, 652 (1993) 149–159.
[12] S. Hjertén, *J. Chromatogr.*, 347 (1985) 191–198.
[13] M.J. Gordon, K.J. Lee, A.A. Arias and R.N. Zare, *Anal. Chem.*, 63 (1991) 69–72.
[14] M. Zhu, R. Rodriguez, D. Hansen and T. Wehr, *J. Chromatogr.*, 516 (1990) 123–131.
[15] A. Emmer, M. Jansson and J. Roeraade, *J. High Resolut. Chromatogr.*, 14 (1991) 738–740.
[16] M.A. Strege and A.L. Lagu, *J. Chromatogr.*, 630 (1993) 337–344.
[17] W.G.H.M. Muijselaar, C.H.M.M. de Bruijn and F.M. Everaerts, *J. Chromatogr.*, 605 (1992) 115–123.
[18] M.M. Bushey and J.W. Jorgenson, *J. Chromatogr.*, 480 (1989) 301–310.
[19] F. Chen, L. Kelly, R. Palmieri, R. Biehler and H. Schwartz, *J. Liq. Chromatogr.*, 15 (1992) 1143–1161.
[20] R.M. McCormick, *Anal. Chem.*, 60 (1988) 2322–2328.
[21] H.H. Lauer and D. McManigill, *Anal. Chem.*, 58 (1986) 166–170.
[22] Y. Walbroehl and J.W. Jorgenson, *J. Microcol. Sep.*, 1 (1989) 41–45.
[23] H. Lindner, W. Helliger, A. Dirschlmayer, M. Jaquemar and B. Puschendorf, *Biochem. J.*, 283 (1992) 467–471.
[24] C.H. Shieh, *US Pat.*, pending.
[25] M. Huang, W.P. Vorkink and M.L. Lee, *J. Microcol. Sep.*, 4 (1992) 135–143.
[26] J.D. McCulloch, *J. Liq. Chromatogr.*, 16 (1993) 2025–2038.
[27] M.J. Gordon, K. Lee, A.A. Arias and R.N. Zare, *Anal. Chem.*, 63 (1991) 69–72.

ELSEVIER

Journal of Chromatography A, 685 (1994) 321–329

JOURNAL OF CHROMATOGRAPHY A

Chiral separations of amino acids by capillary electrophoresis and high-performance liquid chromatography employing chiral crown ethers

Yvonne Walbroehl[1], Joseph Wagner*

Marion Merrell Dow Research Institute, 16 Rue d'Ankara, 67080 Strasbourg, France

Abstract

High-performance liquid chromatography with a chiral crown ether stationary phase and capillary electrophoresis (CE) with a chiral crown ether dissolved in the operating buffer were used for the separation of enantiomers of analogues of DOPA and tyrosine and some analogues of γ-aminobutyric acid (GABA). CE and HPLC yielded similar results for the DOPA and tyrosine analogues. However, for the analogues of GABA, three of the four compounds tested were well resolved by HPLC but only one was well resolved by CE. It was necessary to use an indirect detection scheme for the CE of GABA analogues. The influence of substituents on the different compounds on the resolution factors observed by the two methods is discussed, in addition to the advantages and disadvantages of the two methods in practical applications.

1. Introduction

High-performance liquid chromatography (HPLC) using various types of chiral stationary phases, mobile phase additives and derivatizing agents has been used extensively for the separation of amino acids [1,2]. Capillary electrophoresis (CE) has also been employed for chiral separations of amino acids, but derivatization has usually been required [3]. More recently, Kuhn and co-workers [4,5] described the use of a chiral crown ether for the chiral resolution of various amino acids, peptides and optically active amines without prior derivatization. In this work, we applied both capillary electrophoresis with a chiral crown ether in the operating buffer and HPLC using a crown ether stationary phase to the separation of two series of compounds, analogues of DOPA and tyrosine and analogues of γ-aminobutyric acid (GABA). We explored the influence of the structure of the analyte molecules in a series of analogues on the degree of separation obtained and compared the results obtained for the two series of compounds using the two different procedures.

2. Experimental

All CE experiments were carried out using a Beckman P/ACE 2100 system. The system was interfaced to an IBM-compatible personal com-

* Corresponding author.

[1] Present address: Syntex Discovery Research, 3401 Hillview Avenue, P.O. Box 10850, Palo Alto, CA 94303, USA.

0021-9673/94/$07.00
SSDI 0021-9673(94)00722-5

puter and Beckman System Gold software was used for data collection and manipulation. Separations were carried out in a fused-silica capillary tube (Beckman Instruments, Neuilly, France). For the separation of DOPA and tyrosine analogues, the dimensions of the tube were 27 cm × 50 μm I.D., with the detector located 7 cm from the outlet end of the capillary. A detector slit size of 100 μm × 200 μm was used for experiments with direct detection. The detection wavelength was 280 nm. The capillary was thermostated at 20°C. Most experiments were carried out using 50 m*M* sodium phosphate buffer (pH 2.2) containing 30 m*M* 18-crown-6-tetracarboxylic acid (18-crown-6-TCA). For experiments investigating the effects of the concentration of the crown ether, the concentration of 18-crown-6-TCA was varied from 0 to 100 m*M*. Alternatively, 100 m*M* Tris buffer with the pH adjusted to 2.5 with citric acid and containing 30 m*M* 18-crown-6-TCA was used. Test compounds were dissolved in water at a concentration of ca. 0.25 mg/ml.

For chiral resolutions of the GABA analogues, which have poor UV absorbance, an electrolyte solution containing 6 m*M* benzyltrimethylammonium chloride (BTMACl) and 30 m*M* 18-crown-6-TCA and the pH adjusted to 3.7 with 1 *M* NaOH was used, with indirect detection. The detector wavelength was set at 214 nm. A slit size of 50 μm × 200 μm was used for measurements with indirect detection. A 57 cm × 75 μm I.D. capillary thermostated at 25°C was used for these experiments. Test compounds were dissolved in water at a concentration of ca. 0.5 mg/ml.

HPLC experiments were carried out using a conventional HPLC system consisting of a Waters M590 pump, a Waters WISP 710B autosampler and either a Waters M481 UV detector or a Kratos Spectroflow 773 UV detector. A Crownpak CR(+) column (15 cm × 4 mm I.D., 5-μm packing) obtained form Daicel (Tokyo, Japan) was used. The column was thermostated using either a water-bath or a methanol bath. A guard column (2.1 cm × 2.0 mm I.D.) containing glass beads (30–50 μm diameter) was used. Unless indicated otherwise, the following chromatographic conditions were used for the analogues of DOPA and tyrosine: mobile phase, 0.16 *M* $HClO_4$–10% methanol (pH 1.05); temperature, 20°C; flow-rate, 1 ml/min.; detection wavelength, 280 nm; injection volume, 5 μl. Sample solutions were prepared in the mobile phase at concentrations ranging from about 0.2 to 0.3 mg/ml. The conditions used for the GABA analogues were as follows: mobile phase, 0.11 *M* $HClO_4$ (pH 1.05); temperature, 10°C; flow-rate, 0.5 ml/min; detection wavelength, 210 nm; injection volume, 10 μl. Sample solutions were prepared in the mobile phase at a concentration of ca. 0.6 mg/ml.

Chemicals were of analytical reagent grade, unless stated otherwise. Phosphoric acid, perchloric acid, methanol, sodium hydroxide and 18-crown-6-TCA were obtained from Merck (Darmstadt, Germany). Citric acid was obtained from Prolabo (Paris, France). Benzyltrimethylammonium chloride was obtained from ICN Pharmaceuticals (Plainview, NY, USA). Tris, D,L-DOPA, D-DOPA, tyrosine, L-tyrosine, (±)-ephedrine and (±)-norephedrine were obtained form Sigma (Saint Quentin Fallavier, France). Analogues of DOPA and tyrosine (compounds **1–7**) were synthesized in-house by previously published methods [6–8]. Analogues of GABA (compounds **8–11**) were also synthesized by published procedures [9–12].

3. Results and Discussion

3.1. Results for analogues of DOPA and tyrosine

Influence of structure of analytes on chiral resolution

We investigated a series of analogues of DOPA and tyrosine with various substituents. Structures of the compounds and results of HPLC and CE experiments of this series of compounds are given in Table 1. Structures of the crown ethers used in the experiments are shown in Fig. 1. It can be seen that for compounds having three substituents on the carbon α to the amino group (**1–4**), no resolution was

Table 1
Summary of results obtained by HPLC and CE for analogues of DOPA and tyrosine

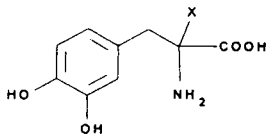

Structure A (compounds **1–4**)

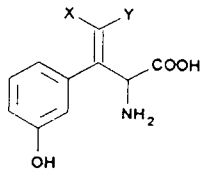

Structure B (compounds **5–7**)

Compound	Structure	X	Y	HPLC results[a]			CE results[b]		
				t_{r1}	t_{r2}	R_s	t_{m1}	t_{m2}	R_s
DOPA				3.24	4.78	4.4	5.84	5.97	1.1
Tyrosine				3.95	5.77	4.4	5.86	6.00	1.0
1[c]	A	CH_2F		3.13	–	0	15.51	–	0
2[c]	A	CHF_2		2.80	–	0	26.84	–	0
3[c]	A	$CH{=}CH_2$		5.20	–	0	11.93	–	0
4[c]	A	$CH{\equiv}CH$		3.44	–	0	24.98	–	0
5	B	H	H	5.73	11.44	7.8	8.69	10.11	6.3
6	B	F	H	5.26	8.00	4.5	9.72	13.31	11.1
6[d]	B	F	H	17.25	23.38	4.3			
7[d]	B	H	F	15.97	17.39	1.1	10.57	11.09	2.0

[a] t_{r1} = Retention time of first-eluting enantiomer and t_{r2} = retention time of second-eluting enantiomer from HPLC column.
[b] t_{m1} = migration time of faster migrating enantiomer and t_{m2} = migration time of slower migrating enantiomer by CE.
[c] CE operating buffer, 100 m*M* Tris–citrate–30 m*M* 18-crown-6-TCA (pH 2.5).
[d] HPLC mobile phase, 0.06 *M* $HClO_4$ (pH 1.5); flow-rate, 0.5 ml/min; temperature, 20°C.

obtained with CE or HPLC. Even using eluents with a higher perchloric acid concentration (0.16 *M*) and no methanol and working at lower temperatures (0–10°C) did not allow the resolution of these compounds. When Behr et al. [13] measured stability constants for complexes of various amines with chiral crown ethers, including 18-crown-6-TCA, they determined that primary amines with three α-substituents formed very weak complexes as compared with analogues with only two substituents at the α-carbon. Kuhn et al. [5] compared results for ephedrine, a secondary amine that does not fit into the crown ether cavity, and norephedrine, its demethylated analogue, by CE using 18-crown-6-TCA in the buffer. They found that whereas the enantiomers of norephedrine were resolved, no resolution was observed for ephedrine. The migration time of ephedrine in the CE system was also significantly faster than those of the norephedrine enantiomers. From this, they concluded that complexation of the ammonium cation with the crown ether is necessary for chiral recognition by CE using 18-crown-6-TCA. In our laboratory, we carried out analogous experiments by HPLC using the Crownpak CR(+) column. We were also unable to resolve the enantiomers of ephedrine, whereas the enantiomers of norephedrine were resolved with longer retention times than that observed for ephedrine. Therefore, the fact that no separation was seen for the α-substituted compounds by either HPLC or CE is most likely due to very weak, if any, complexation of these compounds with the crown ethers.

The remaining compounds have a C=C double bond in the position β to the amino group. All of these compounds were resolved using both CE and HPLC, but there are significant differences in the results. Using HPLC, **5** was better resolved than DOPA and tyrosine. The resolution obtained for **6** was similar to that for DOPA and

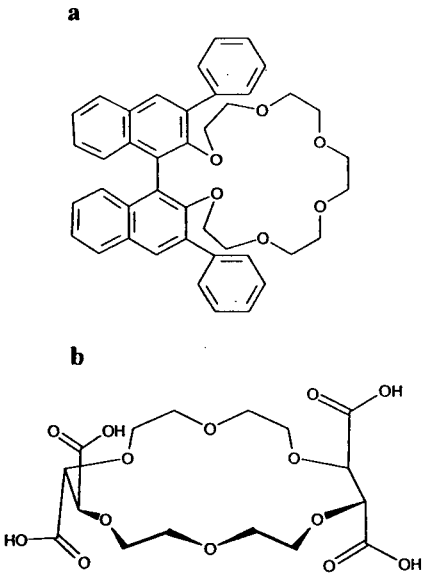

Fig. 1. (a) (*S*)-2,3:4,5-Bis(1,2-3-phenylnaphtho)-1,6,9,12,15,18-hexaoxacycloeicosa-2,4-diene crown ether incorporated into the stationary phase of the Crownpak CR(+) HPLC column; (b) (2*R*,3*R*,11*R*,12*R*)-(+)-1,4,7,10,13,16-hexaoxacyclooctadecane-2,3,11,12-tetracarboxylic acid crown ether used in the capillary electrophoresis operating buffer.

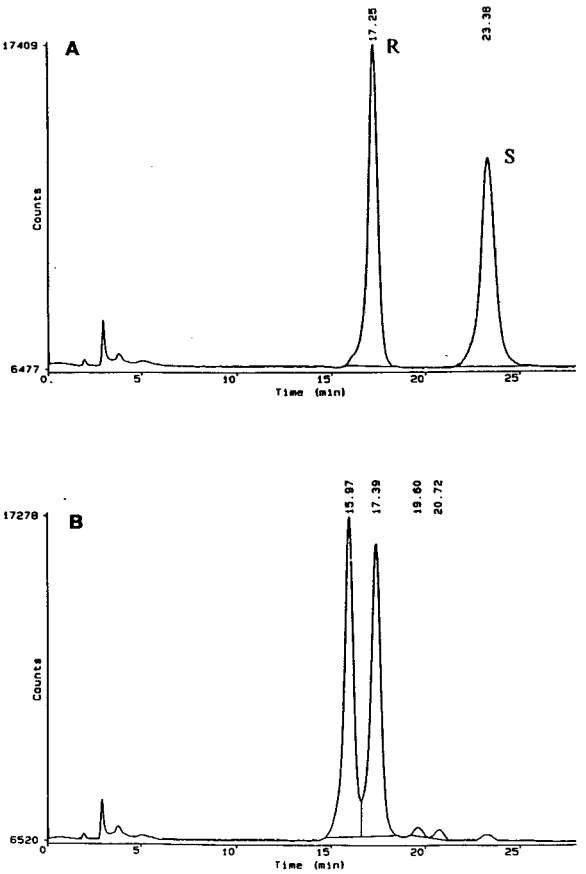

Fig. 2. Representative chromatograms obtained for analogues of tyrosine on the Crownpak CR(+) column. (A) Compound **6**, 1.05 μg injected; (B) compound **7**, 1.5 μg injected. Conditions: mobile phase, 0.06 *M* $HClO_4$ (pH 1.5); temperature, 20°C; flow-rate, 0.5 ml/min; detection wavelength, 280 nm. Peaks for **7** are not chirally identified because the individual enantiomers were not available.

tyrosine. For **7**, the resolution was much poorer than for DOPA and tyrosine. The order of elution was determined for those compounds for which at least one of the individual enantiomers was available (DOPA, tyrosine and **6**). In each instance, the *R*-enantiomer was eluted first, followed by the *S*-enantiomer. This indicates that the *S*-enantiomer forms a stronger complex with the (*S*)-(+)-crown ether. Representative chromatograms are shown in Fig. 2.

However, the CE results were clearly different. Compounds **5** and **6** were much better resolved by CE than DOPA and tyrosine, whereas only a modest increase in resolution was observed for **7**. Representative electropherograms are shown in Fig. 3. The large resolution factors observed for **5** and **6** are in contrast to earlier reports of CE using 18-crown-6-TCA as a chiral selector, where more modest resolution factors, between 0 and 3, were observed [4,5]. Large resolution factors imply that there is a large difference between the stability constants for the complexes of the two enantiomers with the crown ether. The large resolution factors observed for **5** and **6** can probably be explained by the altered geometry at the β-carbon. Apparently, this geometry leads to the stabilization of the complex of 18-crown-6-TCA with one of the two enantiomers. The proximity of the fluorine atom to the amino group in **7** most likely destabilizes this complex and therefore a more modest resolution factor is observed. The rela-

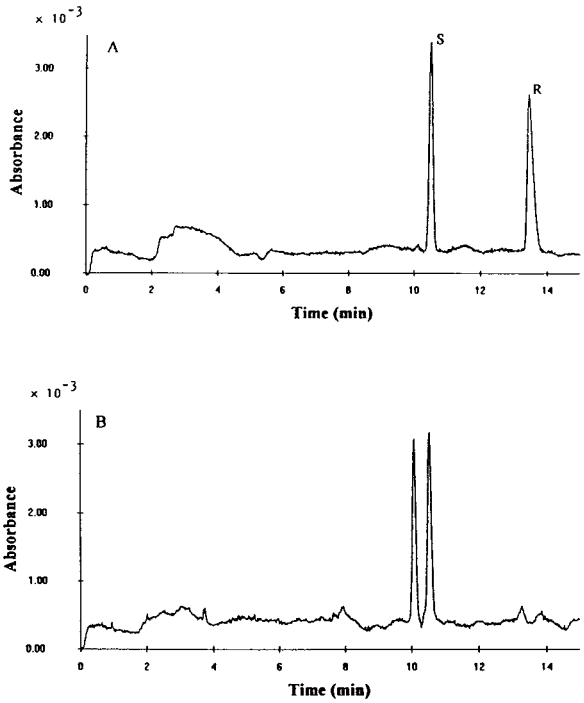

Fig. 3. Representative electropherograms obtained for analogues of tyrosine. (A) Compound **6** (12 ng injected); (B) Compound **7** (ca. 8 ng injected). Conditions: capillary, 27 cm × 50 μm I.D., fused silica; buffer, 50 m*M* sodium phosphate (pH 2.2)–30 m*M* 18-crown-6-TCA; temperature, 20°C; applied voltage, 10 kV; detection wavelength, 280 nm. Peaks for **7** are not chirally identified because the individual enantiomers were not available.

tively poor resolution observed for **7** by HPLC can probably be explained in the same way.

Again, the order of migration was determined for those compounds for which at least one single enantiomer was available. In contrast to the results observed by HPLC, in the CE system the *S*-enantiomer migrated fastest, followed by the *R*-enantiomer for the compounds tested. However, it is not possible to make generalizations with regard to migration order. At least one example exists in the literature in which the *R*-enantiomer migrates fastest in a CE system using 18-crown-6 TCA [14]. The reversal of elution order as compared with HPLC with the Crownpak CR(+) column is not surprising, since that column uses the *S*-enantiomer of the crown ether [15], whereas in the CE experiment the *R*-enantiomer of 18-crown-6 TCA is used [16].

Use of CE to study the interaction between the amino acid and crown ether

By HPLC, it is difficult to obtain information about the relative stability of complexes of analyte species with a chiral selector in the stationary phase, owing to non-stereospecific interactions of the analytes with the stationary phase. However, one can gain this sort of information by CE, in which there are few competing interactions, by varying the amount of chiral selector in the operating buffer. Penn et al. [17] have shown this to be a useful approach to gain information on the kinetics of interactions of compounds with cyclodextrins.

In this experiment, the migration times of the enantiomers of the compounds were measured and plotted as a function of the concentration of 18-crown-6-TCA in the operating buffer. Plots for DOPA and **5**–**7** are shown in Fig. 4. A calculation of the actual stability constants is not possible using these data because the contribution of electroosmotic flow, which is very low at pH 2.2, was not measured. However, it is possible to obtain information on the relative extent of complexation of the two enantiomers.

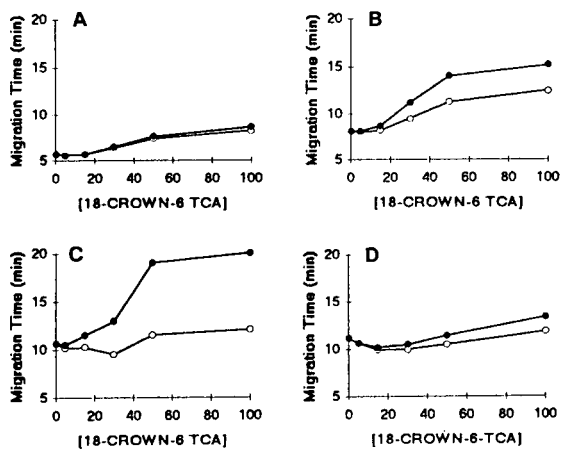

Fig. 4. Effect of concentration of 18-crown-6-TCA in operating buffer on migration times for analogues of DOPA and tyrosine. (A) DOPA; (B) **5**; (C) **6**; (D) **7**. ○ = first peak; **O** = second peak.

For all compounds, the plots show that the migration times initially decrease, then increase as a function of the concentration of crown ether in the buffer, whereas the resolution between the two enantiomers always increases with the crown ether concentration. The initial decrease in migration time is probably a result of an increase in electroosmotic flow as a function of crown ether concentration. Although the electroosmotic flow was very slow and was not measured, it can have a significant effect on the migration time, particularly of slower migrating species. In a separate experiment, the migration time of pyridine, which does not interact with the crown ether, was measured as a function of crown ether in the buffer, and its migration time decreased slightly as the crown ether concentration was increased. As the crown ether is not expected to have any effect on the electrophoretic mobility of pyridine, this is a further indication that electroosmotic flow decreases with increasing crown ether concentration. In the buffer system used in these experiments, 18-crown-6-TCA complexes with sodium ion [13], reducing the amount of sodium in the buffer which is available to shield effectively silanol groups on the capillary walls. Hence the electroosmotic flow is expected to increase with increasing crown ether concentration. For compounds which form complexes with the crown ether, the migration times increase after an initial slight decrease, owing to the reduced electrophoretic mobility of the complexed amino acid compared with the free amino acid. At higher crown ether concentrations this effect dominates the effect of the crown ether on electroosmotic flow.

Distinct differences between the data for well resolved and modestly resolved compounds were observed. For DOPA, a compound that was separated with a modest resolution factor, the migration times of the two enantiomers increased at only slightly different rates with increasing 18-crown-6-TCA concentration. The data for **7** are similar. This indicates that both enantiomers are complexed with the crown ether and that the separation is based on a small difference in the two stability constants. However, for **5** and **6**, which showed high resolution factors under the standard conditions, the migration time of the slower migrating isomer increased much more rapidly with increasing concentration of the crown ether than that of the faster migrating isomer. This behaviour indicates that the slower migrating isomer complexes with the crown ether to a much greater extent than does the faster migrating isomer. No significant decrease in resolution with high concentrations of crown ether, as has been observed in some enantiomeric separations with cyclodextrins [18], was seen. An 18-crown-6-TCA concentration of 100 m*M* was the practical upper limit under the conditions of these experiments. At higher concentrations, the crown ether began to precipitate from the buffer solution.

3.2. Results for analogues of γ-aminobutyric acid

Chiral separations by CE with 18-crown-6-TCA and HPLC using the Crownpak CR(+) column were attempted for a series of four analogues of GABA. The structures of the compounds and the results obtained are given Table 2. The results indicated that for this family of compounds, with various substituents on the carbon attached to the amino group, HPLC is generally more useful for chiral resolution. However, some general trends were observed using both techniques. Ethynyl-GABA (**8**) was well resolved by both HPLC and CE. Vinyl-GABA (**9**) was not resolved by either technique. Methyl-GABA (**11**) was resolved by HPLC only. Although allenyl-GABA (**10**) was resolved by both techniques, the resolution obtained by CE was very poor. A representative HPLC trace for **8** is shown in Fig. 5 and a typical electropherogram is shown in Fig. 6.

It is interesting to note the effect of electrolyte pH on the peak shape obtained for these compounds by CE. When using the conditions recommended by Kuhn et al. [5] for indirect detection and chiral separation, the peak shapes observed for the analogues of GABA were very poor. The peaks were very broad with asymmetric shapes. This indicated that the peak broadening was due to concentration overloading and a

Table 2
Summary of results obtained by HPLC and CE for analogues of GABA

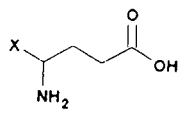

Compound	X	HPLC results[a]			CE results[b]		
		t_{r1}	t_{r2}	R_s	t_{m1}	t_{m2}	R_s
Ethynyl-GABA (**8**)	C≡CH	11.42	18.10	5.27	14.64	16.39	2.97
Vinyl-GABA (**9**)	$CH=CH_2$	14.62	–	0	14.09	–	0
Allenyl-GABA (**10**)	$CH=C=CH_2$	18.74	21.85	2.00	14.53	14.69	<0.5
Methyl-GABA (**11**)	CH_3	7.67	10.23	2.99	12.77	–	

[a,b] See Table 1.

poor mismatch of the conductivities of the sample and the buffer, a phenomenon that is known to cause such peak shapes [19]. The most notable difference between the GABA analogues and the α-amino acids is that the pK_a value for the acid moiety (pK_1) is about 4.1–4.2 for the GABA analogues [20], whereas it is in the range 2.1–2.3 for the α-amino acids [21]. At pH 2.5, the pH used in the work by Kuhn et al., the GABA analogues will have a higher positive charge than the α-amino acids, thus accounting for the difference in conductivity. Therefore, in order to decrease the conductivity of the GABA analogues, the pH of the buffer was increased to 3.7. This resulted in more acceptable peak shapes, as is demonstrated for ethynyl-GABA (**8**) in Fig. 6.

For those compounds for which at least one single enantiomer was available, we found that the *R*-enantiomer always eluted before the *S*-enantiomer in the HPLC system, whereas in the CE system, the *S*-enantiomer of ethynyl-GABA was observed to migrate faster than the *R*-enantiomer. No attempt was made to determine the migration order of allenyl-GABA by CE as the resolution was very poor. The elution and migration orders are the same as those observed for the analogues of DOPA and tyrosine. The effect of the substituents on resolution of the

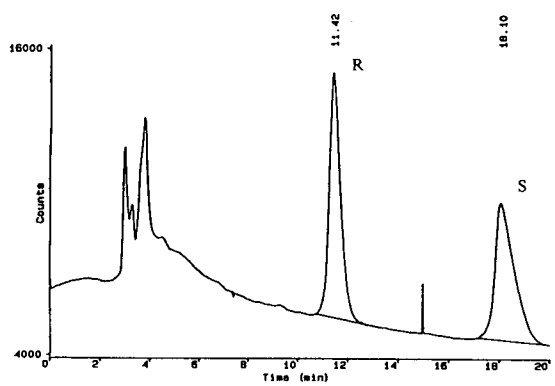

Fig. 5. Chromatogram obtained for **8** (6.5 μg injected) on the Crownpak CR(+) column. Conditions: mobile phase, 0.11 *M* $HClO_4$ (pH 1.05); temperature, 10°C; flow-rate, 0.5 ml/min; detection wavelength, 210 nm.

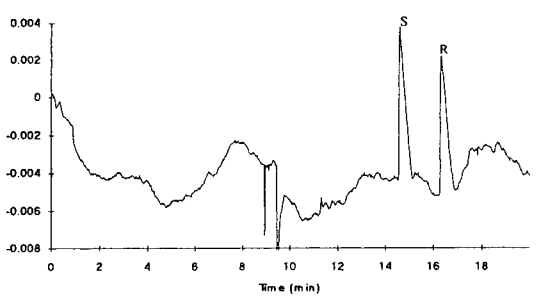

Fig. 6. Electropherogram obtained for **8** (13 ng injected). Conditions: capillary, 57 cm × 75 μm I.D., fused silica; buffer, 6 m*M* BTMACl–30 m*M* 18-crown-6-TCA (pH adjusted to 3.7 with 1 *M* NaOH); temperature, 25°C; applied voltage, 15 kV; detection wavelength, 214 nm.

different analogues is not obvious from the HPLC and CE data. Particularly puzzling is the inability to resolve vinyl-GABA by either procedure. The results were verified by analysis of the individual enantiomers. The resolution of all of these analogues of GABA, as their N-pentafluoropropyl esters, has been previously achieved by capillary GC using a Chirasil-Val stationary phase [22].

4. Conclusions

We have demonstrated the utility of crown ethers in the chiral resolution of two particular groups of amino acids in both HPLC and CE. For analogues of DOPA and tyrosine, we found that for those analogues having a substituent on the carbon α to the amino group, no separation was obtained using either method. There is evidence that this is due to lack of complexation with the crown ether, probably owing to steric hindrance. For a second set of analogues having a C=C on the carbon β to the amino group, large resolution factors were obtained in the CE experiment. The resolution factors were much larger than those observed for DOPA and tyrosine themselves and those reported in the literature for other compounds. When the amount of crown ether in the operating buffer was varied, it was discovered that for these compounds the complex of one enantiomer with the crown ether is significantly more stable than the other. Although no such pattern was observed in the HPLC experiment, these compounds were all adequately resolved by HPLC also. For analogues of GABA, we observed that three of the four compounds tested were well resolved by HPLC, whereas only one was well resolved using CE. Detection was also a significant problem in the CE analysis of GABA analogues. Because the compounds have poor UV absorbance properties, it was necessary to use an indirect detection scheme.

In the chiral resolution of amino acids with good UV absorbance properties, neither technique was found to be clearly advantageous over the other. Capillary electrophoresis is advantageous when the amount of sample available is very small, as is sometimes the case in pharmaceutical research. In routine analysis, CE may also be advantageous because it avoids the high cost of a chiral HPLC column. However, when high sensitivity is required, HPLC is advantageous owing to the larger detector cell volume. In the chiral analysis of compounds that absorb only poorly in the UV region, HPLC is clearly advantageous because of the greater sensitivity possible with this technique. Clearly, at present, HPLC and CE are complementary techniques that both provide numerous possibilities in the area of chiral separations.

Acknowledgements

The authors thank Professor J.M. Lehn for his interest in this work, Mme. Blanche Heintzelmann, M. Alain Renard and Mme. Laurence Breton for their assistance in collecting the HPLC data and Mme. Claudine Froehly for secretarial work. They also thank Dr. Michael Schleimer for his assistance in data collection and helpful insights.

References

[1] A.M. Krstulovic (Editor), *Chiral Separations by HPLC: Applications to Pharmaceutical Compounds*, Ellis Horwood, Chichester, 1989.
[2] H. Brückner and B. Strecker, *J. Chromatogr.*, 627 (1992) 97.
[3] R. Kuhn and S. Hoffstetter-Kuhn, *Chromatographia*, 34 (1992) 34.
[4] R. Kuhn, F. Stoecklin and F. Erni, *Chromatographia*, 33 (1992) 32.
[5] R. Kuhn, F. Erni, T. Bereuter and J. Häusler, *Anal. Chem.*, 64 (1991) 2815.
[6] P. Bey, J.P. Vevert, V. Van Dorsselaer and M. Kolb, *J. Org. Chem.*, 44 (1979) 2732.
[7] I.A. McDonald, J.M. Lacoste, P. Bey, J. Wagner, M. Zreika and M.G. Palfreyman, *J. Am. Chem. Soc.*, 106 (1984) 3354.
[8] B.W. Metcalf and K. Jund, *Tetrahedron Lett.*, 41 (1977) 3689.
[9] B. Lippert, B.W. Metcalf, M.J. Jung and P. Casara, *Eur. J. Biochem.*, 74 (1977) 441.

[10] M.J. Jung, B.W. Metcalf, B. Lippert and P. Casara, *Biochemistry*, 17 (1978) 2628.
[11] P. Casara, K. Jund and P. Bey, *Tetrahedron Lett.*, 25 (1984) 1981.
[12] E. Fischer and A. Groh, *Liebigs Ann. Chem.*, 383 (1911) 370.
[13] J.-P. Behr, J.-M. Lehn and P. Vierling, *Helv. Chim. Acta*, 65 (1982) 1853.
[14] E. Höhne, G.-J. Krauss and G. Gübitz, *J. High Resolut. Chromatogr.*, 15 (1992) 698.
[15] T. Shinbo, T. Yamaguchi, K. Nishimura and M. Sugiura, *J. Chromatogr.*, 405 (1987) 145.
[16] J.-P. Behr, J.-M. Girodeau, R.C. Hayward, J.-M. Lehn and J.-P. Sauvage, *Helv. Chim. Acta*, 63 (1980) 2096.
[17] S.G. Penn, D.M. Goodall and J.S. Loran, *J. Chromatogr.* 636 (1993) 149.
[18] S.A.C. Wren and R.C. Rowe, *J. Chromatogr.*, 603 (1992) 235.
[19] F.E.P. Mikkers, F.M. Everaerts and Th.P.E.M. Verheggen, *J. Chromatogr.*, 169 (1979) 1.
[20] J. Wagner, unpublished results.
[21] R.C. Weast (Editor), *Handbook of Chemistry and Physics*, CRC Press, Boca Raton, FL, 70th ed., 1989, p. D-161.
[22] J. Wagner, E. Wolf, B. Heintzelmann and C. Gaget, *J. Chromatogr.*, 392 (1987) 211.

ELSEVIER

Journal of Chromatography A, 685 (1994) 331–337

JOURNAL OF CHROMATOGRAPHY A

Characterization of food proteins by capillary electrophoresis

Fu-Tai A. Chen*, Anton Tusak

Beckman Instruments Inc., Advanced Technology, 2500 Harbor Boulevard D-20-A, Fullerton, CA 92634, USA

First received 6 June 1994; revised manuscript received 25 July 1994

Abstract

A simple analytical method for characterization of food proteins by capillary electrophoresis (CE) has been developed. Major proteins in chicken eggs and cow's milk are characterized and can be quantitated by the CE technique. Egg white proteins are well resolved while the yolk shows a substantially more complex protein separation pattern than that in the egg white. Caseins and whey proteins in fresh milk were resolved by CE in a similar buffer system. Separation of both milk and egg proteins was performed reliably and reproducibly in an untreated fused-silica column, 25 cm × 20 μm I.D. Diluted egg or milk samples can be directly loaded on an automated instrument with on-line injection, detection and real-time data analysis in less than 10 min.

1. Introduction

Chicken eggs and cow's milk are the two major dairy products rich in protein content. They are also among the most important sources of the daily diet that contains all the essential amino acids. Despite the recent awareness of cholesterol diet intake in dairy products, both chicken's egg and low-fat and non-fat cow's milk are still the primary source of protein intake. Egg whites account for about 58% of the entire egg mass, with 10–12% of the mass being protein and the remainder of the mass being water. Among the proteins in egg whites, ovalbumin, ovomucoid, globulins and conalbumin are the major components constituting 54, 11, 10 and 13%, respectively, with lysozyme as the minor component of about 3.5% [1]. Proteins in the egg yolk, on the other hand, are substantially more complex than those in egg white and not as well characterized. The yolk comprises 32% of the mass of egg, and is about 49% water, 33% fat and 16% protein [2]. Cow's milk contains about 3.2% protein regardless of its fat content [3]. Protein in cow's milk contains mostly caseins, approximately 80%; the remainder being whey proteins.

Separation of both egg white and yolk proteins has been achieved by Shepard and Hottle [4] who used the Longsworth-modified free zone electrophoresis [5] of Tiselius apparatus, with the classical zone electrophoresis. Capillary electrophoresis (CE) has rapidly become the method of choice for most of the analytical applications [6–10]. The feasibility of performing a routine protein analysis by capillary zone electrophoresis in an untreated fused-silica capillary [11–13] was established. Using a high-phosphate-based buffer in conjunction with a capillary with I.D. of 20 μm, we have demonstrated a high-resolution protein analysis of complex mixtures such as human serum, urine and ascites fluid [14]. Addi-

* Corresponding author.

0021-9673/94/$07.00
SSDI 0021-9673(94)00700-4

tion of urea to the high-phosphate buffer allowed us to characterize milk proteins with a reasonably good resolution [15]. This report is an attempt to establish the feasibility of rapid analysis of proteins in egg and milk with a simple borate-based buffer.

2. Experimental

2.1. CE procedures

A P/ACE 2100 automated CE system by Beckman Instruments (Palo Alto, CA, USA) was used with P/ACE system software controlled by an IBM PS/2 Model 55 SX computer. Post-run data analysis was performed on System Gold software by Beckman Instruments (Fullerton, CA, USA). Capillary columns of 25 cm length (18.5 cm to detector window) × 20 μm I.D. (Polymicro Technologies, Phoenix, AZ, USA) were assembled in the P/ACE cartridge format (50 × 200 μm aperture). On-line detection of the P/ACE system was at 200 nm. During electrophoresis, the capillary was maintained at ambient temperature (usually 23°C) with circulating

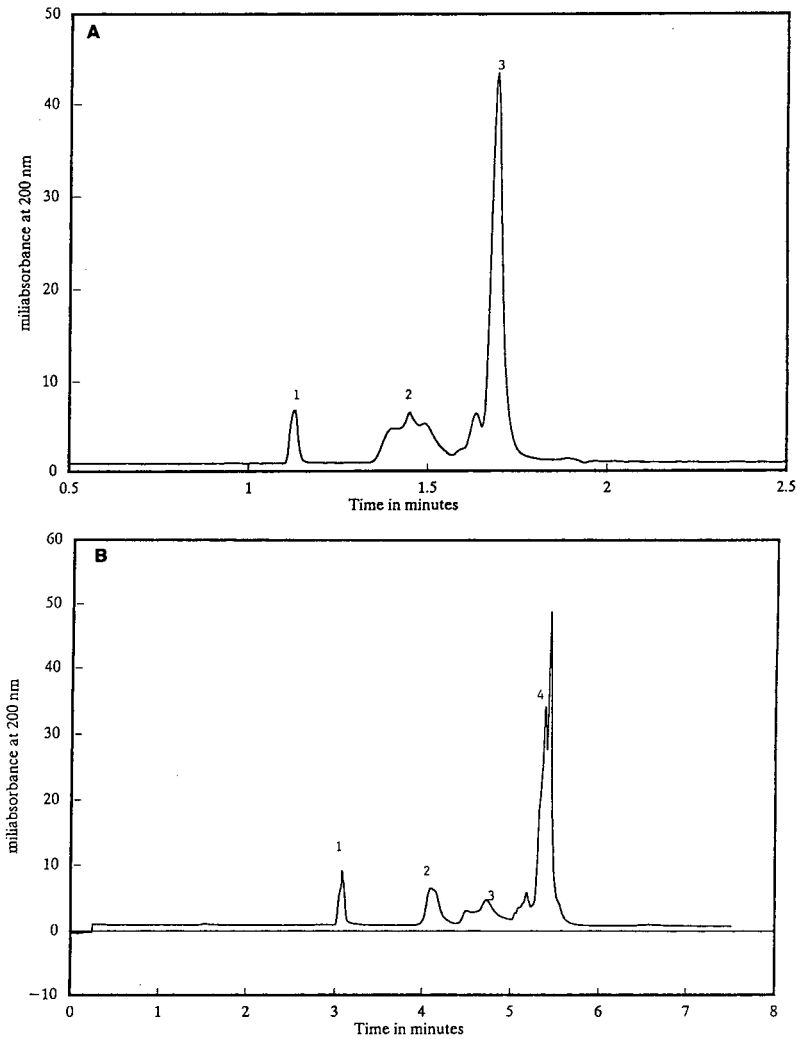

Fig. 1.

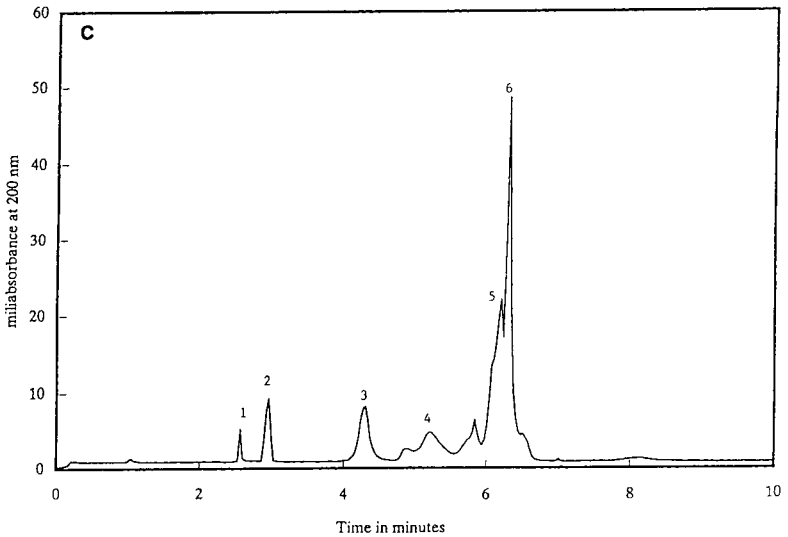

Fig. 1. Electropherograms of egg white proteins. (A) Conditions: untreated fused-silica capillary, 25 cm × 20 μm I.D.; applied potential, 20 kV/17 μA; buffer, 80 m*M* borate at pH 10.0; peaks: 1 = neutral marker (DMF); 2 = conalbumin and globulins; 3 = ovomucoid and ovalbumin. (B) Conditions: untreated fused-silica capillary, 25 cm × 20 μm I.D.; applied potential, 10 kV/17 μA; buffer, 200 m*M* borate at pH 10.0; peaks: 1 = neutral marker and lysozyme; 2 = conalbumin; 3 = globulins; 4 = ovomucoid and ovalbumin. (C) Conditions: untreated fused-silica capillary, 25 cm × 20 μm I.D.; applied potential, 12 kV/26 μA; buffer, 300 m*M* borate at pH 10.0; peaks: 1 = lysozyme; 2 = neutral marker; 3 = conalbumin; 4 = globulins; 5, 6 = ovomucoid and ovalbumin.

coolant surrounding the capillary. Diluted samples were introduced by pressure injection for 15–30 s and electrophoresis was performed at the voltage indicated on the electropherograms. Between runs, the capillary was sequentially washed with 1.0 *M* sodium hydroxide and water (12 s each, with pressure rinsing at 15 p.s.i.; 1 p.s.i. = 6894.76 Pa) followed by reconditioning with the borate buffer (60 s with pressure rinsing at 15 p.s.i.).

2.2. Sample and buffer preparations

Chicken egg albumin, conalbumin, trypsin inhibitor and lysozyme, and milk caseins, α-lactalbumin and β-lactoglobulin A and B, were obtained from Sigma (St. Louis, MO, USA). Borate buffer at pH 10.0 was prepared by dissolving boric acid and adjusting the pH with the addition of sodium hydroxide solution. Fresh milk and chicken egg samples were purchased from a local supermarket. All protein standards were dissolved in buffer containing 75 m*M* sodium chloride, 20 m*M* potassium phosphate, 0.01% sodium azide, pH 7.0 (phosphate-buffered saline, PBS). Each protein concentration was about 0.2 to 0.5 mg/ml. Egg white was obtained from fresh egg and dissolved in PBS at 1:50 dilution. The egg yolk was separated from the egg white and dispersed in PBS at 1:40 dilution followed by delipidation with SeroClear (Calbiochem, San Diego, CA, USA). Dimethylformamide (DMF) as a neutral marker was added to the sample diluent, PBS, at final concentration of 0.01% (v/v).

3. Results and discussion

In the presence of 80 m*M* borate buffer at pH 10, egg white is resolved into two major fractions as shown in Fig. 1A. Conalbumin and globulins

appear as a broad band migrate between 1.3 and 1.55 min while ovomucoid and ovalbumin appear at 1.75 min. Lysozyme is absent, presumably due to adsorption to silica surface, at pH of 10. As the borate buffer increases to 200 m*M*, egg white proteins begin to separate into four zones, conalbumin, globulins, ovalbumin and ovomucoid, shown in Fig. 1B. Lysozyme is missing, presumably migrates along with the neutral marker, DMF. Addition of an authentic sample of lysozyme to the sample showed that lysozyme co-migrates with DMF. Further increase of borate buffer to 300 m*M*, results in better defined separation pattern as evident in Fig. 1C. Lysozyme clearly migrates at 2.6 min, ahead of neutral marker, at 2.9 min, consistent with its isoelectric point of 11.0, which is 1.0 pH unit above the buffer pH. A high salt buffer prevents

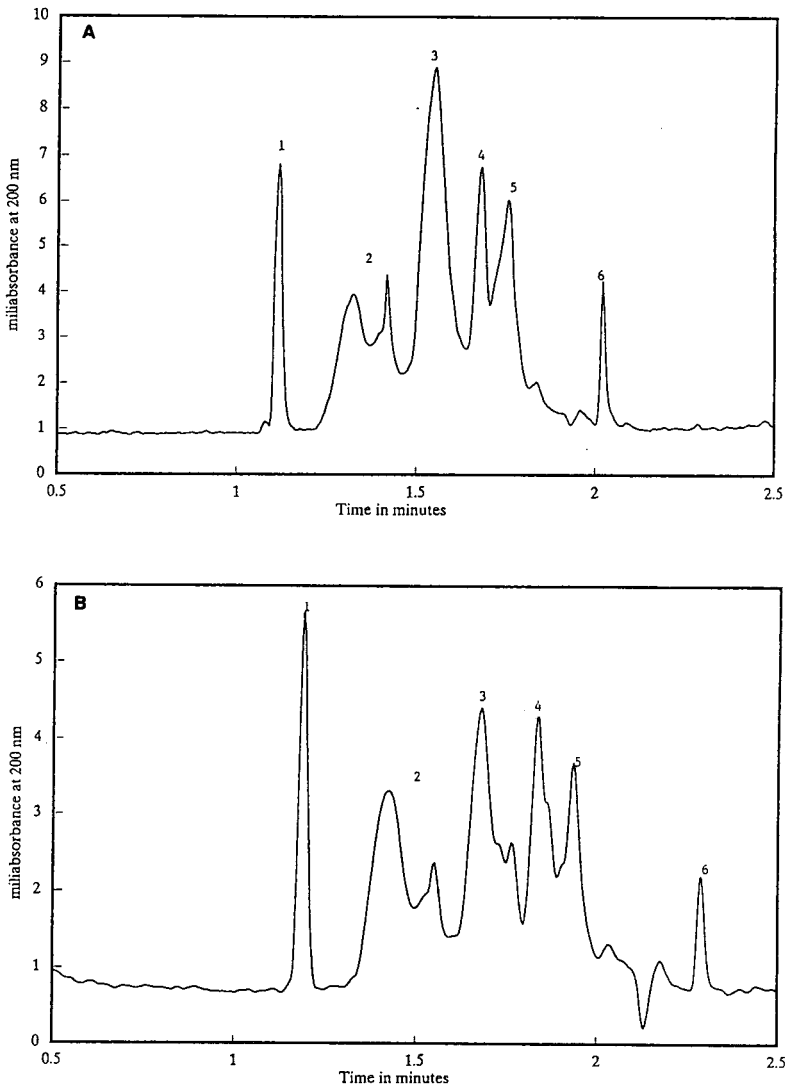

Fig. 2.

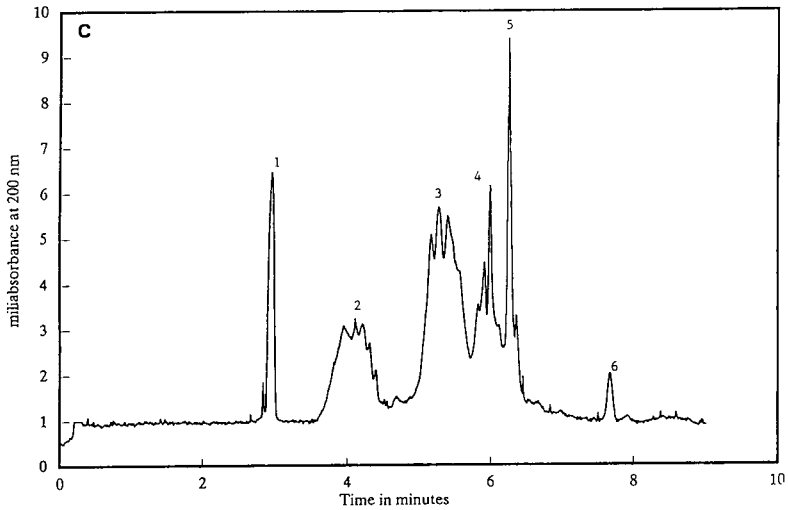

Fig. 2. Electropherograms of egg yolk proteins. (A) Conditions: untreated fused-silica capillary, 25 cm × 20 μm I.D.; applied potential, 20 kV/17 μA; buffer, 80 m*M* borate at pH 10.0. (B) The lipid portion in yolk was extracted with SeroClear; conditions as for (A). (C) Conditions: untreated fused-silica capillary, 25 cm × 20 μm I.D.; applied potential, 10 kV/21 μA; buffer 300 m*M* borate at pH 10.0. Peaks: 1 = neutral marker; 2 = yolk immunoglobulins; 3 = yolk lipoproteins.

lysozyme, a very basic protein, from adsorption on the silica surface [16]. The remainder of the proteins migrate in order according to their isoelectric point. Ovomucoid (p*I* 4.0) and ovalbumin (p*I* 4.6) appear between 6 and 6.6 min, globulin (p*I* 5.5–5.8) migrates as two broad peaks at 5.2 and 5.35 min, and conalbumin (p*I* 6.6), at 4.3 min; they are calculated to be 64, 10 and 14%, respectively, while lysozyme was less than 3.5%.

Egg yolk when dispersed into saline, exhibits a cloudy solution. In the presence of 80 m*M* borate buffer, pH 10.0, it shows primarily six fractions shown in Fig. 2A. Extraction of the cloudy solution with SeroClear, a fluorocarbon, results in a clear solution that exhibits an electropherogram in Fig. 2B, similar to that of Fig. 2A. Protein peaks between 1.5 and 1.8 min appear to be reduced in Fig. 2B in comparison with that in Fig. 2A. Presumably, these are lipid associated species in egg yolk that was extracted into the SeroClear. Each of the four fraction in egg yolk proteins can be resolved substantially in the presence of 300 m*M* borate buffer shown in Fig. 2C. Separation pattern of egg white and yolk proteins by the present method appears to be similar to that obtained by Shepard and Hottle [4] who used the Longsworth-modified free zone electrophoresis [5] of Tiselius apparatus.

Milk proteins were previously analyzed by urea–phosphate buffer that could resolve α- and β-casein, while whey proteins were evident from the electropherogram [15]. In the absence of urea–phosphate buffer whey proteins can be resolved, but caseins migrate as a broad peak, appear to be aggregates [15]. In simplified borate buffer, 0.25 *M* at pH 10.0, the electropherogram of non-fat fresh milk in Fig. 3A shows that β-casein is well separated from α-casein. α-Lactalbumin exhibits as a sharp peak migrating in front of α-casein. β-Lactoglobulin B and A emerge with α-casein. Powdered milk, however, shows broad poorly resolved peaks presumably due to extensive thermal denaturation during the manufacturing process (spray drying process). The absence of the α-lactalbumin and/or β-lactoglobulin in powdered milk shown in Fig. 3B may be used as an indicator for the quantitation of the adulteration in fresh milk.

The utility of egg and milk proteins analysis by

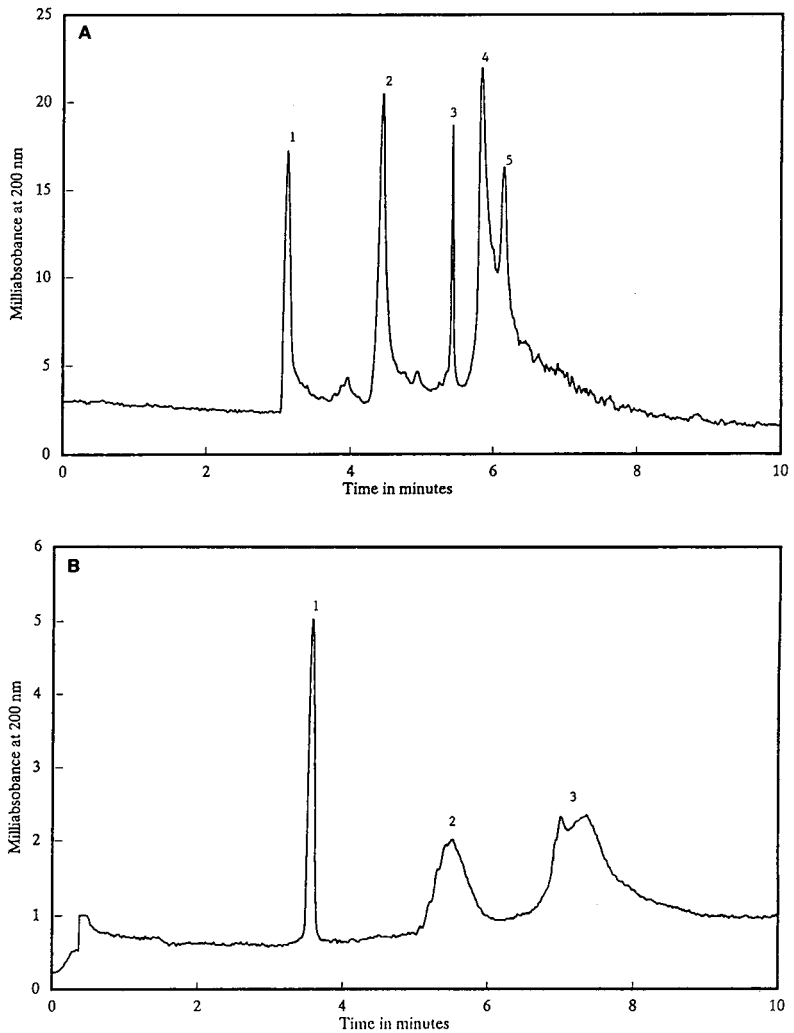

Fig. 3. (A) Electropherogram of the fresh non-fat milk proteins; conditions: untreated fused-silica capillary, 25 cm × 20 μm I.D.; applied potential, 10 kV/15 μA; buffer, 250 m*M* borate at pH 10.0; peaks: 1 = neutral marker; 2 = β-casein; 3 = α-lactalbumin; 4 = α-casein; 5 = β-lactoglobulin. (B) Electropherogram of the powder milk proteins; conditions as for (A); peaks: 1 = neutral marker; 2 = denatured β-casein aggregates; 3 = denatured α-casein aggregates.

CE in an untreated fused-silica column is demonstrated using borate buffer at pH of about 10.0. Increasing the buffer salt concentration results in a better resolution of proteins in both egg and milk proteins. Aggregation of proteins, milk caseins in particular is an analytical problem in which addition of urea to the buffer system is a common practice. The present buffer system with high buffer salt and high pH not only eliminates the casein aggregate problem but also increases the separation efficiency.

References

[1] R.H. Feeney, in H.W. Schultz and A.F. Anglemeir (Editors), *Symposium on Foods: Proteins and Their Reactions*, Avi Publ. Co., Westport, CT, 1964, pp. 209–224.

[2] W.D. Powrie, in W.J. Stadelman and O.J. Cotterill (Editors), *Egg Science and Technology*, Avi Publ. Co., Westport, CT, 1977, pp. 65–91.
[3] S. Patton, *Sci. Am.*, 221 (1969) 58–68.
[4] C.C. Shepard and G.A. Hottle, *J. Biol. Chem.*, 179 (1949) 349–357.
[5] L.G. Longsworth, *Chem. Rev.*, 30 (1942) 323.
[6] F.E.P. Mikkers, F.M. Everaerts and T.P.E.M. Verheggen, *J. Chromatogr.*, 169 (1979) 11–20.
[7] J.W. Jorgenson and K.D. Lukacs, *Anal. Chem.*, 53 (1981) 1298–1302.
[8] M.J. Gordon, X. Huang, S.L. Pentoney and R.N. Zare, *Science*, 247 (1988) 224–228.
[9] A.G. Ewing, R.A. Wallingford and T.M. Olefirowicz, *Anal. Chem.*, 61 (1989) 292A–303A.
[10] S. Terabe, K. Otsuka and K. Ando, *Anal. Chem.*, 57 (1985) 834–841.
[11] F.T.-A. Chen, C.-M. Liu, Y.-Z. Hsieh and J.C. Sternberg, *Clin. Chem.*, 37 (1991) 14–19.
[12] F.-T.A. Chen, *J. Chromatogr.*, 559 (1991) 445–453.
[13] J.W. Jorgenson and K.D. Lukacs, *Clin. Chem.*, 27 (1981) 1551–1553.
[14] F.-T.A. Chen, L. Kelly, R. Palmieri, R. Biehler and H. Schwartz, *J. Liq. Chromatogr.*, 15 (1992) 1143–1161.
[15] F.-T.A. Chen and J.-H. Zang, *J. Assoc. Off. Anal. Chem.*, 75 (1992) 905–909.
[16] H.H. Lauer and D. McManigill, *Anal. Chem.*, 58 (1986) 166–169.

ELSEVIER

Journal of Chromatography A, 685 (1994) 338–343

JOURNAL OF CHROMATOGRAPHY A

Short communication

Fractionation of non-*ortho*-substituted toxic polychlorinated biphenyls on two nitro-containing liquid chromatographic stationary phases

Eva Grimvall[a,1], Conny Östman[b,*]

[a]*Department of Analytical Chemistry, Stockholm University, 106 91 Stockholm, Sweden*
[b]*Division of Analytical Chemistry, National Institute of Occupational Health, 171 84 Solna, Sweden*

First received 30 March 1994; revised manuscript received 15 August 1994

Abstract

Two liquid chromatographic stationary phases, dinitroanilinopropylsilica (DNAP) and tetranitrofluorenimino-propylsilica (TENF), are demonstrated to retain selectively the toxic non-*ortho*-chlorobiphenyl congeners CB-77, CB-126 and CB-169. On the DNAP column, these three congeners elute as a single peak. With hexane as mobile phase all eighteen tested chlorobiphenyl congeners are eluted within 13 min. Carryover effects of CBs in HPLC systems are discussed. To demonstrate the isolation of the three congeners, a sample of Aroclor 1254 was fractionated and analysed by GC with electron-capture detection.

1. Introduction

It is well known that the 209 theoretically possible congeners of chlorinated biphenyls (CBs) possess substantial differences in biological effects. The most toxic congeners are recognized as those which lack chloro substitution in the *ortho* position and in addition have chlorine substituents in both *para* and at least two *meta* positions. These configurations make it possible to obtain a planar structure that resembles the 2,3,7,8-tetrachloro-dibenzo-*p*-dioxin and thus possess similar biological activity [1]. Determination of these congeners, CB-77 (3,4,3′,4′), CB-126 (3,4,5,3′,4′) and CB-169 (3,4,5,3′,4′,5′) [2], demands separation from the bulk of polychlorinated biphenyl (PCB), as they will otherwise be completely covered by the peaks of the more abundant congeners. Group separation is mostly performed by liquid chromatography, in open columns by gravitational flow or by high-performance liquid chromatography (HPLC) [3]. There are also some cases where multi-dimensional gas chromatography (GC) have been applied to achieve a separation [4–6]. The use of two-dimensional GC can be troublesome when there are large concentration differences between the solutes as in samples of PCB.

When liquid chromatography is applied, the use of different kinds of carbon material dominates the published methods for the fractionation of PCB into a non-*ortho* and sometimes a mono-*ortho* subsample of PCB. Those stationary phases include activated carbon such as Amoco

* Corresponding author.
[1] Present address: Division of Analytical Chemistry, National Institute of Occupational Health, 171 84 Solna, Sweden.

0021-9673/94/$07.00
SSDI 0021-9673(94)00786-1

PX-21 [7] and porous graphitic carbon [8]. Carbon materials often require strong solvents such as dichloromethane or toluene and exhibits retention times that can be more than 100 min. However, porous graphitic carbon has occasionally been used with pure hexane as mobile phase [9,10]. Aluminium oxide and Florisil [11,12] have also been shown to retain selectively the toxic non-*ortho*-substituted congeners. Disadvantages of aluminium oxide and Florisil are large batch-to-batch variations and the need for careful control of the adsorbent activity. Haglund et al. [13] showed that a column of 2-(1-pyrenyl)-ethyldimethylsilica (PYE) had a selectivity similar to that of carbon but with weaker adsorption of the solutes. The use of a stationary phase of C60–70 fullerenes bonded to a core of styrene–divinylbenzene to enrich non-*ortho*-substituted CBs has been demonstrated [14]. Reviews of methods for the separation of non-*ortho*-substituted CBs have been published by Creaser et al. [3] and De Voogt et al. [15], who also included biological activity and the occurrence of non-*ortho*-, mono-*ortho*- and di-*ortho*-chlorobiphenyls.

In this paper we present methods for the selective fractionation of non-*ortho*-substituted CBs on two stationary phases, dinitroanilinopropylsilica (DNAP) and tetranitrofluorenimino-propylsilica (TENF). Nitrophenylpropylsilica has been used previously for the clean-up of CBs and other chlorinated pesticides [16], but it does not separate the toxic non-*ortho*-substituted CBs from the bulk of PCB [17].

2. Experimental

2.1. Chemicals

The pure CB congeners were obtained from Ultra Scientific (Kingstown, RI, USA) and the commercial PCB mixture used was Aroclor 1254 (Monsanto, St. Louis, MO, USA).

2.2. Chromatographic conditions

The HPLC system consisted of a Waters (Milford, MA, USA) Model 590 pump, a Rheodyne (Cotati, CA, USA) Model 7125 injector equipped with a 100-μl loop, a Crococil (France) column thermostat set at 25°C and an LKB (Bromma, Sweden) Model 2125 UV detector monitoring the eluent at 225 nm. The two HPLC columns of DNAP and TENF, both 25 cm × 4.6 mm I.D. with 5-μm particles, were obtained from ES Industries (Berlin, NJ, USA). The DNAP particles had a pore size of 60 Å and the TENF particles 100 Å. HPLC-grade hexane (Rathburn, Walkerburn, UK) was used as the mobile phase at a flow-rate of 1.0 ml/min. Capacity factors were determined in triplicate and the dead time was determined from the injection dip in the baseline caused by pentane (Rathburn), which was added to all samples. The volume injected was 30 μl, containing 10–30 ng of individual congeners and ca. 2.5μg of Aroclor 1254.

Gas chromatography was performed in the splitless injection mode on a Varian (Walnut Creek, CA, USA) Model 3400 gas chromatograph equipped with an electron-capture detector and a Jade (Austin, TX, USA) injector. The GC column was RT-5 (60 m × 0.32 mm, I.D., 0.25 μm film thickness) (Restek, Bellefonte, PA, USA). The temperature settings were as follows: injector, 250°C; detector, 300°C; column oven, 70°C held for 2 min and then raised at 10°C/min to 280°C, which was held for 10 min. Hydrogen was used as the carrier gas at a column head pressure of 11 psi and nitrogen was used as the detector make-up gas at a flow-rate of 35 ml/min. The split vent, which was opened after 2 min, was set to a flow rate of 23 ml/min. An ELDS Pro laboratory data system (Chromatography Data Systems, Svartsjö, Sweden) was used to register and process all UV and electron-capture detector signals.

Confirmation of the identity and a check of purity of the fractionated toxic non-*ortho*-PCB congeners were performed by gas chromatography–mass spectrometry (GC-MS). The GC column and the applied column oven temperature programme were the same as for the GC analysis with electron-capture detection (ECD). The transfer line to the mass spectrometer, an INCOS 50 quadropole mass spectrometer (Finnigan MAT, San Jose, CA, USA), was main-

tained at 300°C and the column outlet was directed into the mass spectrometer ion source, which had a temperature of 150°C. The instrument was operated in the electron impact (EI) mode with an electron energy of 70 eV utilizing both full range scan, 250–450 mass units and multiple ion detection monitoring the four most intense ions of the eluting non-*ortho*-CB and CBs with the next two higher degrees of chlorination. The latter was needed for detection of the toxic non-*ortho*-CB at the lowest concentration, CB 169.

2.3. HPLC fractionation

The fraction of toxic non-*ortho*-substituted CBs present in 2.5 μg Aroclor 1254 was separated on the DNAP column, collected between 10.80 and 12.60 min and was then carefully concentrated under a gentle stream of nitrogen to ca. 100 μl. A 2-μl volume of the concentrate was injected on to the gas chromatograph. A larger amount of Aroclor 1254, 15 μg dissolved in 300 μl of hexane, was injected into a 500-μl injection loop in order to check for memory effects due to overloading. A further investigation of memory effects was carried out by the injection of 100 ng of CB-105 dissolved in 50 μl of hexane on the HPLC–DNAP system. Eight fractions of 1 ml each, starting from 1 min before the beginning of the elution of CB-105, were collected. CB-103 (2,4,6,2′,5′) was added as an injection standard in different amounts according to the estimated concentrations of CB-105. The collected fractions were either concentrated or diluted in order to achieve similar absolute concentrations prior to analysis by GC.

3. Results and discussion

3.1. Retention of CB congeners

The capacity factors of eighteen CBs that have been proposed for determination by the Nordic Council of Ministers [1] are shown in Table 1. On both columns the toxic non-*ortho* compounds are the most retained, preceded by a group of mono-*ortho*-substituted congeners and the di-*ortho*-substituted compounds which have the weakest retention. This rule is followed by all tested compounds except CB-170 on the TENF column and CB-170 and CB-138 on the DNAP column, where they elute in the mono-*ortho* fraction. All CB congeners have higher or equivalent capacity factors on the DNAP compared with the TENF stationary phase. Further, it is remarkable that the three toxic non-*ortho*-CB congeners have the same retention time on the DNAP column and hence elute as a single peak, a phenomenon not described in the literature for any other column. This property makes it possible to collect a small fraction for subsequent analysis that should have a potential to contain less non-PCB interferences than the fractions collected after back-flush elution, or collection of the wide non-*ortho* heart-cut fraction obtained from, e.g., graphitized carbon or PYE. When the back-flush technique is utilized, all the components with stronger retention than the CBs will also be trapped in the same fraction.

Table 1
Capacity factors of CBs on the DNAP and TENF stationary phases using hexane as mobile phase

CB No.	Structure	DNAP	TENF
28	2,4,4′	0.85	0.80
47	2,4,2′,4′	0.67	0.65
52	2,5,2′,5′	0.69	0.74
77	3,4,3′,4′	2.43	1.74
101	2,4,5,2′,5′	0.68	0.62
105	2,3,4,3′,4′	1.59	1.10
114	2,3,4,5,4′	1.08	0.75
118	2,4,5,3′,4′	1.12	0.76
122	3,4,5,2′,3′	1.36	1.00
126	3,4,5,3′,4′	2.42	1.55
138	2,3,4,2′,4′,5′	0.96	0.73
153	2,4,5,2′,4′,5′	0.70	0.50
156	2,3,4,5,3′,4′	1.35	0.80
157	2,3,4,3′,4′,5′	1.57	0.96
167	2,4,5,3′,4′,5′	1.11	0.64
169	3,4,5,3′,4′,5′	2.43	1.44
170	2,3,4,5,2′,3′,4′	1.11	0.82
180	2,3,4,5,2′,4′,5′	0.81	0.54

The relative standard deviation in retention time was less than 1.0% on the DNAP column and less than 1.3% on the TENF column ($n = 3$).

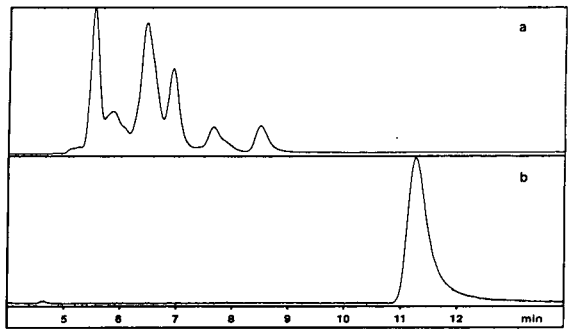

Fig. 1. Chromatograms of (a) Aroclor 1254 and (b) a standard of CB-77, CB-126 and CB-169 separated on a DNAP column. Hexane was used as the mobile phase at a flow-rate of 1.0 ml/min and the UV detector was set at 225 nm.

3.2. Isolation of toxic non-ortho-CB congeners

To illustrate the practical use in clean-up, a solution of the technical product Aroclor 1254 was fractionated on the DNAP column. The HPLC trace is shown in Fig. 1a and that of a standard sample containing CB-77, CB-126 and CB-169 in Fig. 1b. A good separation between the bulk of PCBs and the non-*ortho* congeners is demonstrated. The two groups, bulk and non-*ortho* components, are less resolved on the TENF column (Fig. 2a and b). Hence DNAP is to be preferred to TENF as long as the latter is not shown to have superior separation capabilities for matrix components or other interfering substances. In Fig. 3a and b the GC–ECD traces of Aroclor 1254 and the non-*ortho* fraction from DNAP are shown. Their relative peak heights are roughly in the orders corresponding to the amounts found in Aroclor 1254 [18] or Clophen A50 [13,19]. As it has been shown that on slightly polar GC columns with a 5% diphenyl content, only CBs with higher degrees of chlorination elute close to the toxic non-*ortho*-PCB congeners [20], their identity and purity can be checked by GC–MS. No interfering PCB congeners were found in the peaks of CB-126 and CB-169. For CB-77, a minor amount of a pentachlorobiphenyl, CB-110 [20], was detected in the peak. The detector signal from the pentachlorobiphenyl was 10% of that from CB-77. Hence columns with different polarities or detection by MS using only individual masses, not ranges, should be used for the quantification and identification of CB-77.

3.3. Carryover effects in HPLC systems

It is obvious that there are residues of bulk PCBs in the non-*ortho* chromatogram (Fig. 3b), predominantly from the mono-*ortho*-substituted congeners. This is obtained despite the good separation monitored on the UV detector. Neither rinsing the column outlet with hexane or acetone immediately before collection nor add-

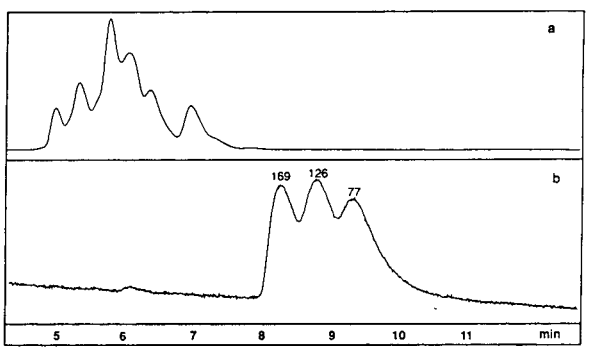

Fig. 2. Chromatograms of (a) Aroclor 1254 and (b) a standard of CB-77, CB-126 and CB-169 separated on a TENF column. Hexane was used as the mobile phase at a flow-rate of 1.0 ml/min and the UV detector was set at 225 nm.

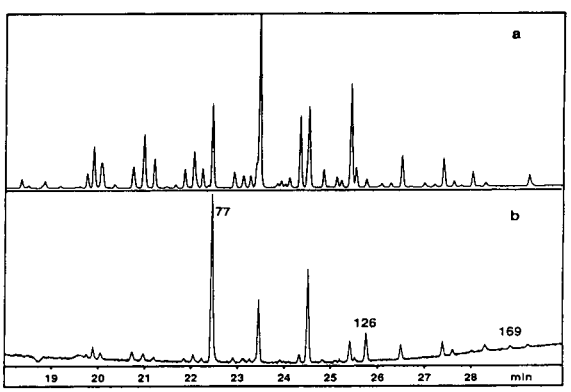

Fig. 3. GC–ECD of (a) Aroclor 1254 and (b) toxic non-*ortho* congeners fractionated from Aroclor 1254 on a DNAP column. A Restek RT-5 GC column (60 m × 0.32 mm I.D.) was used with hydrogen as carrier gas.

ing a modifier such as methyl-*tert.*-butyl ether to reduce adsorption eliminated the problem. The effect remained also after shortening the connecting tubing length to the minimum. There were no signs of overloading as two fractionation experiments with different amounts of Aroclor 1254 yielded the same relative peak heights in the subsequent GC analysis.

Hence, the effect is attributed to peak tailing due to interaction with the stationary phase. This problem becomes particularly evident because of the large concentration differences between the target compounds, i.e., CB-77, CB-126 and CB-169, and the more abundant components of Aroclor 1254. The major peaks of the remaining bulk PCB in the chromatogram of the non-*ortho*-CB congeners (Fig. 3b) correspond to the mono-*ortho* congeners CB-118 at a retention time of 23.5 min and CB-105 at 24.5 min. Of the individual congeners tested, CB-105 elutes closest to the non-*ortho* fraction (Table 1). CB-118 has a capacity factor less than half those of the non-*ortho* congeners on the DNAP column, but it is the second most abundant congener in Aroclor 1254 [20].

Fig. 4 shows the HPLC trace of CB-105 injected on to a DNAP column where eight collected fractions have been marked. The relative distribution of CB-105 in each fraction is listed in Table 2. A much longer tailing is demonstrated by the data in Table 2 compared with the tailing observed on the HPLC–UV trace. Still, in fraction eight, collected about 6 min after the peak apex, 0.2% of the total detected amount of this non-polar compound is present. The non-*ortho* fraction, which corresponds to the second half of fraction 4, fraction 5 and a small part of fraction 6 (10.80–12.60 min), is estimated to contain 1–1.5% of the total amount CB-105. For the purpose of determining CB-105, it can be concluded that collection of fractions 1 and 2 provides a yield of more than 97% of the detected amount.

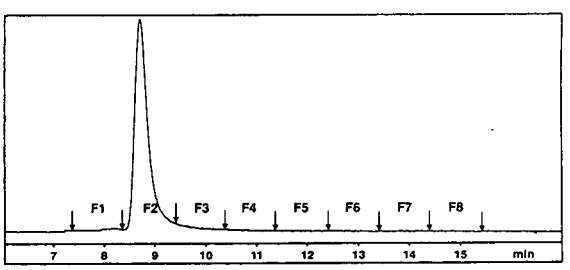

Fig. 4. Chromatogram of CB-105 injected on to a DNAP column. Fractions collected at 1-min intervals are marked. The relative distribution of CB-105 in the different fractions is listed in Table 2. Hexane was used as the mobile phase at a flow-rate of 1.0 ml/min and the UV detector was set at 225 nm.

Table 2
Relative distribution of CB-105 in different fractions as shown in Fig. 4

Fraction No.	Relative distribution (%)
1	0.03
2	92.5
3	5.0
4	1.2
5	0.6
6	0.3
7	0.2
8	0.2

The fractions were analysed by GC as described under Experimental.

The problem with overlap from tailing peaks seems to be present to a larger or smaller extent on all applied liquid chromatographic stationary phases when solutes with concentration differences of the orders found in PCB samples are to be separated [6,8,13,14]. However, as MS with single or multiple ion monitoring is frequently used for detection when determining CB-77, CB-126 and CB-169, residues of CB congeners with masses other than that currently being monitored will not be detected or will yield only small peaks from fragments with the same mass-to-charge ratio.

When the purity of the non-*ortho*-PCB fractions of Aroclor 1254 from a DNAP column and Clophen A50 from a PYE column are compared, it can be noted that the PYE column yields lower residual amounts of CB-105 and CB-118 than the DNAP column. On the other hand, those are the only "bulk PCB" peaks higher than the peak of CB-126 in the collected fraction from the DNAP

column, whereas the fraction collected from the PYE column has at least seven bulk-PCB peaks higher than that of CB-126 [13].

4. Conclusions

Two new alternatives for the selective separation of toxic non-*ortho*-chlorobiphenyls from the bulk PCB have been presented, dinitroanilinopropylsilica and tetranitrofluoreniminopropylsilica. Both stationary phases differ in functionality from the previously used materials based mainly on pure carbon or hydrocarbons. The nitro functionality is expected to provide alternative selectivity also to non-PCB components, a characteristic that might improve clean-up. The unusual retention pattern of CB-77, 126 and 169 on the DNAP column, all in a single peak, provide the possibility of collecting a small fraction for subsequent analysis by GC or on-line coupled LC–GC. These nitro stationary phases can thus be regarded as adequate alternatives for the selective clean-up of toxic non-*ortho*-CBs.

Acknowledgements

This project was financially supported by the Swedish National Environmental Protection Board, grants Nos. 532630-9 and 30359, and the Swedish Work Environment Fund, grant No. 93-0336.

References

[1] U. Ahlborg, A. Hanberg and K. Kenne, *Risk Assessment of PCBs*, Nordic Council of Ministers, Report Nord 1992:26, Copenhagen, ISBN 92 9120 0751, 1992, p. 1.
[2] R. Fischer and K. Ballschmiter, *Fresenius' Z. Anal. Chem.*, 335 (1989) 20.
[3] C.S. Creaser, F. Krokos and J.R. Startin, *Chemosphere*, 25 (1992) 1981.
[4] J.C. Duinker, D.E. Schulz and G. Petrick, *Anal. Chem.*, 60 (1988) 478.
[5] K.K. Himberg and E. Sippola, *Chemosphere*, 27 (1993) 17.
[6] N. Kannan, G. Petrick, D. Schulz, J. Duinker, J. Boon, E. van Arnhem and S. Jansen, *Chemosphere*, 23 (1991) 1055.
[7] T.R. Schwartz, D.E. Tillitt, K.P. Feltz and P.H. Peterman, *Chemosphere*, 26 (1993) 1443.
[8] J. de Boer, C.J.N. Stronck, F. van der Valk, P.G. Wester and M.J.M. Daudt, *Chemosphere*, 25 (1992) 1277.
[9] C.S. Creaser and A. Al-Haddad, *Anal. Chem.*, 61 (1989) 1300.
[10] M.D. Pastor, J. Sanchez, D. Barcélo and J. Albaigés, *J. Chromatogr.*, 629 (1993) 329.
[11] E. Storr-Hansen, M. Cleeman, T. Cederberg and B. Jansson, *Chemosphere*, 24 (1992) 323.
[12] R. Lazar, R.C. Edwards, C.D. Metcalfe, F.A.P.C. Gobas and G.D. Haffner, *Chemosphere*, 25 (1992) 493.
[13] P. Haglund, L. Asplund, U. Järnberg and B. Jansson, *J. Chromatogr.*, 507 (1990) 389.
[14] D.L. Stalling, C.Y. Guo and S. Saim, *J. Chromatogr. Sci.*, 31 (1993) 265.
[15] P. de Voogt, D.E. Wells, L. Reutergårdh and U.A.Th. Brinkman, *Int. J. Environ. Anal. Chem.*, 40 (1990) 1.
[16] V.P. Nero and R.D. Hudson, *Anal. Chem.*, 56 (1984) 1041.
[17] E. Grimvall and C. Östman, *J. Chromatogr. A*, 675 (1994) 55.
[18] N. Kannan, S. Tanabe, T. Wakimoto and R. Tatsukawa, *J. Assoc. Off. Anal. Chem.*, 70 (1987) 451.
[19] M. Athanasiadou, A. Jensen and E. Klasson Wehler, *Chemosphere*, 23 (1991) 957.
[20] D.E. Schulz, G. Petrick and J.C. Duinker, *Environ. Sci. Technol.*, 23 (1989) 852.

ELSEVIER

Journal of Chromatography A, 685 (1994) 344–348

JOURNAL OF CHROMATOGRAPHY A

Short communication

Membrane affinity chromatography of alkaline phosphatase

Wei Guo, Zhenhua Shang, Yinian Yu, Liangmo Zhou*

Dalian Institute of Chemical Physics, Academia Sinica, P.O. Box 100, Dalian 116012, China

First received 16 May 1994; revised manuscript received 2 August 1994

Abstract

A method for the preparation of a microporous cellulose membrane is described. The triazine dyes Cibacron Blue F3GA and Active Red K2BP were immobilized as affinity ligands. Up to 90 mg of Active Red K2BP can be coupled to 1 g of membrane matrix. A membrane cartridge containing red affinity membranes was also prepared. The flux of the cartridge containing 80 sheets of membrane can reach 5.0 ml/min with a pressure drop of 0.1 MPa. On this cartridge, the chromatography of alkaline phosphatase was performed with a 60% recovery of activity and a 40-fold purification.

1. Introduction

Affinity chromatography is a unique method in separation technology as it is the only technique that permits the purification of biomolecules based on biological functions rather than individual physical or chemical properties. The high specificity of affinity chromatography is due to the strong interaction between the ligand and biomolecule of interest. On the other hand, because of the strong interaction, elution of a biomolecule may be very difficult and time consuming, which may seriously lower the activity recovery of samples. To solve this problem, membrane affinity chromatography (MAC) was introduced several years ago [1,2].

Membrane separation allows the processing of a large amount of sample in a relatively short time owing to its structure, which provides a system with rapid reaction kinetics [3]. The integration of membrane and affinity chromatography provides a number of advantages over normal affinity chromatography using columns, especially with regard to time and activity recovery [4,5].

There are two technical problems that have hampered further increases in the use of MAC, the distribution of the sample or mobile phase and the sealing of the bundling system. The former problem was solved by Josic et al. [6] using simple distribution plates but the latter was not so easy, especially because when using many individual membranes as the stationary phase the bundling of thin membranes often leads to leakages in the system, which in turn causes the mobile phase and the sample to flow beyond the edges and therefore past the membranes. One solution to this problem is to add a sealing ring between every two individual membranes, as done by Millipore (Tokyo, Japan) in their commercial membrane cartridge product.

In this work, an affinity membrane medium was prepared from chemically cross-linked cellulose film. The membrane obtained was more

* Corresponding author.

0021-9673/94/$07.00
SSDI 0021-9673(94)00725-X

chemically and mechanically stable than the original cellulose microfiltration membrane, and had a large pore size and high porosity. The triazine dyes Cibacron Blue F3GA and Active Red K2BP were immobilized as affinity ligands. Using a special sealing technique, 80 sheets of cellulose membrane were bonded together. With the addition of two distribution plates, an affinity membrane cartridge was also prepared. The flux of the membrane cartridge can reach 5.0 ml/min with a pressure drop of 0.1 MPa. The membrane cartridge with red dye affinity ligand was used for the purification of alkaline phosphatase.

2. Experimental

2.1. Materials

Quantitative filter-paper Xinhua No. 1 was purchased from Hangzhou Xinhua Paper Manufactory (Hangzhou, China), Sepharose 4B from Pharmacia (Uppsala, Sweden), epoxy propane chloride of analytical-reagent grade from Tianjin Chemical Plant (Tianjin, China), Cibacron Blue F3GA and Active Red K2BP from Serva (Heidelberg, Germany) and Shanghai Eighth Chemical Dyestuff Factory (Shanghai, China), respectively, and alkaline phosphatase and its substrate, *p*-nitrophenyl phosphate, from Dongfeng Biochemical (Shanghai, China).

2.2. Apparatus

The experiments were performed on a Bio-Rad (Richmond, CA, USA) automated Econo System which consists of a Model EP-1 Econo Pump, a Model EM-1 Econo UV monitor with portable optics module equipped with two interchangeable filters (254 and 280 nm), a Model 2110 fraction collector and a Model ES-1 Econo system controller. Chromatograms were recorded and processed on a Hewlett-Packard Model 3394A integrator. The loading of sample on the affinity cartridge was carried out with a Gilson (Middleton, WI, USA) Minipuls 3 peristaltic pump in a refrigerator (3–7°C). The C, H and N contents of the dye-immobilized affinity membrane were determined on a Carla Erla (Milan, Italy) Model 1106 elemental analyser.

2.3. Preparation of cellulose film

An 80-g filter-paper was dispersed in 1000 ml of aqueous solution containing 50 g of NaOH and 5 g of $NaBH_4$ and the mixture was heated and kept boiling until a uniform pulp was achieved. Then the pulp was cast on a glass plate and frozen at −30°C in a freezer for 45 min. After thawing at room temperature, the plate was immersed in 10% HCl for 1 h. The cellulose film was then removed and rinsed with water until neutral. After dipping in acetone for 2.5 h, the cellulose film was dried in air.

2.4. Preparation of affinity membrane

A 12-g amount of NaOH was dissolved in 50 ml of water and 100 ml of dimethyl sulphoxide, to which 20 ml of epoxy propane chloride and 0.5 g of $NaBH_4$ were added. At room temperature, 40 sheets of cellulose films with a diameter of 40 mm were soaked in the above solution individually, then gently shaken for 20 min. The films were then removed, 4 g of NaOH and 10 ml of epoxypropane chloride were added to the remaining solution and the films were soaked individually again in the solution. The solution was heated to 50°C and stirred every 10 min for 3 h, then the cross-linked membranes were washed with hot distilled water until neutral. The membranes were dispersed in 10% ammonia solution for 24 h at room temperature, washed thoroughly to remove residual ammonia and finally soaked in a solution of 2.0 g of Active Red K2BP, 380 ml of water and 20 ml of 15% Na_2CO_3. The temperature was held at 50°C for 20 h with stirring every 10 min. Finally, the red membranes were washed with distilled water until the absorbance at 520 nm of the eluate was zero.

2.5. Methods

The activity of the enzyme was determined with a *p*-nitrophenyl phosphate substrate as described by Schlesinger and Barret [7] and the protein content was determined by the Coomassie Blue method described by Gogstad and Grossberg [8]. The pore size of the prepared cellulose membrane was determined by the method Yasuda and Tsai [9].

3. Results and discussion

One of the most important factors in affinity chromatography is the development of solid supports. In membrane affinity chromatography, the selection of the membrane material and the preparation of the membrane are dominant factors affecting chromatographic performance. We chose cellulose as the best material as it has long been used in membrane preparation and it is a good matrix for affinity coupling. However, the commercially available cellulose derivatives membranes, which usually are produced by a solution casting method, have a relatively low porosity and are not suitable for chromatography owing to the high pressure drop through the bundling of membranes. Therefore, in this work, a new type cellulose microfiltration membrane prepared in our laboratory was used as a membrane matrix. This membrane, consisting of coarse fibres, has a higher porosity and larger pore size (1–2 μm) than ordinary cellulose microfiltration membranes, but is less uniform in structure. To enhance the mechanical and chemical stabilities, cross-linking by epoxypropane chloride was carried out prior to immobilization of triazine dyes.

Sample distribution is one of the main problems, especially when wide but thin membrane cartridges are used in separation. Josic et al. [6] overcame this problem by installing distribution plates before and behind the membrane. They compared over twenty patterns of plates. In this work, distribution plates were prepared according to the optimum conditions described by Josic.

The other main problem in the preparation of membrane cartridges, the sealing of the system, which becomes more serious when the bundling of many single membranes is adopted, was solved with greater effort. In this work, a special bonding method was performed. The circumference with a width of 1 mm on the edge of each individual membrane was saturated with an elastic glue. After removing the excess glue, up to 80 sheets of membrane can be packed and bonded together with mild pressure. The structure of the cartridges prepared using this method was better with regard to both sealing and separation efficiency and, because that the membrane consisted of coarse fibres and had a large pore size and high porosity, the pressure across the cartridge during chromatography can be relatively low. The construction of the membrane cartridge used in the experiment is shown in Fig. 1. The flux through a membrane cartridge containing 80 sheets of membrane is shown in Fig. 2.

For cellulose membrane cross-linking, 2.4 *M* NaOH was used. This concentration exceeded that necessary for the cross-linking only. A high concentration alkali in the cross-linking increased the amount and activity of the hydroxyl groups in the cellulose membrane obtained. In this experiment, two kinds of cellulose membranes was prepared using different cross-linking conditions: one (alkali-treated cellulose mem-

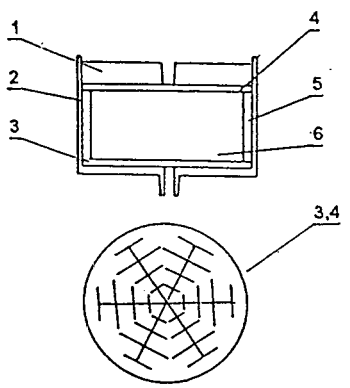

Fig. 1. Construction of the membrane cartridge for membrane affinity chromatography. The diameter of the membranes used was 40 mm. 1 = Rubber cover; 2 = glass holder; 3, 4 = distribution plates; 5 = bonding part; 6 = affinity membranes.

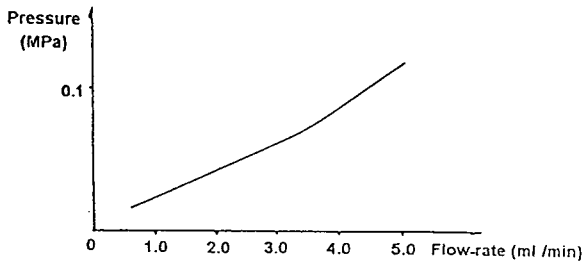

Fig. 2. Flux of membrane cartridge (18 × 40 mm I.D., containing 80 sheets of cellulose membrane).

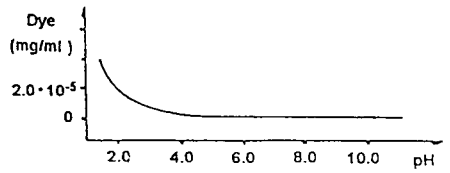

Fig. 3. Ligand leakage of membrane affinity media. 18 × 40 mm I.D. cartridge, containing 80 sheets of Active Red K2BP-immobilized cellulose membrane. Mobile phase, 0.5 *M* NaCl; flow-rate, 0.5 ml/min.

brane) was cross-linked in 2.4 *M* NaOH and the other (initial cellulose membrane) was cross-linked in 0.4 *M* NaOH. Based on elemental analysis, the capacities of these two cellulose membranes for the immobilization of triazine dyes were compared (Table 1).

A major advantage of the triazine dyes as affinity ligands is their stability. Triazine linkages are less prone to ligand leakage than cyanogen bromide-activated polysaccharides [10]. The membrane cartridge prepared in this experiment with Active Red K2BP as ligand was eluted with a pH gradient from pH 1 to 12, and the absorbance of the eluate was determined (Fig. 3). The results showed that when the pH of the eluent was higher than 3.5, no dye released from the stationary phase was observed in the eluate.

Triazine dyes can serve as analogues for nucleotides so that a protein will bind them at nucleotide-binding sites. They have been used successfully in the purification of many enzymes, especially kinases and dehydrogenases. The phosphatase can be purified on a dye-immobilized medium. In this work, commercial alkaline phosphatase from calf intestine was purified on an affinity membrane cartridge containing 80 sheets of red cellulose membrane (Fig. 4). The phosphatase was eluted with 1 *M* NaCl, and an unknown component with a stronger affinity to the ligand was eluted with 60% ethylene glycol. The results of recovery experiments are given in Table 2. The recovery of alkaline phosphatase

Table 1
Effect of alkali treatment of the cellulose membrane on its capacity for the immobilization of triazine dyes

Dye	Capacity (mg/g)	
	Original cellulose membrane	Alkali-treated cellulose membrane
Cibacron Blue F3GA	20	100
Active Red K2BP	39	90

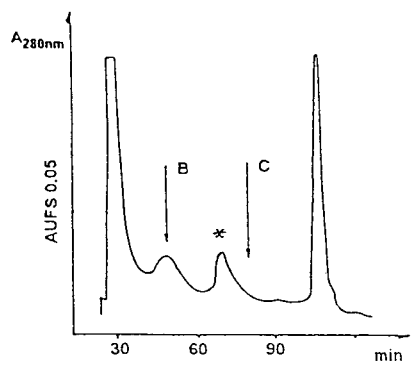

Fig. 4. Membrane affinity chromatography of alkaline phosphatase on Active Red K2BP-immobilized cellulose membranes. A 10.3-mg amount of alkaline phosphatase was dissolved in 2.0 ml of 0.1 *M* NaCl–0.1 *M* NaOAc–HCl buffer (pH 7.5) and was applied to a 18 × 40 mm I.D. cartridge, containing 80 sheets of membrane, at a flow rate of 0.1 ml/min at 4°C. The cartridge, at room temperature, was first equilibrated with 1.0 ml of 0.1 *M* NaCl–0.1 *M* NaOAc–HCl buffer (pH 7.2) (solution A), then the alkaline phosphatase and other impurities were eluted with 1.0 *M* NaCl–0.1 *M* NaOAc–HCl buffer (pH 7.0) (solution B) and 1.0 *M* NaCl–0.1 *M* NaOAc–HCl buffer (pH 7.0) containing 60% ethylene glycol (solution C), respectively. The flow-rate of mobile phase was 0.8 ml/min. The asterisk indicates alkaline phosphatase.

Table 2
Purification of alkaline phosphatase by membrane affinity chromatography

Enzyme	Volume (ml)	Total protein (mg)	Total activity (U)	Specific activity (U/mg)	Enrichment (-fold)	Yield (%)
Initial sample	2.0	10.3	10 800	1050		
Product of MAC	8.0	0.15	6480	$4.2 \cdot 10^4$	40	60

activity was 60% and a 40-fold purification was achieved.

Acknowledgements

This work was supported by the National Natural Science Foundation of China.

References

[1] K.B. Male, J.H.T. Luong and A.L. Nguyen, *Enzyme Microb. Technol.*, 9 (1987) 374.
[2] A.L. Nguyen and J.H.T. Luong, *Biotechnol. Bioeng.*, 34 (1989) 1186.
[3] M. Unarska, P.A. Daview, M.P. Esnouf and B.J. Bellhouse, *J. Chromatogr.*, 519 (1990) 53.
[4] S.Y. Suen and M.R. Etzel, *Chem. Eng. Sci.*, 47 (1992) 1355.
[5] W. Guo, Z.H. Shang, Y.N. Yu, Y.F. Guan and L.M. Zhou, *Biomed. Chromatogr.*, 6 (1992) 95.
[6] D. Josic, H. Reusch, K. Loster, O. Baum and W. Ruetter, *J. Chromatogr.*, 590 (1992) 59.
[7] M.J. Schlesinger and K. Barret, *J. Biol. Chem.*, 240 (1965) 4284.
[8] G.D. Gogstad and S.E. Grossberg, *Anal. Biochem.*, 126 (1982) 355.
[9] H. Yasuda and J.T. Tsai, *J. Appl. Polym. Sci.*, 18 (1974) 805.
[10] P.D. Dean and D.H. Watson, *J. Chromatogr.*, 165 (1979) 301.

ELSEVIER

Journal of Chromatography A, 685 (1994) 349–355

JOURNAL OF CHROMATOGRAPHY A

Short communication

Direct enantiomeric separation of the four stereoisomers of nadolol using normal-phase and reversed-phase high-performance liquid chromatography with Chiralpak AD

James P. McCarthy

Analytical Research and Development, Pharmaceutical Research Institute, Bristol-Myers Squibb, Princeton, NJ 08543, USA

First received 28 April 1994; revised manuscript received 19 August 1994

Abstract

Two enantiomeric separations have been developed which resolve the four stereoisomers of nadolol on Chiralpak AD using high-performance liquid chromatography. The normal-phase method uses hexane, ethanol and diethylamine to baseline resolve all four stereoisomers. The reversed-phase method uses ethanol, water and diethylamine. Both methods were optimized by investigating different mobile phase modifiers, flow-rates and column temperatures. Accuracy and reproducibility were determined for quantitating levels of racemate A and racemate B using the normal-phase method.

1. Introduction

Nadolol, 5 - {3 - [(1,1 - dimethylethyl)amino] - 2 - hydroxypropoxy} - 1,2,3,4 - tetrahydro - *cis* - 2,3 - naphthalenediol is a β-blocker used in the management of hypertension and angina pectoris. Its chemical structure has three chiral centers which allow for eight possible stereoisomers. However, the two hydroxyl substituents on the cyclohexane ring are in the *cis* configuration which precludes four stereoisomers (see Fig. 1). Nadolol is marketed as an equal mixture of the four stereoisomers, designated as the diastereomers "racemate A" and "racemate B". Racemate A is a mixture of stereoisomer I and its enantiomer II, whereas racemate B is a mixture of the most active stereoisomer III and its enantiomer IV.

Many β-blockers have been successfully separated from their enantiomers using Chiralcel OD, a cellulose-based 3,5-dimethylphenyl carbamate HPLC column manufactured by Daicel (Tokyo, Japan) [1–6]. The method developed by Krstulovic et. al. [7] for enantiomeric separation of nadolol used Chiralcel OD to separate nadolol into two peaks. Nadolol however requires an approach different from Chiralcel OD because it contains two diastereomeric pairs of enantiomers, for a total of four compounds to be separated. Most other β-blockers contain only one pair of enantiomers. Daicel's Chiralpak AD HPLC column is amylose based and has a helical structure, whereas Chiralcel OD has a rigid linear structure. Chiralpak AD has the same 3,5-dimethylphenyl carbamate moiety as Chiralcel OD and the same silica support. Therefore, observed differences in separation must be due to the structural differences between cellulose and amylose.

The most recent HPLC methodology for the

0021-9673/94/$07.00
SSDI 0021-9673(94)00803-5

Racemate A

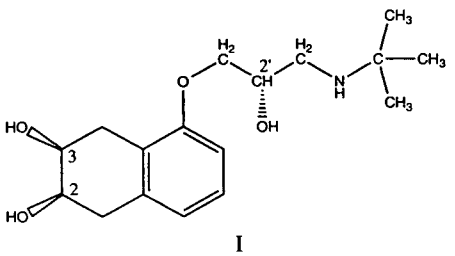

I

2R,3S,2'R (-) ring, (+) side chain

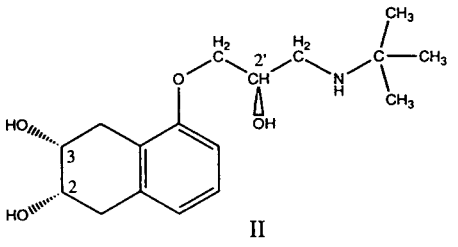

II

2S,3R,2'S (+) ring, (-) side chain

Racemate B

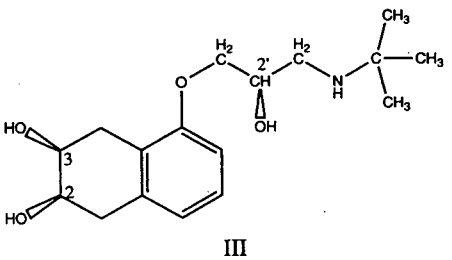

III

2R,3S,2'S (-) ring, (-) side chain

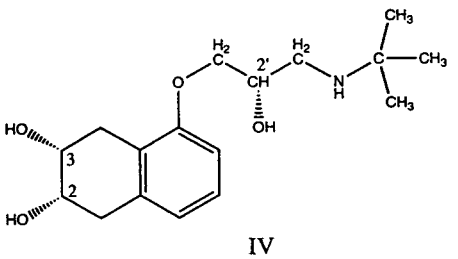

IV

2S,3R,2'R (+) ring, (+) side chain

Fig. 1. Absolute conformation of the four stereoisomers of nadolol.

analysis of nadolol baseline resolves the four stereoisomers using Ultron ES-OVM with a mobile phase of methanol and phosphate buffer [8]. In order to perform preparative-scale isolations of each stereoisomer of nadolol, Hoshino et al. [8] developed a second separation using Chiralpak AD which did not baseline resolve all four stereoisomers. Prior to the Ultron ES-OVM, a method was not available which baseline resolved all four of the stereoisomers without derivatization.

Daicel's cellulose- and amylose-based carbamate columns have been almost exclusively used under normal-phase conditions. Recently, separations have been developed on Chiralcel OD using reversed-phase conditions ("OD-R") [9]. Ishikawa and Shibata [9] successfully separated the enantiomers of two β-blockers, propranolol and pindolol, using 0.1 *M* aq. $NaPF_6$–CH_3CN. Their article detailed a comprehensive study of the effects different mobile phase additives have on the separation of acidic, neutral and basic compounds from their enantiomers. It was determined that acidic compounds are best resolved at pH < 3, neutral compounds can be separated using water and an organic modifier, and basic compounds require the addition of a chaotropic modifier. The chaotropic modifier has an effect similar to ion pairing. Perchlorate and hexafluorophosphate modifiers were determined to be among the best chaotropes for resolving enantiomers of basic compounds.

Detailed in the following article are the separations of the four stereoisomers of nadolol on Chiralpak AD using normal-phase and reversed-phase conditions. The effects of mobile phase composition, flow-rate and column temperature on resolution are discussed. The research by Ishikawa and Shibata [9] prompted the investigation of Chiralpak AD column under revers-

ed-phase conditions detailed below. The conclusions of Ishikawa and Shibata were applied to nadolol in a similar though less comprehensive study.

2. Experimental

2.1. Reagents

Methanol, 85% *n*-hexane and 2-propanol were all Baker HPLC reagents (Phillipsburg, NJ, USA). Ethanol used was dehydrated 200 proof obtained from Pharmco (Bayonne, NJ, USA). The diethylamine was 98% and obtained from Aldrich (Milwaukee, WI, USA). UV-grade acetonitrile was obtained from Burdick & Jackson (Muskegon, MI, USA). Water used in these experiments was drawn from a Milli-Q water system (Millipore, Milford, MA, USA). The nadolol standards were obtained internally. Nadolol, racemate A, racemate B and standards of each individual stereoisomer were available. Structural conformations of the individual stereoisomer standards were confirmed by X-ray diffraction.

2.2. Apparatus

The HPLC system consisted of a Perkin-Elmer Model Series 4 solvent-delivery system (Norwalk, CT, USA), a Perkin-Elmer ISS-100 autosampler and an Applied Biosystems variable-wavelength UV-absorbance detector Model 785A (Foster City, CA, USA) with the wavelength set at 270 nm. Column temperature was maintained by a Euramark Model EU-255 column thermostat (Mt. Prospect, IL, USA) which utilizes Peltier cooling. The stationary phase used was amylose-based tris-3,5-dimethylphenyl carbamate (Chiralpak AD) coated on 10-μm silica gel, 25.0 × 0.46 cm (Daicel) available from Chiral Technologies (Exton, PA, USA). Data collection and reporting was by a VG Multichrom data acquisition system.

The Chiralpak AD-R (reversed-phase) column was created from a standard Chiralpak AD column received from Chiral Technologies. It was gradually changed over from hexane to 2-propanol, then to methanol, and finally ethanol. A slow gradient and low flow-rate were used to avoid too high pressure.

2.3. Chromatographic conditions

All sample solutions were approximately 2 mg/ml dissolved in ethanol. Sample solutions were stable for at least 24 h. A 25μ-l aliquot was injected. The Chiralpak AD column was investigated using both normal-phase (hexane, ethanol, 2-propanol and diethylamine) and reversed-phase (water, ethanol, methanol, 2-propanol, acetonitrile and diethylamine) at various flow-rates and column temperatures. Final normal-phase conditions used a mobile phase of 800 ml hexane, 200 ml ethanol and 3 ml diethylamine. The flow-rate was 1.2 ml/min at 23°C. The reversed-phase conditions used the same column and sample solutions. The mobile phase consisted of 750 ml water, 250 ml ethanol and 5 ml diethylamine. A flow-rate of 0.2 ml/min was used and the column temperature was maintained at 0°C.

2.4. Determination of elution order

All four stereoisomers were analyzed by HPLC individually and compared to analyses of nadolol and racemates A and B. The elution orders are shown in Fig. 2 and Fig. 3. The elution order of the four stereoisomers is the same in both normal- and reversed-phase systems.

3. Results and discussion

Both the normal- and the reversed-phase systems resolve the four stereoisomers of nadolol. Fig. 2 shows the normal-phase separation. All four compounds are baseline resolved. The reversed-phase separation is shown in Fig. 3. Two of the four compounds are baseline resolved. Since the normal-phase separation was superior, it was evaluated for accuracy and reproducibility.

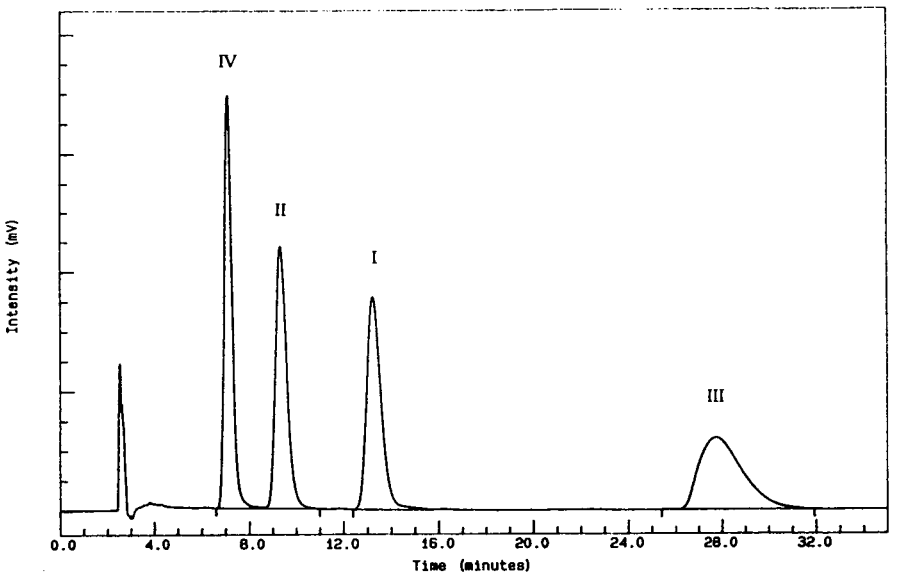

Fig. 2. Resolution of the four stereoisomers of nadolol in normal-phase mode using hexane–ethanol–diethylamine (80:20:0.3).

3.1. Normal-phase separation

During development of the normal-phase system, alcohol type, alcohol concentration, diethylamine concentration, flow-rate and column temperature were varied to determine their effect on resolution. Many combinations baseline resolved all four stereoisomers.

Alcohol type and concentrations were varied in mobile phases containing hexane and diethylamine. Ethanol, 2-propanol and combinations of the two were investigated. A systematic ap-

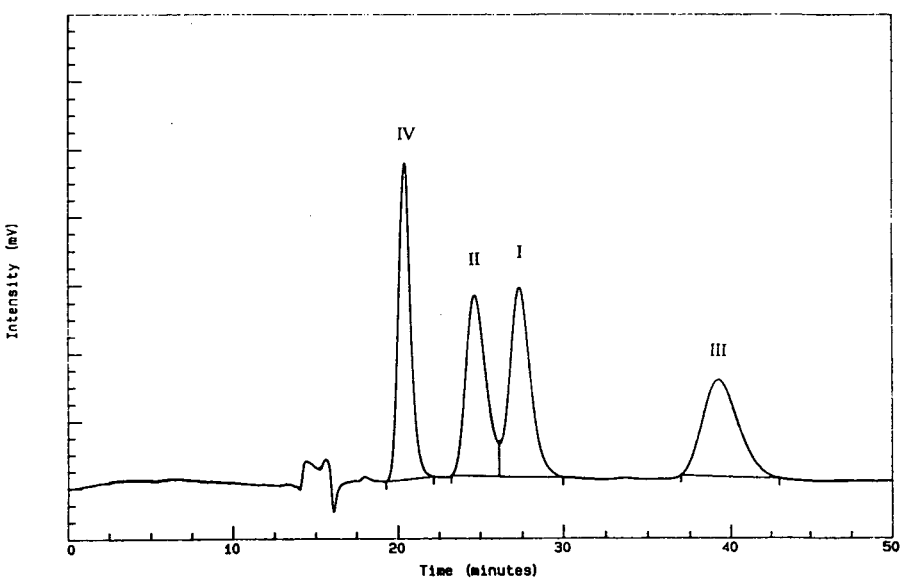

Fig. 3. Resolution of the four stereoisomers of nadolol in reversed-phase mode using ethanol–water–diethylamine (25:75:0.5).

proach was taken varying the alcohol concentrations in 2% increments from hexane–ethanol–2-propanol (75:25:0) to (75:0:25). As the concentration of ethanol decreased and 2-propanol increased, compounds IV and II eluted closer together. Hexane–ethanol (80:20) and hexane–ethanol–2-propanol (77:15:8) baseline resolved all four stereoisomers. When hexane–2-propanol was used without ethanol, compounds IV and II merged and compounds I and III were only partially resolved.

Diethylamine was necessary to separate the four stereoisomers. At concentrations less than 0.3%, the peaks tailed into one another and could not be quantitated. At levels higher than 0.3%, up to 1.0%, neither peak shape nor resolution improved.

Various flow-rates and column temperatures were also investigated. Several combinations of mobile phases at different flow-rates and temperatures baseline resolved all four stereoisomers. Table 1 shows examples of mobile phase/flow-rate/column temperature combinations that baseline resolved all four stereoisomers. As expected, lower column temperatures and less alcohol increased retention. However these changes did not always improve resolution (R_s) or separation (α) of the critical pair (the closest eluting pair of stereoisomers). By increasing the ethanol concentration to 25% and cooling the column to 10°C, resolution and separation of the critical pair compounds IV and II were increased. Since column coolers are sometimes inconvenient and not universally used, the normal-phase conditions at room temperature were studied further.

Accuracy and reproducibility of this method to quantitate levels of the four stereoisomers in synthetic mixtures were determined. Mixtures at ratios of approximately 80:20, 60:40, 40:60 and 20:80 of racemates A:B were weighed and the experimental results were compared to the theoretical levels. Detector response was measured for the individual stereoisomers and corrections were made for contamination of the individual stereoisomers with the other stereoisomers. The averages of four replicate analyses of each mixture are summarized in Table 2. All experimental results were within 99.1–101.5% of theoretical racemate A levels. The mixture of A–B (80:20) was injected five times and statistically analyzed for reproducibility. The relative standard deviations (R.S.D.s) ranged from 0.18 to 1.36%.

In several batches of the individual stereoisomers which were synthesized, trace levels of the other three stereoisomers have been quantitated. Levels as low as 0.10%, measured by area counts, have been quantitated. Linearity, however, was not determined.

3.2. Reversed-phase separation

Nadolol is classified as a basic drug, similar to propranolol and pindolol. Therefore, mobile phases containing chaotropic modifiers, as suggested by Ishikawa and Shibata [9], were investigated. In addition, diethylamine was investigated because it reduces tailing in other normal-phase and reversed-phase chromatographic applications.

Various organic modifiers were evaluated in combination with water. Ethanol was the only modifier which resolved the stereoisomers satisfactorily. Methanol, 2-propanol and acetonitrile were substituted for ethanol and did not resolve nadolol into four peaks. Diethylamine was necessary at a level of 0.5% to reduce tailing and resolve the four peaks. Lowering the column temperature and flow-rate retained nadolol longer and improved the separation. Lowering the concentration of ethanol was investigated as a means of increasing retention but did not improve resolution. The combination of a high concentration of ethanol, low column temperature and low flow-rate were necessary to resolve nadolol. The four stereoisomers were best resolved with ethanol–water–diethylamine (25:75:0.5) at a flow-rate of 0.2 ml/min and column temperature maintained at 0°C. However, compounds II and I were not baseline resolved. The R_s was calculated to be 1.0.

The separation of nadolol on the AD-R column did not behave similarly to propranolol and pindolol on the OD-R column. The chaotropic modifiers $NaPF_6$ and $NaClO_4$ had little or no

Table 1
Resolution and capacity factors under normal-phase conditions

Mobile phase (%)			Flow-rate (ml/min)	Column temperature (°C)	Capacity factors				Critical pair	R_s critical pair	Separation of critical pair
Hexane	Ethanol	2-Propanol			Peak IV	Peak II	Peak I	Peak III			
84	16	0	1.1	23	2.84	3.91	7.06	13.61	IV, II	2.78	1.38
80	20	0	1.2	23	1.71	2.55	4.01	9.46	IV, II	2.94	1.49
80	20	0	1.2	10	2.35	3.41	6.58	13.03	IV, II	2.84	1.45
75	25	0	1.2	0	1.63	2.67	4.74	10.65	IV, II	2.23	1.64
75	25	0	1	10	1.25	2.02	3.17	6.85	IV, II	3.22	1.61
75	25	0	1	19	1.13	1.91	2.49	6.58	II, I	2.5	1.31
75	25	0	1	23	1.13	1.86	2.41	6.4	II, I	2.1	1.29
84	6	10	1.1	23	2.31	2.31	3.99	4.91	IV, II	–	–
78	11	11	1.1	23	1.53	2.02	3.75	6.14	IV, II	1.58	1.33
77	15	8	1.1	23	1.57	2.31	4.24	8.6	IV, II	2.53	1.47
73	18	9	1	23	1.15	1.77	2.98	6.98	IV, II	1.86	1.54
77	20	3	1.1	23	1.57	2.17	4.29	8.06	IV, II	2.74	1.39

Table 2
Accuracy of normal-phase method to quantitate levels of racemates A and B

Racemate A			Racemate B	
Theoretical	Experimental	Accuracy (%A)	Theoretical	Experimental
77.66	78.8	101.47	22.34	21.2
58.86	59.44	100.99	41.14	40.56
40.06	39.71	99.13	59.94	60.29
21.26	21.09	99.20	78.74	78.91

effect resolving nadolol. A complete study of AD-R similar to Ishikawa and Shibata's has not yet been conducted to compare it to OD-R and determine the full versatility of AD-R. Nevertheless, AD-R has been used successfully in this laboratory for applications which were unsuccessful using OD-R. Typically, acetonitrile or methanol and water yield the best separations.

4. Conclusions

Nadolol was best resolved into its four stereoisomers on Chiralpak AD under normal-phase conditions. All four compounds were baseline resolved using hexane–ethanol–diethylamine (80:20:0.3) at room temperature. The final conditions resulted in an R_s value of 2.94 with an α value of 1.49 for the critical pair, compounds IV and II. Cooling the column and increasing the ethanol concentration improved resolution of the critical pair. Resolution of the four stereoisomers was dependent on alcohol type and the presence of diethylamine. The accuracy and reproducibility of this method were determined to be acceptable. This method can be used for determining levels of all four stereoisomers in current nadolol drug substance and can be used to determine trace levels of other stereoisomers in the individual stereoisomers synthesized.

Using the reversed-phase conditions of ethanol–water–diethylamine (25:75:0.5), nadolol could be resolved into four distinct peaks. Compounds IV and III were baseline resolved and compounds II and I had an R_s value of 1.0. Using Chiralpak AD in reversed-phase mode has advantages over normal-phase even though nadolol was baseline resolved for only two of the four stereoisomers. The reversed-phase separation replaces highly flammable hexane with water for utilization in laboratories that prefer to avoid using hexane. This reversed-phase separation may also be adaptable to LC–MS. Utilizing Chiralpak AD in the reversed-phase mode is novel and still in the investigational stage. However, it has been successful in this laboratory for several other applications in which OD-R was unsuccessful. Work is continuing with AD-R.

Acknowledgements

I wish to thank Ms. Rita Fox for synthesizing each of the four stereoisomers of nadolol. Additionally, I wish to thank Dr. Jack Gougoutas for determining the absolute conformations of the stereoisomers by X-ray diffraction.

References

[1] H.Y. Aboul-Enein and V. Serignese, *J. Liq. Chromatogr.*, 16 (1993) 197.
[2] H.Y. Aboul-Enein and R. Islam, *J. Chromatogr.*, 511 (1990) 109.
[3] Th. Hollenhorst and G. Blaschke, *J. Chromatogr.*, 585 (1991) 329.
[4] K. Balmer, A. Persson, P.-O. Lagerstrom, B.-A. Persson and G. Schill, *J. Chromatogr.*, 553 (1991) 391.
[5] V.L. Herring and J.A. Johnson, *J. Chromatogr.*, 612 (1993) 215.
[6] H.Y. Aboul-Enein and M.R. Islam, *Anal. Lett.*, 23(6) (1990) 973.
[7] A.M. Krstulovic, M.H. Fouchet, J.T. Burke, G. Gillet and A. Durand, *J. Chromatogr.*, 452 (1988) 477.
[8] M. Hoshino, E. Matsui, K. Yajima, and A. Okahira, *J. Chromatogr. A*, 664 (1994) 104.
[9] A. Ishikawa and T. Shibata, *J. Liq. Chromatogr.*, 16 (1993) 859.

ELSEVIER

Journal of Chromatography A, 685 (1994) 356–359

JOURNAL OF CHROMATOGRAPHY A

Short communication

Separation and determination of reaction mixtures of anthraquinone by gas chromatography☆

Sajid Husain*, P. Nageswara Sarma, K. Sita Rama Rao, V.V.S. Lakshmi

Analytical Chemistry Division, Indian Institute of Chemical Technology, Hyderabad 500 007, India

First received 8 March 1994; revised manuscript received 26 July 1994

Abstract

Anthraquinone is a valuable organic intermediate commonly prepared by the reaction of phthalic anhydride with benzene and subsequent acid cyclization of the product obtained. Rapid, sensitive and selective analytical methods are essential for monitoring the reactions during process development. A gas chromatographic method using an internal standard is described for the separation and determination of the reaction products obtained during the manufacture of anthraquinone.

1. Introduction

Anthraquinone is a valuable intermediate in the manufacture of dyestuffs and pigments [1] and several methods are available for its preparation. It is generally prepared by the reaction of phthalic anhydride with benzene [2,3] in the presence of a catalyst to give *o*-benzoylbenzoic acid, followed by acid cyclization. Process development for the manufacture of anthraquinone starting from phthalic anhydride and benzene is in progress in our institute. During the process, selective, accurate and rapid analytical methods are required for monitoring the reactions.

A literature search revealed that anthraquinone has been determined in different matrices [4–11] using various instrumental techniques. It has been determined as a by-product in the preparation of benzaldehyde by gas chromatography (GC) [12]. However, no method has been reported for the separation and determination of components of reaction mixtures during the preparation of anthraquinone from phthalic anhydride. This prompted us to undertake the present studies.

A rapid, selective and precise GC method with acenaphthene as an internal standard was developed for the analysis of reaction mixtures obtained during the preparation of anthraquinone from phthalic anhydride.

2. Experimental

2.1. Materials

Acenaphthene was procured from Fluka (Buchs, Switzerland). Phthalic anhydride, benzophenone and anthraquinone were purchased from Loba Chemicals (Bombay, India). OV-17 used as the stationary phase and Chromosorb W

* Corresponding author.

☆ IICT Communication No. 3357.

0021-9673/94/$07.00
SSDI 0021-9673(94)00703-9

AW used as an inert support were obtained from Analabs (North Haven, CT, USA). All other chemicals and solvents were of analytical reagent grade.

2.2. Gas chromatography

A Hewlett-Packard Model 5840A gas chromatograph provided with a flame ionization detector equipped with a microprocessor was used under the following conditions: 15% OV-17 on Chromosorb W AW (80–100 mesh); column, stainless-steel (6 ft. × 1/8 in. I.D.); column temperature, 250°C; injection port temperature, 300°C; detector temperature, 300°C; chart speed, 1 cm/min; carrier gas, nitrogen; flow-rate, 45 ml/min; and injection volume, 1 μl.

2.3. Preparation of standard mixtures

Standard mixtures were prepared in the same proportions as expected in the reaction mixtures using acenaphthene as internal standard. Standard mixtures of various compositions were prepared. Triplicate runs were made for each standard mixture and reaction mixtures.

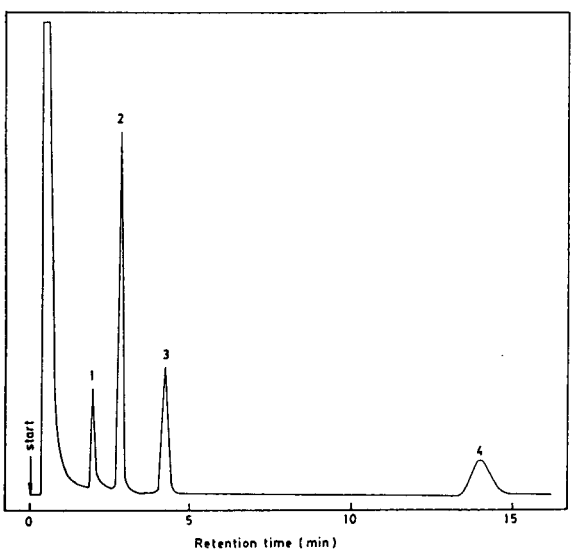

Fig. 1. Typical gas chromatogram showing the separation of a standard mixture of (1) phthalic anhydride, (3) benzophenone and (4) anthraquinone, with (2) acenaphthene as internal standard.

Table 1
Relative retention times (RRT) and relative response factors (RRF) of phthalic anhydride, anthraquinone and benzophenone on OV-17 stationary phase

Compound	RRT	RRF
Phthalic anhydride	0.68	2.56
Anthraquinone	5.01	1.24
Benzophenone	1.49	1.11
Acenaphthene (internal standard)	1.00	1.00

3. Results and discussion

The separation of anthraquinone, benzophenone and phthalic anhydride was studied on various stationary phases. It was found that the resolution was very good on 15% OV-17. A typical chromatogram showing the separation of phthalic anhydride, anthraquinone and benzophenone in a standard mixture containing an internal standard is depicted in Fig. 1. The elution sequence follows the order phthalic anhydride, benzophenone and anthraquinone, which has been confirmed by injecting authentic samples.

The relative retention times and relative response factors of these compounds with respect

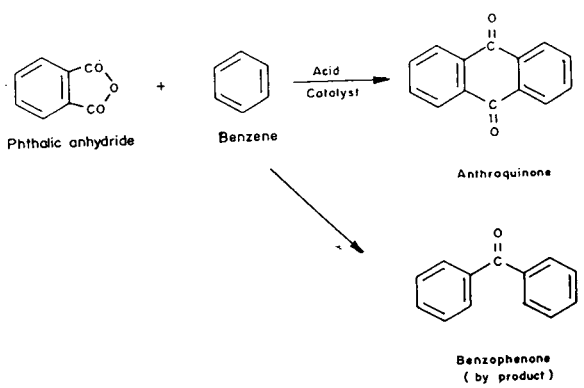

Fig. 2. Reactions for the preparation of anthraqunione.

Table 2
Results of the analysis of standard mixtures of phthalic anhydride, anthraquinone and benzophenone by GC

Compound	Mixture No.				
	1	2	3	4	5
Phthalic anhydride					
Taken (%)	49.40	32.58	29.53	32.06	8.57
Found (%)	49.99	31.78	28.85	31.40	8.24
Standard deviation ($n = 3$)	0.395	0.217	0.310	0.488	0.143
Anthraquinone					
Taken (%)	17.68	40.34	29.07	26.94	62.24
Found (%)	18.17	41.34	29.64	26.43	60.79
Standard deviation ($n = 3$)	0.361	0.481	0.209	0.283	0.671
Benzophenone					
Taken (%)	10.73	8.20	25.28	17.14	9.18
Found (%)	10.62	8.30	25.22	16.75	9.48
Standard deviation ($n = 3$)	0.169	0.008	0.129	0.215	0.103

to acenaphthene (internal standard) are given in Table 1. The relative response factors of phthalic anhydride, benzophenone and anthraquinone are >1, which indicates that the detector response is not 100%. The efficiency of the method was tested with various synthetic mixtures. The results obtained are given in Table 2. It can be observed from Table 2 that the experimental values are in good agreement with the true values and are within the limits of experimental error.

The method of preparation of anthraquinone from phthalic anhydride and benzene is shown in Fig. 2. A number of reaction mixtures obtained during the preparation of anthraquinone were analysed by the developed method and the results are given in Table 3.

A typical gas chromatogram showing the separation of reaction mixtures of anthraquinone is given in Fig. 3. It can be seen that an additional peak is obtained at 5.98 min, and GC–MS was applied to identify this peak. It was concluded

Table 3
Results of the analysis of typical reaction mixtures of anthraquinone

Mixture No.	Phthalic anhydride (%)	S.D. ($n = 3$)	Anthraquinone (%)	S.D. ($n = 3$)	Benzophenone (%)	S.D. ($n = 3$)
1	45.94	0.261	2.36	0.068	16.59	0.014
2	30.33	0.300	8.89	0.090	3.41	0.032
3	27.72	0.202	7.68	0.028	3.56	0.012
4	8.96	0.270	6.48	0.032	2.03	0.040
5	8.04	0.290	3.33	0.043	2.27	0.007

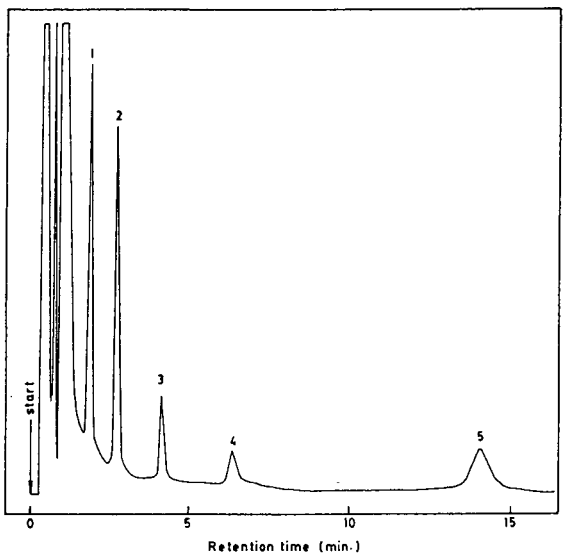

Fig. 3. Typical gas chromatogram showing the separation of anthraquinone reaction mixture. Peaks: 1 = phthalic anhydride; 2 = acenaphthene (internal standard); 3 = benzophenone; 4 = unidentified; 5 = anthraquinone.

that it may be 9-fluorenone. The total time for the analysis was 30 min.

Acknowledgements

The authors thank Dr. A.V. Rama Rao, Director, IICT, for his keen interest and encouragement. They also thank Dr. M. Subrahmanyam and Dr. V. Durgakumari, IICT, for supplying reaction mixtures.

References

[1] A.J. Confrancesco, in M.H. Grant (Editor), *Encyclopedia of Chemical Technology*, Vol. 2, Wiley, New York, 4th ed., 1992, p. 801.
[2] H. Sadamori and T. Okazaki, *Jpn. Pat.*, 74 95 952 (1974); *Chem. Abstr.*, 82 (1975) 43097p.
[3] G. Friedhofen, O. Immel and H. Schwarz, *Ger. Pat.* 2 633 458 (1978); *Chem. Abstr.* 88 (1978) 137904j.
[4] P.P. Rai, T.O. Turner and S.A. Maltin, *J. Chromatogr.*, 110 (1975) 401.
[5] F. Tsutomu, S. Shoji and L. Hidefume, *J. Chromatogr.*, 21 (1966) 116.
[6] Y.A. Tang and W.A. Aue, *Mikrochim. Acta*, 2 (1987) 21; *Chem. Abstr.*, 109 (1988) 16399s.
[7] M. Coskun, *Int. J. Pharmacogn.*, 30 (1992) 151; *Chem. Abstr.*, 117 (1992) 258328a.
[8] V. Stepan and V. Vodehnal, *Collect. Czech. Chem. Commun.*, 36 (1971) 3964; *Chem. Abstr.*, 76 (1972) 78720y.
[9] L.Y. Kheifet and V.D.B. Bezuglyi, *Org. Poluprod. Krasiteli*, (1969) 164; *Chem. Abst.*, 72 (1970) 62117p.
[10] J.P. Hans, *J. Chromatogr.*, 26 (1967) 515.
[11] H. Thielemann, *Sci. Pharm.* 40 (1972) 291; *Chem. Abstr.*, 78 (1973) 75917y.
[12] G.D. Mitra and S.K. Ghosh, *Fert. Technol.*, 17 (1980) 194; *Chem. Abstr.*, 96 (1982) 154747t.

ELSEVIER

Journal of Chromatography A, 685 (1994) 360–364

JOURNAL OF CHROMATOGRAPHY A

Short communication

Resolution of amino acid racemates on borate-gelled guaran-impregnated silica gel thin-layer chromatographic plates

V. Mathur, N. Kanoongo, R. Mathur, C.K. Narang, N.K. Mathur*

Department of Chemistry, JNV University, Jodhpur-342003, India

First received 17 November 1992; revised manuscript received 28 June 1994

Abstract

Borate-gelled guaran-impregnated silica gel TLC plates act as a very good chiral chromatographic media. Tetracoordinated boron is complexed to the *cis*-OH pairs in guaran polysaccharide, creating a chiral environment around boron. The complexed boron can undergo a ligand-exchange reaction or stereoselective dual H-bonding to a bis-oxygen or N,O-ligand, such as conformationally favourable glycol, α-hydroxy acids and α-amino acids. These reactions, due to chiral selectivity, result in a difference in the migration rates of the enantiomers of a racemic mixture on a TLC plate. This provided a simple, rapid and effective method for the resolution of α-amino acid racemates.

1. Introduction

A chiral chromatographic sorbent can recognize molecular chirality of a low-molecular-mass solute owing to the interactions such as host–guest interactions [1], chiral metal complex–ligand exchange [2,3], charge transfer [4] and even weak, but sterically selective, hydrogen bonding association [5]. We have observed certain types of chiral discriminating properties in galactomannan (guaran) polysaccharide [6] which do not occur with anhydroglucose polymers, e.g., starch and cellulose. This has been attributed to the sterically selective dual bonding (or a two-point contact), due to the presence of a pair of *cis*-OH groups in a locked-in conformation of the pyran ring of the hexoses, i.e., galactose and mannose residues of the polysaccharide. The chiral selectivity of galactomannan is further enhanced by introducing an additional chiral stationary selector on the guaran polymer matrix or by carrying out a ligand-exchange reaction of a polymer-bound tetracoordinated borate group with ligands such as chiral 1,2-diol or α-hydroxy acid [7].

1,2-Dihydroxy ligands, α-amino acids and α-amino alcohols can also form borate complexes. We have considered the possibility of developing a rapid TLC method for the separation of amino acid racemates, based on the interaction of amino acids with tetracoordinated borate immobilized on guaran gel. In this paper, we report the effective separation of several amino acid racemates on silica gel impregnated with borate-gelled guaran.

* Corresponding author.

0021-9673/94/$07.00
SSDI 0021-9673(94)00731-4

2. Experimental

Guaran (food grade, with a viscosity of 3800 cP at 1.0% concentration as measured with a Brookfield LVT viscometer spindle No. 3 at 20 rpm) was purified as described earlier [8]. All other reagents were high-purity commercial products and were used as received.

2.1. Preparation of borated guaran-impregnated silica gel TLC plates

A 1.0-g amount of guaran was dissolved in 100 ml of distilled water and 50 g of TLC-grade silica gel was slurried into it using a Waring blender at 3500 rpm for 2 min. This was followed by addition of 0.2 g of sodium tetraborate dissolved in 100 ml of water and the mixture was again blended for 2 min at 3500 rpm. The resulting slurry was coated (0.5 mm) on TLC glass plates (20 × 5 cm) using a Stahl-type applicator. The plates were air dried and stored. For resolution studies, a solution of amino acid racemate (0.001 M, 25 μl) was applied on the TLC plate with a Hamilton syringe along with an equal amount of individual isomers of the same amino acid. For good resolution, the spot diameter was kept to about 2 mm.

The chromatographs were developed in glass jars of suitable size containing 30–40 ml of solvent and with the chamber saturated at 25°C.

As we employed laboratory-made TLC plates, the nature of TLC-grade silica gel and guaran (natural product; the commercially available form can have different molecular masses and viscosities) employed are likely to affect the resolution. Similarly, the reversible borate complexing of guaran and amino acid is pH dependent (optimum pH range 7–8) and at more alkaline pH (ca. >9) the exchange reaction becomes sluggish.

The chromatograms were developed using suitable solvent systems (Table 1) and, after drying, the chromatograms were developed by spraying with a 0.1% ethanolic ninhydrin solution followed by heating for 5 minutes at 90°C. In most instances two distinct and sharp spots corresponding to the D- and L-isomers were clearly visible on the TLC plate. These were identified by measuring and comparing the R_F values with those of co-chromatographed D- and L-isomers (Figure 1).

3. Results and discussion

Two extreme views have been expressed about the mechanism of gelling of galactomannans by

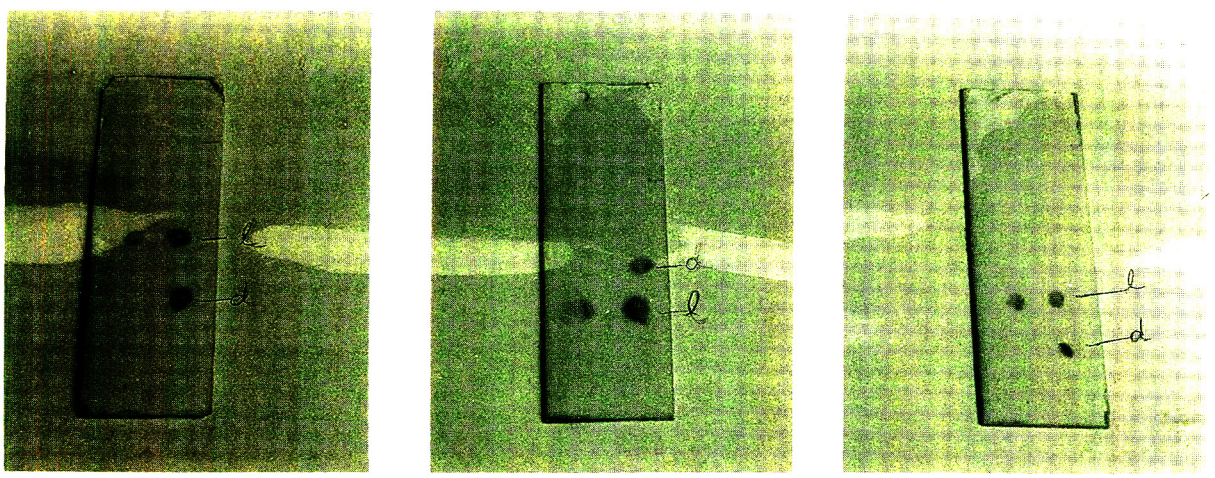

Fig. 1. Typical thin-layer chromatograms showing resolution of amino acid racemates.

borates [9]. According to one of the views, borate forms a bis-diol complex (Fig. 2, Structure 1a) due to the presence of pairs of *cis*-OH groups on the hexose units of the adjacent polymer chains resulting in a pH-dependent cross-linking. According to the other view, the cross-linking results solely due to H-bonding of the tetrahydroxy borate anion with the *cis*-OH groups on the adjacent polymer chains (Fig. 2, Structure 1b) [10]. As the borate gelling of guaran is always accompanied by the liberation of acid, the latter view cannot be considered to be correct. Also, in aqueous medium, there is a predominant possibility of forming a 1:1 diol–borate complex [11,12]. Hence the gelling of galactomannan by borate is best explained as being due to the formation of 1:1 complexes followed by H-bonding to the adjacent polymer chain (Fig. 2, Structure 1c). With this model, we can make a reasonable hypothesis for the chiral discrimination of 1,2-diol and α-amino acid enantiomers by borate-gelled guaran.

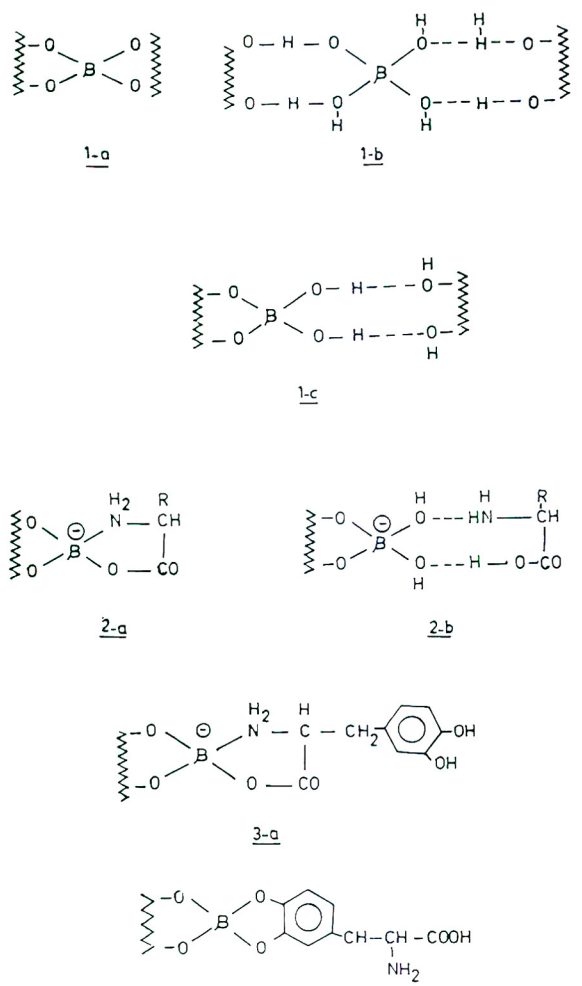

Fig. 2. Modes of interaction of borate and guaran analytes. 1a–1c: Possible modes of complexing of borate with guaran. 2a,2b: Possible interactions of guaran borate complex with amino acids. 3a,3b: Possible interactions of DOPA with guaran–borate complex.

The polymeric borate–guaran diol (1:1) complex interacts steroselectively with one of the amino acid enantiomers to form a mixed bis-complex (Fig. 2, Structure 2a), resulting in the sorption of an amino acid isomer from the mobile phase, the mobility of which is decreased (lower R_F value). Alternatively, the free hydroxyl groups [$B(OH)_2$] in the 1:1 complex interact steroselectively with one of the enantiomers by H-bonding [7] (Fig. 2, Structure b). It is expected that in the former instance, the interaction, which amounts to a ligand-exchange reaction, will have a higher stereoselectivity, but in a counter-current process even the weak stereoselectivity in H-bonding should be sufficient to resolve the enantiomers.

Our contention that bonding due to *cis*-OH groups plays an important role in chiral selectivity is further supported by the fact that even the low-molecular-mass disaccharide lactose (containing a *cis*-OH pair in the galactose half) has been shown to be effective in the separation of certain racemates [13], although no explanation was given.

Table 1 shows representative α-amino acids which have been resolved on borated guaran-impregnated silica gel. The R_F values of the D- and L-isomers are given, along with the solvent systems. It can be observed that the overall difference between the R_F values of D- and L-isomers is sufficient to make a clear distinction between the two enantiomers. However, there is no common solvent system applicable to most of the amino acids. This is to be expected because of the difference in the polarity of various amino acids. There is no common trend for the R_F values of D- and L-isomers, although a decreased

Table 1
Amino acids resolved by TLC on borated guaran-impregnated silica gel

DL-Amino acid	Solvent system[a]	R_F values of isomers[b]	
		L-	D-
Alanine	B	0.60	0.41
Valine	B	0.42	0.61
Leucine	A	0.25	0.44
Isoleucine	A	0.25	0.43
Phenylalanine	C	0.44	0.65
Tyrosine	C	0.41	0.62
DOPA	C	0.38	0.60
Tryptophane	C	0.41	0.61
Serine	C	0.23	0.44
Threonine	C	0.25	0.46
Cystine	A	0.33	0.46
Aspartic acid	C	0.61	0.80
Glutamic acid	C	0.64	0.82
Proline	A	0.62	0.29

[a] Solvent systems: (A) 2-propanol–water (7:3); (B) phenol–water (4:1) [15]; (C) butanol–acetic acid–water (3:1:1). Elution time: 30–45 min.

[b] The R_F values at 25°C are averages of four determinations, the standard deviation being 0.02; 25 μl of 0.001 *M* amino acid solution were spotted in each case.

retention (higher R_F value) has been observed for ten out of thirteen D-isomers studied. (Gupta [14] successfully achieved similar resolution, but with different R_F values.)

A unique separation on borate-gelled guaran is that of DL-DOPA enantiomers, which have a pair of catechol-type OH groups, in addition to the α-aminocarboxylic group common to natural amino acids. Here the interaction of the polymer-coordinated boron and DOPA can be either via aminocarboxylic functionalities (Fig. 2, Structure 3a) or via catchol-type 1,2-OH group pairs (Fig. 2, Structure 3b). In the latter instance, the chiral centre (α-C) of the amino acid is somewhat distant from the boron atom, which cause stereoselectivity, in acquiring chirality. Hence the overall "fit" of one of the enantiomers in the coordination sphere of tetrahedral boron must play an important role in stereoselectivity. No resolution was observed when silica gel was impregnated with guaran alone.

As there are a large number of biologically active molecules and synthetic drugs that have oxygen and/or nitrogen functional groups suitably juxtapositioned to interact with the chiral guaran–borate complex, we expect this system to be applicable to the resolution of a variety of racemates, and work on these lines is in progress.

4. Conclusions

Borated guaran-impregnated silica provides a chiral chromatographic medium for the resolution of not only α-amino acids, but also a large number of bis-oxygen or N,O-ligands such as glycols, α-hydroxy acids and α-amino alcohols which can interact with borate ion. As the chiral galactomannan also forms borate complexes, stereoselectivity is observed in either the formation of mixed bis-borate complex by a ligand-exchange reaction, or H-bonding of the solute to coordinated borate, resulting in enantiometer separation.

Acknowledgements

N.K. and V.M. are grateful to the CSIR and UGC India, respectively, for financial assistance.

References

[1] S.G. Allenmark, *Chromatographic Enantioseparation: Methods and Applications*, Ellis Horwood, Chichester, 1988.
[2] R.C. Helgeson, K. Koga, J.M. Timko and D.J. Cram, *J. Am. Chem. Soc.*, 95 (1973) 3021, and subsequent papers.
[3] S.V. Rogozhin and V.A. Davankov, *Chem. Commun.* (1971) 490.
[4] Y.H. Kim, A Tishbee and E. Gil-Av, *J. Am. Chem. Soc.*, 102 (1980) 5915.
[5] R. Charles, V. Beitler, B. Feibuch and E. Gil-Av, *J. Chromatogr.*, 112 (1975) 121.
[6] R. Mathur, S. Bohra, C.K. Narang and N.K. Mathur, *J. Liq. Chromatogr.* 15 (1992) 573.
[7] R. Mathur, S. Bohra, V. Mathur, C.K. Narang and N.K. Mathur, *Chromatographia*, 33 (1992) 336.
[8] K.C. Gupta, M.K. Sahani, B.S. Rathore, C.K. Narang and N.K. Mathur, *J. Chromatogr.*, 177 (1979) 218.
[9] H. Deuel, H. Nevkom and P. Weber, *Nature*, 161 (1948) 96.

[10] R.J. Chydzikowski, *J. Soc. Cosmet. Chem.*, 22 (1971) 43.
[11] R.F. Nickerson, *J. Inorg. Nucl. Chem.*, 32 (1970) 1401.
[12] K. Kustin and R. Piezer, *J. Am. Chem. Soc.*, 91 (1969) 317.
[13] E. Gil-Av, B. Feiburt and R. Charles-Sigier, *Tetrahedron Lett.*, (1966) 1009.
[14] K.C. Gupta, CSIR Center for Biochemical, Delhi, personal communication.
[15] E. Von Arx and R. Neher, *J. Chromatogr.*, 12 (1963) 329.

ELSEVIER

Journal of Chromatography A, 685 (1994) 365–366

JOURNAL OF CHROMATOGRAPHY A

Book Review

Flow Injection Separation and Preconcentration by Z. Fang, VCH, Weinheim, 1993, XIV + 259 pp., price DM 148.00, £61.00, ISBN 3-527-28308-0.

Professor Fang's book describes separation and preconcentration techniques as implemented in continuous-flow systems. In so doing, it touches on one of the least developed aspects of analytical chemistry to date: preliminary sample treatment steps (e.g., extraction, sorption, dialysis), which are typically time consuming and error prone. Automation of such steps, the ultimate subject matter of the book, is aimed at bringing development of the initial stages of the analytical process nearer to the advanced status of the signal measurement (detection) and computerized processing for the delivery of analytical results. The book is therefore devoted to one of the analytical topics of the greatest current interest.

The book consists of nine chapters. The first introduces readers to flow injection analysis principles and the general characteristics of flow methods involving a separation and/or preconcentration unit. In this respect, the section summarizing the different techniques described in the book is worth special note as it clearly outlines their most distinguishing features through the key factors defining the foundation of the separation and preconcentration techniques. Chapter 2 discusses the basic elements of flow systems (mainly pumps, valves, reactors and detectors) and is followed by a description of specific separation and preconcentration techniques. The reviewed applications of liquid–liquid extraction (Ch. 3) include its conventional implementation by means of a segmenter, coil and phase separator, until the development of other recent innovations avoiding the use of these units, and various applications based on different types of detection. Sorption processes are discussed in Chapter 4, the longest in the book, with special emphasis on such technical aspects as column design, packing and incorporation into flow systems; emerging technology such as that of flow-through sensors is only briefly covered, however. The reviewed gas–liquid separation systems (Ch. 5) are mostly based on gas diffusion; by contrast, hydride generation and cold vapour systems are given little attention, and no mention is made of continuous distillation and evaporation. Dialysis is very briefly considered in Chapter 6, whereas precipitation–dissolution processes are dealt with systematically in Chapter 7. The last two chapters comment on some environmental and agricultural applications of the previously described techniques (Ch. 8), and their use in clinical and pharmaceutical analysis (Ch. 9). The proposed examples testify to the high potential of continuous separation and preconcentration systems for solving a variety of real problems, including application to different complex matrices. Nevertheless, they could have been described at greater length for consistency with the eminently practical nature of the book.

The author, an expert in continuous-flow systems, gives experimental details that will be a

SSDI 0021-9673(94)00710-1

great aid in fine tuning flow systems that include a separation and/or preconcentration unit. Although brief, some coverage of basic and theoretical aspects is provided. The conceptual ordering of the chapters is somewhat inconsistent with the classification made in the Introduction (liquid–liquid, liquid–gas and liquid–solid systems). Electrodeposition and dissolution, not included in the book, should be considered in future editions. There is no doubt that the book will be of considerable use to readers with an interest in automating any of the wide variety of analytical procedures currently used routinely in many control laboratories in order to significantly facilitate the processing of complex samples.

Córdoba, Spain Angel Ríos

Author Index

The Data Analysis Handbook

By **I.E. Frank** and **R. Todeschini**

Data Handling in Science and Technology Volume 14

Analyzing observed or measured data is an important step in applied sciences. The recent increase in computer capacity has resulted in a revolution both in data collection and data analysis. An increasing number of scientists, researchers and students are venturing into statistical data analysis; hence the need for more guidance in this field, which was previously dominated mainly by statisticians.

This handbook fills the gap in the range of textbooks on data analysis. Written in a dictionary format, it will serve as a comprehensive reference book in a rapidly growing field. However, this book is more structured than an ordinary dictionary, where each entry is a separate, self-contained entity. The authors provide not only definitions and short descriptions, but also offer an overview of the different topics. Therefore, the handbook can also be used as a companion to textbooks for undergraduate or graduate courses.

Approximately 1700 entries are given in alphabetical order grouped into 20 topics and each topic is organized in a hierarchical fashion. Additional specific entries on a topic can be easily found by following the cross-references in a top-down manner. Several figures and tables are provided to enhance the comprehension of the topics and a list of acronyms helps to locate the full terminologies. The bibliography offers suggestions for further reading.

©1994 386 pages Hardbound
Price: Dfl. 325.00 (US$185.50)
ISBN 0-444-81659-3

ELSEVIER

An imprint of Elsevier Science

❑ **Yes, please send me ..... copies of:**
The Data Analysis Handbook
By I.E. Frank and **R. Todeschini**
©1994 386 pages Hardbound
Price: Dfl. 325.00 (US$185.50)
ISBN 0-444-81659-3

Send this form to your regular supplier or to
ELSEVIER SCIENCE B.V.
P.O. Box 330, 1000 AH Amsterdam
The Netherlands
Fax: +31 (20) 586 2845

Customers in the USA/Canada, send to
ELSEVIER SCIENCE B.V.
P.O. Box 945, New York
NY 10159-0945
Fax: +1 (212) 633 3680

ORDER FORM

❑ Payment Enclosed: (Bank Draft / Eurocheque / International Money Order / Postal Cheque / Official Purchase Order Form)

❑ Please send me a pro forma invoice

❑ Charge my credit card:

❑ Access ❑ Eurocard ❑ Visa ❑ American Express ❑ MasterCard

Card No. ..... Valid Until .....

Name ..... Initials .....

.....

.....

Signature ..... Date .....

Vat Registration No. .....

US$ prices are valid only for the USA & Canada and are subject to exchange rate fluctuations; in all other countries the Dutch guilder price (Dfl.) is definitive. Customers in the European Union should add the appropriate VAT rate applicable in their country to the price(s). Books are sent postfree if prepaid.

PUBLICATION SCHEDULE FOR THE 1995 SUBSCRIPTION

Journal of Chromatography A and *Journal of Chromatography B: Biomedical Applications*

MONTH	O 1994	N 1994	D 1994	
Journal of Chromatography A	683/1 683/2 684/1	684/2 685/1 685/2 686/1	686/2 687/1 687/2 688/1 + 2	The publication schedule for further issues will be published later.
Bibliography Section				
Journal of Chromatography B: Biomedical Applications				

INFORMATION FOR AUTHORS

(Detailed *Instructions to Authors* were published in *J. Chromatogr. A*, Vol. 657, pp. 463–469. A free reprint can be obtained by application to the publisher, Elsevier Science B.V., P.O. Box 330, 1000 AH Amsterdam, Netherlands.)

Types of Contributions. The following types of papers are published: Regular research papers (full-length papers), Review articles, Short Communications and Discussions. Short Communications are usually descriptions of short investigations, or they can report minor technical improvements of previously published procedures; they reflect the same quality of research as full-length papers, but should preferably not exceed five printed pages. Discussions (one or two pages) should explain, amplify, correct or otherwise comment substantively upon an article recently published in the journal. For Review articles, see inside front cover under Submission of Papers.

Submission. Every paper must be accompanied by a letter from the senior author, stating that he/she is submitting the paper for publication in the *Journal of Chromatography A* or *B*.

Manuscripts. Manuscripts should be typed in **double spacing** on consecutively numbered pages of uniform size. The manuscript should be preceded by a sheet of manuscript paper carrying the title of the paper and the name and full postal address of the person to whom the proofs are to be sent. As a rule, papers should be divided into sections, headed by a caption (*e.g.*, Abstract, Introduction, Experimental, Results, Discussion, etc.). All illustrations, photographs, tables, etc., should be on separate sheets.

Abstract. All articles should have an abstract of 50–100 words which clearly and briefly indicates what is new, different and significant. No references should be given.

Introduction. Every paper must have a concise introduction mentioning what has been done before on the topic described, and stating clearly what is new in the paper now submitted.

Experimental conditions should preferably be given on a *separate* sheet, headed "Conditions". These conditions will, if appropriate, be printed in a block, directly following the heading "Experimental".

Illustrations. The figures should be submitted in a form suitable for reproduction, drawn in Indian ink on drawing or tracing paper. Each illustration should have a caption, all the *captions* being typed (with double spacing) together on a *separate sheet*. If structures are given in the text, the original drawings should be provided. Coloured illustrations are reproduced at the author's expense, the cost being determined by the number of pages and by the number of colours needed. The written permission of the author and publisher must be obtained for the use of any figure already published. Its source must be indicated in the legend.

References. References should be numbered in the order in which they are cited in the text, and listed in numerical sequence on a separate sheet at the end of the article. Please check a recent issue for the layout of the reference list. Abbreviations for the titles of journals should follow the system used by *Chemical Abstracts*. Articles not yet published should be given as "in press" (journal should be specified), "submitted for publication" (journal should be specified), "in preparation" or "personal communication".

Vols. 1–651 of the *Journal of Chromatography*; *Journal of Chromatography, Biomedical Applications* and *Journal of Chromatography, Symposium Volumes* should be cited as *J. Chromatogr.* From Vol. 652 on, *Journal of Chromatography A* (incl. Symposium Volumes) should be cited as *J. Chromatogr. A* and *Journal of Chromatography B: Biomedical Applications* as *J. Chromatogr. B.*

Dispatch. Before sending the manuscript to the Editor please check that the envelope contains four copies of the paper complete with references, captions and figures. One of the sets of figures must be the originals suitable for direct reproduction. Please also ensure that permission to publish has been obtained from your institute.

Proofs. One set of proofs will be sent to the author to be carefully checked for printer's errors. Corrections must be restricted to instances in which the proof is at variance with the manuscript.

Reprints. Fifty reprints will be supplied free of charge. Additional reprints can be ordered by the authors. An order form containing price quotations will be sent to the authors together with the proofs of their article.